Rémi Losno: Inscription au Diplôme d'Habilitation à Diriger les Recherches.

Le cycle atmosphérique des métaux et d'autres éléments chimiques. Exposé des motivations et de l'avancement de notre programme de Recherches.

Sommaire:

1 Introduction: le rôle de l'atmosphère dans le cycle des métaux.

Après l'oxygène et le silicium, les métaux sont les éléments les plus abondants à la surface de la terre (Turekian 1971, Lameyre 1986). A l'état naturel, on les retrouve sous forme d'oxydes (par exemple TiO_2), d'oxohydroxydes (par exemple goethite FeOOH), d'hydroxydes (par exemple gibbsite $AlOH)_3$) ou comme inclusion dans une matrice minérale silicatée (par exemple sodium ou potassium dans du feldspath) (Lameyre 1986). Les activités humaines produisent ces éléments à l'état de corps purs (par exemple cuivre), d'alliages (par exemple bronze), de solides multiphasiques (par exemple une tôle d'acier galvanisée) ou de poussières (fumées d'usine d'incinération). Pour être transférés dans l'atmosphère, les métaux doivent être sous la forme de très fines particules de diamètre inférieurs à une dizaine de micromètres. On appelle ces particules en suspension dans l'air un aérosol solide.

Les forces de frottements et les hautes températures sont les principales causes de la fabrication de telles particules. Ces causes peuvent être activées aussi bien par des phénomènes naturels qu'anthropiques (Colls 1997). Les vents agissent sur un sol sec en mettant en mouvement des particules de taille variées. Ce mouvement engendre un frottement qui va permettre de libérer des particules microscopiques: on appelle cela la saltation (Gillette et al., 1974; Gomes et al., 1990; Alfaro et al., 1997). Aussi, le frottement de l'air sur la surface des océans va créer des vagues qui, en englobant des bulles d'air, vont générer des fines particules de sels de mer (Blanchard 1983, Weisel et al. 1984). Le volcanisme permet à des masses rocheuses en fusion de remonter des profondeurs vers la surface de la terre. Suite à une baisse de pression rapide, les gaz dissous dans le magma à haute température vont s'échapper en emportant avec eux des métaux dans leur état gazeux. Lorsque le gaz se refroidit, les métaux condensent en très fines particules (Colls, 1997). De nombreuses activités humaines utilisent des températures élevées où les métaux sont susceptibles de s'évaporer et ensuite de se condenser à nouveau. Ces phénomènes se produisent dans les panaches des fumées d'usine ou dans l'échappement d'un moteur thermique (Colls, 1997). D'une autre façon, toute pièce mécanique en mouvement va générer des particules par frottement sur les axes ou les pièces en glissement.

Enfin, il arrive que des métaux puissent se trouver à l'état gazeux dans les conditions habituelles de l'environnement. Il y a par exemple le mercure dont la tension de vapeur est suffisamment élevée à température ambiante pour détecter la présence d'atome Hg dans l'air. Des combinaisons organiques des métaux (méthyl étain ou alkyl plomb par exemple) peuvent aussi porter les métaux à l'état gazeux avec une tension de vapeur non négligeable (Donard et Weber, 1988).

Une fois dans l'atmosphère, ces métaux et les aérosols associés subissent des transformations chimiques causées par diverses interactions:

1. Interaction de la lumière sur l'aérosol pendant la journée. Les conséquences de cette interaction sont d'une part des réactions photochimiques et d'autre part une modification du bilan radiatif de l'atmosphère contenant les aérosols car cette interaction dépend de la longueur d'onde des photons (Claquin et al., 1998). On peut d'ailleurs se servir de cette interaction pour une mesure physique à distance de ces aérosols (Kaufmann et al., 1997; Chiapello et al., 2000)
2. Interaction avec des espèces gazeuses. Ces réactions ont lieu à la surface de l'aérosol et peuvent avoir un impact plus ou moins grand sur la chimie troposphérique (Dentener et al. 1996) On peut distinguer les réactions acide-base, par exemple de l'acide nitrique gazeux avec un aérosol de calcite produisant du nitrate de calcium solide et du dioxyde de carbone, et les réactions d'oxydo-réduction, par exemple de l'ozone créant des fonctions oxygénées sur une particule de suie. Parfois, les deux sont liées comme par exemple l'action du dioxyde de soufre SO_2 et de l'oxygène O_2 sur une particule d'aérosol marin humide qui va donner du

sulfate de sodium (oxydation du soufre IV en soufre VI, très acide) et de l'acide chlorhydrique. Ces dernières réactions nécessitent la présence d'eau liquide qui contient de traces de métaux de transition comme catalyseur, et font participer les 3 états solides, liquide et gazeus.

3. Interaction avec l'eau. Cette interaction particulière commence avec la condensation de la vapeur d'eau sur une particule solide (Kölher, 1921; Svenningsson, 1994; Flossmann 1998b & c), se continue par des réactions de dissolution de l'aérosol dans la phase aqueuse ainsi formée (Desboeufs at al., 1999 & 2001, Spokes et al., 1994 & 1996) ou encore par des réactions en phase homogène aqueuse (Graedel et al., 1985 & 1986; Jacob et al., 1989; Walceck et al., 1997, Weschler et al., 1986, Zhu et al., 1993), et se termine par l'évaporation de l'eau ou bien le dépôt de l'ensemble sur le sol au cours d'un épisode pluvieux. Ce sont les nuages qui sont le siège de telles interactions, et les aérosols y subissent de nombreux cycles d'évapo-condensation (Flossmann 1998a & b). Au cours de ces cycles, la surface de l'aérosol est profondément altérée (Desboeufs et al., 1999; Desboeufs et al., 2001) et de la matière peut s'échanger entre différents types d'aérosols présents dans la goutte d'eau, et aussi entre la phase gazeuse et la phase condensée par dissolution de gaz solubles (Audiffren et al., 1996; Lelieveld and Crutzen, 1991). Il est à noter que dans l'atmosphère les aérosols sont omniprésents et l'eau ne se condense jamais spontanément sans un support. On appelle ce support un noyau de condensation (CCN). La facilité de condensation de l'eau sur ce support dépend de l'hygroscopicité de celui-ci et donc de la solubilité de sa surface (Flossmann 1998b, Pradelle et al. 2002a & b). Les modifications chimiques de cette surface vont donc contribuer à modifier le caractère CCN de tel ou tel aérosol, et donc le nombre de CCN disponibles pour former un nuage, donc la densité de gouttes d'un nuage. De ce spectre de goutte dépend les propriétés radiatives du nuage. Il y a donc ici un effet indirect des propriétés chimiques de l'aérosol sur le bilan radiatif de l'atmosphère et donc sur le climat.

On peut remarquer que les systèmes décrits font intervenir des réactions chimiques dans plusieurs phases simultanément. Il s'agit donc de chimie multiphasique. C'est pour alimenter un tel axe de recherche au sein de notre Laboratoire de Recherches (LISA, Universités Paris 7, Paris 12 et CNRS), que j'ai orienté mes travaux dans cette direction. Cet axe est soutenu par les plans quadriennaux engageant le Laboratoire auprès de ses tutelles Universitaires et du CNRS. Les questions auxquelles nous avons à répondre pour faire avancer nos connaissances dans ce domaine sont multiples et seront développés dans les chapitres suivants de ce fascicule.

Il s'agit tout d'abord de problèmes de Chimie Analytique afin de fournir une observation correcte des phénomènes que nous voulons décrire. Les concentrations en métaux dans l'environnement sont heureusement très faibles mais très variables dans le temps et dans l'espace. Des techniques particulières doivent être développées pour assurer la qualité des résultats analytiques car s'il est possible de répéter une expérience menée en laboratoire, il est impossible d'obtenir deux fois la même situation lorsque l'on se trouve dans le milieu naturel. En effet, les concentrations en aérosols, en gaz réactifs, en eau, l'intensité lumineuse ne se produisent jamais deux fois à l'identique car ces paramètres dépendent étroitement des conditions météorologiques qui ont permis le transport de la matière au lieu d'observation, des sources d'émissions de matière dans l'atmosphère et des condition de dépôt de cette matière hors de l'atmosphère. Il y a trop de degrés de liberté pour qu'une même situation se représente à l'identique à l'échelle de quelques années, voire du siècle. A cause de ce manque de reproductibilité, la précision, la justesse, la fiabilité et donc la validité des analyses chimiques pratiquées dans l'environnement sont donc fondamentaux pour pouvoir mener une discussion scientifique.

Nous exposerons ensuite différents aspects de la chimie atmosphérique des métaux qui vont de leur implication dans des cycles catalytiques de photo-oxydo-réduction à leur action sur le caractère CCN. Puis nous nous intéresserons à leur impact et aux informations qu'ils peuvent apporter au

géochimiste lorsqu'ils se déposent hors de l'atmosphère, que ce soit sur un sol végétal ou bien dans l'océan.
Tous les travaux présentés dans la suite de ce fascicule ont été réalisés en travail d'équipe, les noms des différents chercheurs et apprentis chercheurs concernés apparaissent comme co-auteurs dans les publications listées plus loin et dans la liste de mes encadrements de 3ème cycle.

2 L'analyse des métaux dans l'atmosphère

Comme nous l'avons indiqué dans l'introduction, la maîtrise des outils chimiques d'analyse est un passage indispensable pour alimenter notre réflexion scientifique sur le sujet proposé. Cette maîtrise commence par le prélèvement lui-même et se termine par l'obtention de données quantitatives validées. Nous avons donc du développer des méthodes et des protocoles spécialement adaptés à la maîtrise de la contamination, à la conservation d'échantillons très peu concentrés en analyte et à la détermination de très petites quantités d'éléments chimique mais concernant la plus grande proportion possible du tableau périodique. Cette dernière action passe nécessairement par l'acquisition et la maintenance d'une d'instrumentation performante, donc coûteuse.

2.1 L'instrumentation analytique

Nous avons du maîtriser un des aspects souvent cachés de la recherche car souvent ingrat, qui est l'obtention de financements à la hauteur de la centaine de millier d'Euros. Ces fonds ont été obtenus grâce à de nombreux partenariats contractuels avec nos tutelles qui sont les Universités Paris 7 et Paris 12 et le CNRS, avec d'autres laboratoires de recherche (par exemple le Laboratoire de Géochimie des Eaux, l'Université Paris7), avec d'autres organismes publics partenaires de la recherche et habilités à la financer (Ministère de l'Environnement, ADEME) ou encore des sociétés de droit privée ou d'économie mixte (agences de l'air). Nous avons contribué par notre activité au financement d'un Spectromètre de Fluorescence X, d'une absorption atomique à four graphite et à génération d'hydrure, et enfin d'un spectromètre d'émission atomique de plasma. Cette course à l'instrumentation nous permet de contribuer à l'avancement des concepts de travail dans la communauté scientifique. Longtemps, nous avons du raisonner en suivant le comportement d'un nombre restreint de métaux, à cause des contrainte analytiques. Le développement récent de techniques performantes d'analyse élémentaire permet de multiplier par 10 ou 20 le nombre d'éléments chimiques analysés en même temps tout en améliorant les limites de détection et la justesse de la détermination. Nous pouvons donc maintenant suivre le comportement dans l'environnement non pas de tel ou tel élément particulier, mais de groupes entiers d'éléments chimiques, comme par exemple les alcalins, les alcalino-terreux, la première série des métaux de transition, etc... Nous pouvons passer avec le même investissement en temps et en argent d'une analyse descriptive restreinte au comportement de tel ou tel élément à une analyse explicative de ce comportement en comparant les membres d'un même groupe et l'évolution des comportements individuels le long d'une même colonne du tableau périodique par exemple. Dans ce cas, la productivité d'un instrument d'analyse a un effet direct considérable sur la productivité scientifique de son utilisateur.

2.1.1 Fluorescence X

La fluorescence X permet une analyse multi élémentaire directe et sans préparation lourde, d'échantillons solides en couche mince, tels que se présentent des aérosols après filtration de l'air sur une membrane. Bien que très intéressante pour nos travaux, une telle application n'est pas prévue par les constructeurs car elle ne représente aujourd'hui qu'un marché très réduit. Il nous a donc fallu participer au développement de la méthode analytique optimale pour l'analyse d'aérosols en couche mince. Nous avons abouti à la définition d'un protocole d'étalonnage par filtration de standards géochimiques (roche en poudre ou poussières industrielles) en suspension dans du cyclohexane et

par dépôt de gouttes de solutions salines des éléments à doser. Les limites de détection sont, pour la plupart des éléments analysés, de l'ordre du nano gramme de matière déposé sur la membrane. On peut lire une application de cette méthode d'analyse l'annexe jointe: "Origins of the Atmospheric Particulate Matter over the North-Sea and the Atlantic Ocean".

2.1.2 L'émission de plasma et l'absorption atomique

Ces deux méthodes nécessitent d'avoir des échantillons en solution, la première est une méthode multi élémentaire, la seconde mono élémentaire mais plus sensible. Notre travail a consisté à obtenir des limites de détection les plus basses possibles afin d'avoir accès au plus grand nombre possible d'éléments chimiques. Nous avons aussi procédé à une validation interne de nos résultats analytiques par des intercalibrations internes et avec d'autres laboratoires. Ces intercalibrations consistent à mesurer des séries d'échantillons avec des techniques analytiques différentes.

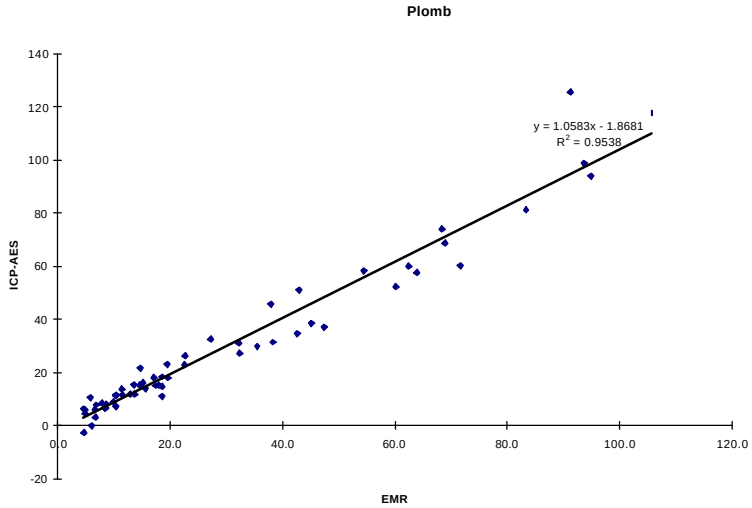

Cette figure montre par exemple le résultat d'une intercalibration pour le plomb entre l'absorption atomique (abscisse, EMR) et l'émission plasma (ordonnée, ICP-AES). Il s'agit d'échantillons de retombées atmosphériques collectées en Corse et conservées dans des récipients en polyéthylène, en milieu acide nitrique 1%. Les axes sont gradués en ppb, soit des µg par litre. Une autre particularité de cette intercalibration est qu'elle concerne des échantillons conservés 10 ans. On montre également la pertinence de nos procédures de conservation d'échantillons liquides. Il existe aussi dans le commerce des stocks homogènes d'échantillons qui ont été analysés de nombreuses fois et que l'on peut acheter ou en obtenir un exemplaire pour valider sa propre méthode. Nous avons contribué à l'élaboration de tels standards sur les ions majeurs d'une eau de composition voisine d'une rivière et d'eau de pluie.

Les limites de détection sont, pour l'émission plasma que nous employons, de l'ordre du nano gramme pour 10 mL de solution, et pour l'absorption atomique 10 à 100 fois plus faibles. A part la reconnaissance que nous apportent nos pairs dans l'usage de ces techniques lors de nos échanges scientifiques, nous participons à l'organisation de séminaires de formation à ces techniques dans le cadre de formation continue en partenariat avec le monde industriel.

2.2 L'environnement analytique

Les limites de détection qui sont obtenues par nos méthodes instrumentales n'ont de sens que si l'échantillon n'est pas contaminé par le milieu ambiant tout au long de la procédure d'analyse. Travaillant dans l'environnement, nous devons avoir la capacité d'analyser des échantillons provenant de zones ou les concentrations ambiantes en métaux sont très différentes, en fait très inférieures à celles rencontrées dans nos environnements urbains. Nous avons donc du développer des systèmes de confinement qui permettent de travailler dans un environnement toujours plus pur que celui où a été prélevé l'échantillon. Il s'agit de salles blanches chimiques où, au sein d'une

structure de laboratoire, nous avons crée des zones de travail où l'environnement est jusqu'à un million de fois plus pur que celui du reste du laboratoire. Notre expertise dans ce domaine est là encore reconnue au-delà du monde scientifique car nous sommes sollicités par des partenaires industriels pour organiser des stages de formation aux techniques de salle blanche chimiques et d'analyses d'ultra-traces.

Cet environnement nous a permis de mettre au point des techniques de conservation de l'échantillon minéral en phase dissoute grâce à la très grande propreté des récipients et réactifs utilisés. En effet, pour bien conserver un échantillon, il faut empêcher à la fois toute adsorption sur les parois du flacon le contenant, et aussi toute désorption de contaminant vers la solution. A plus long terme, c'est à dire sur des périodes plus longues qu'un mois, on peut noter un effet notable de diffusion des espèces chimiques à travers la matière constitutive du flacon. Comme il est impossible d'éviter l'adsorption sans favoriser la désorption, il faut faire en sorte qu'il ne reste plus rien à désorber susceptible de contaminer l'échantillon. Pour cela, nous avons mis au point un protocole très long de lavage des flacons où les étapes ultimes consistent à laisser reposer pendant plusieurs mois le flacon plein d'une solution acide ultra-pure. Un tel protocole ne peut se concevoir que dans l'enceinte d'une salle blanche chimique car, sinon, un trempage avec une solution contaminée, même faiblement, et dans un environnement empoussiéré aboutit à l'inverse du but recherché, c'est à dire un enrichissement du flacon en différentes substances contaminantes. L'évolution de l'instrumentation rend les appareils de plus en plus sensibles pour de plus en plus d'éléments, ce qui rend les procédures de décontamination de plus en plus lourdes à réaliser et à mettre au point car il faut les optimiser pour de plus en plus d'éléments à la fois. On peut voir dans les figures suivantes, où on représente les analyses récentes (1999) en fonction d'analyses plus anciennes (1988) que la concervation peut être bonne pour certains éléments (Mn) et pas d'autres (Cd) à des concentrations plus ou moins fortes. Toutes les valeurs sont exprimées en ppb ($\mu g.L^{-1}$ d'élément).

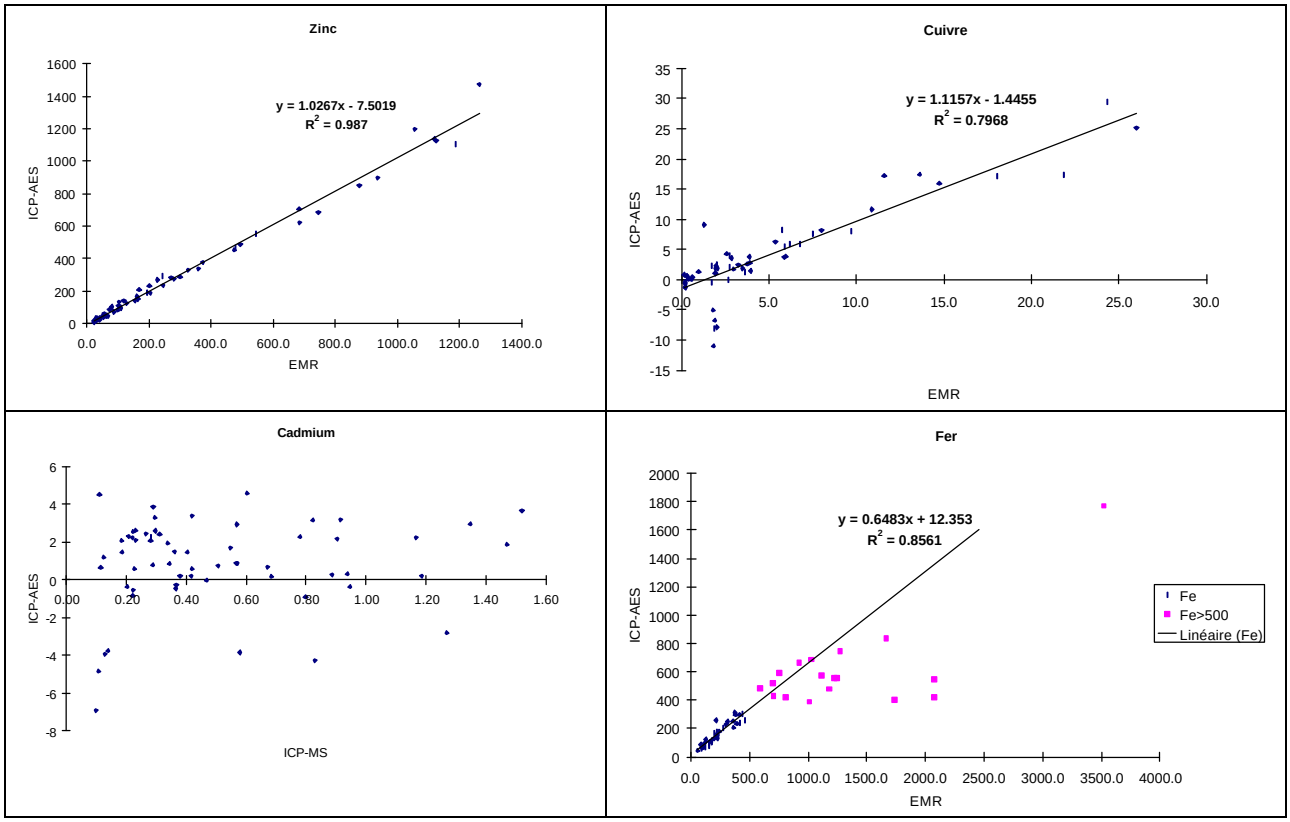

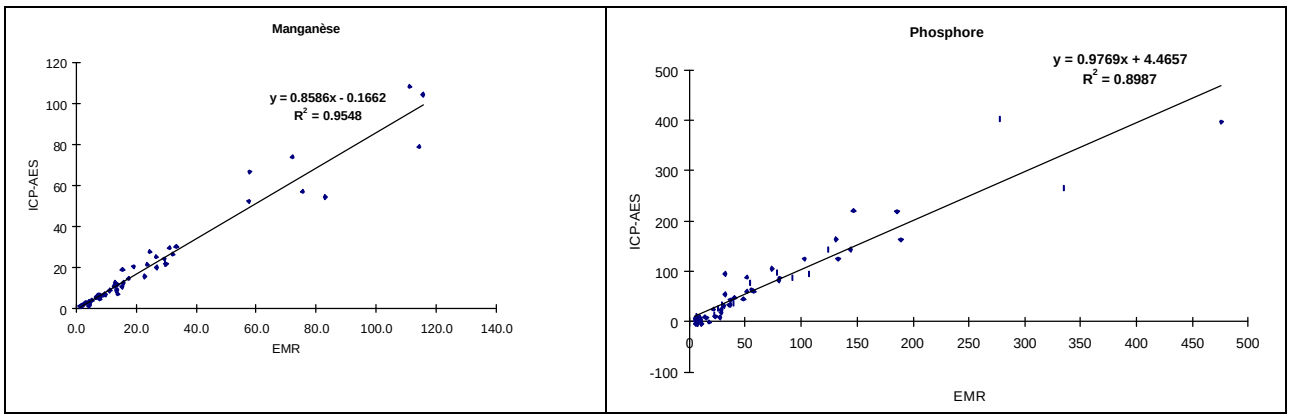

On peut voir dans cette figure plusieurs cas de dégradation ou de conservation dans cette série d'intercalibrations à 10 ans d'intervalle, qui porte sur des échantillons de retombées totales (Remoundaki et al., 1991) prélevées en Corse entre 1986 et 1988. Le zinc et le phosphore, présents en forte concentration se conservent bien sur toute la gamme, le fer s'est mieux conservé dans les échantillons les moins concentrés, le cuivre au contraire présente des anomalies pour les faibles concentrations, on a perdu tout signal sur le cadmium, et le manganèse est au contraire très bien conservé, même sur les faibles valeurs, comme le montre l'agrandissement suivant:

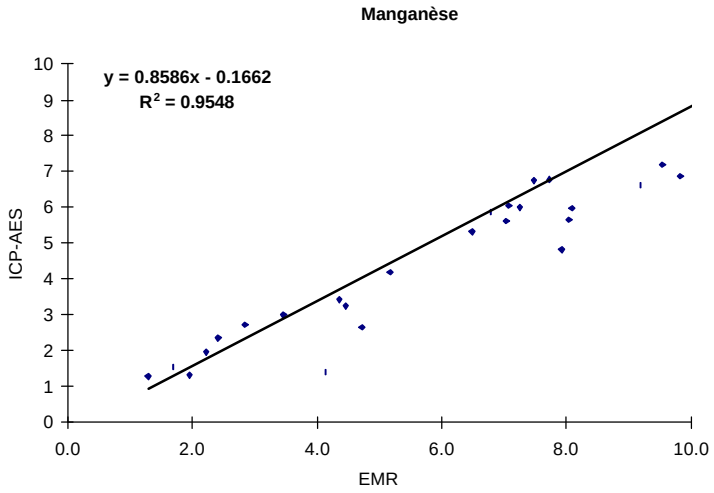

En abscisse, on a les valeurs "EMR" correspondant à l'absorption atomique en mode flamme ou four selon la concentration, sauf pour le phosphore où il s'agit d'une méthode colorimétrique au molybdate d'ammonium.

2.3 Le prélèvement

Les techniques analytiques maîtrisées, il s'agit de transférer dans l'appareil d'analyse des parties représentatives du milieu étudié. Comme l'atmosphère est un système multiphasique, une des premières préoccupations sera de séparer les phases.

2.3.1 L'aérosol

Si nous nous intéressons à l'aérosol, alors nous pourrons séparer la phase solide de la phase gaz par filtration ou impaction. La première méthode consiste à forcer de l'air à passer à travers une membrane filtrante ou un filtre fibreux. La plupart des particules solides se déposent alors sur le support solide qui leur est présenté. L'efficacité de piégeage dépend du débit de l'air à travers le filtre et de la taille de la particule à piéger. En général, les particules les plus grosses (>1µm) et les plus petites (<50 nm) se déposent facilement. On obtient un minimum d'efficacité (80 à 90%) pour des particules d'une taille de l'ordre de 0,2 µm. La seconde méthode consiste à projeter un jet d'air sur

une paroi. Les particules les plus grosses vont impacter sur la paroi alors que les plus petites suivront les flux d'air. En réglant l'intensité du jet d'air, on peut contrôler la taille des particules piégées sur la plaque. Si on met plusieurs systèmes de ce genre en série, on forme un impacteur en cascade où, pour chaque taille et chaque étage, on peut affecter une probabilité de rétention encore appelée fonction d'efficacité de l'étage. On obtient ainsi un dispositif permettant une sélection granulométrique de l'aérosol. Nous n'avons pas contribué à des développements révolutionnaires des systèmes de filtration, mais encore une fois nous nous sommes attachés à mettre au point des méthodes de prélèvement assurant l'absence de contamination des échantillons et sa représentativité par rapport à la masse d'air étudiée. Comme le prélèvement s'étale souvent sur plusieurs heures, voire sur plusieurs jours dans des régions où il y en a très peu (par exemple au Groenland), nous devons éviter de mélanger plusieurs situations météorologiques. Nous avons donc mis au point un couplage entre une station météorologique locale et un système de prélèvement d'aérosol afin d'utiliser les données de vent local pour n'autoriser le prélèvement que pour des situations homogènes.

2.3.2 Les pluies

En ce qui concerne la phase aqueuse, toujours mélangée à des phases solides comme nous l'avons vu dans l'introduction, elle se sépare par gravité de la phase gazeuse lors d'une pluie, si les gouttes sont assez grosses. Nous avons développé des procédures de collecte d'eau de pluie dans des conditions ultra propres, et avec une séparation en ligne des phases solides et aqueuse. Ces procédures incluent la définition de la position des collecteurs pour maximiser la récolte de pluie au détriment de particules qui ne sont pas des gouttes de pluie (voir l'annexe jointe "Non-rain deposition significantly modifies rain samples at a coastal site").

2.3.3 Les nuages

Lorsque les gouttes d'eau sont trop petites, alors elles ne tombent pas et on doit agir pour les séparer de l'air qui les entoure. Nous sommes actuellement en plein développement d'un tel système qui devra être monté sur un avion car les nuages sont souvent largement au-dessus du sol. La difficulté d'un tel système réside presque entièrement dans la difficulté à maintenir propre et non contaminé un préleveur devant être monté par des mécaniciens dans un hall d'aéroport, puis subissant tout l'environnement des pistes de décollage balayées par les gaz d'échappement des avions.

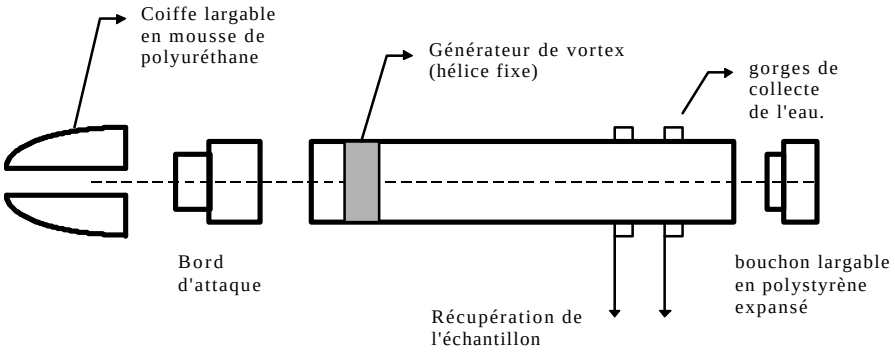

Schéma du collecteur d'eau nuageuse

3 La chimie atmosphérique des métaux

Nous arrivons maintenant à un point où nous disposons de données fiables sur les métaux dans l'atmosphère et sur les variations de leurs concentrations. Nous pouvons alors tenter d'expliquer leur comportement soit par la modélisation chimique, soit par simulation dans un réacteur chimique.

Cette deuxième alternative n'excluant absolument pas la première. Le projet de recherche INCHAAC, malheureusement non financé, mais joint en annexes constitue une bonne description du travail à faire dans ce domaine, et que nous persistons à vouloir réaliser.

3.1 Les métaux catalyseurs

C'est par le biais de la modélisation en cinétique et thermodynamique chimique que nous avons abordé ce problème (voir article joint: "Trace metals acting as catalysts in a marine cloud: a box model study" pour les détails). Nos travaux ont tout d'abord consisté à montrer le rôle de catalyseur qu'ont les métaux de transition naturellement présents dans l'atmosphère lorsqu'ils se dissolvent dans les gouttes d'eau nuageuse. Nous nous sommes dans un premier temps appuyés sur des valeurs mesurées de concentrations en métaux dissous. En région non polluée, la chimie aqueuse atmosphérique est largement dominée par le peroxyde d'hydrogène H_2O_2 et le peroxyde de méthyle CH_3OOH, ce dernier provenant de l'oxydation du méthane omniprésent dans la troposphère (partie de l'atmosphère en contact avec le sol, haute d'environ 10 km). Par photodissociation, H_2O_2 produit des radicaux OH susceptibles d'oxyder n'importe quelle molécule dissoute dans l'eau, et aussi H_2O_2 où on obtient alors le radical HO_2. HO_2 peut à son tour donner un radical OH ou bien réagir avec un autre HO_2 pour donner H_2O_2. On obtient alors des cycles de photo-oxydo-réduction qui maintiennent des concentrations stables en radicaux dans la goutte d'eau. L'introduction de traces de métaux de transition va considérablement accélérer la vitesse de rotation du cycle HO_2/OH car ces métaux sont susceptible de changer facilement de degré d'oxydation. Ainsi, nous avons la suite de réactions:

N°	Réaction			vitesse de réaction ($L.mol^{-1}.s^{-1}$, sauf 01, 21et 22 en s^{-1})
(01)	$h\nu + H_2O_2$	→	2 OH	J=5.7E-07
(02)	$HO_2 + OH$	→	$O_2 + H_2O$	k=7.0E+09
(03)	$O_2^- + OH$	→	$O_2 + OH^-$	k=1.1E+10
(04)	$H_2O_2 + OH$	→	$HO_2 + H_2O$	k=2.7E+07
(05)	$O_3 + OH$	→	$HO_2 + O_2$	k=2.0E+09
(06)	$HO_2 + HO_2$	→	$H_2O_2 + O_2$	k=8.6E+05
(07)	$HO_2 + O_2^- + H_2O$	→	$H_2O_2 + O_2 + OH^-$	k=1.0E+08
(08)	$H_2O_2 + HO_2$	→	$OH + H_2O + O_2$	k=5.0E-01
(09)	$H_2O_2 + O_2^-$	→	$OH + OH^- + O_2$	k=1.3E-01
(10)	$O_3 + O_2^- + H_2O$	→	$OH + 2\ O_2 + OH^-$	k=1.5E+09
(11)	$OH + Mn^{2+}$	→	$Mn^{3+} + OH^-$	k=3.4E+07
(12)	$HO_2 + Mn^{2+} + H_2O$	→	$Mn^{3+} + H_2O_2 + OH^-$	k=6.0E+06
(13)	$O_2^- + Mn^{2+} + 2\ H_2O$	→	$Mn^{3+} + H_2O_2 + 2\ OH^-$	k=1.1E+08
(14)	$HO_2 + Mn^{3+}$	→	$Mn^{2+} + O_2 + H^+$	k=2.0E+04
(15)	$O_2^- + Mn^{3+}$	→	$Mn^{2+} + O_2$	k=1.5E+08
(16)	$H_2O_2 + Mn^{3+}$	→	$Mn^{2+} + HO_2 + H^+$	k=3.2E+04
(17)	$HO_2 + Fe^{3+}$	→	$Fe^{2+} + H^+ + O_2$	k=2.0E+04
(18)	$HO_2 + Fe(OH)^{2+}$	→	$Fe^{2+} + H^+ + O_2$	k=2.0E+04
(19)	$O_2^- + Fe^{3+}$	→	$Fe^{2+} + O_2$	k=1.5E+08
(20)	$O_2^- + Fe(OH)^{2+}$	→	$Fe^{2+} + O_2 + OH^-$	k=1.5E+08
(21)	$h\nu + Fe^{3+}\ (+H_2O)$	→	$Fe^{2+} + OH + H^+$	J=6.4E-07
(22)	$h\nu + Fe(OH)^{2+}$	→	$Fe^{2+} + OH + OH^-$	J=3.9E-04
(23)	$HO_2 + Fe^{2+}$	→	$Fe(OH)^{2+} + H_2O_2$	k=1.2E+06
(24)	$O_2^- + Fe^{2+}$	→	$Fe(OH)^{2+} + H_2O_2$	k=1.0E+07
(25)	$OH + Fe^{2+}$	→	$Fe(OH)^{2+}$	k=3.0E+08
(26)	$O3 + Fe^{2+}\ (+H_2O)$	→	$Fe(OH)^{2+} + OH + O_2$	k=1.7E+05
(27)	$Fe^{2+} + Mn^{3+}$	→	$Fe(OH)^{2+} + Mn^{2+} + H^+$	k=2.1E+04
(28)	$H_2O_2 + Fe(OH)^+$	→	$Fe(OH)^{2+} + OH + H_2O$	k=1.9E+06
(29)	$O_2 + Fe^{2+}\ (+H_2O)$	→	$Fe(OH)^{2+} + O_2^- + H^+$	k=7.9E-04
(30)	$Fe^{3+} + Cu^+$	→	$Fe^{2+} + Cu^{2+}$	k=1.0E+07
(31)	$Fe(OH)^{2+} + Cu^+$	→	$Fe^{2+} + Cu^{2+} + OH^-$	k=1.0E+07
(32)	$OH + Cu^+$	→	$Cu^{2+} + OH^-$	k=3.0E+08
(33)	$HO_2 + Cu^+\ (+H_2O)$	→	$Cu^{2+} + H_2O_2 + OH^-$	k=1.5E+09
(34)	$O_2^- + Cu^+$	→	$Cu^{2+} + H_2O_2$	k=1.0E+10
(35)	$H_2O_2 + Cu^+$	→	$Cu^{2+} + OH + OH^-$	k=4.0E+05
(36)	$Mn^{3+} + Cu^+$	→	$Cu^{2+} + Mn^{2+}$	k=2.1E+04
(37)	$HO_2 + Cu^{2+}$	→	$Cu^+ + O_2 + H+$	k=1.0E+08
(38)	$O_2^- + Cu^{2+}$	→	$Cu^+ + O_2$	k=5.0E+09

Il apparaît alors deux cycles catalytiques imbriqués:

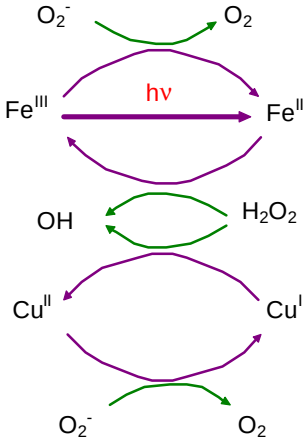

On mesure l'importance de ces cycles lorsque l'on simule par le calcul un scénario où on fait alterner des périodes sombres (LIGHT OFF) et claires (LIGHT ON). Le modèle utilisé est un modèle pas à pas explicite à pas variable que nous avons écrit pour l'occasion en visual basic. En sortie, nous avons les concentrations calculées en espèces réactives. La figure de gauche (a) montre une sortie sans participation des métaux et celle de droite une sortie avec participation des métaux (b).

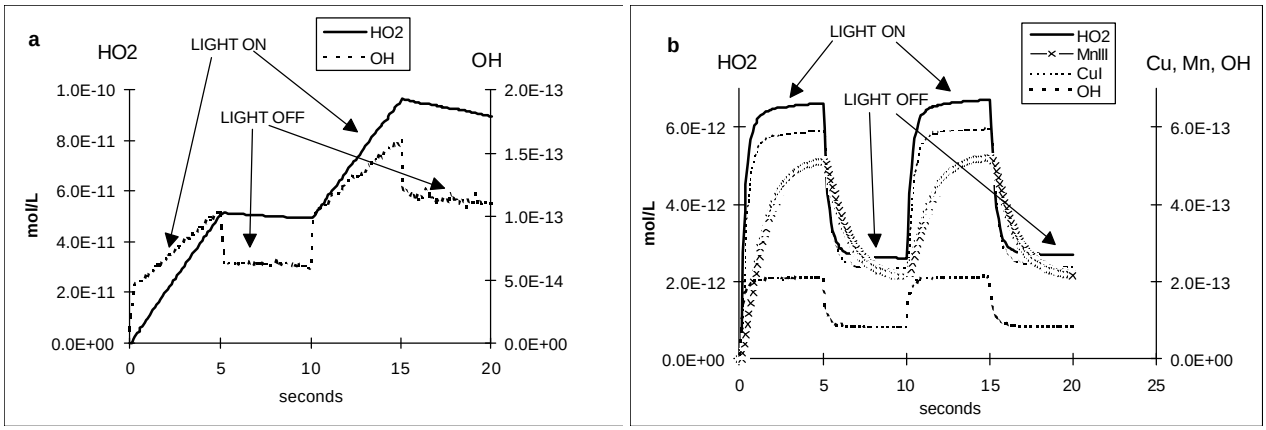

La principale conclusion que nous inspire ces figure est que le cycle catalytique évoqué plus haut provoque une relaxation très rapide du système, alors que en l'absence de ce cycle, notre système garde la mémoire de son histoire comme l'attestent des niveaux de radicaux HO_2 et OH qui dépendent du numéro du cycle, alors que dans le scénario b ils n'en dépendent pas. Sur la figure suivante, on peut suivre l'évolution à plus long terme (l'abscisse est en minutes) des concentrations des deux espèces de fer aux degrés d'oxydations II ou III:

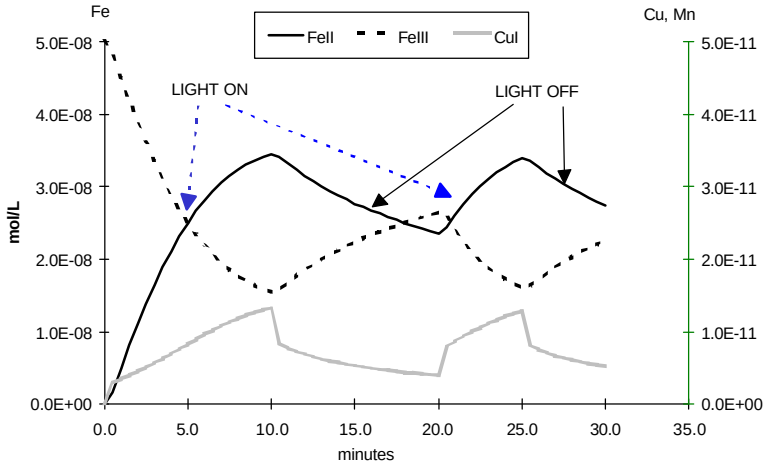

Contrairement au cuivre, on s'aperçoit que le temps de relaxation du fer entre les formes II et III est beaucoup plus long que pour le cuivre (I et II), alors que les concentrations des deux espèces du fer sont du même ordre de grandeur. Nous pouvons en tirer argument pour développer une technique analytique de séparation du fer II et du fer III. Le temps de relaxation est suffisamment long pour permettre une manipulation de l'échantillon en quelques minutes sans perte de l'information contenue dans l'échantillon.

Un dernier aspect concerne la sensibilité du système défini par rapport à l'ajout d'un réducteur, comme par exemple du méthanol, lui aussi produit de l'oxydation du méthane. On a aussi rajouté un oxydant, de l'ozone gazeux en équilibre avec la phase aqueuse. La figure suivante présente la variation de concentration en radicaux OH (mol.L^{-1}) au cours du temps.

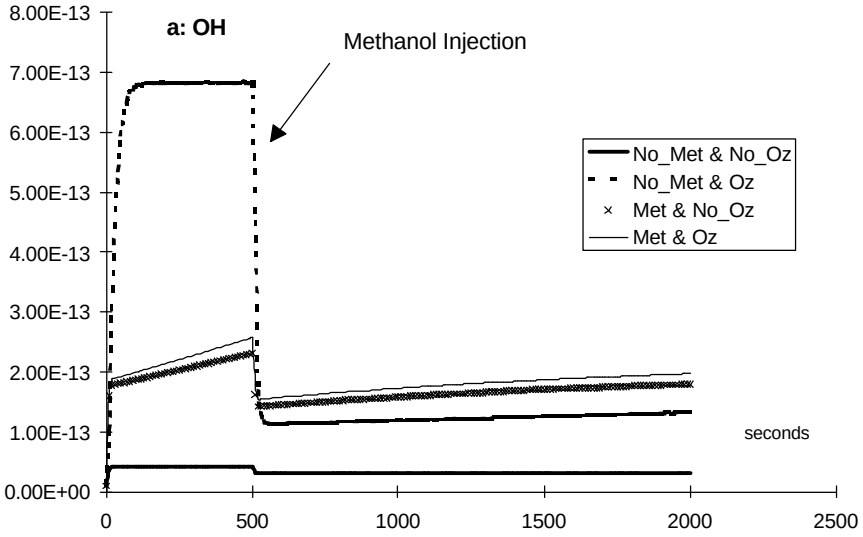

Dans le cadre de ce modèle, on peut tout d'abord observer avant l'ajout du méthanol, que le système sans métaux est très sensible à la présence d'ozone (No_Met & No_Oz, No_Met & Oz) alors que le système contenant des métaux l'est beaucoup moins. Dans le système sans métaux, la réaction (10) est une des réactions les plus rapides, alors qu'elle est plus beaucoup plus lente avec les métaux car les réactions avec les métaux sont très rapides, et que la concentrations en ion O_2^-, base conjuguée de HO_2, est plus faible. Lorsqu'on ajoute le méthanol, la concentration en radicaux OH s'effondre dans le cas où c'est l'ozone qui est le principal pourvoyeur d'OH (No Met & Oz), alors qu'elle ne varie pas beaucoup dans le cas où la concentration d'OH est gouvernée par le cycle catalytique des métaux (Met & Oz, Met & No_Oz).

3.2 La dissolution des métaux

Ce problème a été traité d'abord du point de vue thermodynamique, par exemple avec l'aluminium, dans la publication jointe en annexe: "Aluminium solubility in rainwater and molten snow". Toutes les données relatives à ces études ont été obtenues grâce à des expériences de collecte sur le terrain, afin d'obtenir la plus grande variété possible de situations différentes et réelles. Cependant, il nous est apparu que l'aspect thermodynamique n'était pas capable de rendre compte des processus de dissolution particulièrement pour les métaux de transition où leur implication dans des schémas réactionnels photo-oxydo-réducteur empêchent les équilibres de solubilité de s'établir. Comme il était difficile de suivre l'évolution d'un système sur le terrain, nous avons développé une stratégie d'expériences en laboratoire.

Nous avons mis en oeuvre un simulateur de goutte d'eau nuageuse en milieu hétérogène afin d'étudier des réactions photochimiques qui prennent place à l'intérieur des nuages (voir publications jointes: 'The pH-dependent dissolution of wind-transported Saharan dust" et "Factors influencing aerosol solubility during cloud process"). Ces réactions sont hétérogènes car elles font intervenir des transferts de matière entre les phases gazeuses et liquide et liquide et solide. Nous nous sommes focalisés sur l'aspect liquide-solide en pratiquant une étude de processus plutôt qu'une simple tentative de simulation de la goutte d'eau nuageuse. Pour cela, nous avons conçu un premier réacteur où, dans les échanges entre les phases solides et la phase aqueuse, seul la dissolution peut se produire. Il faut pour cela maintenir un déséquilibre constant au détriment de la formation de sels insolubles des métaux étudiés. Nous avons résolu œ problème en travaillant avec un réacteur en circuit ouvert où la solution altérante est constamment renouvelée. L'équation de fonctionnement d'un tel réacteur permet de relier la vitesse $\mathbf{v_{diss}}$ de la réaction de dissolution aux concentrations **C** en éléments dissous mesurées en sortie de réacteur, sachant que la solution altérante entrante est analytiquement exempte de cet élément. On obtient:

$$\mathbf{v_{diss} = D.C + V\ dC/dt}$$

où **V** est le volume du réacteur et **D** le débit de la solution altérante.

Les hydroxydes sont en général des minéraux précipitant d'autant plus facilement que le pH est moins acide. Afin de maintenir un déséquilibre de solubilité en faveur de la phase dissoute à des pH allant jusqu'à 6, il nous a été nécessaire de travailler à de très basses concentrations en métaux, de l'ordre de la nano mole par litre. Nous avons pu ici mettre à profit pour une cause purement chimique notre expertise acquise dans le maniement des solutions très diluées. Un deuxième réacteur a été fabriqué pour étudier l'influence de cycles d'évapo-condensation sur le comportement des métaux dans l'atmosphère. De tels cycles sont imposés à l'aérosol par les formations nuageuses qui transportent les masses d'air dans un mouvement vertical. Lorsque la masse d'air s'élève, elle se refroidit et l'eau se condense sur la particule. Lorsqu'au contraire elle descend, la température s'élève et l'eau s'évapore. Un tel cycle dure de quelques minutes à quelques heures suivant l'intensité de la turbulence convective. Nous avons simulé cette contrainte en mouillant notre aérosol puis en faisant s'évaporer l'eau par un courant d'azote chaud. Les deux figures suivantes sont des schémas des deux réacteurs décrits.

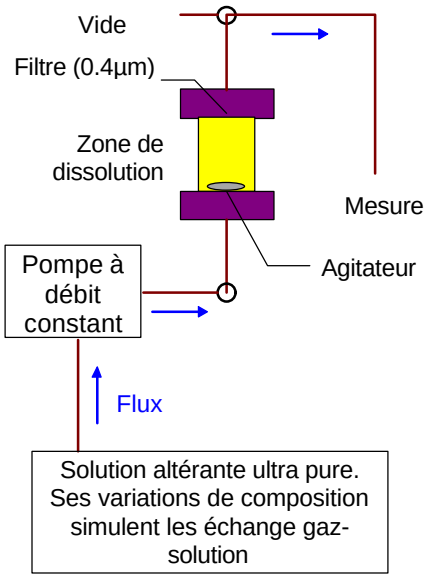

Schéma de la cellule de dissolution

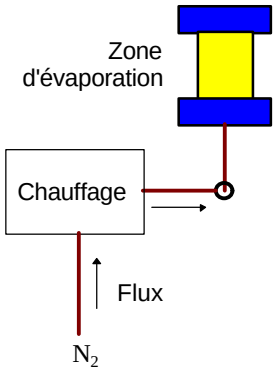

Schéma de la cellule d'évaporation

Les transferts de matière aux interfaces solides/liquide étaient bien compris lorsqu'on étudiait l'interaction d'écoulements d'eau sur ou dans le sol à l'échelle des temps géologiques, mais très mal documentés jusqu'alors aux échelles de temps qui nous intéressent, de l'ordre de l'heure. Nous avons commencé par détailler l'influence du pH et des cycles d'évapo-condensation en l'absence de lumière sur deux types de particules: des particules d'origine purement crustale (loess du Cap Vert) et des particules d'origine industrielle (centrale d'incinération d'ordures). Le comportement différent de ces deux aérosols s'explique d'une part par leur morphologie différente et d'autre part par leur pouvoir neutralisant de l'acidité, pouvoir qui est nul pour les cendres volantes et important pour les loess. La figure suivante montre un exemple des résultats acquis avec ce type d'expériences avec le comportement du manganèse. On peut y voir la variabilité du comportement du manganèse lorsqu'il est altéré, à pH 4.7, par une solution d'acide sulfurique diluée (ici, 10^{-5} M). Le temps, en min, est en abscisse alors que les ordonnées expriment la vitesse de dissolution du manganèse en pourcentage de sa masse totale pour 5 types de poussières: AD est "Arizona dust", poussières de désert américain, UP est "Urban Particles", poussières urbaine prélevées dans une ville américaine près de Détroit, FAP et FAV sont des cendres volantes collectées dans les dépoussiéreurs de centrales électriques au fuel, et Loess un loess récolté à l'île de Sal, au Cap Vert. Les deux premiers échantillons correspondent à des standards analytiques commerciaux.

La figure suivante illustre la sensibilité de la vitesse de dissolution aux variations de pH. Dans l'exemple suivant concernant le manganèse dans le loess, nous avons fait subir une brusque variation du pH de la solution altérante, le pH passant de 3 à 6 au bout de 100 min puis de 6 à 3 à 200 min.

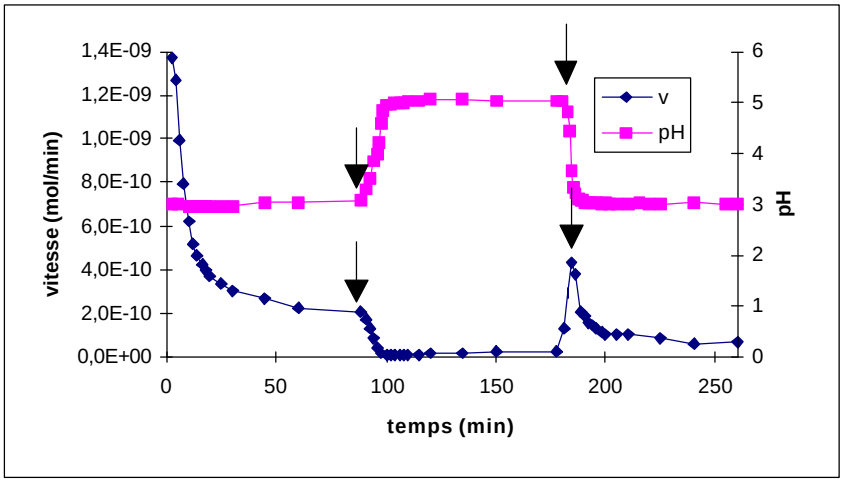

On peut observer que la vitesse de dissolution du manganèse est fortement corrélée à la variation de pH. Une autre simulation expérimentale a consisté à faire subir à un loess une série de cycles d'évapo-condensation. On voit nettement dans les deux figures suivantes l'influence du premier cycle pour la solubilité du calcium, alors que ces cycles sont moins importants dans le cadre de la solubilité du sodium.

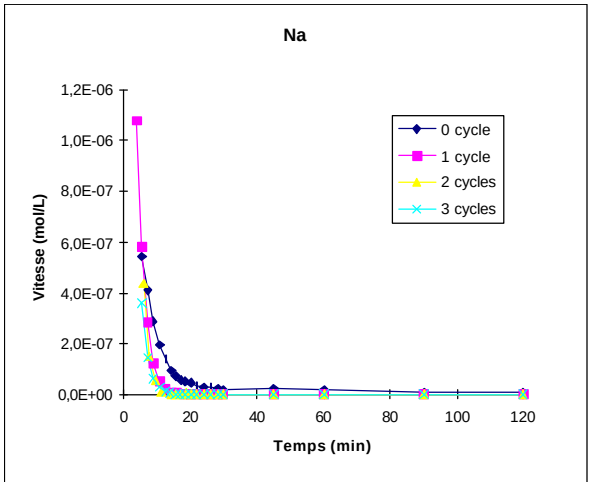

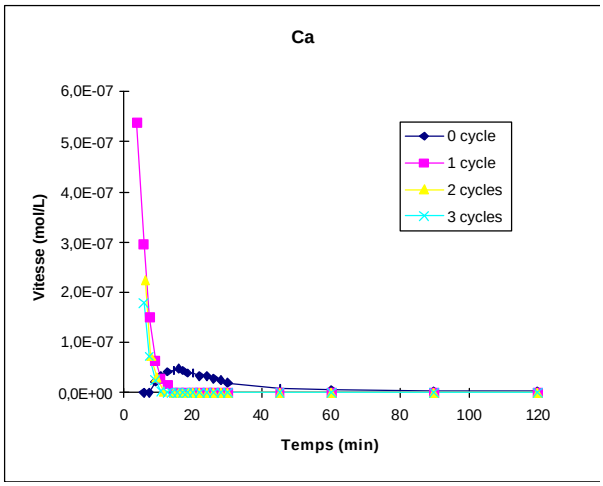

Nous avons pu aller plus loin dans notre description cinétique des réactions de dissolution de l'aérosol solide en proposant un modèle où l'aérosol solide est composé d'un mélange interne d'au moins 3 phases solides qui sont altérés successivement au cours du temps que dure nos expériences. Pour cela, nous avons établi un modèle où la cinétique d'altération de chaque phase est d'ordre 1. En portant une fonction du logarithme de la quantité dissoute en fonction du temps, nous voyons apparaître dans la figure suivante pour l'exemple du fer, 3 droites de pente distinctes correspondant à l'épuisement successif des 3 phases solides, respectivement au bout de 5, 15 min et à la fin de l'expérience. Le terme X/(X-S) en ordonnée correspond au rapport de la quantité totale de X solubilisable et de la différence entre la quantité totale X et la quantité S solubilisée au temps t. Cette quantité X correspond à la quantité totale de chaque phase solide, et a été calculée en portant le logarithme de la vitesse de dissolution en fonction du temps suivant l'équation:

$$\ln v = \ln(kX) - kt$$

où v est la vitesse de dissolution mesurée, X la quantité totale de la phase considérée et k la constante de vitesse de dissolution du premier ordre.
Les deux figurent suivantes illustrent ces calculs:

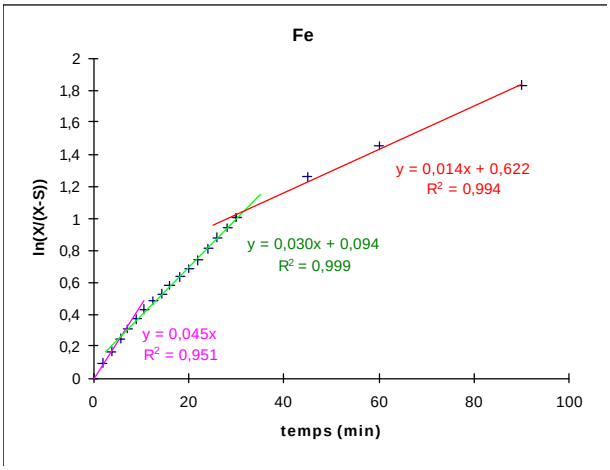

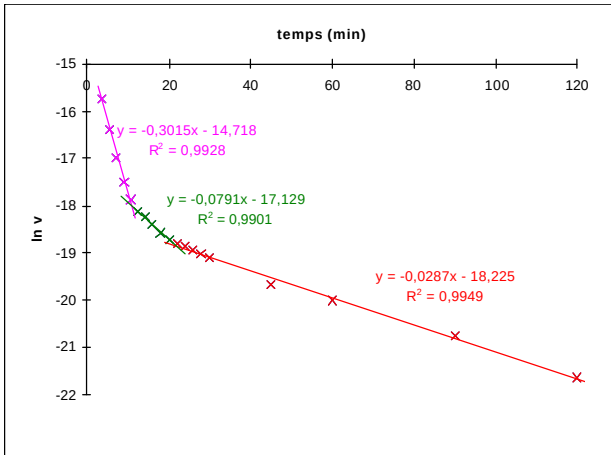

Nous avons ainsi pu proposer des valeurs de X pour plusieurs éléments chimiques dans le loess, en moles pour 20 mg de matière (d'après Desboeuf, thèse 2001):

Elément	X calculée respectivement pour les 3 étapes	Somme des X pour les 3 étapes	X mesuré après 2h de dissolution	quantité totale mesuré dans le loess
Al	$1,48\ 10^{-7}$ $1,87\ 10^{-7}$ $2,08\ 10^{-7}$	$5,43\ 10^{-7}$	$3,58\ 10^{-7}$	$6,22\ 10^{-5}$
Ba	$1,75\ 10^{-8}$ $1,27\ 10^{-8}$ $2,17\ 10^{-9}$	$3,23\ 10^{-8}$	$3,05\ 10^{-8}$	$3,35\ 10^{-7}$
Ca	$2,10\ 10^{-6}$ $7,67\ 10^{-7}$ $3,51\ 10^{-7}$	$3,21\ 10^{-6}$	$2,91\ 10^{-6}$	$1,89\ 10^{-5}$
Fe	$3,72\ 10^{-9}$ $9,04\ 10^{-9}$ $5,70\ 10^{-9}$	$1,84\ 10^{-8}$	$1,02\ 10^{-8}$	$2,72\ 10^{-5}$
K	$7,93\ 10^{-6}$ $1,51\ 10^{-6}$ $3,62\ 10^{-7}$	$9,80\ 10^{-6}$	$5,85\ 10^{-6}$	$6,65\ 10^{-6}$
Mg	$1,34\ 10^{-6}$ $4,60\ 10^{-7}$ $4,23\ 10^{-7}$	$2,22\ 10^{-6}$	$1,60\ 10^{-6}$	$2,30\ 10^{-5}$
Mn	$5,05\ 10^{-9}$ $5,18\ 10^{-9}$ $5,61\ 10^{-9}$	$1,58\ 10^{-8}$	$1,29\ 10^{-8}$	$4,73\ 10^{-7}$
Na	$1,21\ 10^{-5}$ $6,30\ 10^{-7}$ $3,21\ 10^{-7}$	$1,30\ 10^{-5}$	$1,02\ 10^{-5}$	$1,40\ 10^{-5}$
Si	$3,87\ 10^{-7}$ $4,20\ 10^{-7}$ $4,95\ 10^{-7}$	$1,30\ 10^{-6}$	$9,32\ 10^{-7}$	$1,62\ 10^{-4}$
Sr	$5,26\ 10^{-8}$ $1,73\ 10^{-8}$ $1,21\ 10^{-8}$	$8,2\ 10^{-8}$	$5,98\ 10^{-8}$	$7,30\ 10^{-7}$

Nous avons poursuivi ces travaux sur le pH par la mise en place d'une cellule de simulation nuageuse photochimique comportant de la matière solide en suspension. Cette cellule est voisine de

celle utilisé pour les expériences précédentes, mais elle possède une fenêtre en quartz par laquelle on amène de la lumière artificielle proche du spectre solaire grâce à une fibre optique. Dans cette cellule, nous étudions l'influence des propriétés RedOx du milieu ambiant sur le cycle de dissolution des aérosols, d'origine unique ou en mélange. On utilise le peroxyde d'hydrogène, dont les propriétés photochimiques sont fortement exaltées en présence de métaux de transition. Les premières études où seule l'influence des photon a été mesurée semblent montrer une action réelle sur les métaux de transition (Fe, Mn, Cu, etc...), mais aucune sur les métaux ne possédant qu'un seul degré d'oxydation en solution aqueuse (Mg^{2+}, K^{+}). On peut observer ce phénomène sur la figure suivante où on a porté en ordonnée les concentrations en Mg (insensible), Mn et Fe (métaux de transition sensibles) en fonction du temps. L'expérience commence dans le noir, puis on allume la lampe à t= 30 min. On observe alors une réaction sensible du fer et du manganèse à l'éclairement par une augmentation visible de leur concentration en sortie de cellule alors que le magnésium ne réagit pas. Lorsque l'on coupe l'éclairage, alors les concentrations redescendent à des niveaux très inférieurs, surtout pour le fer.

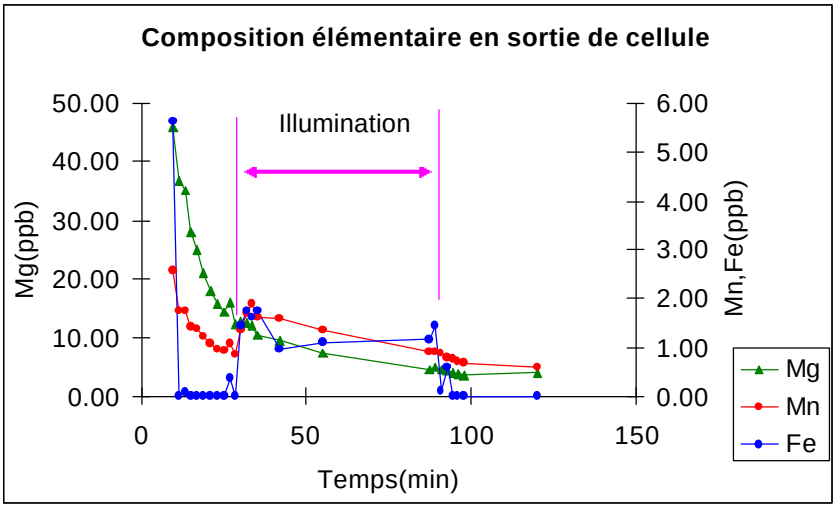

Ces résultats préliminaires demandent non seulement à être confirmés mais encore proprement quantifiés, et c'est une de nos priorités pour les années futures.

4 Le dépôt des métaux

4.1 Approche classique

La dernière phase de l'étude du du comportement des métaux dans l'atmosphère concerne leur sortie par dépôt. L'une des voies majeures de dépôt concerne les précipitations, de neige dans les zones froides et de pluie dans les zones plus tempérées ou chaudes. Ce dépôt a des conséquences au niveau de l'atmosphère lui-même car les quantités présentes à un moment donné dans l'air sont le résultat du bilan de l'émission et du dépôt. Le milieu récepteur est également sensible à ce transfert de matière en provenance de l'atmosphère. A ce niveau, les espèces solubles auront beaucoup plus d'impact que les espèces insolubles. On voit donc apparaître une autre application des études de solubilité de l'aérosol, application qui concerne un aspect biogéochimique de l'impact d'un apport de métaux sur un écosystème. Nos études portent d'une part sur l'apport de nutriments au milieu marin. Il s'agit là de métaux rares dans l'eau de mer car insolubles: fer, manganèse, mais aussi de non-métaux comme le phosphore ou l'arsenic. D'autre part, nous travaillons sur l'impact des métaux en milieu terrestre, essentiellement sous la forme de métaux lourds qui peuvent présenter une certaine toxicité comme le zinc, le cadmium, le plomb ou le mercure, mais aussi des non métaux comme l'arsenic. Cette dernière direction ainsi que celle décrite dans le paragraphe suivant sont très récentes

et n'ont pas encore donné lieu à la production de communications ni de publications scientifiques notables, hormis des rapports de contrat.

4.2 Les bio-capteurs

Dans ce milieu terrestre, il existe une grande variété d'espèces biologiques qui recouvrent les surfaces continentales. Parmi celles-ci, il s'en trouve qui n'ont de fort contact d'échange qu'avec l'atmosphère. Ces espèces sont donc à priori plus sensibles aux conditions atmosphériques qu'à la composition du sol sur lequel elles poussent. C'est une direction de recherche très récente qui s'intéresse aux variations de composition en métaux et non-métaux de mousses terrestres, afin d'en déduire dans un premier temps les variations de la composition de l'atmosphère avec lequel elles sont en contact, puis d'en tirer un bilan sur l'évolution de la pollution au point de collecte des mousses. De tels travaux sont déjà nombreux à être publiés, mais ils restent tous à un niveau qualitatif aussi bien sur la résolution temporelle des mesures que sur la valeur de la fonction de transfer entre la pollution atmosphérique et les teneurs mesurées dans les végétaux. Le succès d'une telle recherche permettra d'obtenir une mesure de l'extension géographique des zones polluées à n'importe quelle échelle puisqu'elle ne repose pas sur l'installation à priori d'un réseau d'instruments de mesure mais utilise une végétation naturelle.

Nous venons d'achever en novembre 2002 la phase d'analyse élémentaire d'une série de 530 prélèvements de mousse terrestre du programme "Mousses 2000" piloté par l'ADEME. Ce travail s'insère dans le programme français de mesure des retombées métalliques d'origine atmosphérique utilisant les mousses comme bio-accumulateurs de métaux, en association avec le Muséum Nationnal d'Histoire Naturelle. En pleine collaboration avec le Muséum, nous avons tout d'abord conseillé les équipes de collecte sur les moyens à mettre en œuvre pour prévenir toute contamination accidentelle des échantillons de mousse, puis suivi les étapes de conditionnement des végétaux jusqu'à leur broyage et séchage pour l'obtention d'une poudre homogène destinée à la minéralisation et l'analyse. Puis nous avons proposé et appliqué un protocole analytique permettant une analyse élémentaire validée sur une trentaine d'éléments. Outre les difficultés analytiques inhérentes à l'analyse multiélémentaire, nous avons du organiser une base de donnée permettant le traitement de l'ensemble des résultats (16000 mesures) sans erreur. Les figures suivantes montrent, pour le sodium, une indubitable influence marine de son dépôt, alors que le plomb est fortement lié à l'activité urbiane.

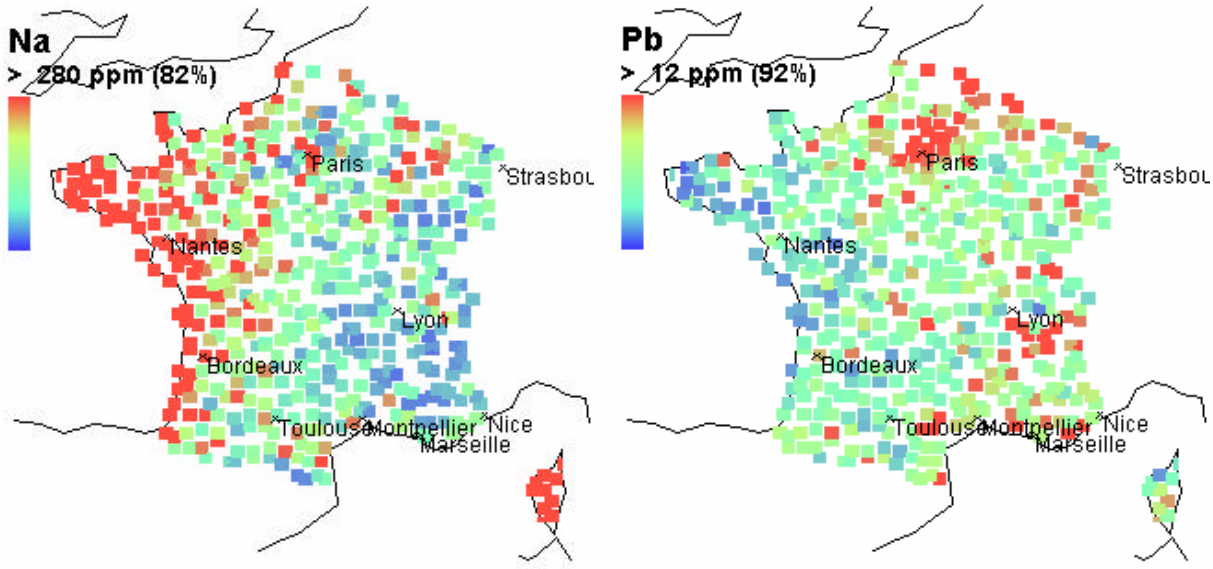

Concentrations en sodium et en plomb dans les échantillons de mousse.

La grande quantité d'éléments mesurées dans cette campagne (Li, Na, K, Rb, Be, Mg, Ca, Sr, Ba, Al, Ti, V, Cr, Mn, Fe, Co, Ni, Cu, Zn, Zr, Ag, Cd, Hg, Pb, Si, Ge, Sn, P, S, As, Sb) est en train de permettre l'interprétation du comportement des éléments chimiques en temps que groupe dans le tableau périodique, par exemple en comparant Mg, Ca, Sr et Ba, ou tout se groupe avec les éléments de transition, etc… Dans ce sens, une telle étude est susceptible d'apporter un type d'informations voisin des analyses isotopiques sur les sources et les cycles biogéochimiques. On peut ainsi espérer trouver une mesure quantitative de la dispersion géographique de la pollution.
La thèse de S. Leblond en cours d'achèvement permettra de relier la variabilité de concentration dans les mousses avec la variabilité du dépôt atmosphérique. Pour cela, nous procédons à une étude de suivi temporel dans une région rurale loin de toute source de pollution (Vouzon, Loir et Cher) afin de pouvoir comparer l'évolution de la retombée atlosphérique avec l'évolution de la concentration en métaux des mousses.

5 Conclusion et prospectives

La recherche que je mène au LISA s'inscrit dans l'étude chimique et géochimique de l'atmosphère, et particulièrement dans ses aspects décrivant l'interaction entre les aérosols solides et les phases aqueuse et gazeuse. Il s'agit ici de chimie et de physique multiphasique puisqu'elle fait intervenir des échanges de matière entre différentes phases: une phase gazeuse, une phase liquide (solution aqueuse) et de très nombreuses phases solides. Ces phases solides, que l'on dénomme aérosols solides, correspondent au minéraux et solides organiques très variés en suspension dans l'atmosphère sous la forme de très fines particules (entre 0.01 et 10 µm de diamètre). Je suis actuellement, au sein du laboratoire, le coordonateur d'une action thématique regroupant les aspects de terrain, de laboratoire et de modélisation de cette chimie multiphasique atmosphérique. Elle implique également des développements importants dans les techniques analytiques liées à la manipulation de traces et d'ultra-traces (de l'ordre de la nanomole par litre en solution, et de la dizaine de nanogramme pour des solides).
Les nuages, mélange d'eau de particules solides et de gaz, constituent les réacteurs chimiques et photochimiques les plus importants de la phase aqueuse atmosphérique. Cela m'amène à développer:

- des outils de modélisation photochimiques, thermodynamiques et cinétiques multiphasiques.
- des expériences de laboratoire pour la mesure de constantes photochimiques et cinétiques hétérogènes (solide-liquide).
- un préleveur aéroporté d'eau nuageuse capable de mesurer les métaux en traces.
- le prélèvement des minéraux atmosphériques en suspension (aérosols) ou en dépôt.

Les programmes en cours que je pilote ou auxquels je participe concernent d'une part la description chimique des interactions entre la surface des aérosols solides et l'eau liquide atmosphérique, et d'autre part l'application de ces recherches à l'impact de la retombée atmosphérique. Par exemple sur la retombée (Piren-Seine) et la biodisponibilité des métaux lourds en milieu continental (Programme Mousse 2000 de l'ADEME/Ministère de l'Environnement) ou sur le pouvoir altérant des pluies (Étude de l'altération du verre architectural financé par l'ADEME, action thématique CNRS-INSU: PNCA). Enfin, une dernière voie de recherche qui vient de se réactiver pour moi après plusieurs années de mise en someil, concerne les échanges entre l'atmosphère et la couche de surface des océans (PROOF). C'est l'exploration de cette direction qui m'a motivé pour accepter ma participation au comité scientifique de PROOF et ma responsabilité de représentant français du programme internationnal SOLAS. Elle me permettra de mettre au profit de la communauté des océanographes l'expérience que j'ai pu acquérir sur les transformations et les cycles des métaux et des non métaux dans l'atmosphère. La principale sortie de ces cycles atmosphérique concerne la solubilité et la biodisponibilité de ces éléments une fois transférés dans le milieu océanique.

Les mécanismes chimiques qui sont étudiés ici permettent de comprendre la manière avec laquelle de nouveaux minéraux ou matériaux organiques sont synthétisés au cours de l'évolution de l'aérosol dans l'atmosphère. Cette évolution dure en moyenne dix jours et s'accompagne d'épisodes de condensation d'eau liquide pendant laquelle l'activité chimique est à son maximum. Ces nouveaux minéraux et matériaux organiques possèdent des propriétés chimiques différentes des espèces présentes à la source d'émission des aérosols, ces derniers pouvant même être émis sous forme gazeuse. Nous sommes en train de démontrer que l'évolution de cet aérosol se fait toujours dans le sens d'une plus grande solubilité dans l'eau et d'on d'un plus grand caractère hydrophile des nouvelles espèces créées en surface (Desboeufs et al., 2001). Cette solubilité supérieure peut rendre mobile des métaux lourds toxiques ou bien encore d'autres éléments nutients (P, Fe, Mn…) emprisonnés à l'origine dans une matrice silicatée. Il s'agit directement d'un effet d'augmentation de la biodisponibilité.
Pour les éléments majeurs, cette augmentation de la solubilité va s'accompagner d'une augmentation de l'hygroscopicité des aérosols solides. Celle-ci va favoriser la condensation de vapeur d'eau sur ces particules et donc modifier le spectre des gouttes d'un nuage et par conséquent son bilan radiatif. On voit ici comment la chimie multiphasique atmosphérique permet d'apporter des éléments de réponse à une demande sociale forte concernant la toxicité des retombées atmosphériques (métaux lourds) et l'effet de serre (bilan radiatif).

Les travaux que je souhaite continuer à mener dans le cadre de mon activité de recherche s'inscrivent dans la continuité des projets qui ont été présentés dans mon mémoire. Il y a tout d'abord deux axes concernant une étude de processus couplés qui sont l'altération de la surface de l'aérosol et l'impact de la dissolution de l'aérosol sur le pouvoir oxydant de l'atmosphère:

Le premier concerne l'exploration des propriétés de surface des aérosols via la mesure en laboratoire des interactions entre l'aérosol solide et l'eau dans des conditions aussi proches que possible de conditions nuageuses réelles, tout en restant parfaitement contrôlées. Ce travail a été proposé avec succès pour l'appel d'offre 2002 du CNRS dans le cadre du Pnca. Une première étude, qui a permis la rédaction d'une thèse de doctorat (K. Desboeufs) et de 2 publications parues, a permis de documenter l'influence du pH sur les vitesses d'interactions entre les phases aqueuse et particulaires. Nous proposons maintenant de compléter ceci en y ajoutant l'aspect photochimique qui inclut la participation de réactions d'oxydo-réduction aux processus de dissolution. J'ai pu faire effectuer un travail préliminaire dans le cadre de deux DEA (Kui, 2001, Velay, 2002) où il a été clairement montré que l'irradiation d'un système hétérogène aérosol-solution aqueuse perturbait sensiblement et sélectivement la dissolution des métaux de transition. Ce comportement est cohérent avec la sensibilité bien connue des métaux de transition à des variations du pouvoir oxydo-réducteur de la solution avec laquelle ils sont en contact.
Nous disposons, pour ces expériences, d'un réacteur de simulation photochimique. Ce réacteur, utilisable en phase mixte gaz/particule ou eau/particule est constitué d'une enceinte en Téflon de 50 mL irradiée à l'aide d'une lampe à spectre quasi-solaire, par l'intermédiaire d'une fibre optique. Ce réacteur peut fonctionner suivant deux modes: mode fermé ou mode ouvert (à écoulement). Dans le mode fermé, on isole le réacteur du milieu extérieur, on procède à l'expérience et on analyse les produits de réaction à la fin. Dans le mode ouvert, le réacteur est constamment balayé par un flux de fluide (gaz ou liquide), ce qui permet d'une part une analyse continue de la composition du fluide sortant et d'autre part de mettre en place des conditions stationnaire pour cette composition. Nous nous proposons donc de mesurer l'évolution de l'interaction de la surface de l'aérosol avec la phase aqueuse lorsque l'ensemble de ce système est soumis à une irradiation équivalente à celle reçue par un nuage. Nous mènerons les expériences suivantes:

1. Évaluation de l'influence de la lumière sur la solubilisation d'un aérosol minéral modèle sans que soit introduit d'espèces solubles photo réactives.
2. Évaluation de l'influence de la lumière sur la solubilisation d'un aérosol minéral en présence d'espèces solubles photo réactives
3. Évaluation de l'influence de la lumière sur un cycle d'évapo-condensation.

Les données récoltées au cours de ces manipulations devraient nous permettre de quantifier l'impact du flux lumineux sur les modifications des propriétés d'interaction entre la surface de l'aérosol et l'eau. En particulier, nous pourrons distinguer les processus où les photons sont utilisés via des espèces dissoutes, et ce sont alors les photo-radicaux qui agissent, des processus où les photons sont directement utilisés par les métaux présents à la surface du solide. Une innovation majeure apportée dans cette étude sera des mesures de spéciation rédox du fer (fer^{II} et fer^{III}). Ces mesures, aussi importante pour la chimie minérale que le sont les quantifications des groupes fonctionnels en chimie organique nous permettrons d'accéder à l'évolution de la capacité oxydante de l'aérosol.

Le deuxième axe concerne l'impact de la chimie hétérogène solide-dissous sur les propriétés oxydantes de l'atmosphère. C'est un des thèmes principaux développé dans le projet "INCHAAC" annexé en fin du mémoire, et dont j'ai assuré la conception et la coordination et qui décrit à mon sens parfaitement ce qu'il convient de faire. Cette étude s'appuie bien évidemment sur les progrès réalisés grâce à l'axe précédent, mais aussi sur des mesures de terrain et de la modélisation. Bien que le financement de tout ce travail n'ait pas été acquis, c'est une direction que nous souhaitons continuer à explorer. Les métaux de transition jouent un rôle majeur dans les mécanismes d'oxydo-réduction actifs dans les nuages, rôle qui dépend quantitativement de la quantité de métal dissout disponible. Le but de cette recherche est de quantifier ce rôle de manière précise, c'est-à-dire de calculer les quantités de métaux présents à tout instant dans la goutte de nuage pour pouvoir l'utiliser dans des modèles de chimie atmosphérique. Actuellement, ces modèles ne prennent, dans le meilleur des cas, qu'une estimation exprimée en pourcentage d'élément dissout; c'est évidemment très insuffisant lorsqu'on observe la sensibilité du système chimique aqueux à la concentration de métaux de transition dissout (Losno, 1999). Compte tenu de la complexité du système chimique qui opère dans un nuage, seules des mesures sur le terrain seront capables de valider les concepts et les équations exprimées dans ce travail de modélisation chimique. Nous disposons pour cela d'un collecteur d'eau nuageuses aéroporté spécialement conçu pour permettre un prélèvement de nuage sans contamination. Bien évidemment, c'est par le biais de collaborations avec des équipes spécialisés dans les modèles chimiques, microphysiques et de transport que nous pourrons parvenir au terme de ce projet.

Un troisième axe est en train de se dévelloper et concerne le dépôt atmosphérique dans une dimension continentale en mesurant la dispersion spatiale de la pollution grâce aux bio-capteurs ou en mesurant la qualité du dépôt atmosphérique en terme de biodisponibilité. Les mousses et les lichens présentent l'avantage d'avoir le maximum d'échange avec l'atmosphère, par rapport à d'autres végétaux qui échangent beaucoup avec le sol sur lequel ils poussent. L'analyse des variations de la composition élémentaire de ces espèces donne donc l'espoir de pouvoir remonter aux variations de la pollution atmosphérique en métaux dans l'ambiance de ces végétaux. On pourra ainsi, grâce à l'utilisation des métaux comme traceurs de source, établir des cartes de dispersion de la pollution, voire même de les séparer en cartes de pollution automobile, sidérurgique, par incinérateur d'ordures ménagères, etc… Nous sommes fortement impliqués, à titre exploratoire, dans un tel programme qui est actuellement soutenu par l'ADEME. Ce programme consiste dans un premier temps à mesurer une dispersion géographique de la contamination des mousses terrestres en métaux lourds, au niveau de la France, et de le comparer au niveau Européen. Parallèlement, nous avons choisi un site

particulièrement homogène dans le centre de la France pour faire une étude de la fonction de transfert entre l'atmosphère et les mousses.

Tous les acquis des axes couplés 1 et 2 permettront enfin de comprendre et de prévoir quelle est la part du dépôt atmosphérique dans l'apport de nutrients au milieu océanique. En effet, la mesure des retombées atmosphériques globales ne suffit pas à quantifier cet apport car seule la partie soluble ou solubilisable de la matière particulaire qui tombe dans l'océan est susceptible de pénétrer l'écologie du système récepteur. Or, il se trouve que c'est au cours de son transport atmosphérique que l'aérosol, porteur des nutrients, subit le plus de changements quant à sa composition minéralogique, essentiellement au cours de cycles d'évapo-condensation dans des nuages. Ces changements vont toujours dans le sens d'une augmentation de cette solubilité (Desboeufs et al., 2001). C'est au cours de mesures de retombées ou de composition atmosphérique dans différents milieux océaniques (Océan Indien, Pacifique Sud, Méditerranée) que nous pourrons quantifier l'évolution de la biodisponibilité des minéraux en les couplant à nos études de processus en laboratoire.

6 Bibliographie hors celle personnelle décrite au §7.2.1

Alfaro, S.C., A. Gaudichet, L. Gomes and M. Maille, (1997), **Modeling the size distribution of a soil-aerosol produced by sandblasting**. *J. Geophys. Res.*, **102**, 11239-11249.

Audiffren N., N. Chaumerliac, and Renard, M. (1996), **Effects of a polydisperse cloud on tropospheric chemistry.**, *J. Geophys. Res.*, **101,** 25949-25966.

Blanchard D.C. (1983), **The production, distribution and bacterial enrichment of the sea salt aerosol**, NATO: Asi serie C N°108, Air-Sea exchange of gases and particles, P.S. Liss and W.G.N. Slinn ed, 108, 407-454.

Chiapello, I., P. Goloub, D. Tanré, J. Herman, O. Torres, and A. Marchand, (2000) **Aerosol detection by TOMS and POLDER over oceanic regions**, *J. Geophys. Res*, 105, 7133-714

Colls J. (1997), **Air Pollution**, ISBN 0-419-20650-7, E & FN Spon Londres, 341.

Claquin, T., M. Schulz, Y. Balkanski, and O. Boucher, (1998) **Uncertainties in modelling radiative forcing by mineral dust**, *Tellus*, 50B, 491–505.

Colin, J.L., Jaffrezo, J.L. and Gros, J.M. (1990) Solubility of major species in precipitation : factors of variation. *Atmos. Environ*., **24A**, 537-544.

Dentener, F., Carmichael, G., Zhang, Y., Crutsen, P. and Lelifeld, J. (1996) **The role of mineral aerosols as a reactive surface in the global troposphere**, *J. Geophys Res*., **101 D17**, 22869-22890.

Donard, O.F.X. and J.H. Weber (1988), **Volatilization of tin as stannane in anoxic environments**. Nature, 339-341.

Flossmann A.I., (1998a), **Clouds and Pollution**. *Pure & Appl. Chem.*, **70**, 1345-1352.

Flossmann A.I., (1998b), **Interaction of aerosol particles and clouds**. *J. Atmos. Sci.*, **55**, 879-887.

Flossmann A.I., (1998c), **Richard Goody : Principles of atmospheric physics and chemistry**. *J. Atmos. Chem*, **30**, 314-317.

Gillette, D.A., I.H. Blifford Jr. and D.W. Fryrear, (1974), **The influence of wind velocity on size distribution of aerosols generated by wind erosion on soils.** *J. Geophys. Res.*, **79**, 4068-4075.

Gomes, L., G. Bergametti, G. Coudé-Gaussen and P. Rognon, (1990), **Submicron desert dusts : a sandblasting process.** *J. Geophys. Res.*, **95**, 13 927-13 935.

Götz, G., Meszaros & Vali, **Atmospheric particles and nucleï** , *Akademia Kiado, Budapest*, 1991.

Graedel T.E., Weschler C.J and Mandich M.L. (1985), **Influence of Transition Metal Complexes on Atmospheric Droplet Acidity.** *Nature* **317,** 240-242.

Graedel T.E., Mandich M.L. and Weschler C.J. (1986), **Kinetic Model Studies of Atmospheric Droplet Chemistry: 2. Homogeneous Transition Metal Chemistry in Raindrops**, *J. Geophys. Res.*, **91 D4**, 5205-5221.

Kölher, H. (1921), *Meteor. Z.*, ***38***, 168.

Jacob D.J., Gottlieb E.W. and Prather M.J. (1989), **Chemistry of a Polluted Cloudy Boundary Layer**, *J. Geophys. Res.*, **94 D10**, 12975-13002.

Kaufman Y.J., Tanré D., Gordon H.R., Nakajima T., Lenoble J., Frouin R., Grassl H., Herman B.M., King M., Teillet P.M. (1997), **Passive Remote Sensing of Tropospheric Aerosol and Atmospheric correction for the Aerosols Effects**, *J. Geophys. Res.*, 102, 16815-16830.

Lameyre J. (1986), **Roches et Minéraux**, ISBN 2-7040-0499-4, Doin Paris, 350 pp.

Lelieveld J. and Crutzen P.J. (1991), **The role of Clouds in Tropospheric Photochemistry**, *J. Atmos. Chem.*, **12**, 229-267.

Pradelle F., G. Cautenet and I. Jankowiak, (2002a) **Radiative and microphysical interactions between marine stratocumulus clouds and Saharan dust. Part 1: Remote sensing observations**. *J.Geophys.Res.*, sous presse.

Pradelle, F. and G. Cautenet, (2002b) **Radiative and microphysical interactions between marine stratocumulus**

clouds and Saharan dust. Part 2: modeling. *J.Geophys.Res.*, sous presse.

Spokes, L. J., Jickells, T.D. and Lim, B. (1994) **Solubilisation of aerosol trace metals by cloud processing : a laboratory study.** *Geochem. Cosmochim. Acta*, **58**, 3281-3287.

Spokes, L.J. and Jickells, T.D. (1996) **Factors controlling the dissolved-particulate distribution of aerosol trace metals in the atmosphere and on mixing to seawater.** *Aquatic Geochemistry*, **1**, 355-374.

Svenningsson, B., Hansson, H.C., Wiedensohler, A., Noone, K., Ogren, J., Hallberg, A. & Colvile, R. (1994), **Hygroscopic growth of aerosol particles and its influence on nucleation scavenging in cloud: Experimental results from Kleiner Feldberg.**, *J. Atmos. Chem.*, ***19***, 129-152.

Turekian K.K. (1971), **Geochemical distribution of the elements**, *Encyclopedia of Sciences and Tecnologie*, vol 4., Mc Graw Hill ed.

Walcek C. J., Yuan H.H., and Stockwell W.R. (1997) **The influence of aqueous-phase chemical reactions on ozone formation in polluted and nonpolluted clouds**, *Atmos. Environ.*, **31**, 1221-1237.

Weisel C.P., Duce R.A., Fasching J.L. et Heaton R.W. (1984), **Estimates of the transport of trace metals from the ocean to the atmosphere**., *J. Geophys. Res*., **89 n°D7**, 11607-11618.

7 Annexes: Curriculum Vitae incluant les titres et travaux publiés

Rémi LOSNO, 40 ans, (décembre 1961)

Adresse professionnelle enseignement: UFR de Sciences, Bâtiment Lavoisier, Université de Marne-la-vallée, 5 Bd Descartes, Champs sur Marne, 77454 MARNE LA VALLEE CEDEX 2
Adresse professionnelle recherche: LISA, Université Paris 7 Paris 12, Faculté des Sciences, 61 avenue du général de Gaulle, 94010 Créteil CEDEX.

N° de téléphone: (33) 1 45 17 15 98
Adresse e-mail: losno@lisa.univ-paris12.fr
Adresse Web: http://www.lisa.univ-paris12.fr

Fonctions: Maître de Conférence en Chimie à l'Université de Marne la Vallée, chercheur au LISA en Chimie de l'atmosphère.

7.1 Titres et diplomes:

- Ancien élève de l'École Normale Supérieure de Saint-Cloud (1981-1985).
- Agrégation de Chimie en juillet 1984.
- D.E.A. : Chimie de la pollution, physique, énergétique et chimie de l'atmosphère.
- **Analyse par fluorescence X en couche mince des aérosols atmosphériques : détermination expérimentale des conditions optimales de validité.** Laboratoire de Physico-Chimie de l'Atmosphère, Université PARIS 7, 1985.
- Thèse de Doctorat en Sciences à l'Université PARIS 7:
- **Chimie d'éléments minéraux en trace dans les pluies méditerranéennes**, soutenue le 24 mai 1989 à l'Université PARIS 7. Le jury était composé de MM.: Pr. G. Mouvier (Président et directeur de la thèse, Univeristé Paris 7), G. Bergametti (Rapporteur, CNRS), P. Buat-Ménard (Rapporteur, CNRS), Pr. B. BIGOT (Examinateur, Professeur à l'École Normale Supérieure de Lyon), R. Delmas (Examinateur, CNRS), Pr. T.D. Jickells (Examinateur, Professeur à l'Université d'East-Anglia, UK).

7.2 Publications scientifiques:

7.2.1 Publications à comité de lecture de rang international

Losno R., G. Bergametti and G. Mouvier; **Determination of optima conditions for atmospheric aerosols analyses by X-Ray fluorescence.**, *Envir. Tech. Letters*, **8**, 77-87, 1987.

Losno R., Bergametti G. and Buat-Ménard P.; **Zinc partitioning in Mediterranean rainwater**, *Geophys. Res. Lett.*, **15**, 1389-1392, 1988.

Bergametti G., Dutot A.L., Buat-Ménard P., Losno R. and Remoudaki E.; **Seasonal variability of the elemental composition of atmospheric aerosol particles over the Northwestern Mediterranean.**, *Tellus*, **41B**, 353-351, 1989.

Losno R., Bergametti G., Carlier P. et Mouvier G.; **Major ions in marine rainwater with attention to sources of alkaline and acidic species.**, *Atmos. Environ.* 25A, 763-770, 1991.

Tedesco D., Toutain J.P., Allard P. and Losno R.; **Chemical variations in fumarolic gases at Vulcano Island (Southern Italy): seasonal and volcanic effects.**, *J. of Volcanology and Geothermal Res.*, 45, 325-334, 1991.

Remoudaki E., Bergametti G. and Losno R.; **On the dynamic of the atmospheric input of copper and manganese into the Western Mediterranean Sea.**, *Atmos. Environ.* 25A, 733-744, 1991.

Losno R., Bergametti G. et Carlier P.; **Origin of the atmospheric particulate matter over the North-Sea and the Atlantic Ocean.** *J. of Atmos. Chem.*, 15, 333-352, 1992.

Bergametti G., Remoudaki E., Losno R., Steiner E., Chatenet B. et Buat- Ménard P.; **Source, transport and deposition of atmospheric phosphorus over the Northwestern Mediterranean.** *J. of Atmos. Chem.*, 14, 501-513, 1992.

Losno R., Colin J.L., Le Bris N., Bergametti G., Jickells T. et Lim B.; **Aluminium solubility in rainwater and molten snow.** *J. of Atmos. Chem.*, 17, 29-43, 1993.

B. Lim, R. Losno, T.D. Jickells and J.L. Colin; **The solubilities of aluminium, lead, copper and zinc in rain samples in the marine environment over the North Atlantic Ocean and the Mediteranean Sea.** , *Global Biogeochemical Cycles*, 8, 349-362, 1994.

Quisefit J.P., Garivait S., Losno R. and Steiner E.; **X-Ray fluorescence spectrometry to characterise the chemical composition of ashes produced by the burning of savannah grasses.**, *The Nucleus.*, **32**, 135-142, 1995.

François F., W. Maenhaut, J.L. Colin, R. Losno, M. Schulz, T. Haster, L. Spokes and T. Jickells; **Intercomparison of elemental concentrations in total and size-fractionated aerosol samples collected during the Mace Head experiment, April 1991**. *Atmos. Environ.*, 27, 837-849, 1995.

Losno R., Colin J.L., Spokes L., Jickells T., Schulz M., Reberts A., Leermakers M., Meulemann C. and Bayens W.; **Non-rain deposition significantly modifies rain samples at a coastal site.** *Atmos. Environ.*, **32**, 3445-3455, 1998.

Losno R.; **Trace Metals Acting as Catalysts in a Marine Cloud: a Box Model Study**. *Phys. Chem. Earth* (B), **24** N°3, 286-286, 1999.

Desboeufs K., Losno R., Vimeux F. and Cholbi S., **pH dependent dissolution of wind transported Saharan dust**, *J. GeoPhys. Res.*, 21287-21299, 1999.

Monna.F, Loizeau J.L., Thomas B., Guégen C., Favarger P.Y., Losno R. and Dominik J., **Noise identification and sampling frequency determination for precise Pb isotopic measurements by quadrupole-based Inductively Coupled Plasma Mass Spectrometry**, *Analusis*, 28, 750-757, 2000.

Marion T., P.E. Perros, R. Losno, E. Steiner, **Ozone production efficiency in savanna and forest areas during EXPRESSO experiment**, *Journal of Atmospheric Chemistry*, 38, n°1, 3-30, 2001.

Desboeufs K.V., Losno, R. and Colin J.L., **Factors influencing aerosol solubility during cloud processes**, *Atmos. Environ.*, **35**, 3529-3537, 2001

7.2.2 Autres publications et actes de congres

Masclet P., P. Pistikopoulos, G. Bergametti, G. Mouvier and R. Losno; **Determination by PAH analysis of the age of air mass contamination in area remote from sources of pollution.** in *Physicochemical behaviour of atmospheric pollutants,* D.Reidel publishing company, pp 588-595, 1986.

Bergametti G., Buat-Ménard P., Chatenet B., Dutot A.L., Losno R. et Remoudaki E.; **Atmospheric transport and deposition of trace elements to the Western Mediterranean Sea**, in *"Airbone Pollution of the Mediterranean Sea", Report and proceeding of a WMO-UNEP workshop*, 141-149, Map technical series N°31, UNEP, Athène 1989.

Losno R., Carlier P., Remoudaki E. et Bergametti G.; **Concentration and sources of trace elements over the Atlantic Ocean.** in *Physico-Chemical Behaviour of Atmospheric Pollutants, Restelli and Angeletti eds., Kluwer Academic Publishers, Dordrecht*, 711- 716, 1990.

Remoudaki E., Bergametti G., Losno R., Chatenet B. et Mouvier G.; **Temporal variability of atmospheric Pb, Cu and Mn concentrations and fluxes over the Western Mediterranean Sea.** in *Physico-Chemical Behaviour of Atmospheric Pollutants, Restelli and Angeletti eds., Kluwer Academic Publishers, Dordrecht*, 141-169, 1990.

Marticorena B., A. Youssfi, R. Losno and G. Mouvier; **Wavelet transform of atmospheric particulate matter concentration.** Proceedings of Geophysics and Environment: Background air pollution, *Bolletino Geofisico, XV, N°5*, 107-120, 1992.

Schulz M., Dannecker W., Church T., Colin J.L., Haster T., Leermakers M., Losno R., Meulemann C., and Spokes L.; **Intercomparison of rain sampling at Mace Head/Ireland.** *Annales Geophysicae,* Suppl. II to Vol 10, 1992.

Kanakidou M., Poisson N., Lattuati M., Aumont B., Beekmann M., Bey I., Behra P., Chaumerliac N., Grégoire P., Hauglustaine D., Huret N., Losno R., Maalez A., Martin D., Martinerie P., Mercier P., Pham M., Pirre M., Ramaroson R. et K. Suhre, **Comparaison entre 11 modèles utilisés en France pour la description de la chimie troposphérique**, *Atelier de Modélisation de l'Atmosphère*, Toulouse, 283-283, volume II, 28-30 novembre 1995.

Losno R. et P. Behra, **Influence des métaux de transition sur la composition chimique des nuages**, *Atelier de Modélisation de l'Atmosphère*, Toulouse, 407-407, volume II, 28-30 novembre 1995.

R. Losno, **Modification du préleveur d'eau nuageuse "NUAC" pour l'étude des traces**, *Atelier "Expérimentation et instrumentation"*, Toulouse, 15-17 octobre 1996.

Desboeufs K. and R. Losno, **The Influence of trace metals leaching from mineral atmospheric aerosols an atmospheric photochemistry**, *proceedings of the second Workshop of the EUROTRAC-2 Subproject CMD, APP 2*, Karlsruhe, 23-25 september 1998.

Losno R. and K. Desboeufs, **Modelling trace metals acting as catalysts in clouds: Multiphase chemistry in non polluted aerea**, *proceedings of the second Workshop of the EUROTRAC-2 Subproject CMD, APP 8*, Karlsruhe, 23-25 september 1998.

K.V. Desboeufs, R. Losno and J.L. Colin, **Atmospheric particle dissolution process in the cloud droplets**, J. Aerosol Sci., 32 supplement 1, S273-S274, 2001.

K.V desboeufs, R. Losno and J.L. Colin, **Mechanisms of physicochemical modifications of Saharan Aerosol during cloud process,** *Proceedings in: Physico-Chemical Behaviour of atmospheric pollutants,* 17-20 septembre 2001, Torino. Electronic publication (CD-ROM).

R. Losno, K.V. Desboeufs, J. Kui and J.L. Colin, **Influence of simulated sun irradiation on aerosol dissolution rate**, *Proceedings in: Physico-Chemical Behaviour of atmospheric pollutants*, 17-20 septembre 2001, Torino. Electronic publication (CD-ROM).

A. Sofikitis, J.L. Colin, S. Costes and R. Losno, **Analytical method for speciation of iron in rainwater**, *Proceedings in: Physico-Chemical Behaviour of atmospheric pollutants,* 17-20 septembre 2001, Torino. Electronic publication (CD-ROM).

Alexandra Sofikitis, Jean Louis Colin, Karine Desboeufs and Rémi Losno, **Iron dissolution rate in various minerals**. *EUROTRAC-2 symposium*, Garmisch-Partenkirschen, march 2002, *Proceedings* CD-ROM.

Karine Desboeufs, Rémi Losno, and Jean-Louis Colin, **Aerosol Alkalinity depends on pH**. *EUROTRAC-2 symposium*, Garmisch-Partenkirschen, march 2002. *Proceedings* CD-ROM.

7.2.3 Communications à des congrès internationaux

Losno R., G. Bergametti and P. Buat-Ménard, **The solubility of zinc, lead and manganese in Western Mediterranean rain water.**, *International Conference on Global and Regional Environmental Atmospheric Chemistry*, Pekin, 3-10 mai 1989.

Remoudaki E., R. Losno, G. Bergametti and P. Buat-Ménard, **Source, transport and deposition of lead in the Mediterranean atmosphere.** *International conference on Aerosols and Background Pollution*, Galway, juin 1989.

Losno R., P. Carlier and G. Bergametti, **Concentration Profiles of trace elements over the North Sea and the Atlantic Ocean: Anthropogenic and Natural Contribution.** *International conference on Aerosols and Background Pollution*, Galway, juin 1989.

R. Losno, G. Bergametti, P. Carlier and G. Mouvier, **Ionic Balances in marine rainwater with a special emphasis on sources of alkaline and acidic species**, *International Conference on Aerosols and Background pollution*, Galway, 13-15 juin 1989 (Poster).

R. Losno, P. Carlier, E. Remoudaki and G. Bergametti, **Concentration and sources of trace elements over the atlantic ocean**, *International Conference on Aerosols and Background pollution*, Galway, 13-15 juin 1989 (Poster).

Losno R., G. Bergametti, J.L. Colin and P. Buat-Ménard; **Partitioning of trace metals in Mediterranean rainwater**, *Eurotrac/ASE Meeting*, Bordeaux, 23-25 novembre 1989.

Jickells T.D., B. Lim, X. Zhu, J. Prospero, R. Losno and G. Bergametti, **Particulate and dissolved trace metal distribution in North Atlantic Precipitations**, *AGU Fall Meeting*, San Francisco, 4-8 décembre 1989.

Bergametti G., E. Remoudaki, R. Losno, E. Steiner and P. Buat-Ménard, **Source, transport and deposition of atmospheric particulate phosphorus over the Western Mediterranean sea.** *VII CACGP Symposium on Chemistry of the Global Atmosphere*, Champrousse, 5-11 septembre 1990.

Losno R., J.L. Colin, N. Le Bris, B. Chatenet, G. Bergametti, T.D. Jickells and B. Lim, **Chemistry of the dissoltion of atmospheric Al and Fe in marine rainwaters**. *VII CACGP Symposium on Chemistry of the Global Atmosphere*, Champrousse, 5-11 septembre 1990.

Dulac F., G. Bergametti, R. Losno, E. Remoudaki, L. Gomes, U. Ezat and P. Buat-Ménard, **Dry deposition of aerosol particles in the marine atmosphere: a critical evaluation of current field and modeling approaches**, *5th International Conference on Precipitation Scavenging and Atmosphere-Surface Exchange Processes*, Richland (USA), 15-19 juillet 1991 (Poster).

Donard O.F.X., C.R. Quétel, F. Grousset, R. Losno and J.L. Colin; **Determination of trace metals in rain waters by ICP/MS and biogeochemical implications.** *European Geophysical Society, XVII General Assembly*, Edinburgh , 6-10 April 1992.

M. Schulz, W. Dannecker, T. Church, J.L. Colin, T. Hasler, M. Leermakers, R. Losno, C. Meulemann and L. Spokes, **Intercomparison of rain sampling at Mace Head**, *17th EGS Assembly*, Edimbourg, 6-10 April 1992 (Poster).

N. Le Bris, J.L. Colin, R. Losno and B. Chatenet, **Dissolved-particulate distribution of iron and manganese in remote marine rain samples**, *17th EGS Assembly*, Edimbourg, 6-10 April 1992 (Poster).

Marticorena B., A.Youssfi, R. Losno and G. Mouvier, **Wavelet Transform of Atmospheric Particulate Matter Concentration.** *Geophysics and environment: Background air pollution*, Rome, 16-18 juin 1992.

R. Losno and J.L. Colin; **Influence of sea-salts and marine spray on marine rainwater sampling.** *Eurotrac/ASE MaceHead and Nose Meeting*, Paris, 13-15 octobre 1992.

I. Vassalli, R. Losno and J.L. Colin, **Ligands in rainwater.** *Eurotrac/ASE meeting*, Arcachon, 25-29 octobre 1993.

Colin J.L., N. Le Bris, B. Lim, M.Tisserant and R. Losno, **Heterogenous chemistry in marine atmosphere**, *A.S.E. Workshop on Air-Sea Exchange*, Arcachon, 25-29 Octobre 1993.

Losno R. and J.L. Colin; **Organic ligands in the atmosphere. Measurements on the field of Porspoder in March 1994**. *A.S.E. Workshop on Air-Sea Exchange*, Riso, Roskilde (Dannemark), 19-22 October 1994.

J.P. Quisefit, R. Losno and S. Garivait, **Quantitatives analyses of biomass burning residues by X-ray fluorescence and ionic chromatography**, *DC" 94 MONTREUX 2nd SAS*, Montreux, 1994.

R. Losno, S.Loyaux, A.L.Devillard and J.L.Colin, **Anions in marine rain waters.** *A.S.E. Workshop on Air-Sea Exchange*, Mayence, 1-5 novembre 1995.

Losno R., S.Cholbi and J.L.Colin; **pH dependence of dissolution rates of iron and manganese-Preliminary results.** *A.S.E. Workshop on Air-Sea Exchange*, Mayence, 1-5 novembre 1995.

Colin J.L., Bergametti G. and Losno R., **Mechanisms and modelling of sea-air exchange of trace metals : solubility of trace metals**. *Conférence invitée au Workshop on Sea-Air Exchange: processes and modeling*, Oslo, 11-13 juin1997.

Losno R., **A model describing trace metals acting as catalyst in a marine cloud**, *EGS plenary assembly*, Nice, 20-24 avril 1998.

Dulac F., D. Filippi, H. Cachier, U. Ezat, J.C. Le roulley, D. Paronis, P. Chazette, E. Hamonou, N. Mihalopoulos, G. Kouvarakis, A. Gaudichet, S. Caquineau, R. Losno, G. Malingre, J.P. Quisefit, F. Albers, M. Wirth and M. Krautstrunk, **Characterization of tropospheric aerosols in the eastern Mediterranean from airborne and other measurements during the June 1997 STAAARTE campaign**, *EGS plenary assembly*, Nice, 20-24 avril 1998.

Desboeufs K. and R. Losno, **The Influence of trace metals leaching from mineral atmospheric aerosols an atmospheric photochemistry**, *Second Workshop of the EUROTRAC-2 Subproject CMD*, Karlsruhe, 23-25 septembre 1998.

Losno R. and K. Desboeufs, **Modelling Trace metals as catalysts in clouds: multiphase chemistry in non polluted area**, *Second Workshop of the EUROTRAC-2 Subproject CMD*, Karlsruhe, 23-25 septembre 1998 (Poster).

R. Losno, K. Desboeufs, S. Costes, J.L. Colin and J.P. Quisefit, **The use of ICP-AES for the determination of trace levels below ppb in environmental samples,** *European Winter Conference on Plasma Spectrochemistry*, Pau, 10-15 janvier 1999 (Poster).

K. Desboeufs, Losno R. and Colin J.L. **Evolution of aerosol mineral solubility during cloud process and its impact on aerosol surface**, *IGAC conference*, Bologne, 13-18 septembre 1999 (Poster).

R. Losno, Colin J.L., Perros P. and Pereira S., **Hydrogen peroxide variations at Mace-Head (Ireland) and Porspoder (Brittany)**, *IGAC conference*, Bologne, 13-18 septembre 1999 (Poster).

R. Losno and Desboeufs K., **Trace Metals Supply and Acid-Base Reactions in Cloud and Rain Water**, *Third Workshop of the EUROTRAC-2 Subproject CMD*, Aachen, 21-23 septembre 1999.

R. Losno, K. Desboeufs and J.L. Colin, **Dissolved Transition Metals Affecting Atmospheric Chemistry**, *EGS plenary assembly*, Nice, 25-29 avril 2000.

K.V. Desboeufs, R. Losno and J.L. Colin, **Atmospheric particle dissolution process in the cloud droplets,** *EAC 2001*, Leipzig, 3-7 septembre 2001**.**

K.V desboeufs, R. Losno and J.L. Colin, **Mechanisms of physicochemical modifications of Saharan Aerosol during cloud process,** *Physico-Chemical Behaviour of atmospheric pollutants*, 17-20 septembre 2001, Torino.

R. Losno, K.V. Desboeufs, J. Kui and J.L. Colin, **Influence of simulated sun irradiation on aerosol dissolution rate**, *Physico-Chemical Behaviour of atmospheric pollutants*, 17-20 septembre 2001, Torino.

A. Sofikitis, J.L. Colin, S. Costes and R. Losno, **Analytical method for speciation of iron in rainwater**, *Physico-Chemical Behaviour of atmospheric pollutants*, 17-20 septembre 2001, Torino.

Alexandra Sofikitis, Jean Louis Colin, Karine Desboeufs and Rémi Losno, **Iron dissolution rate in various minerals**. *EUROTRAC-2 symposium*, Garmisch-Partenkirschen, march 2002, poster.

Karine Desboeufs, Rémi Losno, and Jean-Louis Colin, **Aerosol Alkalinity depends on pH**. *EUROTRAC-2 symposium*, Garmisch-Partenkirschen, march 2002. Poster.

Jean-Michel Velay, Karine Desboeufs, Rémi Losno and Jean-Louis Colin, **Aerosol dissolution enhancement by light irradiation**. *EUROTRAC-2 CMD meeting*, 9-11 sptembre 2002, Paris.

Alexandra Sofikitis, Jean Louis Colin, Karine V.Desboeufs and Rémi Losno, **Experimental Simulation of Iron Cycling**. *EUROTRAC-2 CMD meeting*, 9-11 sptembre 2002, Paris.

Losno, R., Gombert, S., Colin, J.L., Leblond, S. & Rausch de Traunbenberg, C.,(2002). **French spatial estimation of trace metal deposition using moss as biomonitor**. *Joint CACGP/IGAC 2002 international symposium*, Atmospheric chemistry within the earth system: from regional pollution to global change, 18-25 September 2002, Creta Maris, Hersonissos. Poster.

F. Dulac, P. Chazette, C. Moulin, U. Ezat, J.-F. Leon, M. Kanakidou, N. Mihalopoulos, G. Kouvarakis, I. Kavouras, E. Stephanou, I. Chiapello, M. Legrand, O. Pancrati, R. Losno, J.-P. Quisefit, G. Malingre, **Overview of observational results from the Mediterranean Dust Experiment (MEDUSE) and correlative measurements**, *Joint CACGP/IGAC 2002 international symposium*, Atmospheric chemistry within the earth system: from regional pollution to global change, 18-25 September 2002, Creta Maris, Hersonissos. Poster.

7.2.4 Communications à des congrès nationaux

Losno R.; **Application de la fluorescence X à l'analyse d'aérosols atmosphériques.** *Journée du G.A.M.S.* du 2 février 1987 sur la fluorescence X, Paris.

Losno R.; **Analyse de traces en absorption atomique. Méthodes de décontamination et de non contamination. Application à l'étude de précipitations.** *Journée du G.A.M.S.* du 20 octobre 1988 sur l'absorption atomique sans flamme, Paris.

Dulac F., Gomes L., Losno R., Steiner E. et Ezat U.; **Distribution granulométrique d'aérosols mesurée à l'aide d'impacteurs en cascade: procédure statistique de déconvolution des spectres et de correction des effets de rebond des particules**, Paris, *7ème journées COFERA du GAMS*, 28 novembre 1990.

Quétel C.R., O.F.X. Donard, F. Grousset, R. Losno and J.L. Colin; **Application de l'ICP/MS à l'étude de signatures géochimiques métalliques en ultra-trace dans l'environnement,** *European Meeting on Mass Spectrometry*, Metz, 22-24 Septembre 1992.

Kanakidou M., Poisson N., Lattuati M., Aumont B., Beekmann M., Bey I., Behra P., Chaumerliac N., Grégoire P., Hauglustaine D., Huret N., Losno R., Maalez A., Martin D., Martinerie P., Mercier P., Pham M., Pirre M., Ramaroson R. et K. Suhre, **Comparaison entre 11 modèles utilisés en France pour la description de la chimie troposphérique**, *Atelier de Modélisation de l'Atmosphère*, Toulouse, 28-30 novembre 1995.

Losno R. et Behra P.; **Influence des métaux de transition sur la composition chimique des nuages**. *Atelier de Modélisation de l'Atmosphère*, Toulouse, 28-30 novembre 1995.

R. Losno et G. Malingre, **Modification du préleveur d'eau nuageuse "NUAC" pour l'étude des traces**, *Atelier "Expérimentation et instrumentation"*, Toulouse, 15-17 octobre 1996 (Poster).

7.2.5 Rapports de contrats

Bergametti G., Buat-Ménard P., Chatenet B., Losno R. et Remoudaki E.; **Apport de métaux par voie atmosphérique à la Méditerranée Occidentale**, *Rapport SRETIE/Ministère de l'Environnement, 87-092*, 22pp, 1988.

G. Bergametti, R. Losno, J.L. Colin, H. Cachier, P. Buat-Ménard and M.P. Brémond; **Aerosol and rain chemistry over European sea areas.** *Rapport Eurotrac Air Sea Exchange*, 8pp, 1989.

J.L. Colin, M. Tisserant, S. Madec, R. Losno, H. Cachier, J. Ducret et C. Liousse; **Processus d'incorporation et spéciation des espèces de l'aérosol minéral et carboné dans les précipitations marines.** *Rapport EUROTRAC/A.S.E.*, 1993.

R. Losno et D. Martin, **NUAC: une approche de la base de donnée. première analyse de cohérence et de qualité. perspectives d'utilisation**, *Rapport au Ministère de l'Environnement*, 14 pp, février 1995.

J.L. Colin, R. Losno, N. Le Bris, M. Tisserant, I. Vassali, S. Madec, S. Cholbi, F. Vimeux, G. Bergametti. **Aerosol and Rain Chemistry in Marine Environment**, *EUROTRAC/ASE, Rapport Final*, 15pp, 1997.

P.E. Perros, T. Marion, F. Steiner et R. Losno, **MONA (Measurement Of Nitrogen compounds onboard Aircraft)**, *Rapport INSU/CNES*, Novembre 1997.

J.P. Quisefit and R. Losno, **Dayly based sampling and elemental analyses of aerosol in Creta Island**, in *MEDUSE, Rapport CEE*, 4pp, juin 1998.

R. Losno, K. Desboeufs, J.L. Colin and S. Costes, **Trace metals dissolution affecting aqueous chemistry (APP 7)**, in *EUROTRAC/CMD-APP 1998 Annual Report*, 4pp, février 1999.

J.L. Colin, G. Varrault, R. Losno and S. Costes, **Influence of d-block metals on photochemistry within clouds**, in *EUROTRAC/PROCLOUD 1998 Annual Report*, 4pp, février 1999.

P.E. Perros, T. Marion, F. Steiner et R. Losno, **MONA (Measurement Of Nitrogen compounds onboard Aircraft)**, *Rapport final INSU/CNES*, Septembre 1999.

R. Losno, K. Desboeufs, J.L. Colin and S. Costes, **Trace metals dissolution affecting aqueous chemistry (APP 7)**, in *EUROTRAC/CMD-APP 1999 Annual Report*, 4pp, février 2000.

R. Losno, K. Desboeufs and J. Daoudi, **Trace metals dissolution and photochemistry (APP 7)**, in *EUROTRAC/CMD-APP 2000 Annual Report*, 3pp, avril 2001.

Rémi Losno, Jean-Louis Colin, Sandrine Gombert, Sylvie Costes, Sébastien Leblond, Catherine Rausch et Daniel Cossa, **Les dosages des retombées métalliques d'origine atmosphérique en France par l'utilisation de mousses comme bioaccumulateurs des métaux (campagne 2000) - Heavy-metal atmospheric fallout measurements in France using mosses as bio-accumulators (field experiment 2000)**. *Rapport final du contrat Ademe 00 62 011*, décembre 2001.

7.2.6 Conférences invité

R. Losno; **Retombées de la pollution atmosphérique sur les écosystèmes.** Journée Chimie et Environnement Prolabo, Paris, 27 mai 1991.

R. Losno; **Les exigences pour l'analyse de traces**, *Journées de l'analyste "Trace et Spéciation"*, Paris, 8-9 avril 1997.

R. Losno; **Analyse d'Ultra-Traces en Spectrométrie d'Absorption Atomique Electrothermique dans les eaux de pluies peu polluées**, *Journeé Thermo-Optek*, Paris, 12 mars 1998.

R.Losno; **Le rôle de l'atmosphère en biogéochimie Marine**, Villefranche-sur-mer, Juin 2001.

7.2.7 Autres publications

- Traduction d'un glossaire de chimie dans le cadre d'une encyclopédie éditée par France Loisirs (1990).
- Traduction du volume "La Chimie" de la Nouvelle Encyclopédie des Sciences éditée par France-Loisir (1997).

7.3 Activités pédagogiques

7.3.1 Formation initiale

- Premier cycle universitaire (DEUG A et B) (1984-1992).
- Instrumentation en maîtrise de chimie physique (Absorption Atomique et polarographie) (1984-1992).
- Préparation à l'agrégation de physique (Chimie générale et minérale) à l'E.N.S. de Sèvres-Montrouge. (1989).
- Préparation à l'agrégation de physique (Chimie pour physiciens) au C.N.E.D. de Vanves. (1988-1992).
- Enseignement des sciences physiques en lycée (2nd et terminale D) (1990-1991).
- Mise en place du DEUG Sciences à l'antenne Paris 7 de Marne-la-Vallée (1991-1992).
- Enseignement en premier cycle Universitaire à Marne-la-Vallée (DEUG Sciences, 1991→).
- Enseignement en second cycle à l'Université de Marne-la-Vallée (1994, 1996→).
- Enseignement en 3ème cycle (DEA de Chimie et pollution atmosphérique, Université Paris 7, 1996→).
- Mise en place des travaux pratiques de l'option "Chimie Inorganique" de la licence des matériaux de l'Université de Marne-la-Vallée (1996-1997).
- Cours, Travaux Dirigés et Travaux Pratiques de la licence des matériaux de l'université de Marne-la-Vallée (1997-1998): Chimie minérale.
- Cours, Travaux Dirigés et Travaux Pratiques de la Licence de Chimie physique de l'université de Marne-la-Vallée (1998→): Chimie minérale.
- Cours, Travaux Dirigés et Travaux Pratiques de la Maîtrise de Chimie physique de l'université de Marne-la-Vallée (1999→): Physico-Chimie de l'environnement.
- Cours et Travaux Pratiques de la Maîtrise de Chimie physique de l'université de Marne-la-Vallée (2000-2001): Option: calcul numérique en chimie.
- Cours, Travaux Dirigés et Travaux pratiques du DESS "Génie Chimique de l'Environnement" à l'Université de Marne-la-Vallée (1999→): Écologie et chimie; Le prélèvement; Méthodes d'analyses atomiques.

7.3.2 Encadrement de 3ème cycle:

- I. Vassalli, *DEA de Chimie de la pollution atmosphérique*, (1992-1993), **Mesure du pouvoir complexant d'une eau de pluie**. Bourse de thèse de la Région Centre (Orléans), 1992-1993.
- S. Madec, *DEA de Chimie de la pollution atmosphérique*, (1993-1994) **Mise en évidence de la complexation dans une eau de pluie non polluée en milieu marin**. emploi en milieu hospitalier.
- A.L. Devillard, *DEA de Chimie de la pollution atmosphérique*, (1994-1995) **Mesure du pouvoir complexant organique d'une eau de pluie**. Bourse MRT.
- S. Cholbi, *DEA de Chimie de la pollution atmosphérique*, (1994-1995) **Étude cinétique de dissolution de métaux de transition dans un loess**, service militaire puis emploi dans une société informatique.
- F. Vimeux, *DEA de Chimie de la pollution atmosphérique*, (1995-1996) **Simulation de la dissolution du fer, du manganèse et du cuivre dans un nuage. Étude cinétique**. Bourse MRT.

- K. Desboeufs, *DEA de Chimie de la pollution atmosphérique*, (1996-1997) **Contribution à l'étude des processus d'altération de l'aérosol dans les nuages**. Bourse MRT.
- K. Desboeufs (pour 90%), Thèse, **Altération de l'aérosol dans un nuage et son effet sur la photochimie aqueuse**, 1997,2001, ATER à l'Université Paris 7. Directeur de Thèse Pr. J-L Colin.
- J. Kui, *DEA de Chimie de la pollution atmosphérique*, (1999-2000) **Réactions photochimiques de métaux en phase aqueuse**, emploi dans une société informatique.
- C. Blondelot, **Mise en œuvre d'un capteur aéroporté d'eau nuageuse**, 2000-2001.
- Alexandra Sofikitis (pour 20%), Thèse, **Le cycle du fer dans l'atmosphère**, 2000 →. Directeur de Thèse Pr. J-L Colin.
- S. Leblond (pour 20%), Thèse, **Transfert de la pollution atmosphérique en métaux**, 2000 →. Directeur de Thèse Pr. J-L Colin.
- J.M. Velay, **Photodissolution des métaux dans l'aérosol,** 2001-2002**.** Bourse MRT
- J.M. Velay, Thèse, **Photochimie hétérogène d'un système eau-aérosol**, 2002→.

7.3.3 Formation continue

7.3.3.1 Organisation

- Salle Blanche et Analyse Chimique (juin 1995, avril 2000, novembre 2001)
- Analyse de traces par ICP-AES (juin 1997)

7.3.3.2 Participation et animation

Formation continue au cours de stages de chimie analytique (1992→). Cours de statistiques et d'interprétation de résultats analytiques, cours et travaux pratiques de comportement en salle blanche, cours et travaux pratiques d'ICP-AES. 2 à 3 stages par an.

7.4 RESPONSABILITES COLLECTIVES:

7.4.1 Responsabilités scientifiques

Membre du comité scientifique de PROOF
Responsable français du programme SOLAS pour la partie atmosphère.

7.4.2 Autres tâches

- Membre élu du conseil scientifique de l'U.F.R. de Chimie de l'université Paris 7 (1988-1992).
- Aménagement des salles de travaux pratiques de Chimie pour l'implantation de l'UST-P7 à Marne-la-Vallée, future Université de Marne-la-Vallée (4 salles, 800 kF, 1990).
- Construction de deux petites salles blanches sur le campus de Jussieu (80 kF, 1991 et 1997).
- Construction d'une salle blanche (100 m²) pour l'installation du LISA sur le site de Créteil, Université Paris12-val-de-Marne (600 kF, 1992).
- Aménagement de 2 salles de laboratoire de Recherche pour préparer le déménagement du laboratoire de Jussieu (Paris 7) à Créteil (Paris 12).
- Vice-Président de la commission de spécialité de l'Université de Marne-la-Vallée. (1993-1998).
- Membre élu des commissions de spécialistes des sections de Sciences de la matière à l'Université de Marne-la-Vallée, nommé de la 31ème section de l'université Paris7 Denis Diderot (1998-2001) et de la 31ème section de l'Université Paris12 val de Marne.
- Membre du Conseil de Laboratoire du LISA (1992→)
- Responsable du réseau informatique du LISA (1998→) à Créteil. Il s'agit de gérer la connexion aux réseaux d'une centaine de postes comprenant des ordinateurs personnels, des serveurs et des stations de travail réparties sur 2 sites à Créteil et à Jussieu (Paris). Il a fallu trouver des solutions

pour permettre le transfert entre les différentes machines du laboratoire des très gros fichiers (de l'ordre du Go) générés par les programmes de modélisation. D'autre part, le laboratoire possède son propre domaine Internet (Dns, e-mail, Web, Ftp, ...) dont il faut assurer la maintenance et garantir le fonctionnement permanent.

- Reprise de l'aménagement des salles de Travaux Pratiques de 1er cycle de l'Université de Marne-la-Vallée (5 salles, budget 300 kF, 1999).

8 Choix de publications jointes en intégralité

8.1 Trace metals acting as catalysts in a marine cloud: a box model study.

R. Losno

LISA (Laboratoire Interuniversitaire des Systèmes Atmosphériques)
Universités Paris 7 Paris 12 - UMR CNRS 7583
Faculté des Sciences, 61 avenue du G[al] de Gaulle
F- 94010 Créteil Cedex France
e-mail: losno@lisa.univ-paris12.fr

Abstract:

A marine cloud includes a limited number of reactive compounds. Major species are hydrogen peroxide and ozone which are activated by photochemistry and RedOx cycling with trace metals. If we put the trace metals into the reactivity scheme, catalytic cycles appear and completely drive the reactivity even at the very low concentrations found in non polluted areas. This increases the speed of the reactions involving OH, HO_2 and O_2^- radicals. Under these conditions, the reaction of an added dissolved reactive species can be well fitted by a first order law decrease of the degraded compound. This leads to significant simplifications in a reaction mechanism which is suitable for modelling aqueous phase chemistry in unpolluted marine clouds.

1 Introduction

The cloud, fog and rain chemistry have a chemical impact at a regional or more global scale, taken into account in recent publications (Matthijsen et al., 1997; Walceck et al., 1997; Sander & Crutzen 1996) but pointed out several years ago (Lelieveld & Crutzen 1991; Jacob et al., 1991). Modelling this chemistry in transport models including gas phase and 3D wind fields is difficult because of the large amount of chemical equations added to take into account the cloud water chemistry. A lot of minor reactions should be neglected, and simplified reaction scheme proposed to allow a reasonable calculation time. We will propose here a case study in non polluted area to point out the importance of the trace metals catalytic effect, especially of dissolved copper and iron.

A cloud water droplet condenses itself always on a solid particle, everywhere present as an aerosol particle in the atmosphere, even in remote oceanic area (e.g. Losno et al., 1992). Trace metals are introduced into the aqueous phase through the partial dissolution of these aerosols into the water. If the droplet size increases, it forms rain and could be collected for elemental analyses. Various field experiments report values of measured dissolved trace metals into rainwater (Jickells et al., 1984; Lim at al., 1994) and also laboratory experiments which demonstrate the transfer of trace metal from the solid to the dissolved phase (Spokes et al. 1994). We have chosen to investigate several situations with and without trace metals, with and without ozone, and with and without species consuming OH. All the concentrations are consistent with those encountered in non polluted area. A box model including photochemistry is used. We will show how two catalytic cycles driven by Fe^{III}/Fe^{II} and Cu^{2+}/Cu^{+} respectively can explain all the reactive species concentrations into the modelled cloud drop.

Correspondence to: R. Losno

2 Model used and initial conditions

Our model have several parts which run together. The first is a kinetic explicit calculation with a variable time step. For each step (date t), the global concentration variation rate of each species by all the introduced reactions is computed. The step length (Δt) is calculated so that no more than 5% of the most reactive species vary in a linear interpolation. A new concentration set is then calculated at $t + \Delta t$. The second part involves equilibrium in aqueous phase, especially acid/base and aqua/hydroxy complex exchange, and is numerically solved at each step.

The third part concerns the exchange between gas and solution for reactive species which can be kinetically or thermodynamically controlled. The mass transfer between gaseous and dissolved phase is expressed as:

$$\Delta C_i = \Delta P_i \frac{1.0\ 10^5\ (\mathrm{Pa.g.bar^{-1}.L^{-1}})}{W\ R\ T}$$

- C_i is the concentration variation in the aqueous phase ($mol.L^{-1}$)
- ΔP_i is the partial pressure variation (bar) in the gas phase of compound i.
- W the liquid water content expressed in $g.m^{-3}$, taken here at 1.0 $g.m^{-3}$.
- R the gas constant (8.314 $J.K^{-1}.mol^{-1}$)
- T the absolute temperature (K), being in this study 298 K.

For the gas-dissolved transfer, we used a kinetic model expressed in Sander and Crutzen (1996) for a typical cloud droplet size distribution. If the transfer reaction is fast enough, an Henry's equilibrium can be assumed and then the mass transfer continuously adjusted.

The last part of the model is a time dependent external forcing, which allows us to change the irradiation intensity or add compounds at selected time during the run. The utilised reactions are listed in Table 1 and extract from Graedel & Mandich (1986), Jacob et al. (1989), Lelieveld & Crutzen (1991), Sander & Crutzen (1996) and Walcek et al. (1997):

N°	Reaction			rate constant ($L.mol^{-1}.s^{-1}$, except 01, 21 and 22 in s^{-1})
(01)	$hv + H_2O_2$	→	$2\ OH$	J=5.7E-07
(02)	$HO_2 + OH$	→	$O_2 + H_2O$	k=7.0E+09
(03)	$O_2^- + OH$	→	$O_2 + OH^-$	k=1.1E+10
(04)	$H_2O_2 + OH$	→	$HO_2 + H_2O$	k=2.7E+07
(05)	$O_3 + OH$	→	$HO_2 + O_2$	k=2.0E+09
(06)	$HO_2 + HO_2$	→	$H_2O_2 + O_2$	k=8.6E+05
(07)	$HO_2 + O_2^- + H_2O$	→	$H_2O_2 + O_2 + OH^-$	k=1.0E+08
(08)	$H_2O_2 + HO_2$	→	$OH + H_2O + O_2$	k=5.0E-01
(09)	$H_2O_2 + O_2^-$	→	$OH + OH^- + O_2$	k=1.3E-01
(10)	$O_3 + O_2^- + H_2O$	→	$OH + 2\ O_2 + OH^-$	k=1.5E+09
(11)	$OH + Mn^{2+}$	→	$Mn^{3+} + OH^-$	k=3.4E+07
(12)	$HO_2 + Mn^{2+} + H_2O$	→	$Mn^{3+} + H_2O_2 + OH^-$	k=6.0E+06
(13)	$O_2^- + Mn^{2+} + 2\ H_2O$	→	$Mn^{3+} + H_2O_2 + 2\ OH^-$	k=1.1E+08
(14)	$HO_2 + Mn^{3+}$	→	$Mn^{2+} + O_2 + H^+$	k=2.0E+04
(15)	$O_2^- + Mn^{3+}$	→	$Mn^{2+} + O_2$	k=1.5E+08
(16)	$H_2O_2 + Mn^{3+}$	→	$Mn^{2+} + HO_2 + H^+$	k=3.2E+04
(17)	$HO_2 + Fe^{3+}$	→	$Fe^{2+} + H^+ + O_2$	k=2.0E+04
(18)	$HO_2 + Fe(OH)^{2+}$	→	$Fe^{2+} + H^+ + O_2$	k=2.0E+04
(19)	$O_2^- + Fe^{3+}$	→	$Fe^{2+} + O_2$	k=1.5E+08
(20)	$O_2^- + Fe(OH)^{2+}$	→	$Fe^{2+} + O_2 + OH^-$	k=1.5E+08
(21)	$hv + Fe^{3+}\ (+H_2O)$	→	$Fe^{2+} + OH + H^+$	J=6.4E-07
(22)	$hv + Fe(OH)^{2+}$	→	$Fe^{2+} + OH + OH^-$	J=3.9E-04
(23)	$HO_2 + Fe^{2+}$	→	$Fe(OH)^{2+} + H_2O_2$	k=1.2E+06
(24)	$O_2^- + Fe^{2+}$	→	$Fe(OH)^{2+} + H_2O_2$	k=1.0E+07
(25)	$OH + Fe^{2+}$	→	$Fe(OH)^{2+}$	k=3.0E+08
(26)	$O3 + Fe^{2+}\ (+H_2O)$	→	$Fe(OH)^{2+} + OH + O_2$	k=1.7E+05
(27)	$Fe^{2+} + Mn^{3+}$	→	$Fe(OH)^{2+} + Mn^{2+} + H^+$	k=2.1E+04
(28)	$H_2O_2 + Fe(OH)^+$	→	$Fe(OH)^{2+} + OH + H_2O$	k=1.9E+06
(29)	$O_2 + Fe^{2+}\ (+H_2O)$	→	$Fe(OH)^{2+} + O_2^- + H^+$	k=7.9E-04
(30)	$Fe^{3+} + Cu^+$	→	$Fe^{2+} + Cu^{2+}$	k=1.0E+07
(31)	$Fe(OH)^{2+} + Cu^+$	→	$Fe^{2+} + Cu^{2+} + OH^-$	k=1.0E+07
(32)	$OH + Cu^+$	→	$Cu^{2+} + OH^-$	k=3.0E+08
(33)	$HO_2 + Cu^+\ (+H_2O)$	→	$Cu^{2+} + H_2O_2 + OH^-$	k=1.5E+09
(34)	$O_2^- + Cu^+$	→	$Cu^{2+} + H_2O_2$	k=1.0E+10
(35)	$H_2O_2 + Cu^+$	→	$Cu^{2+} + OH + OH^-$	k=4.0E+05
(36)	$Mn^{3+} + Cu^+$	→	$Cu^{2+} + Mn^{2+}$	k=2.1E+04
(37)	$HO_2 + Cu^{2+}$	→	$Cu^+ + O_2 + H+$	k=1.0E+08
(38)	$O_2^- + Cu^{2+}$	→	$Cu^+ + O_2$	k=5.0E+09
(39)	$OH + CH_3OH\ (+O_2)$	→	$CH_2O + HO_2 + H_2O$	k=9.7E+08
(40)	$OH + CH_2O\ (+O_2)$	→	$HCOOH + HO_2$	k=7.7E+08
(41)	$OH + HCOOH\ (+O_2)$	→	$HO_2 + CO_2 + H_2O$	k=1.1E+08
(42)	$OH + HCOO^-\ (+O_2)$	→	$HO_2 + CO_2 + OH^-$	k=3.1E+09

Table 1: Set of reactions used for the kinetic model

Equilibrium occurring between acid & base and gas & solution are listed in table 2.

The model starts with initial concentrations corresponding to a cloud condensation in a non polluted air mass, typical of a marine area, containing some hydrogen peroxide, ozone and aerosols which release trace metals by partial dissolution. The initial dissolved concentrations (Table 3) were extracted from published data measured in marine rainwater, and calculated from Henry's law equilibrium for O_3 assuming a 25 ppb gaseous concentration, typical of remote areas.

Equilibrium	$\log_{10} K$	
$H_2O = OH^- + H^+$	-14	K_w
$HO_2 = O_2^- + H^+$	-4.68	$K_{a,HO2}$
$Fe^{3+} + H_2O = Fe(OH)^{2+} + H^+$	-2.04	$K_{a,Fe3+}$
$Fe^{2+} + H_2O = Fe(OH)^+ + H^+$	-9.5	$K_{a,Fe2+}$
$HCOOH = HCOO^- + H^+$	-3.74	$K_{a,form}$
$HO_{2,gas} = HO_{2,dissolved}$	+3.95	
$H_2O_{2,gas} = H_2O_{2,dissolved}$	+4.87	
$O_{3,gas} = O_{3,dissolved}$	-1.92	$K_{H,O3}$

Table 2: homogeneous and heterogeneous equilibrium constants. Metal acidity values are from Turner et al. (1981), other from Sander & Crutzen (1996).

Compound	Initial concentration	Reference
O_3	3.0 E-10 $mol.L^{-1}$	25 ppb gaseous
H_2O_2	10 $\mu mol.L^{-1}$	Willey et al. 1996
H^+	10 $\mu mol.L^{-1}$, pH 5	Losno et al. 1998, Losno et al. 1991
Soluble Fe	5.0 E-8 $mol.L^{-1}$	Hoffman et al. 1997, Jickells et al. 1984
Soluble Mn	3.0 E-9 $mol.L^{-1}$	Le Bris 1993, Losno 1989, Lim et al. 1994
Soluble Cu	1.0 E-9 $mol.L^{-1}$	Ross 1987, Spokes et al. 1994

Table 3: initial non zero concentrations.

Several runs were experienced, with different situations:

- "non trace metal model" where metal concentrations are set to zero,
- "non ozone model" where ozone concentration is set to zero

In each the four possible cases, we have tested the addition of an amount of methanol to look at the behaviour of the system if an OH consuming compound is introduced. The choice of methanol was done because it exhibits a simple aqueous chemistry. It allows us to focus easily on the intensity of the perturbation brought for OH and HO_2. An initial concentration of 0.1 µM was used.

3 Results and discussion

3.1 Importance of the phase exchange

Hydrogen peroxide is very soluble (table 2), and most of its mass is included in the aqueous phase with a long life time, so mass transfer does not have a great importance.

Because we do not join our aqueous phase model to a gaseous one, we do not know the concentrations of OH and HO_2 radicals in the gas phase. As one of their major sources is H_2O_2 which is removed from the gas, their concentration should be depleted, and the soluble phase may be rather a source for the gas phase. On an other hand, the life time of OH is very short and HO_2 is very soluble in water (table 2), so we have not taken into account here the phase exchange. For ozone, which is present mainly in the gas phase and only

$$[O_2^-] = \left(\frac{K_{a;HO2}}{[H^+] + [K_{a;HO2}]}\right)\left(\frac{2\,J_1\,[H_2O_2] + J_{22}\,[Fe(OH)^{2+}] + k_{28}[H_2O_2][Fe(OH)^+] + k_{35}[H_2O_2][Cu^+]}{k_{19;20}\,[Fe^{III}] + k_{38}\,[Cu^{2+}]}\right) \quad \textbf{(1)}$$

$$[OH] = \left(\frac{2\,J_1\,[H_2O_2] + J_{22}\,[Fe(OH)^{2+}] + k_{28}[H_2O_2][Fe(OH)^+] + k_{35}[H_2O_2][Cu^+]}{k_4[H_2O_2]}\right) \quad \textbf{(2)}$$

$$\frac{[Cu^+]}{[Cu^{2+}]} = \frac{k_{38}\,[O_2^-]}{k_{35}\,[H_2O_2]} \quad \textbf{(3)}$$

destroyed in the aqueous (no listed reactions produce ozone) we have tested the influence of the mass transfer kinetic, and compared to a continuous Henry's law equilibrium.

The dynamic of this exchange is fast enough and do not exhibit any differences with a continuous equilibrium hypothesis. We therefore have made our calculation without taking into account the kinetic of the phase exchange, to spare computing time.

3.2 Chemical dynamics of the system

3.2.1 Irradiation dependence

We used here the external forcing feature of our model to switch on the light (all J to their standard values) and off (all J to zero) at very short time intervals (5 s). Figure 1a and 1b show very different shapes.

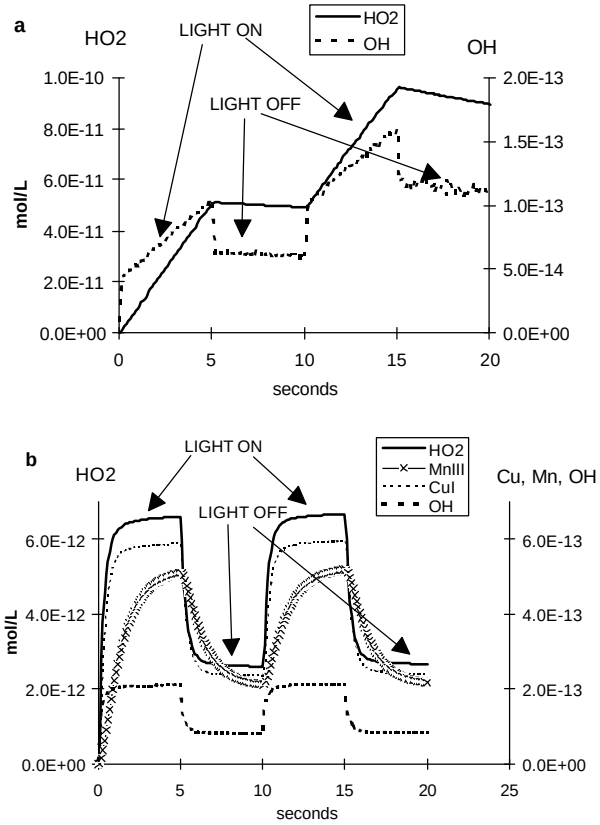

Figure 1a and 1b: Short time simulation with dark and illuminated periods. a is without any trace metal, b with the concentrations listed table 3.

In Figure 1a, where no trace metals are added, the system does not recover the previous state after a light switching period, but radical concentrations remain unchanged in the dark, and are dependent on the concentrations reached during the lightened period. Figure 1b shows the same variation of all the reactive species, whatever the previous cycle. The characteristic time for the system reaching a steady state is less than 2 s for all the reactive species, except manganese which is around 5s. In the dark period, the HO_2 and OH concentrations in the model with trace metals are very low compared to those found without any trace metal, which remain close to the levels reached during the irradiation time.

Iron does not appear in figure 1b because it exhibits a different behaviour underlined for longer run times in Figure 2. The Fe^{II} and Fe^{III} relative concentrations vary as a continuous function of time and are not discontinuously affected by dark to light switching. Large amounts of Fe^{II} are slowly produced during irradiated periods and consumed during dark (Figure 2), as also described in Zuo & Hoigné (1992) or Weschler et al. (1986). Measurements of Fe^{II}/Fe^{III} ratio becomes possible if the samples are analysed within the minutes of their collection, which is not the case for Cu^{I} because it reacts faster.

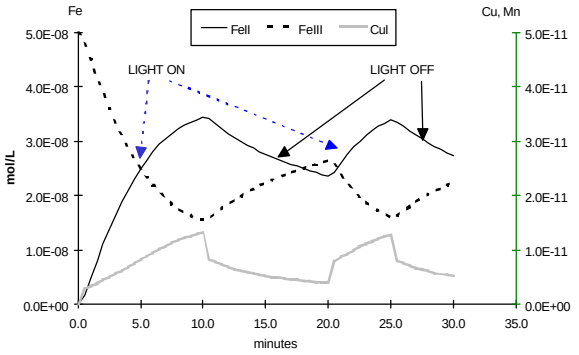

Figure 2: Iron species and copper I concentration variation with illuminated and dark periods of a few minutes.

3.2.2 System reduction

Examining the different reactions allows us to extract the fastest ones and better understand what is important or less. More than 90% of the chemical fluxes can be explained by a set of 7 reactions:

- N° 01 and 04 involving hydrogen peroxide, photons and OH,
- N° 19-20, 22 and 28 involving Fe^{II}/Fe^{III} cycling,
- and N° 35 and 38 with Cu^{II}/Cu^{I} cycle.

Such oxidation-reduction cycles were also cited by Behra & Sigg (1990), but in a polluted region with the participation of sulphur oxides. This system is summarised in figure 3. Manganese does not have any

major influence in this scheme, but copper does, despite its very low concentration (~ 1 nmol.L^{-1}).

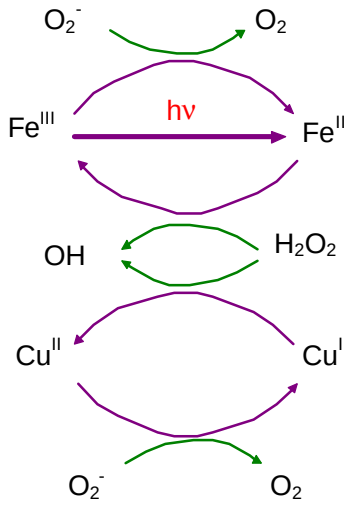

Figure 3: Copper and Iron RedOx cycles.

The balance of the source and sink of the reactive species lets us state photostationarity for HO_2 & O_2^-, OH and Cu^I/Cu^{II} writing the equations displayed at the top of this page (equations 1 to 3). Fe^{III} is the sum of Fe^{3+} and $Fe(OH)^{2+}$, $Fe(OH)^{2+}$ represents both $Fe(OH)^{2+}$ and $Fe(OH)_2^+$ because of the very close values of the photolysis constant of both hydroxy complexes ($Fe(OH)^{2+}$ and $Fe(OH)_2^+$). Moreover, at pH greater than 4, Fe^{3+} is less than 1% of the total Fe^{III}, and can be neglected; so $Fe(OH)^{2+}$ is Fe^{III}.

Taking into account the very low value of the $[Cu^+]/[Cu^{2+}]$ ratio, Cu^{2+} can be taken as total dissolved Cu ($[Cu_{total}]$). The relative iron speciation appears to be important in this case because there is no fast photostationary state, as shown in Figure 2. The reaction is slow, mainly because Fe^{II} is much less reactive than Cu^+ and then shows higher concentrations. However, a slow steady state is reached when:

$$\frac{[Fe^{II}]}{[Fe^{III}]} = \frac{k_{19;20}\,[O_2^-] + J_{22}}{k_{28}\,Ka_{Fe2+}\,[H^+]^{-1}\,[H_2O_2]} \qquad \textbf{(4)}$$

3.3 Addition of other reactive compounds

3.3.1 Influence of ozone and a reducing agent

One property of the scheme proposed is the very fast rate of the two cycles which produce high source and sink for OH and HO_2 radicals, and then is difficult to disturb. As an example, we have simulated the addition of C_o = 0.1 µM of methanol, which acts simply as an OH sink. This concentration is taken very high, balancing the poor reactivity of methanol and derivatives. Methanol itself represents only a simple example of a typical reducing species, with a sink given at the beginning with $k_{39}.C_o = 10^2\ s^{-1}$ applied to OH. This test was done on 4 cases, two with metals (one with and one without ozone) and two without metals (one with and one without ozone).

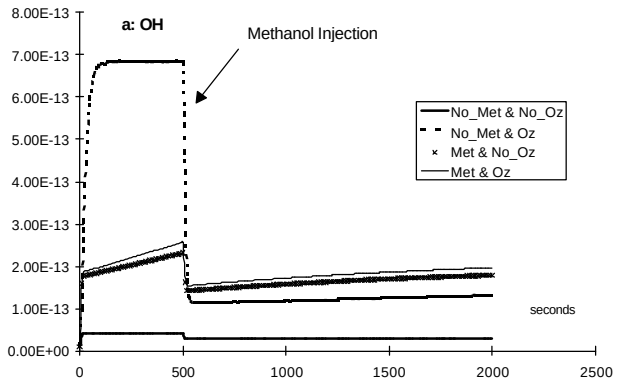

Figure 4a: Effect of addition of methanol on [OH] to the modelled system. Four cases are displayed: with metal and ozone (Met & Oz), with metal and without ozone (Met & No_Oz), without metal and with ozone (No_Met & Oz) and without metal nor ozone (No_Met & No_Oz).

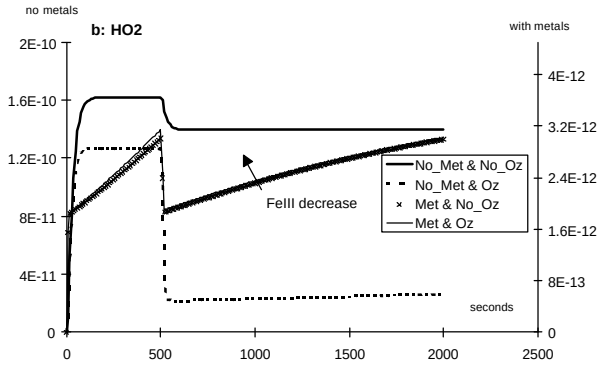

Figure 4b: Effect of addition of methanol on [HO_2].

Figure 4a and 4b summarise the behaviour of the proposed system on both OH and HO_2 radical concentrations, showing two main results: a simple radical scheme is not reactive at pH 5 without ozone, but introducing trace metals activate hydrogen peroxide so much that ozone reactions become negligible. An ozone containing drop is about five times more sensitive to the input of methanol if it does not include metals than if it does. This is a direct consequence of the faster chemical dynamics with trace metals.

3.3.2 First order approximation

This suggests the OH concentration is mostly independent on the methanol concentration, and then it is consumed with an apparent first order kinetic law, expressed like:

$[CH_3OH] = [CH_3OH]_o \exp(-k_{app}\, t)$

where

- k_{app} is the apparent degradation constant ($L.mol^{-1}.s^{-1}$), here $k_{app} = k_{39}\,[OH]$
- t is time (s)

$\log_e [CH_3OH]$ is a straight line if expressed as a function of time.

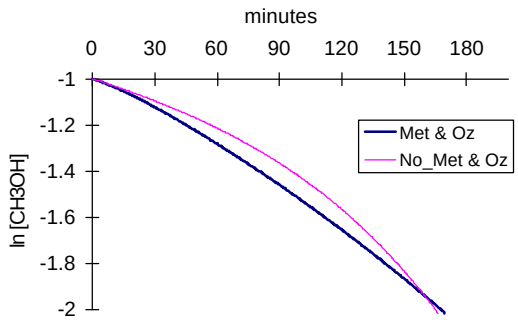

Figure 5: First order approximation for the oxidation of methanol. Plot of $\log_e [CH_3OH]$ as function of time, with (Met & Oz) and without (No_Met & Oz) trace metals.

[OH] is given by equation 2 and depends on the iron speciation. After several minutes, the Fe^{III}/Fe^{II} ratio reach an equilibrium given by equation (4) and [OH] stays constant, imaged by the straight line on figure 5. This is absolutely not the case in the simulation where no metal is added, and a deviation from the 1st order is obvious.

3.4 Model sensitivities

The trace metal concentrations are the engine of the proposed system; therefore its concentrations are a major parameter to drive the reaction rate. Figure 6 shows the effect of various trace metal concentrations on the methanol oxidation rate, maintaining the ratios between copper, iron and manganese constant. The trace metal concentrations used in this model are median values of those published in the references cited for table 3, but exhibit large variations from an event to another. It appears therefore very important to quantify and model the dissolution of trace metals from the included aerosol particles to the water drop.

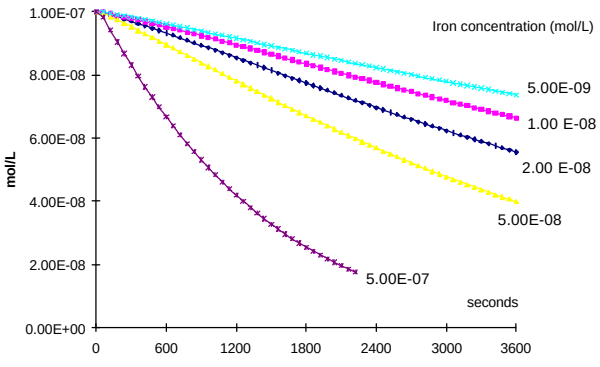

Figure 6: Sensitivity of the model to trace metal concentrations. Methanol concentration versus time.

4 Conclusion

Adding trace metals completely changes the reaction scheme, and so cannot be considered as a "fine tuning" of existing aqueous phase models, even in remote areas. But beside the large amount of reactions that must be added, adding trace metals speeds up most of the major reactions and allows more stationary situations. Consequently, reactions which appeared important without trace metals in the model become small disturbances and can be considered as pseudo-first order.

The system is very sensitive to the trace metal concentrations which were here estimated from rainwater measurements. We must therefore learn more about the solid to soluble phase transfer mechanisms, about the availability of the dissolved metals (noticed in Spokes et al., 1996, concerning copper complexation by organic matter), and finally about the trace metal dissolved concentrations directly measured inside the clouds.

5 References

Behra Ph. and Sigg L. (1990), "Evidence for redox cycling of iron in atmospheric water droplets", *Nature*, **344 6265**, 419-421.

Graedel T.E., Mandich M.L. and Weschler C.J. (1986), "Kinetic Model Studies of Atmospheric Droplet Chemistry: 2. Homogeneous Transition Metal Chemistry in Raindrops", *J. Geophys. Res.*, **91 D4**, 5205-5221.

Hoffmann P., Dedik A.N., Deutsch F., Sinner T., Weber S., Eichler R., Sterkel S., Sastri C.S. and Ortner H.M. (1997), "Solubility of single chemical compounds from an atmospheric aerosol in pure water, *Atmos. Environ.*, **17**, 2777-2785.

Jacob D.J., Gottlieb E.W. and Prather M.J. (1989), "Chemistry of a Polluted Cloudy Boundary Layer", *J. Geophys. Res.*, **94 D10**, 12975-13002.

Jickells T.D., Knap A.H. and Church T.M. (1984), "Trace Metals in Bermuda Rainwater", *J. Geophys. Res.*, **89 D1**, 1423-1428.

Le Bris N. (1993), "Contribution à l'étude de la distribution particulaire-dissous de métaux-trace dans les précipitations", *PhD Thesis*, Université Paris 7, 246 pp.

Lelieveld J. and Crutzen P.J. (1991), "The role of Clouds in Tropospheric Photochemistry", *J. Atmos. Chem.*, **12**, 229-267.

Lim B., Losno R.,. Jickells T.D and Colin J.L. (1994), "The solubilities of aluminium, lead, copper and zinc in rain samples in the marine environment over the North Atlantic Ocean and the Mediteranean Sea." , *Global Biogeochemical Cycles*, **8**, 349-362.

Losno R., (1989), "Chimie d'éléments minéraux en trace dans les pluies méditerranéenes", *PhD Thesis*, Université Paris 7, 215 pp.

Losno R., Bergametti G., Carlier P. and Mouvier G. (1991), "Major ions in marine rainwater with attention to sources of alkaline and acidic species", *Atmos. Environ.*, **25A**, 763-770.

Losno R., Bergametti G. and Carlier P. (1992), "Origin of the atmospheric particulate matter over the North-Sea and the Atlantic Ocean", *J. Atmos. Chem.*, **15**, 333-352, 1992.

Losno R., Colin J.L., Spokes L., Jickells T., Schulz M., Reberts A., Leermakers M., Meulemann C. and Bayens W. (1998), "Non-rain deposition significantly modifies rain samples at a coastal site", *Atmos. Environ.*, **20**, 3445-3455.

Matthijsen J., Builtjes P.J.H., Meijer E.W. and Boersen G. (1997), "Modelling cloud effects on ozone on a regional scale: a case study", *Atmos. Environ.*, **31**, 3227-3238.

Ross H.B. (1987), "Trace metals in precipitation in Sweden", *Water Air and Soil Pollution*, **36**, 349-363.

Sander R. and Crutzen P.J. (1996), "Model study indicating halogen activation and ozone destruction in polluted air masses transported to the sea", *J. Geophys. Res.*, **101 D4**, 9121-9138.

Spokes L.J., Jickells T.D. and Lim B. (1994), "Solubilisation of aerosol trace metals by cloud processing: a laboratory study", *Geochim. Cosmochim. Acta*, **58**, 3281-3287.

Spokes, L.J., Campos, M.L.A.M. and Jickells, T.D. (1996), "The role of organic matter in controlling copper speciation in precipitation", *Atmos. Environ.*, **30**, 3959-3966.

Turner D.R., Whitfield M. and Dickson A.G. (1981), "The equilibrium

speciation of dissolved components in freshwater and seawater at 25°C and 1 atm pressure", *Geochimica et Cosmochimica Acta*, **45**, 855-881.

Walcek C. J., Yuan H.H., and Stockwell W.R. (1997) "The influence of aqueous-phase chemical reactions on ozone formation in polluted and nonpolluted clouds", *Atmos. Environ.*, **31**, 1221-1237.

Weschler C.J., Mandich M.L. and Graedel T.E. (1986), "Speciation, Photosensitivity, and Reactions of Transition Metal Ions in Atmospheric Droplets", *J. Geophys. Res.*, **91 D4**, 5189-5204.

Willey J.D., Kiebert R.J. and Lancaster R.D. (1996), "Coastal Rainwater Hydrogen Peroxide: Concentration and deposition", *J. Atmos. Chem.*, **25**, 149-165.

Zuo Y. and Hoigné J. (1992), "Formation of Hydrogen Peroxide and Depletion of Oxalic Acid in Atmospheric Water by Photolysis of Iron(III)-Oxalato Complexes", *Environ. Sci. & Technol.*, **26**, 1014-1022.

8.2 The pH-dependent dissolution of wind-transported Saharan dust

Karine V. Desboeufs, Rémi Losno, Françoise Vimeux, and Sylvain Cholbi

Laboratoire Interuniversitaire des Systèmes Atmosphériques, Universités Paris 7 et 12, Créteil, France, UMR CNRS 7583, Créteil, France. (desboeufs@lisa.univ-paris12.fr; losno@lisa.univ-paris12.fr), (Received November 19, 1998; revised April 6, 1999; accepted April 7, 1999.)

 Paper number 1999JD900236.0148-0227/99/1999JD900236$09.00

Abstract. An open flow reactor was developed and used to study the pH dependency of atmospheric aerosol weathering. Under ultraclean conditions, this reactor enables experiments below the saturation of hydroxy salts and over the short time span (2 hours) that is typical for weathering by rain and cloud water. The weathering simulations show a two-step process of dissolution rates: First, the rate increases quickly during the hydration of the solid particle surface, then after a maximum, it progressively decreases. In general, there is an increase in the dissolution rate of dissolved elements as the pH is lowered. However, between pH 3.80 and 5.30, the dissolution rate for Fe and Cu depends on both H^+ and OH^- concentrations and exhibits a minimum as a function of pH. This minimum can be related to pH_{pzc} of the mineral containing these elements. The affinity of minerals for H^+ was also determined by correlating hydration constants and pH.

1. Introduction

Dissolved trace metals are an important key in understanding atmospheric aqueous phase chemistry: For example, they probably control catalytic oxidation of SO_2 producing acid precipitation [*Hoffmann and Boyces*, 1983; *Graedel et al.*, 1985; *Berresheim and Jaeschke*, 1986; *Clarke and Radojevic*, 1987]. Trace amounts of transition metals, for example, Fe, Mn, and Cu, readily modify oxidation and reduction paths in droplets [*Graedel et al.*, 1986; *Jacob et al.*, 1989; *Faust and Hoigné*, 1990, *Walcek et al.*, 1997; *Losno*, 1999] because they control the concentration of free radicals. These metals are also involved in a number of organic processes that occur in atmospheric droplets, that is, production and destruction of alkyl-hydroperoxides, and chemical chains that link RO_2 radicals to stable alcohols and acids and oxidation of aliphatic aldehydes to form organic acids [*Weschler et al.*, 1986].

On a global scale, desert aerosols are the main sources of trace metals to the atmosphere [*Lantzy and Mackenzie*, 1979; *Nriagu and Pacyna*, 1988]. Prior to removal by wet or dry deposition processes, aerosol particles are subjected to multiple cycles of wetting and drying during cloud condensation and evaporation [*Junge*, 1964]. They undergo partial weathering, which causes the solubilization of elements from minerals and metals. This initial leaching process establishes the chemistry of the aqueous solution that will define several subsequent atmospheric chemical processes, for example, mineral dusts from crustal weathering can neutralize acidic precipitation [*Khemani et al.*, 1987; *Losno et al.*, 1991]. This weathering process can modify the solid aerosol surface and so affect the optical and chemical properties [*Lowe et al.*, 1996; *Herrmann and Hänel*, 1997].

Wet atmospheric deposition is a major source of trace metals and nutrients to the oceans [*Patterson and Settle*, 1987; *Duce et al.*, 1991]. It has been suggested that Fe [*Brand et al.*, 1983; *Martin and Fitzwater*, 1988] and Mn [*Sunda et al.*, 1981; *De Baar et al.*, 1989] may act as limiting nutrients for phytoplankton growth. Free metals, rather than the total or chelated metal concentrations, control the biological availability [*Anderson and Morel*, 1982; *Rich and Morel*, 1990]. This input of trace metals to the oceans may thus influence the global climate via stimulation of dimethyl sulfide production by phytoplankton [*Zhuang et al.*, 1992] or CO_2 uptake [*Smith and Mackenzie*, 1991; *Martin et al.*, 1994].

Despite the obvious importance of solubilization of metals from dust in atmospheric waters, experimental works on this subject are scarce. Experiments simulating the timescales representative of those in cloud and rainwater showed a strong relationship between the dust mineralogy, pH of the solution and the solubility of transition metals for Saharan aerosol [*Spokes et al.*, 1994], and fuel ash and industry steel dust particles [*Williams et al.*, 1988]. Several studies using natural or artificial rainwater have suggested that the pH is a major factor controling solubility in rain and snow [*Maring and Duce*, 1987; *Prospero et al.*, 1987; *Losno et al.*, 1988; *Statham and Chester*, 1988; *Colin et al.*, 1990; *Lim and Jickells*, 1990].

In this study, we used a flow-through reactor of the same type that was used previously to simulate terrestrial mineral weathering [*Chou and Wollast*, 1984; *Mast and Drever*, 1987; *Schnoor*, 1990; *Bruno et al.*, 1991]. This reactor enables us to reproduce the rapid kinetic interactions between particulate and aqueous phases in atmospheric water. We discuss here the performance of this reactor when applied to the dissolution of mineral phases in part of conditions encountered in clouds where ionic strength remains low. Despite its importance for solubility history and bioavailability [*Zhu et al.*, 1997; *Spokes and Jickells*, 1996], in this paper we will not consider evaporation of a cloud droplet when ionic strength becomes very high and pH is very low. During evaporation, cloud conditions can be compared to the aerosol solution described by *Zhu et al.* [1992]. In our experiments, we have determined simultaneously the pH-dependent dissolution of the elements: Na, Mg, Si, K, Ca, Mn, Fe, Cu, Sr, and Ba at timescales representative of evaporation-condensation cycles in atmospheric cloud droplets. Our objectives were to identify and quantify the individual steps of mineral aerosols'weathering as they enter into a cloud.

2. Materials and Method

2.1. Method Used

The apparatus was designed to prevent equilibration of solid aerosol particles with insoluble salts. We used an open-flow reactor, wherein it was possible to maintain levels of dissolved species concentrations well below the saturation. The initial dissolution of the solids was exclusively studied without interference from secondary precipitation reactions. Evaluations of the effects of various chemical conditions on the dissolution of the introduced samples were possible by changing the composition of the input weathering solution.

2.2. Description of the Reactor

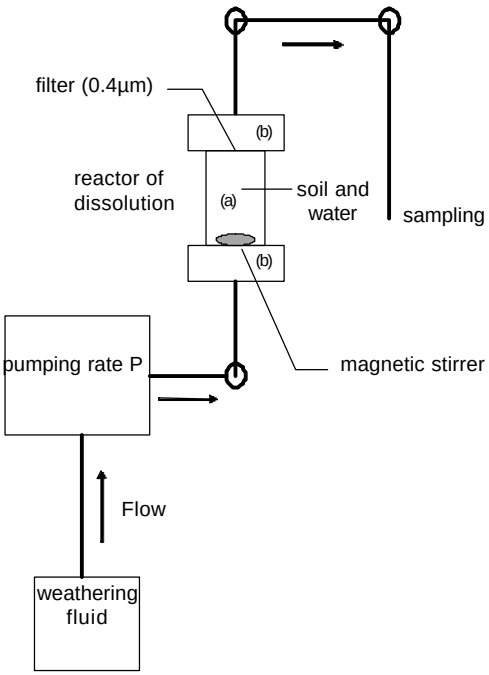

Figure 1. Schematic of dissolution reactor that includes a main body of transparent polycarbonate (labeled a) surrounded by two Teflon™ pieces (labeled b). The lower piece holds a perforated Teflon™ stand which carries the particulate sample at the beginning of the experiment. The upper piece houses a 0.4 µm porosity Nuclepore™ filter. All tubing and vanes are manufactured from Teflon™ and connect the chamber to the pump and the sample area.

This reactor (Figure 1) was designed to work under ultraclean conditions. The dissolution chamber consists of a cylinder, a perforated stand, and a 0.4 µm porosity Nuclepore™ filter. This porosity defines what is soluble and what is not [e.g., *Lim and Jickells*, 1990]. The pump induces an upward circulation of the weathering solution. The solution containing the dissolved elements is collected at the outlet at regular intervals. A magnetic stirrer maintains a homogeneous suspension in the dissolution chamber. An experimental check of homogeneous mixing was performed.
The dissolution rate is expressed as

$$R = \frac{dn}{dt} = F(C_i - C_x) + V\frac{dC}{dt} \qquad (1)$$

where

C solute concentration at time t inside the reactor (mol.L^{-1});
C_i and C_x concentrations of solute in the entering solution and the outgoing solution, respectively (mol L^{-1});
F flow rate (L min^{-1});
R rate of reaction in moles per time unit (mol min^{-1});
V volume of reactor (L);
Dn dissolved mole during dt period.

2.3. Particulate Phase

The < 20 µm diameter fraction of a dry segregated loess sample collected on the northeastern part of Sal Island (Capo Verde Islands) was used as particulate phase. It is aeolian dust from Niger, deposited during the Holocene [*Coudé-Gassen et al.*, 1994; *Rognon et al.*, 1996]. We used loess, which can be considered as an analog to aerosol, to ensure enough quantity of the same material. This loess simulates atmospheric aerosols of a crustal origin, in particular of Saharan dust. It has the size distribution of a natural crustal aerosol particle, ranging from 1 to 100 µm [*Junge*, 1979; *Slinn*, 1983; *Coudé-Gaussen et al.*, 1987; *Betzer et al.*, 1988].

An elemental analysis of this loess sample by X ray fluorescence and inductively coupled plasma atomic emission spectrometry (after acid digestion) is presented in Table 1. The aluminium normalized element ratios in the loess are close to those measured for Saharan dust aerosols [*Bergametti*, 1987] except for Na which is due to local enrichments.

Table 1a. Percentage of Elements Present in the Loess Sample

Element	Percentage
Si	22.7*
Al	8.4*
Fe	7.6*
Ca	3.8*
Mg	2.8*=
K	1.3*=
Na	1.1=
Ba	0.23=
Mn	0.13*=
Sr	0.032=
Cu	0.007=

Mg, K, and Mn measured by both the methods are in good agreement.
The value for Na has a large uncertainty.
*Values are determined by XRF.
=Values are determined by ICP-AES.

X ray diffraction examination of the loess sample was carried out on a Siemens D50 with a cobalt anticathode, covering a large angular field for detection of clay minerals, other silicates, and carbonates. The diffractogram indicates that this loess is made up of two parts: (1) a crystalline component of quartz plus sodic and potassic feldspars and micas (muscovite) and augite and (2) an amorphous component containing the clay minerals (kaolinite) and possibly iron oxo-hydroxides. We interpret these data as a weathering layer of amorphous silica with disordered clay minerals on top of crystalline material feldspars, micas, and probably augite [*Pye*, 1987]. Part of this amorphous layer was formed during postdeposition incipient meteorological alteration [*Coudé-Gaussen et al.*, 1994].

Table 1b. Comparison of Elements at Normalized Element Ratio

	Ca/Al	Fe/Al	Mn/Al	K/Al	Na/Al	Si/Al
X/Al [*Bergametti*, 1987]	0.50	0.94	0.033	0.21	0.03	2.73
X/Al (this study)	0.45	0.90	0.015	0.15	0.13	2.70

2.4. Experimental Procedure

Experiments were conducted using 20 mg of loess that was weathered with about 4 L of fresh solution for about 2 hours. This period is consistent with the lifetime of cloud droplets due to reevaporation [*Junge*, 1964; *Warneck*, 1989]. The volume of the aqueous phase is very large in comparison with the small amount of loess, which is consistent with the observed cloud conditions.

In order to determine the effect of pH on aerosol dissolution, the weathering solution was prepared by dilution of a primary solution of Milli-Q^{TM} water, exactly acidified at $[H^+] = 1.00\ 10^{-2}$ mol L^{-1}. This raw solution was made with ultrapure Prolabo™ Normatom® hydrochloric acid and measured by a classical NaOH conductimetric titration. Input pH values of 3.80, 4.00, 4.30, 4.70, 5.00, and 5.30 were used for transition metals (Cu, Fe, and Mn) and pH values of 4.00, 4.70, and 5.00 were used for Na, Mg, Si, K, Ca, Sr, and Ba. These values are similar to those in rainwater [*Lim and Jickells*, 1990] and cloud water [*Römer et al.*, 1985]. The flow of input and output solution was fixed to 18 mL min^{-1}. The regularity of the flow was checked all along the experiments by measuring the volume of each sample because this parameter is a key parameter in calculations of the dissolution rate (F in (1)). Each sample took about 1 min and 30 s. The samplings were spaced by gaps ranging from 15 s at the beginning to 30 min at the end of the experiment. Sample solution was collected in polyethylene or polypropylene bottles that were carefully washed to remove species that could contaminate the solution [*Losno et al.* 1991]. The collected sample solutions were acidified at pH 1 with ultrapure Prolabo™ Normatom® HNO_3 to allow proper analyses. Four to seven blank samples were made for each experiment.

Table 2. Element Detection Limits

Elements	Detection Limits, ppb
Inductively Coupled Plasma Atomic Emission Spectrometry	
Barium	0.5
Calcium	0.6
Iron	1
Magnesium	0.01
Potassium	0.5
Silicium	1
Sodium	0.3
Strontium	0.005
Atomic Absorption Spectrometry	
Copper	0.002
Iron	0.005
Manganese	0.004

Detection limits are defined as 3 times the standard deviation of at least 10 measurements near blank levels.

The concentrations of Na, Mg, Si, K, Ca, Fe, Sr, and Ba released into the solution were measured with a Perkin-Elmer Optima 3000 inductively coupled plasma atomic emission spectrometry (ICP-AES), and those of Mn, Fe, and Cu were measured with an Unicam TGH Solaar 929 graphite furnace atomic absorption spectrometry (GFAAS). The detection limits are summarized in Table 2. Because the reported data may include values obtained with both instruments, we ensured the correspondence of results between the two analytical methods. Results given by both instruments were compared for iron which exhibited a wide overlapping analytical range. The result of this intercalibration shows good agreement within the analytical instrument performance (Figure 2) and allows us to use one or the other of the analytical methods.

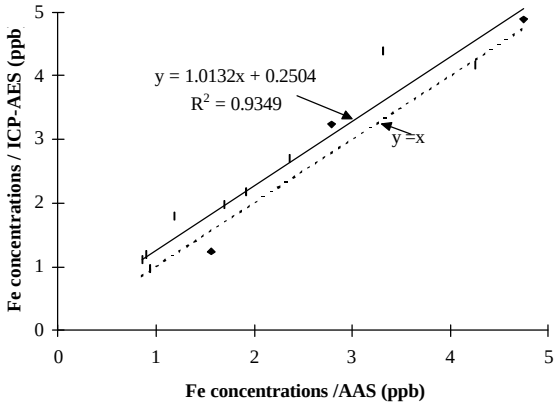

Figure 2. Intercalibration of atomic absorption spectrometry (AAS) / inductively coupled plasma atomic emission spectrometry (ICP-AES) for Fe at a concentration greater than 1 ppb. This value is the lower limit for reasonably good ICP measurements for the conditions used in our

The experimental conditions enabled us to use very low concentrations of about µg L^{-1} (ppb) or less. To avoid extraneous contamination and to ensure very low detection limits, all dissolution experiments and analyses were conducted in a clean room (class < 1000) and with laminar-flow ultraclean benches (class < 10), using ultraclean trace metal protocols [*Boutron et al.*, 1990; *Losno et al.*, 1991]. The temperature in the clean room was maintained between 20° and 22°C.

3. Experimental Conditions

3.1. Blanks

Two experiments were carried out without any particulate phase to demonstrate the absence of contamination during the experimental protocol. The results of these blanks were reproducible. In general, none of the investigated elements were detected except during the first 10 min of each experiment. During these first minutes, blank values were never below detection limit but remained negligible. The worst case was for Ba at pH 4.7 and 9 min and showing blank concentration less than 10% of experimental concentration (Figure 3). This probably resulted from a late rinsing of the system which cannot be changed without a much more extensive cleaning protocol; this was not considered necessary based on the results shown in Figure 3. We believe that the measured values represent dissolution of the loess sample and that they are free of contamination.

3.2. Ionic Composition of Medium

Table 3. Percentages of Major Ions Composition of Solution at pH 4.00 and 5.00

pH	Time Elapsed During Experiment	H^+, %	Na^+, %	K^+, %	Ca^{2+}, %
4.00	1 min	50.0	43.2	5.50	0.90
	30 min	96.7	0.40	0.50	1.30
	90 min	99.6	0.03	0.04	0.30
5.00	3 min	24.1	69.4	4.70	0.70
	30 min	68.7	7.30	5.00	12.6
	45 min	74.8	6.90	4.50	9.40

Table 4. Amount of Loess Captured on the Filter at Three Different Manipulation Times

	Amount at 7 Min, mg	Amount at 15 Min, mg	Amount at 30 Min, mg
Experiment 1	3.5	3.6	5.6
Experiment 2	7.0	7.0	6.9
Experiment 3	2.7	3.1	4.2
Experiment 4	6.1	6.1	3.1
Median	4.80 (24.00%)	4.85 (24.25%)	4.90 (24.50%)
Standard deviation	2.05 (10.2%)	2.12 (10.6%)	1.65 (8.25%)

The initial quantity in each experiment was 20 mg.

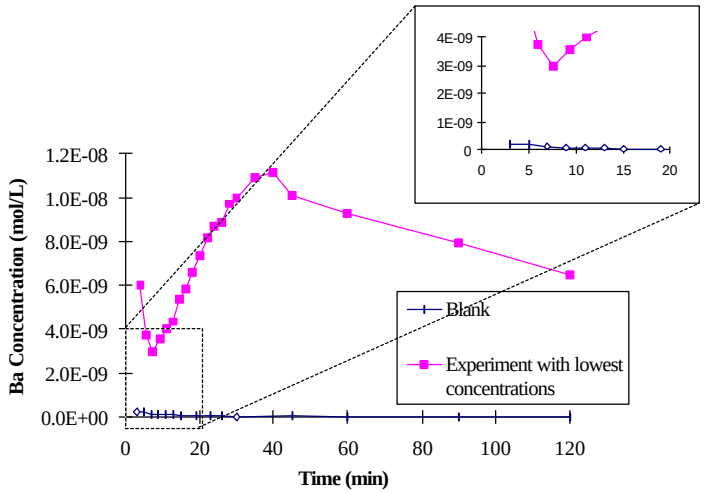

Figure 3. Dissolution concentration curves of the blank and nonblank experiments for Na and Ba

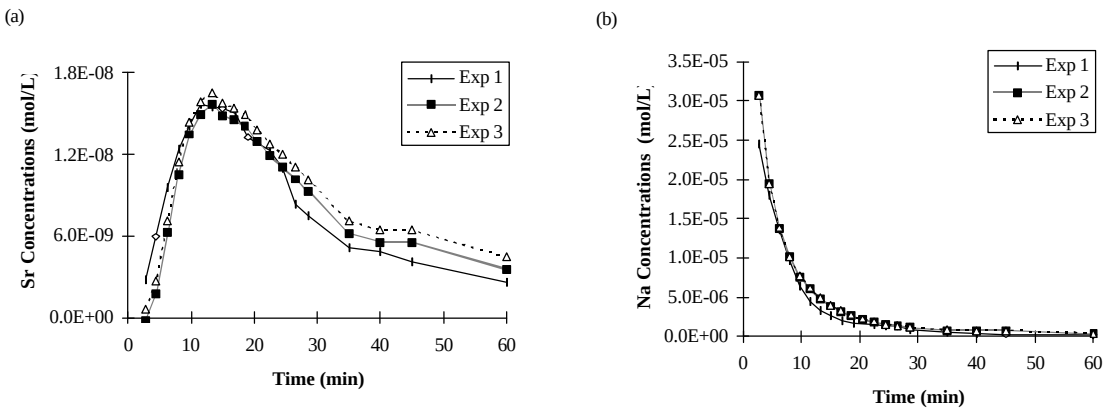

Figure 4. Example of reproducibility of three experiments carried out in the same conditions but at different days for (a) Sr, and (b) Na

The weathering solution initially contained water and acid. During the experiment other ions are released by particle dissolution, especially Na^+. The pH of the weathering solution was checked with a pH meter (0.02 units sensitivity) before the

Table 5. [Fe^{III}_{tot}] in Equilibrium With Ferrihydrite $Fe(OH)_3$ at Different pH Values

$Fe(OH)_3$	pH=3.8	pH=4	pH=4.3	pH=4.7	pH=5	pH=5.3
$Fe_{tot\ max}$, ppb	257.73	142.80	63.41	23.55	11.72	6.04
$Fe_{meas\ max}$, ppb	2.65	4.54	5.01	7.04	7.48	4.78

Log Ks = 3.96 [*Stumm and Morgan*, 1996].

experiment, after 30 min, and again at the finish of each experiment. The pH did not vary between entry and exit of the reactor and matched the anticipated pH values after dilution of the raw solution. We compared the H^+ concentrations with respect to the concentrations of other major cations as a function of time during the experiments (Table 3). The results show that H^+ is not the major ion after 1 min, but it becomes dominant at 30 min.

3.3. Reproducibility

Some fraction of the loess adhered to the top filter during the experiment. Several experiments were carried out to test this issue. The filter was removed from the system, dried, and weighed after 7, 15, and 30 min. The filter caught 10 to 30% of loess (Table 4). Three replicate experiments were carried out, and the maximum difference between concentrations found in the outgoing solution was ~ 5% for the first 30 min and ~ 15% at the end of the experiments (Figures 4a and 4b). In this last case, the concentrations were close to the detection limits and were prone to greater analytical errors. From these results, we deduced that the amounts of captured loess on the filter did not significantly affect the measured dissolution rates.

3.4. Dissolution Equilibrium

For the elements studied here, the solubility product was never reached with the possible exception being Fe^{III} with respect to crystalline oxo hydroxy salts. *Faust and Hoigné* [1990] and *Flynn* [1984] showed that the very insoluble crystalline forms of Fe^{III} salts (especially FeOOH, Goethite) are dissolved or formed too slowly. These salts do not affect our experiments that were completed after 120 min. *Faust and Hoigné* [1990] and *Flynn* [1984] also showed that amorphous hydroxides can interfere with equilibrium conditions. Thus, to prove that our cell operated well below the saturation limit, we made several calculations to evaluate the more probable amorphous form, that is, $Fe(OH)_3$ (ferrihydrite).

The relevant equilibria at 25°C are (Stumm and Morgan, 1996; Turner et al., 1981):

$Fe(OH)_{3(solid)} + 3\ H^+ = Fe^{3+} + 3\ H_2O$ $\quad \log K_S = 3.96$ (2)

$Fe^{3+} + H_2O = FeOH^{2+} + H^+$ $\quad \log \beta_1 = -2.19$ (3)

$Fe^{3+} + 2H_2O = Fe(OH)_2^+ + 2H^+$ $\quad \log \beta_2 = -5.67$ (4)

$Fe^{3+} + 3H_2O = Fe(OH)_3^0 + 3H^+$ $\quad \log \beta_3 = -12.0$ (5)

$Fe^{3+} + 4H_2O = Fe(OH)_4^- + 4H^+$ $\quad \log \beta_4 = -21.6$ (6)

$Fe^{3+} + Cl^- = FeCl^{2+}$ $\quad \log \beta_{Cl} = 1.48$ (7)

The chloride complex is negligible $\beta_{Cl}[Cl^-]<1$ thus

$$[Fe_{tot}] = [Fe^{3+}] + [FeOH^{2+}] + [Fe(OH)_2^+] + [Fe(OH)_3] + [Fe(OH)_4^-]$$

$$[Fe_{tot}] = [Fe^{3+}]\,(1 + \beta_1 [H^+]^{-1} + \beta_2 [H^+]^{-2} + \beta_3 [H^+]^{-3} + \beta_4 [H^+]^{-4})$$

and

$$[Fe^{3+}]_{max} = Ks\,[H^+]^3$$

$$\log [Fe_{tot}]_{max} = \log Ks + \log \left(10^{-3pH} + 10^{\log\beta 1 - 2pH} + 10^{\log\beta 2 - } \right.$$

$$\left. + 10^{\log\beta 3} + 10^{\log\beta 4 + pH}\right)$$

Table 5 gives [Fe_{tot}]$_{max}$ for the pH values of interest to our study. Note that in the range of the studied pH (3.80-5.30), Fe^{III} is always undersaturated with respect to solid $Fe(OH)_3$. This result suggests that Fe^{III} concentrations in our experiments were not affected by salt formation.

4. Results and Discussion

4.1. Dissolution Rate

When plotting reaction rate versus time, two types of curves were obtained, that is, a bell-shaped curve for Mg, K, Ca, Mn, Sr and Ba (Figure 5a) or an experimental decrease in the dissolution rate to relatively low values for Na, Si, Fe, and Cu (Figure 5b). Although the results from long-term dissolution studies are not specifically relevant to aerosol dissolution, these studies also showed similar initially high dissolution rates, such as a parabolic rate law in the case of batch reactor experiments [*Wollast*, 1967; *Luce et al.*, 1972; *Lagache*, 1976; *Holdren and Berner*, 1979; *Schott et al.*, 1981; *Holdren and Speyer*, 1985; *Tole et al.*, 1986; *Carroll-Webb and Walther*, 1988]. In order to explain the parabolic dissolution kinetics, two different mechanisms have been proposed. First, it was assumed that the rate of weathering was controlled by a surface layer through which the reactants and reaction products diffused [*Wollast*, 1967; *Luce et al.*, 1972; *Paces*, 1973; *Chou and Wollast*, 1984; *Wollast and Chou*, 1985; *Holdren and Speyer*, 1985]. Second, surface controlled dissolution of fine-grained material, high-

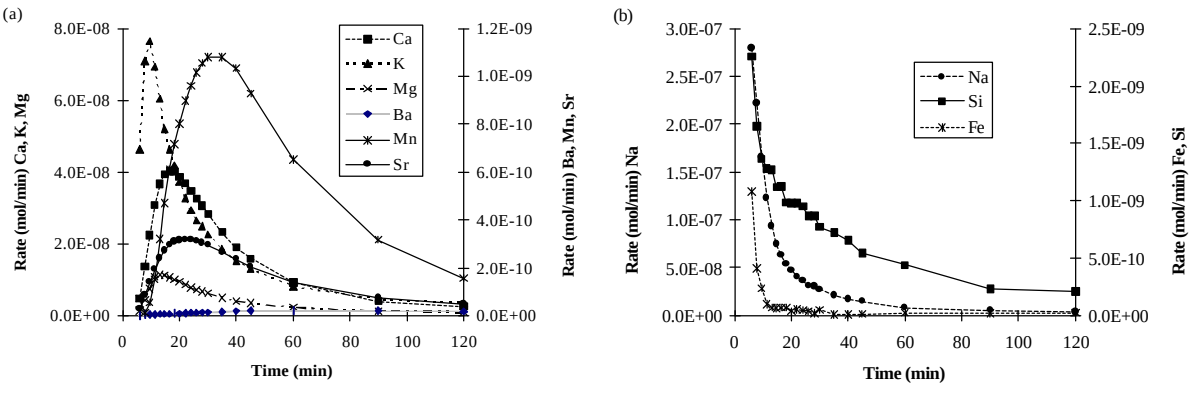

Figure 5. Shapes of dissolution rate curves for the elements: (a) bell shaped dissolution curves at pH 4.7, showing initially strong increasing dissolution rates followed by a gradual decrease, and (b) monotonically decreasing dissolution rates at pH 4.7.

strain areas on large grains, defects and grain boundary diffusion [*Holdren and Berner*, 1979; *Schott et al.*, 1981; *Petrovich*, 1981, *Helgeson et al.*, 1984; *Lasaga*, 1984] were assumed.

To explain the bellshape of our curves, we applied the surface complex-controlled dissolution approach by *Stumm and Furrer* [1987], *Stumm and Wollast* [1990], and *Stumm and Morgan* [1996]. The surface of hydrous oxides and hydrated silicates contains hydroxyl surface groups that are able to coordinate with H^+ and OH^-, that is, surface protonation and deprotonation. Surface protonation polarizes, weakens, and tends to break the critical metal-oxygen lattice bonds enabling the detachment of central metal cations that enter the solution. Dissolution reactions may start as an attack by protons of the mineral surface preferentially at points of excess surface energy. A simple scheme of the proton adsorption can be proposed to explain the increased rates:

$$k'_H = [H^+]^n \, k_H$$

$$[S\text{-}X] + nH^+ \rightarrow [SH_n\text{-}X] \quad (8)$$

$$[SH_n\text{-}X] \xrightarrow{k_L} S_{aqueous} + nH^+ + X \quad (9)$$

the dissolution rate during the first phase of dissolution, when the rates increase can be written as

$$R = k_L[SH_n\text{-}X]$$

Assuming a first order law for [S-X] in reaction (8)

$$d[SH_n\text{-}X] / dt = k'_H ([S\text{-}X]_0 - [SH_n\text{-}X]_t)$$

$$R = k_L[S\text{-}X]_0(1 - e^{-k'_H t}) \quad (10)$$

where

R the dissolution rate (mol cm^{-2} min^{-1});
k_L the rate constant of X release (min^{-1});
$[S\text{-}X]_0$ number of the free surface sites for t = 0 (mol cm^{-2});
k_H and k'_H the rate constant and the apparent rate constant of surface protonation, respectively.

In this scheme, increasing dissolution rates at the front of the bell-shaped curve are caused by the exchange of H^+ at the surface. H^+ is not always the major cation in the solution (Table 3), and a contribution of Na^+ to ion exchange cannot be excluded. During the initial phase, fast surface protonation is followed by the slow and rate-determining release of element from mineral. The dissolution of amorphous rather than crystalline minerals probably dominates the earliest dissolution. After this first stage, either of the two previously mentioned hypotheses might explain the decrease in dissolution rates because the hydrated layer thickens or the surface reactivity is reduced by the complete dissolution of fine grains.

As both bell-shaped and monotonically decreasing curves are obtained, it appears that some elements are more prone to go into solution than others. The monotonic curves for Na, Si, Fe, and Cu could be interpreted as bell-shaped but with k'_H too high for observation. Copper and iron are mostly in amorphous fraction of loess and should be highly reactive. Silicon comes from the mineral lattice or from amorphous SiO_2 at the surface. Sodium may be released swiftly because of rapid exchange of

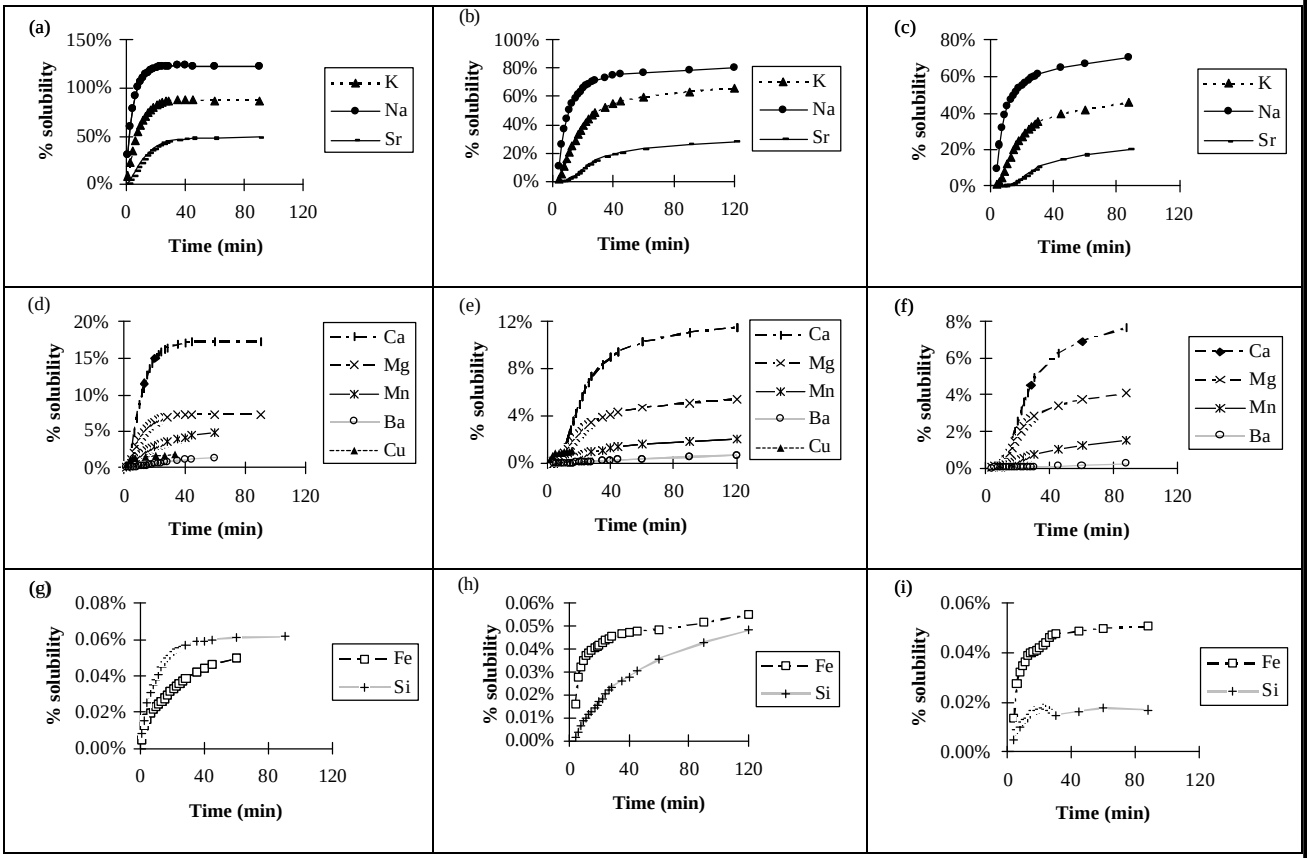

Figure 6. Evolution of the element solubility shown as solubility percentage versus time for the analyzed elements at (a), (d), and (g) pH 4, (b), (e), and (h) pH 4.7, and (c), (f), and (i) pH 5. The value larger than 100% for Na at pH 4 is due to uncertainties for the total Na concentration in the sample (Table 1).

protons at feldspar surfaces and by dissolution of halite crystals.

The relative rate of release of the elements can be expressed as the percentage of the accumulated dissolved mass at the end of each experiment. The observed sequence of increasing solubility becomes Si < Fe < Ba <Mn < Mg < Ca < Sr < K < Na (Figure 6). This relative order was also obtained by *Hoffmann et al.* [1997] for the same elements, and for Fe and Mn [*Spokes et al.*, 1994], in other dissolution experiments. Alkaline and alkaline-earth ions (Na, K, Mg, and Ca) inserted in the lattice dissolve more rapidly than other metals. Silicon, being the primary network constituent, is the least soluble. For all elements except Fe and Cu (Figure 6b, 6c, 6e, 6f, 6h, 6i), releases into the solution increase when pH decreases (Figure 6a-6i). This is in agreement with our proposed hydration mechanism. It also partially explains the different levels found in rainwater, which *Spokes et al.* [1994] pointed out.

The elements have different hydration reactivity as shown by the shift of maxima of bell shaped dissolution curves as a function of time. Fe and Si are released slower than the other elements. They exhibit monotonic dissolution behavior, suggesting that the hydration process is very fast and is well-advanced before we collected the first sample. This behavior supports the hypothesis that Fe and Si are dissolved from an amorphous phase. For Fe, this is in good agreement with the presumed nonreactivity of crystalline oxo-hydrated salts.

4.2. The pH Influence

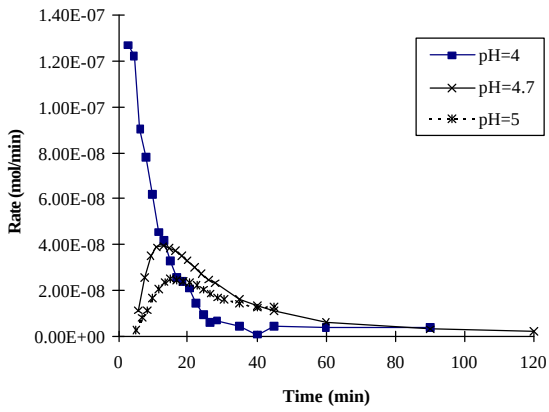

Figure 7. Examples of the effect of pH on Ca dissolution curves. Evolution of bell shaped curve toward monotone curve as pH decreases.

Na, Mg, Si, K, Ca, Mn, Sr, and Ba dissolution and hydration rates generally increase with decreasing pH. Moreover, the shapes of the dissolution curves become monotonic at pH 4.00 for all elements (as shown for Ca in Figure 7). This is in good agreement with the increase of the protonation step expressed in (8) and (10): at pH 4.00, the protonation rate is too fast to be observed and occurs before the first sample collection. The Fe and Cu curves have similar shape and do not exhibit large variations in the range of pH studied (Figure 8a and 8b; see below).

The pH dependency of dissolution can be explained by the approach outlined above, as the apparent rate constant decreases with decreasing pH. The value of k'_H was calculated for pH 4.70 and 5.00 in the step of increasing dissolution rate for the experiments that produced the bell-shaped curves, assuming constant k_L:

$$\frac{dR}{dt} = -k_L [S\text{-}X]_o \, k'_H e^{-k'_H t}$$

$$\ln\left(\frac{dR}{dt}\right) = \ln (k_L [S\text{-}X]_o \, k'_H) - k'_H t$$

The plot of $\ln\left(\frac{dR}{dt}\right) = f(t)$ is used to calculate k'_H, the slope of the linear regression (Table 6) at two different pHs. The exponent n is then calculated as

$$n = \log [(k'_{H1} / k'_{H2}) / (pH_2 - pH_1)]$$

Table 6. Calculation of the k'_H Hydration Constant (min^{-1}) of Mineral Surface Sites and *n* Values

	pH	Ba	Ca	Mg	Mn	Sr
k'_H	4.7	0.2667	0.0650	0.1068	1.2269	0.1298
	5	0.1011	0.0446	0.0631	0.1752	0.1051
n		1.4	0.55	0.75	2.81	0.3

The n value is the parameter of affinity of these sites with protons obtained from the ln (dv/dt) = f(t) plots.

Between pH 4.70 and 5.00, k'_H decreases, and n is positive (Table 6). It is interesting to note that the pH dependency of the rate constants follows, at least qualitatively, the pH dependency of mineral solubility. Thus n values in the range [0.3 - 2.81] are found to decrease for elements in the same column of the periodic table, that is. Mg to Sr (see Table 6). The results emphasize that the affinity of a mineral to form complexes with H^+ varies according to the elements that compose this mineral. The elements with the highest percentages of release have the lowest values of n, and they require the exchange of less H^+ to be leached (Ca < Mg < Mn). However, keeping in mind that only two points were used to calculate n, the values in Table 6 are only approximations.

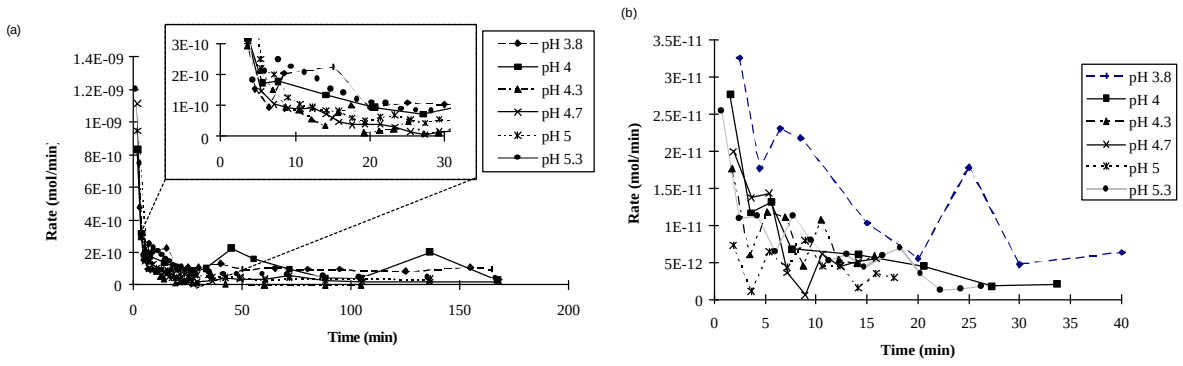

Figure 8. Effect of pH on the shape of the dissolution curve for (a) Fe and (b) Cu. The influence of pH is less obvious than for the others elements.

Figure 7 shows that the dissolved rate for calcium is much faster at the beginning for pH 4.00 than at higher pH. Yet the curve for pH 4.00 crosses the high pH curves after 10 to 20 min and then becomes lower. To point out the effects of varying pH values on dissolution rates, a more useful parameter for comparison will be the reaction progress ξ defined as

$$\xi = \int_{tin}^{t} R \; dt$$

Using equation (1) for R,

$$\xi = \int_{tin}^{t} \left(C(t)F + V\frac{dC}{dt} \right) dt = F \int_{tin}^{t} C(t)dt + V \int_{tin}^{t} \frac{dC}{dt} dt$$

$$\xi = F \int_{tin}^{t} C(t)dt + V\,[C(t)-C(t_{in})]$$

Thus the total amount of dissolution of particulate phase can be calculated for different times:

$$R = C(\xi)\,F + V\,\Delta C/\Delta t$$

We express the percentage of *x* dissolved as

$$(x)_{dissolved}\,\% = \frac{\xi\, Mx}{0.020\; Pc(x)}$$

where

ξ	reaction progress in moles;
M*x*	atomic mass of element *x* (g mol^{-1});
0.020	amount of loess introduced in the reactor (g);
Pc(*x*)	percentage of *x* in the loess (Table 1).

Fe and Cu dissolution are cast in this form and shown in Figure 9. Early Fe dissolution increases uniformly with pH (Figure 9a). Note that later fractions reach a minimum rate at pH 4.3, suggesting that two different dissolution mechanisms operate over longer periods of time; at pH > 4.3 and at pH < 4.3. The same behavior can be inferred for Cu with a rate minimum between pH 4.5 and 5 (Fig. 9b). These observations suggest that Cu and Fe are released by different mechanisms at the beginning and at the end of the experiment. This probably reflects two different mineralogical forms of Cu and Fe in the loess sample. The first form that was regularly influenced by pH changes is probably an amorphous phase which seems to be completely removed after several minutes of dissolution.

The dissolution rate law can be obtained by adding both mechanisms:

$$R = k[H^+]^a + k'[H^+]^{-b} \qquad (11)$$

$$\log R = \log \left(k[H^+]^a + k'[H^+]^{-b}\right)$$

with two different situations.

1. If $k[H^+]^a << k'[H^+]^{-b}$; log R = log k' + b pH**.** This equation represents the part of the line with positive slope. As the H^+/OH^- equilibrium is always very fast, we obtain $k'[H^+]^{-b} = k'\,K_w^{-b}\,[OH^-]^b$ to emphasize reaction control by OH^-s (K_w is the equilibrium constant of water ionic dissociation).
2. If $k[H^+]^a >> k'[H^+]^{-b}$; log R = log k - a pH. This equation represents the part of the line where the slope is negative. The reaction is controlled by protons.

The best fit with rate laws and the rate coefficients are given in Table 7. Similar compound rate laws describing mineral dissolution have been summarized by *Stumm and Morgan* [1996] who introduced the zêta pH of a mineral (pH_{pzc}). Typically, the proton-controlled mechanism dominates dissolution at pH < pH_{pzc}, and hydroxyl-controlled dissolution dominates the overall dissolution at pH > pH_{pzc}. A similar pH-dependence law was also reported by *Brady and Walther* [1989], who considered the detachment rates of the silicate oxide components through surface protonation-deprotonation reactions. The pH_{pzc} estimated from our rate measurements ranges between pH 4.2 and 4.7 for Fe and between pH 4.6 and 5.1 for Cu. The point of zero charge of the mineral depends on the pH, the concentrations of all ions, the degree of hydration, and the degree of crystallinity of the dissolving solids [*Stumm and Morgan*, 1996]. The differences found for pH_{pzc} are probably explained by different hydrated oxides and minerals that contain the studied elements.

Table 7. Values of Kinetic Parameters of Copper and Iron Dissolution as a Function of pH Values at Different Solubility Percentages

Solubility, %	a	log k	b	log k'
		Cu		
0.64	0.90	-8.45	0.80	-16.46
0.77	0.81	-8.96	0.65	-15.71
0.91	1.14	-7.73	0.67	-16.11
		Fe		
0.03	1.43	-5.44	1.91	-19.77
0.04	1.03	-7.32	0.62	-14.30
0.05	1.55	-5.42	0.69	-15.10

The k value is expressed in $min^{-1}mg^{-1}$.

Table 8. Kinetic Parameter Values for Ba, Ca, K, Mg, and Sr Dissolution as a Function of pH Values at Different Solubility Percentages

Element	Solubility, %	a	log k
Ba	0.06	1.35	-5.6
	0.12	1.47	-5.0
	0.16	0.45	-9.9
	0.50	0.71	-8.8
Ca	0.74	0.79	-5.0
	2.64	0.71	-5.3
	4.75	0.72	-5.4
	6.33	0.75	-5.4
K	0.47	0.73	-5.3
	0.58	0.77	-5.2
	0.69	0.82	-5.0
	0.79	0.87	-4.8
Mg	0.41	0.76	-5.5
	1.37	0.77	-5.4
	2.48	0.74	-5.7
	3.53	0.77	-5.6
Sr	4.52	0.74	-7.4
	8.90	0.71	-7.6
	13.82	0.75	-7.4

The k value is expressed in $min^{-1}.mg^{-1}$.
The K percent solubility is low in respect to the maximum percent solubility, because the total reaction curves are very different.

For the other elements, rates decrease with increasing pH, and no hydroxyl-controlled dissolution is observed (Figures 10a-10e), suggesting that the pH_{pzc} point for these elements is greater than 5.30. Rate coefficients for these elements are shown in Table 8. The behavior of Mn is somewhat of an exception with a break of slope at pH 4 (see Fig. 10 f) that was also observed by *Statham and Chester*

[1988]. The composite rate law cannot be applied because the point at pH 4 corresponds to a maximum.

5. Conclusion

An open flow reactor was used to study the aerosol dissolution in atmospheric waters. The simultaneous measurements of the elements Na, Mg, Si, K, Ca, Mn, Fe, Cu, Sr, and Ba allowed us to model the mechanistic steps involved in the weathering of Saharan derived dust aerosol weathering. Our primary observations are as follows:

1. Aqueous dissolution is a two-stage process. The first step consists of an attack by H^+ or OH^- of an amorphous and a crystalline phase. We have quantified this protonation by measuring hydration constants k'_H, which characterize the fixation of protons on surface sites. This allowed us to model the interactions between the particulate and the aqueous phases at the onset of cloud droplet condensation.

2. We have measured the release variations of these elements as a function of pH ranging from 3.80 to 5.30 and found that Fe appears to be the least soluble element after Si, which is in good agreement with the previously observed trends [see *Spokes et al.*, 1994].

3. The pH has a critical role in the dissolution of elements. Typically, a decrease in pH will accelerate dissolution. For the transition metals Fe and Cu, a compound rate law operates: protons control the dissolution at acid pH, and hydroxyls control the dissolution at less acid pH. The operation of a compound rate law points to the necessity to cover a large interval of pH values and does not allow the extrapolation from experimental results obtained at lower pH values.

The study reported here has exposed aerosol analogs to conditions similar to those encountered in clouds during their condensation phase. These results provided a first mechanistic approach to understanding aerosol dissolution in cloud droplets, and they offer a fundamental basis for modeling of the fluxes of dissolved elements, particularly trace metals, from mineral aerosols. This work also showed that the solubility is predictable in terms of the pH/solubility relationship, which is important to qualify and quantify the chemistry of trace metals in the atmospheric aqueous phase and so their role in models of atmospheric chemistry [see *Berglund and Elding*, 1995; *Walcek et al.*, 1997, *Losno*, 1999]. The identification of the atmospheric mechanisms which control the trace metals input due dissolved-particulate distributions contributes to characterizing the atmospheric fluxes in the world's oceans. Future research on the complete evaporation-condensation cycles and their incorporation in photochemical cloud models will be critical.

Acknowledgments. We acknowledge the reviewers of this paper for their useful and constructive comments. We would like to thank Franz Rietmeijer of University of New Mexico for his English assistance.

References.

Anderson, M.A., and M.M. Morel, The influence of aqueous iron chemistry on the uptake of iron by the coastal diatom Thalassiosira Weissflogii, *Limnol. Oceanogr., 27*, 789-813, 1982.

Bergametti, G., Apports de matière par voie atmosphérique à la Méditerranée occidentale: Aspect géochimique et météorologique, Thèse doctoral, Univ. Paris VII, Paris, 1987.

Berglund, J., and L. I. Elding, Manganese-catalysed autoxidation of dissolved sulfur dioxide in the atmospheric aqueous phase, *Atmos. Environ., 29*, 1379-1391, 1995.

Berresheim, H., and W. Jaeschke, Study of metal aerosol systems as a sink for atmospheric SO_2, *J. Atmos. Chem., 4*, 311-334, 1986.

Betzer, P.R., et al., Long-range transport of giant mineral aerosol particles, *Nature, 336*, 568-571, 1988.

Boutron, C.F., C.C. Patterson, and N.I. Barkov, The occurrence of zinc in Antartic ancient ice and recent snow, *Earth Planet. Sci. Lett., 101*, 248-259, 1990.

Brady, P.V., and J.V. Walther, Controls on silicate dissolution rates in neutral and basic pH solutions at 25°C, *Geochim. Cosmochim. Acta, 53*, 2823-2830, 1989.

Brand, L.E., W.G. Sunda, and R.R.L.Guillard, Limitations of marine phytoplankton reproductive rates by zinc, manganese, and iron, *Limnol. Oceanogr., 28*, 1182-1198, 1983.

Bruno, J., I. Casas, and I. Puigdomènech, The kinetics of dissolution of UO_2 under reducing conditions and the influence of an oxidized surface layer (UO_{2+x}): Application of a continuous flow-through reactor, *Geochim. Cosmochim. Acta, 55*, 647-658, 1991.

Carroll-Webb, S.A., and J.V. Walther, A surface complex reaction model for the pH-dependence of corundum and kaolinite dissolution rates, *Geochim. Cosmochim. Acta, 52*, 2609-2623, 1988.

Chou, L., and R. Wollast, Study of the weathering of albite at room temperature and pressure with a fluidized bed reactor, *Geochim. Cosmochim. Acta, 48*, 2205-2218, 1984.

Clarke, A.G., and M. Radojevic, Oxidation of SO_2 in rainwater and its role in acid rain chemistry, *Atmos. Environ., 21*, 1115-1123, 1987.

Colin, J.L., J.L. Jaffrezo, and J.M. Gros, Solubility of major species in precipitation: Factors of variation, *Atmos. Environ., Part A, 24*, 537-544, 1990.

Coudé-Gaussen, G., P. Rognon, G. Bergametti, L. Gomes, B. Strauss, J.M. Gros, and M.N. Le Coustumer, Saharan dust over Fuerteventura Island (Canaries): Chemical and mineralogical characteristics, air mass trajectories and probable sources, *J. Geophys. Res., 92*, 9753-9771, 1987.

Coudé-Gaussen, G., P. Rognon, and M. Le Coustumer, Incorporation progressive de poussières sahariennes aux limons des îles orientales, *C.R. Acad Sci., Ser. II, 319*, 1343-1349, 1994.

De Baar, H.J.W., A.G.J. Buma, G. Jacques, R.F. Nolting, and P.J. Tèguer, Iron and manganese effects on phytoplankton growth, *Ber. Polarforschung, 65*, 34-43, 1989.

Duce, R.A., P.S. Liss, et al., The atmospheric input of trace species to the world ocean, *Global Biogeochem. Cycles, 5*, 193-259, 1991.

Faust, B., and J. Hoigné, Photolysis of FeIII-hydroxy complexes as sources of OH radicals in clouds, fog and rain, *Atmos. Environ., Part A, 24*, 79-89, 1990.

Flynn, C.M., Hydrolysis of inorganic iron (III) salts, *Chem. Rev., 84*, 31-41, 1984.

Graedel, T.E., C.J. Weschler, and M.L. Mandich, Influence of transition metal complexes on atmospheric acidity, *Nature, 315*, 240-242, 1985.

Graedel, T.E., M.L. Mandich, and C.J. Weschler, Kinetic model studies of atmospheric droplets chemistry, 2, Homogeneous transition metal chemistry in raindrops, *J. Geophys. Res., 91*, 5205-5221, 1986.

Helgeson, H.C., W.M. Murphy, and P. Aagaard, Thermodynamic and kinetic constraints on reaction rates among minerals and aqueous solutions, II, Rate constants effective surface area, and the hydrolysis of feldspar, *Geochim. Cosmochim. Acta, 48*, 2405-2432, 1984.

Herrmann, P., and G. Hänel, Wintertime optical properties of atmospheric particles and weather, *Atmos. Environ., 31*, 4053-4062, 1997.

Hoffmann, M.R., and S.D. Boyces, Catalytic autoxidation of aqueous sulphur dioxide in relationship to atmospheric systems, *Adv. Environ. Sci. Technol., 12*, 147-189, 1983.

Hoffmann, P., A.N. Dedik, F. Deutsch, T. Sinner, S. Weber, R. Eichler, S. Sterkel, C.S. Sastri, and H.M. Ortner, Solubility of single chemical compounds from an atmospheric aerosol in pure water, *Atmos. Environ., 17*, 2777-2785, 1997.

Holdren, G.R., and R.A. Berner, Mechanism of feldspars weathering, I, Experimental studies, *Geochim. Cosmochim. Acta, 43*, 1161-1171, 1979.

Holdren, G.R., and P.M Speyer, pH dependent changes in the rates and stoichiometry of dissolution of an alkali feldspar at room temperature, *Am. J. Sci., 285*, 994-1026, 1985.

Jacob, D.J., E.W. Gottlieb, and M.J. Prather, Chemistry of a polluted cloudy boundary layer, *J. Geophys. Res., 94*, 12975-13002, 1989.

Junge, C.E., The modification of aerosol size distribution in the atmosphere, final technical report, *Contract Da 91-591-EVC 2979*, U.S. Army, San Diego, 1964.

Junge, C., The importance of mineral dust as an atmospheric constituent, in *Saharan Dust: Mobilization, Transport, Deposition*, edited by C. Morales, pp. 49-60, John Wiley, New York, 1979.

Khemani, L.T., G.A. Momin, M.S. Naik, P.S. Rao, and P.D. Safai, Influence of alkaline particulates on the pH of cloud and rainwater in India, *Atmos. Environ., 21*, 1137-1145, 1987.

Lagache, M., New data on the kinetics of the dissolution of alkali feldspar at 200°C in CO_2 charged water, *Geochim. Cosmochim. Acta, 40*, 157-161, 1976.

Lantzy, R.J., and F.T. Mackenzie, Atmospheric trace metals: Global cycles and assessment of man's impact, *Geochim. Cosmochim. Acta, 43*, 511-525, 1979.

Lasaga, A.C., Chemical kinetics of water-rock interactions, *J. Geophys. Res., 89*, 4009-4025, 1984.

Lim, B., and T.D. Jickells, Dissolved, particulate and acid leachable trace metal concentrations in North Atlantic precipitation collected on the Global Change Expedition, *Global Biogeochem. Cycles, 4*, 445-458, 1990.

Losno R., Trace metals acting as catalysts in a marine cloud: A box model study, *Phys. Chem. Earth, 24*, 281-286, 1999.

Losno, R., G. Bergametti, and P. Buart-Ménard, Zinc partitioning in Mediterranean rainwater. *Geophys. Res. Lett., 15*, 1389-1392, 1988.

Losno, R., G. Bergametti, P. Carlier, and G. Mouvier, Major ions in marine rainwater with attention to sources if alkaline and acidic species, *Atmos. Environ., Part A, 25*, 763-770, 1991.

Lowe, J.A., M.H. Smith, B.M. Davison, S.E. Benson, M.K. Hill, C.D. O'Dowd, R.M. Harrison, and C.N. Hewitt, Physicochemical properties of atmospheric aerosol at South Uist, *Atmos. Environ., 30*, 3765-3776, 1996.

Luce, R.W., R.W. Bartlett, and G.A. Parks, Dissolution kinetics of magnesium silicates, *Geochim. Cosmochim. Acta, 36*, 35-50, 1972.

Maring, H.B., and R.A. Duce, The impact of atmospheric aerosols on trace metal chemistry in open ocean surface seawater, 1, Aluminium, *Earth Planet. Sci. Lett., 84*, 281-392, 1987.

Martin, J.H., and S.E. Fitzwater, Iron defiency phytoplankton growth in the north-east Pacific subarctic, *Nature, 331*, 341-343, 1988.

Martin J.H., et al., Testing the iron hypothesis in ecosystem of the equatorial Pacific ocean, *Nature, 371*, 123-129, 1994.

Mast, M.A., and J.I. Drever, The effect of oxalate on the dissolution rates of oligoclase and tremolite, *Geochim. Cosmochim. Acta, 51*, 2559-2568, 1987.

Nriagu, J.O., and J.M. Pacyna, Quantitative assessment of worldwide contamination of air, water and soils by trace metals, *Nature, 333*, 134-199, 1988.

Paces, T., Steady-state kinetics and equilibrium between ground water and granitic rock, *Geochim. Cosmochim. Acta, 37*, 2641-2663, 1973.

Patterson, C.C., and D.M. Settle, Review of data on eolian fluxes of industrial and natural lead to the lands and seas in remote regions on a global scale, *Mar. Chem., 22*, 137-162, 1987.

Petrovich, R., Kinetics of dissolution of mechanically comminuted rock-forming oxides and silicates, II, Deformation and dissolution of oxides and silicates in the laboratory and at Earth's surface, *Geochim. Cosmochim. Acta, 45*, 1675-1686, 1981.

Prospero, J.M., R.T. Nees, and M. Uematsu, Deposition rate of dissolved and particulate aluminium derived from Saharan dust in precipitation at Miami, Florida, *J. Geophys. Res., 92*, 14723-14731, 1987.

Pye, K., Loess, in *Eolian Dust and Dust Deposits*, pp. 198-265, Academic,San Diego, Calif., 1987.

Rich, H.W., and F.M.M. Morel, Availability of well-defined iron colloids to the marine diatom Thalaasiosira Weissflogii, *Limnol. Oceanogr., 35*, 652-662, 1990.

Rognon, R., G. Coudé-Gaussen, M. Revel, F.E. Grousset, and P. Pedemay, Holocene saharan dust deposition on the Cape Verde Islands: Sedimentological and Nd-Sr isotopic evidence, *Sedimentology, 43*, 359-366, 1996.

Römer, F.G., J.W. Viljeer, L. Van Den Beld, H.J. Slangewal, A.A. Veldkamp, and H.F.R. Reijnders, The chemical composition of cloud and rainwater. Results of preliminary measurements from an aircraft, *Atmos. Environ., 19*, 1847-1858, 1985.

Schnoor, J.L., Kinetics of chemical weathering: A comparison of laboratory and field weathering rates, in *Aquatic Chemical Kinetics*, edited by W. Stumm, pp 475-504, Wiley-Interscience, New York, 1990.

Schott, J., R.A. Berner, and E. Lennart Sjöberg, Mechanism of pyroxene and amphibole weathering, I, Experimental studies of iron-free minerals, *Geochim. Cosmochim. Acta, 45*, 2123-2135, 1981.

Slinn, W.G.N., Air-to-sea transfer of particles, in *Air-Sea Exchange of Gases and Particles, NATO ASI Ser.*, edited by P.S. Liss and W.G.N. Slinn, pp. 299-405, D. Reidel, Norwell, Mass., 1983.

Smith, S.V., and F.T. Mackenzie, Comments on the role of oceanic biota as a sink for anthropogenic CO_2 emissions, *Global Biogeochem. Cycles, 5*, 189-190, 1991.

Spokes, L.J., and T.D. Jickells, Factors controlling the solubility of aerosol trace metals in the atmosphere and on mixing into seawater, *Aquat. Geochem., 1*, 355-374, 1996.

Spokes, L.J., T.D. Jickells, and B. Lim, Solubilisation of aerosol trace metals by cloud processing: A laboratory study, *Geochim. Cosmochim. Acta, 58*, 3281-3287, 1994.

Statham, P.J., and R. Chester, Dissolution of manganese from marine atmospheric particulates into seawater and rainwater, *Geochim. Cosmochim. Acta, 52*, 2433-2437, 1988.

Stumm, W., and G. Furrer, The dissolution of oxides and aluminium silicates; Examples of surface-coordination-controlled kinetics, in *Aquatic Surface Chemistry*, edited by Werner Stumm, pp. 197-220, Wiley-Interscience, New York, 1987.

Stumm, W., and J.J. Morgan, Kinetics at the solid-water interface: Adsorption, dissolution of minerals, nucleation, and crystal growth, *in Aquatic Chemistry*, 3rd rd., edited by J.L. Schnoor and A. Zehnder, pp. 760-817, Wiley-Interscience, New York, 1996.

Stumm, W., and R. Wollast, Coordination chemistry of weathering: Kinetics of the surface-controlled dissolution of oxides minerals, *Rev. Geophys., 28*, 53-69, 1990.

Sunda, W.G., R.T. Barber, and S.A. Huntsman, Phytoplankton growth in nutrient rich seawater: Importance of copper-manganese cellular interactions, *J. Mar., Res., 39*, 567-586, 1981.

Tole, M.P., A.C. Lasaga, C. Pantano, and W.B. White, The kinetics of dissolution of nepheline ($NaAlSiO_4$), *Geochim. Cosmochim. Acta, 50*, 379-392, 1986.

Turner, D.R., M. Whitfield, and A.G. Dickson, The equilibrium speciation of dissolved components in freshwater and seawater at 25°C and 1 atm pressure, *Geochim. Cosmochim. Acta, 45*, 855-881, 1981.

Walcek, C.J., H.H. Yuan, and W.R. Stockwell, The influence of aqueous-phase chemical reactions on ozone formation in polluted and nonpolluted clouds, *Atmos. Environ., 31*, 1221-1237, 1997.

Warneck, P., *Chemistry of the Natural Atmosphere*, Academic, San Diego, Calif., 1989.

Weschler, C.J., M.L. Mandich, and T.E. Graedel, Speciation, photosensitivity, and reaction of transition metal ions in atmospheric droplets, *J. Geophys. Res., 91*, 5189-5204, 1986.

Williams, P.T., M. Radojevic, and A.G. Clarke, Dissolution of trace metals from particles of industrial origin and its influence on the composition of rainwater, *Atmos. Environ., 22*, 1433-1442, 1988.

Wollast, R., Kinetics of the alteration of K-feldspar in buffered solution at low temperature, *Geochim. Cosmochim. Acta, 31*, 635-648, 1967.

Wollast, R., and L. Chou, Kinetic study of dissolution of albite with a continuous flow-through fluidized bed reactor, in *The Chemistry of Weathering*, edited by Drever J.I., pp. 75-96, D. Reidel, Norwell, Mass., 1985.

Zhu, X., J.M. Prospero, F.J. Millero, D.L. Savoie, and G.W. Brass, The solubility of ferric ion in marine mineral aerosol solutions at ambient relative humidities, *Mar. Chem., 38*, 91-107, 1992.

Zhu, X., J.M. Prospero, and F.J. Millero, Diel variability of soluble Fe(II) and soluble total Fe in North African dust in the trade winds at Barbados, *J. Geophys. Res., 102*, 21297-21305, 1997.

Zhuang, G., Z. Yi, R.A. Duce, and P.R. Brown, Link between iron and sulphur cycles suggested by detection of Fe(II) in remote marine aerosols, *Nature, 355*, 537-539, 1992.

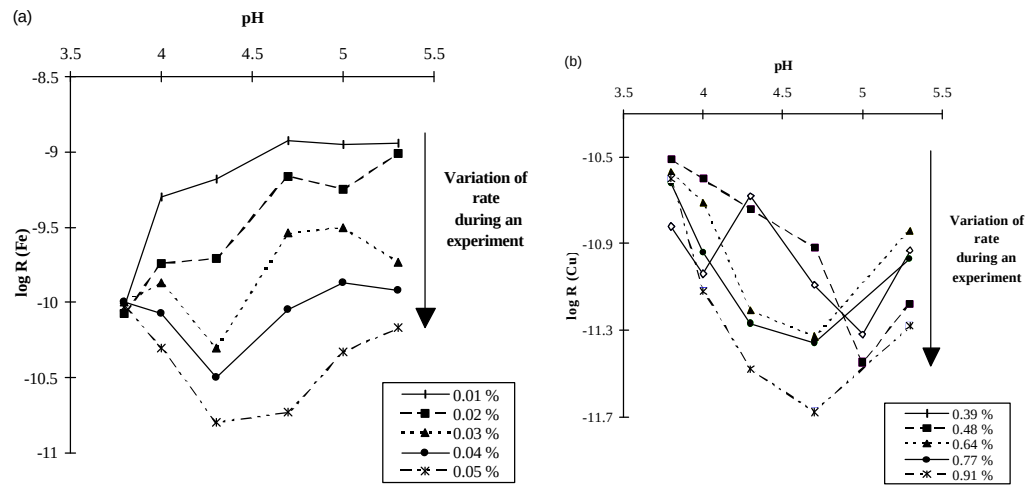

Figure 9. Evolution of release rate as a function of pH for different dissolved fractions and calculations of pH_{pzc} for (a) Cu and (b) Fe.

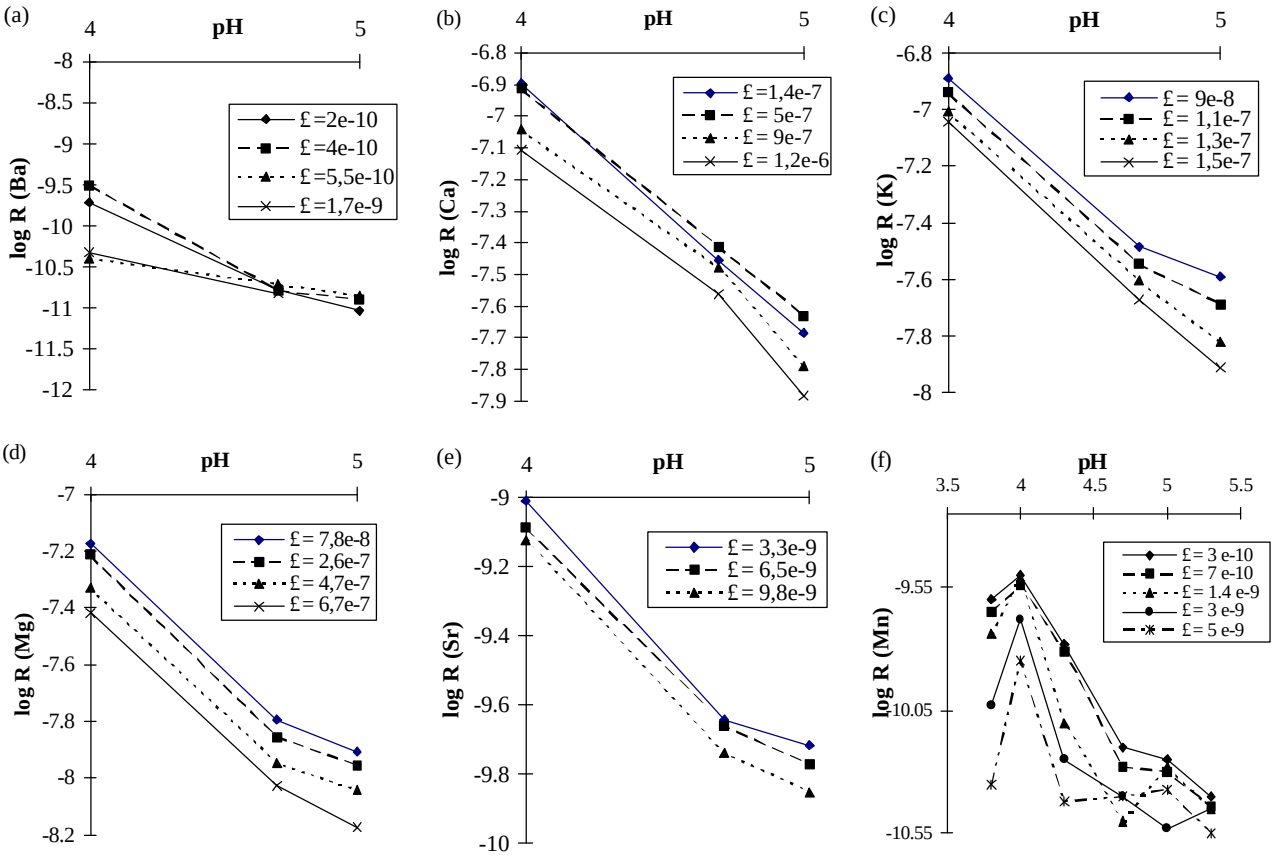

Figure 10. Evolution of dissolution rate as a function of pH for different dissolution steps, for (a) Ba, (b) Ca, (c) K, (d) Mg, (e) Sr, and (f) Mn.

8.3 Factors influencing aerosol solubility during cloud process

K. V. Desboeufs, R. Losno, and J. L. Colin
Laboratoire Interuniversitaire des Systèmes Atmosphériques (LISA), Universités Paris 7 et Paris 12, F 94010 Créteil cedex , France.
desboeufs@lisa.univ-paris12.fr
fax: 33 (1) 45-17-15-64

Abstract: The water-soluble fraction of the aerosol has a great importance for its chemical and physical properties. The aerosol origin and the atmospheric transport are known to influence the fraction of soluble material. In this study, cloud process simulations have been conducted on Saharan and Anthropogenic aerosols. The kinetic of solubilisation was followed and the results show that the solubility of the anthropogenic aerosol is notably higher than the mineral dust one. The investigation on the effect of condensation/evaporation cycles show that the wetting and drying steps increase the solubility of aerosol particles. The pH of the aqueous phase turns out to be the most important factor controlling the aerosol solubilisation and cloud processing. Thereby the alkalinity or acidity of the particles are closely related with the observed dissolution rates.

Keywords: Evaporation/condensation cycles, Weathering, Aerosol composition, pH, Heterogeneous chemistry

Introduction

Aerosols play a critical role in many atmospheric processes. Different species can be produced in the atmospheric aqueous phase as a consequence of the incorporation of water soluble substances contained in aerosol particles and by the dissolution of trace gases in cloud water. The acid rain event and the free radicals cycles depend upon the aqueous chemistry into the cloud droplets. Indeed, several studies emphasise that the dissolved transition metals ions have a potential to act as catalyst in process such as SO_2, O_3 and organic pollutants transformation (Hoffmann and Jacob, 1984; Graedel, et al., 1986; Weschler, et al., 1986; Martin, 1988; Jacob, et al., 1989; Erel, et al., 1993; Sedlak and Hoigné, 1993; Hoigné, et al., 1994; Matthijsen, et al., 1995; Sedlak, et al., 1997). Furthermore, atmospheric aerosols can affect climate via the role they play on the Earth's radiation budget. They can influence the radiative transfer by absorption and scattering of solar and terrestrial radiation, and by changing the optical properties of clouds through modification of the distribution of cloud condensation nuclei (CCN) (Charlson, et al., 1992). One of the paramount parameters which depends on the direct and indirect effect of dust is the water-soluble fraction (Ahr, et al., 1989; Eichel, et al., 1996; Levin and Ganor, 1996). Obviously, the aerosol solubility characterisation is crucial to understand the atmospheric impact of the aerosols particles on the Earth's atmosphere.

Several individual factors have an influence on the aerosol solubility. The aqueous phase pH and the particle mineralogical composition are the major ones (Gatz, et al., 1984; Moore, et al., 1984; Losno, et al., 1988; Statham and Chester, 1988; Colin, et al., 1990; Zhu, et al., 1992; Zhuang, et al., 1992; Chester, et al., 1993; Losno, et al., 1993; Spokes, et al., 1994; Spokes and Jickells, 1996; Gieray, et al., 1997; Ebert and Baechmann, 1998; Desboeufs, et al., 1999). During their transport in the atmosphere, aerosols sustain typically around 10 condensation/evaporation cycles (Pruppacher and Jaenicke, 1995). The aerosol resulting from evaporation of cloud droplets is likely to be quite different from that which entered the cloud, due to in-cloud processes. During their existence as cloud droplets, other particles are caught and mixed in the droplet. Therefore, a large fraction of the resulting aerosols should be a blend of various aerosol types. Alternatively, these cloud drops can take up water-soluble atmospheric trace gases such as HNO_3, SO_2 and NH_3, which could play on the amount of water soluble material, since they strongly modify the pH of the aqueous phase. If these drops evaporate in a dissipating cloud, a certain amount of the scavenged gases will presumably remain in the released aerosol particles as salts. When a cloud condensation nuclei grows into a cloud droplet, its soluble content dissolves in the condensed water, determining the initial composition of the droplet itself. Part of the dissolved fraction from the leached mineral will be deposited back on the particle surface during the evaporation step. Particles may result with significantly larger water-soluble fraction than those initially activated. Thus, cloud processes contribute to weather the particle and so modify its chemical and physical properties.

In this paper, we present results on the evolution of water soluble fraction versus the evaporation-condensation cycles for mineral and anthropogenic aerosols. We have conducted experimental dissolution and evaporation simulations in conditions probably encountered in clouds. We have determined the evolution of the dissolution rate as a function of simulated cloud processing.

Material and method

For this study, two types of aerosol particle are considered, one aerosol crustally dominated and one anthropogenic. The first one is a loess which simulates a Saharan aerosol like material. The sample was collected on the north-eastern part of Sal Island (Cape Verde Islands). They are the < 20µm diameter fraction of a dry segregated loess. The mineralogical and elementary composition of this solid phase are described in Desboeufs, et al. (Desboeufs, et al., 1999). According to BET method, the specific surface of this loess is 50.1 $m^2.g^{-1}$ (Boerensen, personal communication). The second aerosol used is fresh fly-ash (FA) from heavy fuel oil combustion. The granulometric fraction lower than 100 µm was used for the experiments. These particles were collected from the electrostatic filters of an electrical power plant. The chemical, granulometric and mineralogical characteristics of these fly-ash have been reported elsewhere (Ausset, et al., 1999). The elementary composition for the two studied aerosol types are resumed in Table 1.

Table 1: Elemental chemical composition (in weight %) of loess and fly-ash particles.

	Al %	Ba %	Ca %	Fe %	K %	Mg %	Mn %	Na %	Si %	Sr %
Loess	8.40	0.23	3.80	7.60	1.30	2.80	0.13	1.10	22.70	0.032
Fly-ash	1.40	0.03	1.26	3.50	0.06	0.12	0.03	1.46	3.70	0.03

Table 2: Recapitulative Table of experimental sets.

	Aerosol type		First cycle	Second cycle	Three cycle
Set 1	Loess	initial pH	4.7	4.7	4.7
		particulate charge	1.2 g	450 mg	200 mg
Set 2	Loess	initial pH	0.5	4.7	4.7
		particulate charge	1g	500 mg	200 mg
Set 3	Fly-ash	initial pH	4.7		
		particulate charge	100 mg		

The condensation is simulated by mixing aerosols with acidified MilliQ water. Then this mixture is placed in an evaporation reactor (Fig.1). The particulate charge used for the manipulations is 43.6 g/L. The evaporation time is extended in the range of 2 to 10 hours depending to the experimental conditions. The aerosols used can sustain up to three times this simulation protocol. This simulates several passages of aerosols in clouds. Three sets of condensation simulation are carried out. The first one corresponds with 3 successive experimental protocol for loess with H_2SO_4 to 10^{-5} $mol.L^{-1}$ (pH = 4.7). The second one is compound by a first condensation carried out on the original loess with H_2SO_4 to 0.3 $mol.L^{-1}$ (pH = 0.5) in order to limit the neutralising capacity of the mineral phase, and two wetting and drying cycles with H_2SO_4 to 10^{-5} $mol.L^{-1}$ (pH = 4.7). The third one corresponds with FA sustaining one condensation/evaporation protocol with H_2SO_4 to 10^{-5} $mol.L^{-1}$ (pH = 4.7). The H_2SO_4 is used to simulate the scavenging of gaseous SO_2 and further oxidation into H_2SO_4. Table 2 recapitulates the experimental sets.

These weathered aerosol are recuperated and their dissolution kinetic is studied according Desboeufs et al. (1999). Leaching experiments were carried out on 20 mg

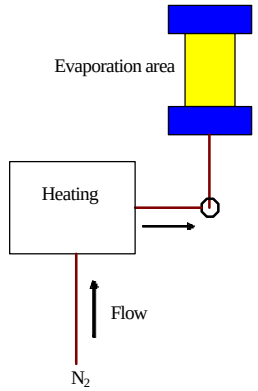

Figure 1: This reactor is compound by a polycarbonate cell in which the sample with acidified water are exposed to a hot N_2 flow. This bubbling enables to maintain the particle in suspension and to evaporate water. The N_2 flow is kept until all the liquid was evaporated, and the solid phase dried.

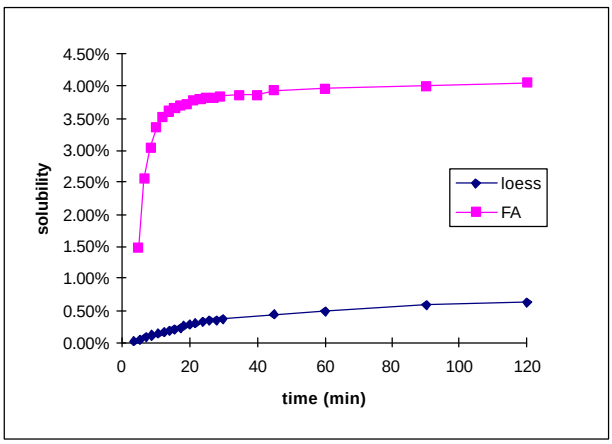

Figure 2: Comparison of mineral matrix solubility (Al, Fe and Si as oxides) for loess and fly-ash versus time in the case of pH 4.7 dissolution experiment.

of solid phase which correspond to 100 cm^2 of loess surface. The material was put in an open flow reactor, described in more detail elsewhere (Desboeufs, et al., 1999). The weathering solution was composed of Milli-Q™ water and ultra pure Prolabo™ Normatom® H_2SO_4 like acidifying agent. In addition, parallel experiments were carried out where pH was continuously measured.

The aliquots were analysed by ICP-AES (Inductive Coupled Plasma- Atomic Emission Spectrometry) method combined with an ultrasonic nebuliser.

Results and discussion

Fresh material solubility: Source and pH influence

Dissolution experiments were conducted on the original aerosols at pH 4.7, which is a median pH for cloud droplets (Li and Aneja, 1992). The solubility of mineral oxides as a function of time is shown in Fig. 2 for both aerosols types. The solubility % of all elements after 120 min. of leaching is given Table 3. The results show that for all the investigated elements, the solubility is clearly higher in the fly-ash compared to loess, except Na which is already very soluble in the loess. This clearly confirms what several studies have already emphasised, crustal aerosols are less soluble than marine or anthropogenic aerosols (Colin, et al., 1990; Jickells, et al., 1992; Spokes, et al., 1994; Ebert and Baechmann, 1998). This variability of solubility as a function of aerosol types has been rationalised in part using the solid state speciation (Jickells, et al., 1992; Chester, et al., 1993; Spokes, et al., 1994). The exchangeable association determines the extent of metals solubility (Chester, et al., 1993). For the fly-ash, all the elements present a high solubility (greater than 60 %) after 120 min., except for the matrix element i.e. Al, Si and Fe. Fly-ash particles are characterised by superficial enrichment of metals due to process associated with the combustion. This compositional heterogeneity can explain the rapid metal solubilisation, since metals are present as oxides or salts, whereas Al, Fe and Si are bound up as high-temperature alumino-silicates (Williams, et al., 1988). For the loess, the highest observed solubility is for Na, which a large fraction comes from marine source (Desboeufs, et al., 1999). The alkaline, the alkaline-earth and Mn are an intermediate solubility since they are the inserted elements in the aluminosilicate lattices. On the contrary, Al, Fe and Si constitute this mineral network, and so are nearly insoluble. These elements are respectively 430, 950 and 13times more soluble in FA than in loess. Indeed, it is possible that the mineral matrix is more soluble for the fly-ash than for loess, because of the cryptocristalline nature of fly-ash lattice (Jickells, et al., 1992). Although the exchangeability seems to be a determinant parameter, the surface could have also an effect to explain the different solubilities found for both aerosol types. We have not the specific surface of the fly-ash, however observations by Scanning Electron Microscopy (SEM) show a spongy or porous morphology for these ones (Ausset, et al., 1999). We can so suppose, despite a larger median diameter, that the FA surface is greater than the one of loess. Nevertheless, even if the exchange surface plays on the difference of aerosol solubility, this parameter can explain only in part the observed behaviours. The solubility difference between loess and FA corresponds with a factor around 1000 for Fe and only 10 for Si. Consequently, the surface effect cannot explain the solubility variation range. Thus, the main source effect is due to the chemical and mineralogical speciation of the elements.

Table 3: Solubility % of element after 120 min of leaching for loess and fly-ash.

	Al %	Ba %	Ca %	Fe %	K %	Mg %	Mn %	Na %	Si %	Sr %
Loess	0.1	0.5	8.1	0.04	46.1	6.1	2.0	88.5	0.06	29.9
Fly-ash	42.9	99.2	100	38.2	100	100	97	100	0.8	61

On the other hand, it has been established that the pH can play a significant role on the aerosol solubility (Maring and Duce, 1987; Prospero and Nees, 1987; Losno, et al., 1988; Statham and Chester, 1988; Colin, et

al., 1990; Losno, et al., 1993; Desboeufs, et al., 1999). Typically, a decrease in pH accelerates dissolution rates in the pH range of 3.8 to 5.3, except for Fe and Mn (Desboeufs, et al., 1999). With loess, during the leaching experiment, an increase of around 1 pH units is observed as a result of the neutralising capacity of minerals present within this material (Fig.3a). In contrast, the pH behaviour in the leaching experiments conducted with fly-ash, showed an initial pH decrease of 0.6 of a pH unit (Fig.3b). All these pH excursions are restrictive to the 20 first minutes of the leaching experiments. These data are in agreement with the field and laboratory observations concerning to the acidity and alkalinity of aerosol (Loÿe -Pilot, et al., 1986; Khemani, et al., 1987; Statham and Chester, 1988; Losno, et al., 1991). The loess sample present a significant acid neutralising capacity (ANC) caused by the probable carbonate liberation. This ANC has been measured by determination of carbonate release from the loess as a function of time (Fig.4). The concentrations of H_2CO_3 and HCO_3^- were thus estimated from the measurement of the pH of water used during the experiments and from the first dissociation constant of carbonic acid (Meites, 1963):

$CO_{2aq} = HCO_3^- + H^+$ $\quad K_{a1} = 10^{-6.4}$ (R1)

$HCO_3^- = CO_3^{2-} + H^+$ $\quad K_{a2} = 10^{-10.3}$ (R2)

Measured pH is always less than 6, the reaction (R2) is quantitative, but a fast acid-base equilibrium occurs for (R1)

$$[H^+]_{cons} = [H^+_{ini}] - [H^+_{meas}] = 2[CO_{2aq}] + [HCO_3^-] \quad (1)$$

Where $[H^+]_{cons}$, $[H^+_{ini}]$, and $[H^+_{meas}]$ are respectively the consumed H^+, the introduced H^+ and the remaining H^+ measured in the outflow of the reactor.

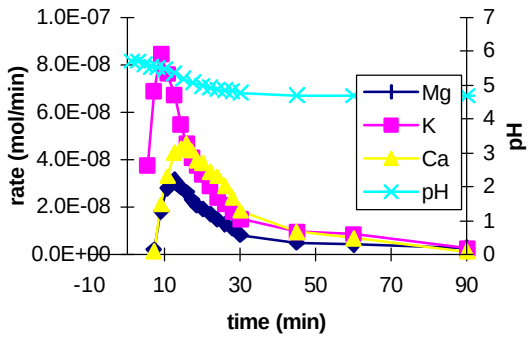

Figure 3a

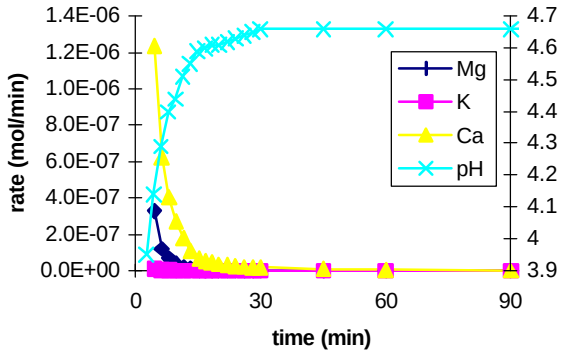

Figure 3b

Figure 3: Dissolution rate curves for Mg, K, Ca, and pH variation as a function of time for loess sample (a) and FA sample (b).

We have compared the evolution of the elementary dissolution rate and the pH variation (Fig.3a and 3b). For the loess leaching experiment, most of the elements present a bell-shaped curve (Fig.3a). Whereas the dissolution rate for the elements coming from FA decreases progressively (Fig.3b). The pH decreases when the dissolution rate of elements associated with mineral dust increase. On the contrary, for the fly-ash experiments, pH increase and no bell-shaped curve are obtained. We can suppose that the observed rate maximum is due in part to this pH decrease. However, the pH influence is not the only parameter determining the bell-shaped curve, since the leaching time of dissolution rate maximum widely depends upon the investigated elements. Thus, the source of the element is again a crucial factor to determine aerosol solubility, since the ANC of the aerosol govern in part the pH of the aqueous phase.

Effect of one condensation-Evaporation cycling

For pH 4.7 solution addition, the loess solubilisation releases carbonate ions which creates a larger pH increase of the aqueous phase than for leaching experiment because the amount of loess is much higher. If we suppose that the carbonates release is proportional to the aerosol concentrations, we can calculate the dissolved carbonates for process to pH 4.7. This amount is around 2.10^{-5} moles of carbonates, for an initial proton amount of $5.5\ 10^{-7}$ moles. It appears that the dissolved carbonates amount is higher than the one of protons. The aqueous phase pH is so controlled by the carbonates equilibrium. Consequently, the evaporation happens in an alkaline solution for these loess samples. Moreover, the experiments are under N_2 flow, which so removes CO_2 and makes the pH more alkaline than naturally in clouds for loess. On the

contrary for a pH 0.5 solution addition, pH measurements show that the pH is constant. All the loess alkalinity is neutralised since the H^+ amount is largely higher than the released carbonates. Thus, the loess simulation take place in an acidic medium. In the same way, the FA evaporation at pH 4.7 happens in the acidic medium, because these aerosol particles released acidifying agent. The aerosols source can plays directly on the solubility since it relates with the aerosol nature. According to these results, it could play also indirectly on this solubility since it can fix the aqueous phase pH via the alkalinity or acidity of the aerosol. Here, the simulations correspond to a neutral non-polluted cloud for the loess at pH 4.7 and an acidic polluted cloud for the loess at pH 0.5 and FA at pH 4.7.

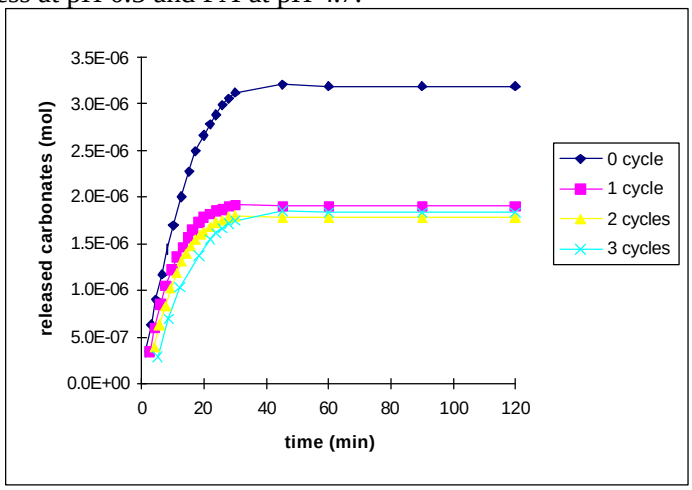

Figure 4: Solubilisation of carbonates over time from original Saharan aerosol or previously subjected to various evaporation/condensation cycles.

Table 4: Solubility % of element after 120 min of leaching for original loess and one cycle weathered loess

	Al %	Ba %	Ca %	Fe %	K %	Mg %	Mn %	Na %	Si %	Sr %
0 cycle	0.1	0.5	8.1	0.04	46.1	6.1	2.0	88.5	0.06	29.9
1 cycle basic	0.1	0.5	12.4	0.04	61.1	9.0	2.8	92.0	1.5	37.7
1 cycle acid	21.7	20.0	20.6	28.3	70.1	42.7	85.5	89.2	0.4	100

It appears that, in these conditions, the sum of silicates matrix solubility increases with one pH cycle (Fig. 5a, 5b and 5c). For the loess samples, the results are different according to the considered element. Several elements are showing a higher solubility after one cycle of alkaline evaporation: Ca, K, Mg, Mn, Si, and Sr (Table 5). This improvement of the solubility is included between 18 % (Si) and 55% (Ca). On the contrary, for Al, Ba, Fe and Na, the solubility is not modified by one condensation/evaporation cycle (Table 4). Na is already almost completely soluble, so its solubility cannot increase with the simulated cloud processes. In contrast, one cycle of acidic evaporation on the loess enables a significant increase of the solubility for all the elements except Si (Table 4). The Si is know to be more soluble in alkaline medium. This improvement of the solubility is included between 52% (K) and 70000% (Fe), and it is always greater than the one observed for the alkaline evaporation. The kinetics of dissolution observed further leaching experiments are also very different depending to the type of evaporation sustained by the loess. The results show that the bell-shaped curves persist with one alkaline wetting and drying cycle, and that the maxima are not significantly modified (Fig.6). Whereas for the acidic simulation the dissolution rate curves become monotone with a rapid decrease of dissolution rate in the first minutes (Fig. 7).

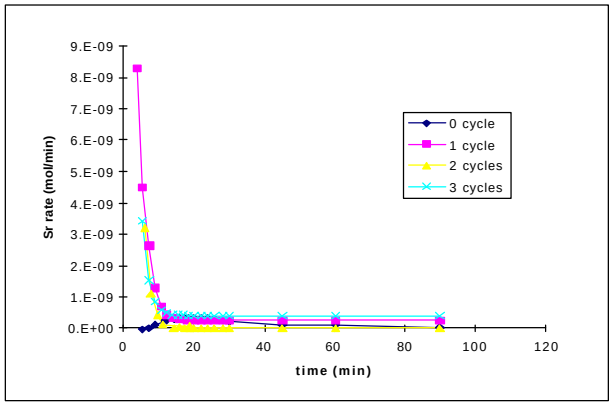

Figure 7: dissolution rate curves

Considering the results on the fresh aerosol particles, the ANC has been calculated from the measured pH during the leaching experiments. The released carbonates amount for the 0 cycle experiment is twice as great as for the experiment with mineral dust after one alkaline cloud process (Fig.4). For the loess sustaining an evaporation in acidic medium, the ANC is totally neutralising. The initial pH decreases of almost 1 pH unit, then the pH increases during the first minutes of the leaching experiment to reach again 4.7 (Fig. 8). A parallel behaviour is so obtained between acidified loess sample and FA, i.e. monotone dissolution curves are found with the pH increase. As we have seen earlier, pH plays on the dissolution rate and so on the solubility, it is therefore not surprising that an improvement of the solubility with the evaporation/condensation cycle is observed, and in particular with the acidic simulation. These results can be clarified in considering the conclusions of Desboeufs et al. (1999). A protonation mechanism was implied in the increasing rate phase. Here, we can suppose that the low initial pH improve the protonation step and when the pH increase, this step is slowed down, and the dissolution rate decrease. Thus the origin of the particles, in particular their initial capacity to influence pH, is a crucial parameter to understand their solubility.

No solubility change is observed for the elements classified as insoluble for the alkaline cycling simulation. In contrast, the solubility of these elements is completely modified in the acidic cycling simulation, their solubility is found around 20% higher, except for Si which remains insoluble. Moreover, the maxima of the bell-shaped curves was not influenced by this ANC change (Fig. 6) but is dependent on the considered elements. Thus, the response to the modification of the experimental protocol depends on the considered elements. The mineralogical nature and the chemistry of the elements seem to play also a role in the aerosol solubility change during the cloud process. If we compare the influence of pH and the one of the dissolved elements, we can try to conclude on the difference of solubility found for the alkaline and acidic evaporation. The more initial pH is low, the more mineralogical structure is disturbed, and more the solubility of the insoluble elements, containing in the mineral network, increases. However, if we consider that the mineralogical structure is higher modified, the specific surface effect can not be excluded. The specific surface has not been measured after the evaporation simulation, but it can also contribute to explain the solubility difference observed between the two dissolution experiments. Indeed, for the fly-ash, the effect of one cloud process is significantly positive for all the elements which have a solubility lower than 100%, except for Fe for which no solubility evolution is noted. No modification in the shape of dissolution rate curves is observed. Yet, the pH variations is not significantly modified between the 0 and 1 cycle experiments.

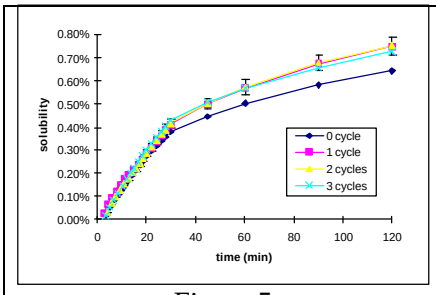

Figure 5a

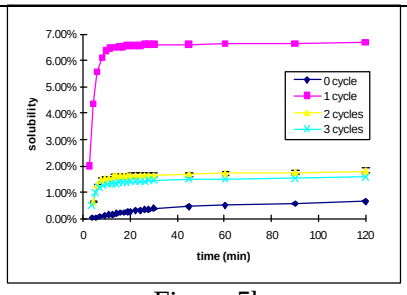

Figure 5b

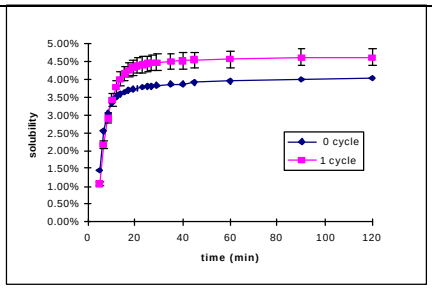

Figure 5c

Figure 5: Sum of major element expresed as oxides solubility over time by condensation/evaporation cycles from loess (a) and FA (b).

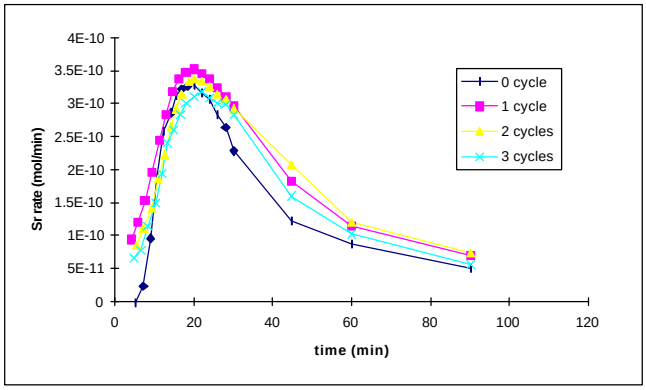

Figure 6: Dissolution rate over time for Sr from loess weathered or not.

Effect of several condensation-evaporation cycling

These experiments has been only carried out for the mineral dust sample. It appears that the solubility remains constant after several cycles in the case of alkaline evaporation (Fig. 5a). The dissolution rate curve shape are not modified in both alkaline and acidic simulation (e.g. Fig. 6). During the first cycle, The ANC of the aerosol seems to be a crucial factor playing on the solubilisation, since the carbonate release triggers off a pH variation. Here, the investigation on the ANC effect show that no significant change appears on the carbonates release between the different alkaline cloud processes (Fig. 4). The preceding conclusions on the role of the ANC of the aerosol are so supported. Moreover, as the ANC change appears only for the first cycle of alkaline evaporation, we can suppose that this ANC modification results from a mineralogical composition change. During the condensation/evaporation cycle, the dissolved elements are deposited back on the surface in a different way that in the original structure. This new surface structure enables a more rapid release of carbonates, and consequently the soluble-water fraction of the aerosol is modified. Concerning to the acidic cycles, the solubility decreases after the first acidic evaporation then remains constant (Fig. 5b). The pH variations during leaching of loess weathered has been also followed. It appears that they did not vary between the successive cycles (Fig. 8). Thus, as different from the alkaline evaporation, the pH measured during the leaching experiments can not explain the observed behaviour. The experimental protocol of the first cycle consists of a condensation with a pH 0.5 solution, whereas for the others cycles the condensation step is carried out at pH 4.7. The solubility seems to depend on the pH of the condensation step. We can so suppose that the initial pH water during the wetting and drying cycle determine the solubility of the aerosol. Since the solubility decreases between first and the other cycles, we can consider that the weathering is a reversible process, where the conditions prevailing into the droplets determine principally the water-soluble fraction for a type of particles. However, the 2 and 3 cycles of acidic evaporation give solubilities always greater than the various alkaline cycles despite the same pH of condensation solution. The only difference between these experiments is a first acidic or alkaline. Consequently, the history of the aerosols particles must be also considered to estimate the aerosol solubility. Finally, although the pH is the direct factor playing on the aerosol solubility, the observed change might be due to an indirect effect as a mineralogical surface modification.

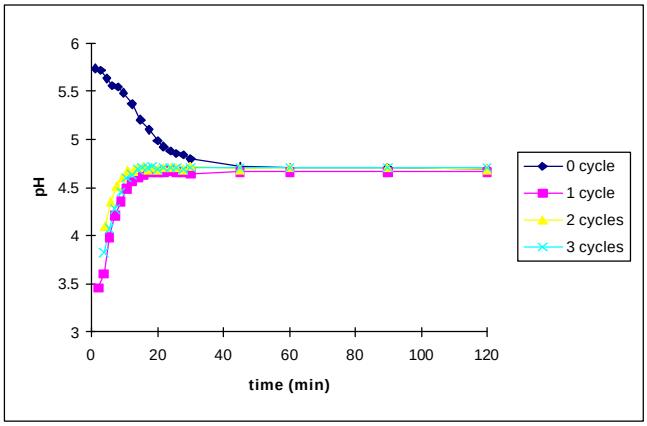

Figure 8: pH variations depending on the evapo-condensation cycle

Conclusion

Based on the results of the original or fresh aerosol dissolution, we were able to point out the importance of several factors acting on the aerosol solubility. We found that the solubility of crustal aerosols is lower than the fly-ash solubility for almost all the elements. The origin of aerosol particles was emphasised like a crucial factor playing on the aerosol solubility, since it governs the mineralogical nature and the aqueous phase pH. For one, we have determined effectively that the difference of solubility could be due to the mineralogical composition of particles by virtue of the exchangeability of elements. For another, the pH which is at least in part determined by the ANC of the aerosol, is a major control of the solubility. We found also that the solubility of aerosol weathered by one condensation/evaporation cycle is improved, all the more so as the condensation step is acidic.

Our results do not conclude on the atmospheric transport effect on aerosol solubility, but suggest, however, that the condensation/evaporation cycles influence the water-soluble fraction of the aerosol and so the CCN availability. We can provide some suggestions on the atmospheric events which could play on the aerosol solubility. The scavenging in the aqueous phase of gas species is a critical point, since it can modify the aqueous phase pH. Moreover, the incorporation in the aqueous phase of several types of aerosols could modify pH and liquid phase composition. The aerosol, generated after a cloud evaporation, could be completely different that the entering ones. Thus, our work will enhance the conclusions of the authors which have put forward the idea that the cloud process contributes to weather the particle and modify its hygroscopicity and its radiative properties (Ahr, et al., 1989; Pruppacher and Jaenicke, 1995; Eichel, et al., 1996).

References

Ahr, M. A., A. I. Flossman and H. R. Pruppacher, 1989. On the effect of the chemical composition of atmospheric aerosol particles scavenging and the formation of a cloud interstitial aerosol. J. Atmos. Chem. 9, 465-478.

Ausset, P., M. Del Monte and R. A. Lefèvre, 1999. Embryonic sulphated black crusts on carbonate rocks in atmospheric simulation chamber and in the field: Role of carbonaceous fly-ash. Atmos. Environ. 33, 1525-1534.

Charlson, R. J., S. E. Schwartz, J. M. Hales, R. D. Cess, J. A. Coakley, J. E. Hansen and D. J. Hofmann, 1992. Climate forcing by anthropogenic aerosols. Science 255, 423-430.

Chester, R., K. J. T. Murphy, F. J. Lin, A. S. Berry, G. A. Bradshaw and P. A. Corcoran, 1993. factors controlling the solubilities of trace metals from non-remote aerosols deposited to the sea surface by "dry" deposition mode. Marine Chem. 42, 107-126.

Colin, J. L., J. L. Jaffrezo and J. M. Gros, 1990. Solubility of major species in precipitation: Factors of variation. Atmos. Environ. 24A, 537-544.

Desboeufs, K., R. Losno, F. Vimeux and S. Cholbi, 1999. pH dependent dissolution of wind transported Saharan dust. J. Geophys. Res. 104, 21287-21299.

Ebert, P. and K. Baechmann, 1998. Solubility of lead in precipitation as a function of raindrop size. Atmos. Environ. 32, 767-771.

Eichel, C., M. Krämer, L. Schütz and S. Wurzler, 1996. The water-soluble fraction of atmospheric aerosol particles and its influence on cloud microphysics. J. Geophys. Res. 101, 29,499-29,510.

Erel, Y., S. O. Pehkonen and M. R. Hoffmann, 1993. redox Chemistry of Iron in Fog and Stratus Clouds. J. Geophys. Res. 98, 18,423-18,434.

Gatz, D. F., B. K. Warner and L. C. Chu, 1984. Solubility of metal ions in rainwater. H. B.B. Deposition both Wet and Dry. 4, 133-151, Ann Arbor, MI.

Gieray, R., P. Wieser, T. Engelhardt, E. Swietlicki, H. C. Hansson, B. Mentes, D. Orsini, B. Martinsson, B. Svenningsson, K. J. Noone and J. Heintzenberg, 1997. Phase partitioning of aerosol constituents in cloud based on single-particle and bulk analysis. Atmos. Environ. 31, 2491-2502.

Graedel, T. E., M. L. Mandich and C. J. Weschler, 1986. Kinetic model studies of atmospheric droplet chemistry, 2. Homogeneous transition metal chemistry in raindrops. J. Geophys. Res. 91, 5225-5221.

Hoffmann, M. R. and D. J. Jacob, 1984. Kinetics and mechanism of the catalytic oxidation of dissolved sulfur dioxide in aqueous solution: an application to nighttime fog water chemistry. C. J.G. Acid Precipitation Series. 3, 101-172, Boston.

Hoigné, J., Y. Zuo and L. Nowell, 1994. Photochemical reactions in Atmospheric waters: Role of dissolved iron species. Z. R. G. Helz G.R., &Crosby P.G. eds. Aquatic and surface photochemistry. Boca Raton F.L.

Jacob, D. J., E. W. Gottlieb and M. J. Prather, 1989. Chemistry of a polluted cloudy boundary layer. J. Geophys. Res. 94, 12,975-13,002.

Jickells, T. D., T. D. Davies, M. Tranter, S. Landsberger, K. Jarvis and P. Abrahams, 1992. Trace elements in snow samples from the scottish highlands: Sources and dissolved/particulate distributions. Atmos. environ. 26 A, 393-401.

Khemani, L. T., G. A. Monin, M. S. Naik, P. S. Pakasa Rao, P. D. Safai and A. S. R. Murty, 1987. Influence of alkaline particulates on pH of cloud and rain water in India. Atmos. Environ. 21, 1137-1145.

Levin, Z. and E. Ganor, 1996. The effect of desert particles on cloud and rain formation in the eastern Mediterranean. S. Guerzoni and R. Chester. The impact of Desert dust across the Mediterranean. 77-86, Dordrecht.

Li, Z. and V. P. Aneja, 1992. Regional analysis of cloud chemistry at high elevations in the Eastern United States. Atmos. Environ. 26A, 2001-2017.

Losno, R., G. Bergametti and P. Buat-Ménard, 1988. Zinc partitioning in Mediterranean rainwater. Geophys. Res. Lett. 15, 1389-1392.

Losno, R., G. Bergametti, P. Carlier and G. Mouvier, 1991. Major ions in marine rainwater with attention to sources of alkaline and acidic species. Atmos. Environ. 25, 771-777.

Losno, R., J. L. Colin, N. Lebris, G. Bergametti, T. Jickells and B. Lim, 1993. Aluminium solubility in rainwater and molten snow. J. Atmos. Chem. 17, 29-43.

Loÿe -Pilot, M. D., J. M. Martin and J. Morelli, 1986. Influence of Saharan dust on rain acidity and atmospheric input to the Mediterranean. Nature 321, 427-428.

Maring, H. B. and R. A. Duce, 1987. The impact of atmospheric aerosols on trace metal chemistry in open ocean surface seawater-1- Aluminium. Earth and Planetary Science Letters 84, 381-392.

Matthijsen, J., P. J. H. Builtjes and D. L. Sedlak, 1995. Cloud model experiments of the effect of iron and copper on tropospheric ozone under marine and continental conditions. Met. Atmos. Phys. 57, 43-60.

Meites, L., 1963. Handbook of analytical chemistry. (Ed), McGraw-Hill book compagny, New-York.

Moore, R. M., J. E. Milley and A. Chatt, 1984. The potential for biological mobilization of trace elements from aeolian dust in the ocean and its importance in the case of Iron. Oceanologica Acta 7, 221-228.

Prospero, J. M. and A. T. Nees, 1987. Deposition rate of particulate and dissolved Aluminium derived from Saharan Dust in precipitation at Miami, Florida. J. Geophys. Res. 92, 14,723-14,731.

Pruppacher, H. R. and R. Jaenicke, 1995. Processing of water vapor. Atmos. Res. 38, 283.

Sedlak, D. L. and J. Hoigné, 1993. The role of copper and oxalate in the redox cycling of iron in atmospheric waters. Atmos. Environ. 27A, 2173-2185.

Sedlak, D. L., J. Hoigné, M. M. David, R. N. Colvile, E. Seyffer, K. Acker, W. Wiepercht, J. A. Lind and S. Fuzzi, 1997. The cloudwater chemistry of iron and copper at Great Dun Fell, UK. Atmos. Environ. 31, 2515-2526.

Spokes, L. J. and T. D. Jickells, 1996. Factors controlling the solubility of aerosol trace metals in the atmosphere and on mixing into seawater. Aquatic Geochem. 1, 355-374.

Spokes, L. J., T. D. Jickells and B. Lim, 1994. Solubilisation of aerosol trace metals by cloud procesing: a laboratory study. Geochim. Cosmochim. Acta 58, 3281-3287.

Statham, P. J. and R. Chester, 1988. Dissolution of manganese from marine atmospheric particulates into seawater and rainwater. Geochim. Cosmochim. Acta 52, 2433-2437.

Weschler, C. J., M. L. Mandich and T. E. Graedel, 1986. Speciation, Photosensitivity, and reaction of transition metal ions in atmospheric droplets. J. Geophys. Res. 91, 5189-5204.

Williams, P. T., M. Radojevic and A. G. Clarke, 1988. Dissolution of trace metals from particles of industrial origin and its influence on the composition of rainwater. Atmos. Environ. 22, 1433-1442.

Zhu, X., J. M. Prospero, F. J. Millero, D. L. Savoie and G. W. Brass, 1992. The solubility of ferric iron in marine mineral aerosol solutions at ambient relative humidities. Mar. Chem. 38, 91-107.

Zhuang, G., Z. Yi, R. A. Duce and P. R. Brown, 1992. Chemistry of iron in Marine aerosols. Gobal Biochem. Cycles 6, 161-173.

8.4 Non-rain deposits disturb significantly the determination of major ions in marine rainwater

R. Losno and J.L. Colin, **L**aboratoire **I**nteruniversitaire des **S**ystèmes **A**tmosphériques (**LISA**), Universités Paris 7-Paris 12, Faculté des Sciences, 61 av. du Gal de Gaulle, 94010 Créteil CEDEX, France.
L. Spokes and T. Jickells, **S**chool of **E**nvironmental **S**ciences (**SES**), University of East Anglia, Norwich NR4 7TJ, England.
M. Schulz and A. Rebers, **I**nstitut für **A**norganische und **A**ngewandte **C**hemie (**IAAC**), Universität Hamburg, Martin-Luther-King-Platz 6, 20146 Hamburg, Germany.
M. Leermakers, C. Meuleman and W. Baeyens, **A**nalytical **C**hemistry **D**epartment (**ACD**), Free University Brussels, Pleinlaan 2, B-1050 Brussels, Belgium.

8.4.1 Abstract

Simultaneous rain water sampling in marine areas was undertaken by four groups involved in the EUROTRAC **A**ir **S**ea **E**xchange project. First results show large variations between the data obtained by the different rain collectors for the same rain event. The main cause of variation is the "non rain deposition" (marine brine and sea salt) during the sampling period. The non rain deposition is shown to be largely influenced by the exposure geometry of the sampler with regard to wind direction and speed. Conclusions given by this work should be taken into account to ensure the data quality of joint multi-site experiments.

8.4.2 Introduction

The first step in environmental experimental science is often collecting representative samples prior any analyses. Rain water seems to be straightforward to sample, simply by leaving a clean funnel exposed during a rain event. In this paper, we show that, in marine areas, results given by more than one team operating together at the same time at the same site can produce as many different results as involved samplers, but that observed differences are, for major ion, explained by large variation of the "non rain deposition". Field experiments are conducted at Mace Head (Ireland, Connemara, April 1991), 300 m from the sea, at the Atmospheric Research Station of the University College Galway. This site, covered entirely with grass or stones, generally samples air from the west. This air has been over the ocean for several days and is relatively little impacted by anthropogenic sources but is heavily impacted by marine salts. To test the reliability of rain water measurements in remote areas, four different research teams have sampled simultaneously for an intercalibration exercise.

8.4.3 Sampling.

According to the purpose of the experiment, each team had its own cleaning and sampling protocol. Dates of rain events are listed in table 1. In addition to each group individual sampling, two bulked samples were also collected (named AQC1 and AQC2 respectively) with a polyethylene funnel and bottle provided by IAAC. Subsamples were distributed by IAAC to the groups to serve as an analytical quality control. Details of collectors and cleaning procedures used by each group are listed below.

	Rain 1	**Rain 2**	**Rain 3**	Rain 4
Date begin	9-Apr-93 12:20	9-Apr-93 14:20	9-Apr-93 16:30	9-Apr-93 22:30
Date End	9-Apr-93 14:20	9-Apr-93 16:30	9-Apr-93 22:30	10-Apr-93 10:00
Rain high	5 mm	4 mm	8 mm	13 mm
Wind speed	14 m/s	14 m/s	12 m/s	11 m/s
Wind direction	191 °	195 °	195 °	190 °

	Rain 5	**Rain 6**	**Rain 7**
Date begin	10-Apr-93 10:00	10-Apr-93 17:15	11-Apr-91 19:10
Date End	10-Apr-93 17:15	10-Apr-93 22:30	11-Apr-91 23:00
Rain high	7 mm	3 mm	6 mm
Wind speed	11 m/s	10 m/s	5 m/s
Wind direction	175 °	184 °	200 °

Table 1: rain sampling conditions at Mace Head.

8.4.3.1 LISA

LISA uses single-use polyethylene funnels (24 cm diameter) and bottles (500ml) for both major ion and trace metal collection in a single sampling. Sufficient quantity of funnels and bottles are washed in the laboratory before the field experiment. All the polyethylene material, including polyethylene bags used to cover the funnels, is first brushed with a soft brush in a domestic detergent, then rinsed with water and soaked in 2% Decon™ laboratory detergent for 24 hours. Then this material is rinsed with deionized water and soaked in 0.1 molar hydrochloric acid for 24 hours. After this pre-cleaning period, the bottles are rinsed firstly with deionized water and secondly with Milli-Q™ water (3 times). They are then filled with ultrapure 0.2 molar hydrochloric acid (Prolabo Normatom™) for one week. Then the bottles are rinsed (5 times) and filled with Milli-Q water for one week, the water is changed every two days. After this period, the bottles are rinsed again with Milli-Q water and left to dry in a laminar clean hood for about six hours. The bottles are then closed and placed in sealed polyethylene bags. Funnels and their bags are also washed in ultrapure hydrochloric acid, but are not soaked in the acid at this stage. In the horizontal laminar flow of a clean hood, acid and Milli-Q water are poured on the funnel walls for several minutes, and after the last rinsing stage, they are dried for 4 to 6 hours. Then the funnels are put in their own cleaned bag, sealed, and put in a second non-cleaned polyethylene bag (Losno et al., 1988, Losno 1989, Losno et al. 1991).

At the start of the rain event, the funnel and bottle are removed from their double polyethylene bag and deployed at a high of 2m above the ground. At the end of the rain, the sample is filtered through a 0.4 µm pore size Nuclepore™ membrane and two aliquot (60 ml each) are kept for major ion analyses in the home laboratory, one preserved with 0.1 ml chloroform and both stored refrigerated.

8.4.3.2 SES

SES uses polyethylene funnels (28.5 cm diameter) and bottles (250 ml) and separately collects samples for trace metals and major ion analysis. For major ion, collection bottles and funnels are initially rinsed with acetone and deionized water, washed with detergent and then thoroughly rinsed with deionized water. After this stage funnels are soaked in a 5% Decon™ bath for 24 hours, rinsed with deionized water and then soaked in deionized water to ensure complete removal of the Decon™. After 24 hours the funnels are removed, rinsed extensively with Milli-Q™ water and then soaked for 24 hours in Milli-Q water. After this time, the bottles are refilled with fresh Milli-Q water, double bagged and stored until required. Bottles are filled with 5% Decon™, soaked for 48 hours, rinsed and then filled with Milli-Q™ water, double bagged and stored until required. The Milli-Q™ water serves, during deployment, as a source of clean water able to wash and blank the funnels prior to use. Funnels and bottles are removed from their bags at the start of a rain event and exposed after washing and blanking with Milli-Q water. At the end of the event the sample is removed from the field, bagged and either frozen or refrigerated if a freezer is unavailable. Once back in the home laboratory the sample is stored frozen until analysis. Funnels are reused after they were washed and blanked with 0.4% HNO3 and Milli-Q water before.

8.4.3.3 IAAC

All funnels (PTFE, Polyethylene (PE) and Quartz) and the polyethylene and PTFE bottles for sample collection are precleaned in several steps using distilled ethanol, deionized water, quartz double distilled water and 10% nitric acid, analytical grade. Funnels are rinsed with ethanol and wiped out with paper, rinsed well with deionized water, soaked more than 48 hours in nitric acid, extensively rinsed with deionized water and finally with quartz double distilled water. They are then packed in new polyethylene bags until sample collection. Bottles are filled with nitric acid and also soaked for more than 48 hours, rinsed with deionized water (5 times) filled with double distilled water 48 hours and finally rinsed 5 times with double distilled water. At Mace Head, rain was collected in three different collectors: PTFE funnel (11.5 cm diameter), polyethylene funnel (25 cm diameter) and Quartz funnel (25 cm diameter) which was situated in an automatic rain collector that only opened when the rainfall intensity was above a reasonable value. All collectors are pre-cleaned as above and used both for trace metal and major ions sampling. The collectors are reused during the same campaign and rinsed with Milli-Q water to investigate memory effects and provide "cleaned" surfaces. Sampling with polyethylene and PTFE funnels is carried out by opening them manually, between rain events they are covered with clean polyethylene bags. Once collected the samples are packed in bags and refrigerated until analysis.

8.4.3.4 ACD

ACD uses polyethylene funnels (20 cm diameter) and bottles. This material is cleaned consecutively with a detergent wash (Decon 90™), deionized and Milli-Q™ water rinses. Funnels are double bagged for storage. The funnel is covered with a plastic bag between rain events. For dry periods longer than one day, the funnel is removed and rinsed with Milli-Q™ water. After the rain event, the samples are bagged and stored without pretreatment in the refrigerator.

8.4.4 Analyses

As soon as possible after the end of the rain event, a 5 ml aliquot was separated from each groups sample to enable measurements of conductance, pH and temperature (table 2). These determinations were made, in the field, never more than 1 hour after collection by the same method, apparatus and operator. Conductance was measured with a 1 cm² plated platinum cell (Tacussel™) with a precision better than 5%, after calibration with a KCl 10^{-4} M solution. Then, conductivity is calculated at the measured temperature using these data. pH is measured with a glass electrode (Metrhom™) after calibration with pH 7 and pH 4 standard solutions, the accuracy is ±0.05 unit.

Anions are measured by High Pressure Liquid Ionic Chromatography (HPLIC) with a Dionex™ ionic chromatograph for LISA, SES and IAAC and an Hamilton™ PRPx100 column for ACD. Detection limits are better than 1 µmol.l^{-1} for Dionex.

	Rain 1	**Rain 2**	**Rain 3**	**Rain 4**	**Rain 5**	**Rain 6**	**Rain 7**
Temperature	15 °C	16 °C	17 °C	16 °C	17 °C	17 °C	17 °C
pH							
LISA	5.49	5.34	5.44	5.53	5.24	5.23	5.21
IAAC Q	5.27	5.27	5.2	5.27	5.22	5.26	5.26
IAAC PE	4.93	5.05	5.15	5.27	5.09	5.2	5.16
ACD	5.72	5.52	5.32	5.42	5.41	5.29	5.54
SES	5.22	5.34	5.19	5.35	5.39	5.38	5.38
Λ (µS.cm)							
LISA	40.5	82.9	68.7	35.4	20.2	21.2	48.9
IAAC Q	15.9	28.6	24.7	21.4	14.1	9.8	47.3
IAAC PE	44.3	73.9	53.7	26.3	40.4	25.2	48.9
ACD	23.0	41.4	37.6	24.1	25.2	22.2	47.3
SES	19.7	33.6	33.3	25.7	19.7	15.1	42.6

Table 2: on field measurements. Λ is conductivity after cell constant correction.

Ammonium is measured at IAAC, SES by the classic indophenol blue method. ACD uses both colorimetric and HPLIC methods.

Other major cations (sodium, magnesium, potassium and calcium) are determined by Atomic Absorption Spectrometry at LISA, ACD, SES or by Inductively Coupled Plasma Atomic Emission Spectrometry at ACD and IAAC or by ICP-Mass Spectrometry at ACD and IAAC.

8.4.5 Results and discussion

8.4.5.1 Analytical quality control

Samples AQC1 and AQC2 were analyzed by each group with their own method, to provide samples not influenced by sampling effects. Results for the analytical quality control samples are given in table 3. They show that between group, variability for sample analysis is small except for K^+ and NO_3^- in samples analyzed by ACD and Mg^{2+} in AQC Rain1 by IAAC. In this last case, the magnesium excess is reflected in the ionic balance. It appears therefore that all laboratories can obtain comparable results for the same sample in major ion measurements.

8.4.5.2 Non rain deposit

The large differences in measured conductivity for simultaneously sampled rain events (see figure 1) confirms that a large variability in major ions concentrations (table 2) has to be attributed to sampling artefacts. The only event, where this variability is less obvious may be Rain 7. Moreover, table 2 shows results for each ion which confirm these conductivity measurements. Since the results obtained for AQ1 and AQ2 agree well, it appears that this variability is not the results of error associated with the differing analysis techniques of the groups involved. It suggests that the major ion concentration is explained by sea salt or seawater dilution in rain water and by sea salt and sea spray deposition on the collecting funnel (usually called "dry deposition"). As each collector has a specific exposure geometry, the amount of dry deposition should be different between each collector.

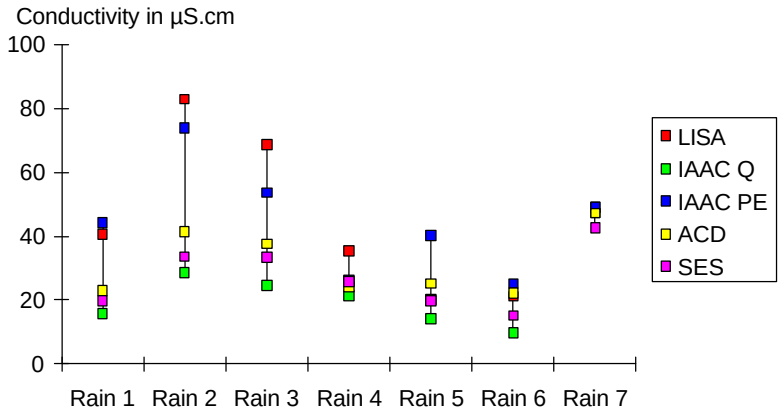

Figure 1: Comparisons of the conductivity measured in each separate sample. Values are in µS.cm.

Rain 7, where results are close between each group is associated with lower wind speed (5m/s) than others (>10m/s). This lower wind speed produces less sea spray and aerosols, and consequently less dry deposition. The sampler denoted IAAC-Q is an automatic rain sampler, which closes itself when insufficient rain intensity occurs.

	Laboratory	IAAC	SES	ACD	LISA
H^+ (µmol/l)	AQC Rain 1				6
Cl^- (µmol/l)	AQC Rain 1	231	234	214	219
SO_4^{2-} (µmol/l)	AQC Rain 2 AQC Rain 1	328 12	14	352 16	350 13
NO_3^- (µmol/l)	AQC Rain 2 AQC Rain 1	22 1.3	1.4	24 3.1	23 1.1
Na^+ (µmol/l)	AQC Rain 2 AQC Rain 1 acid	5.7 199	202	6.9 200	5.0 201
K^+ (µmol/l)	AQC Rain 2 acid AQC Rain 1 acid	308 6	5	309 9	336 4
NH_4^+ (µmol/l)	AQC Rain 2 acid AQC Rain 1	9	2	13 3	7
Mg^{2+} (µmol/l)	AQC Rain 2 AQC Rain 1 acid	62	22	23	23
Ca^{2+} (µmol/l)	AQC Rain 2 acid AQC Rain 1 acid	30 6	3	39 9	33 4
sum of cations	AQC Rain 2 acid AQC1	7 347	0 265	7 282	7 265
sum of anions	AQC1	258	265	250	247

Table 3: AQC results (µmol.l^{-1}). Sum of anions include bicarbonate calculated from pH, assuming an equilibrium between dissolved and gaseous CO_2.

	Rain 1	Rain 2	Rain 3	Rain 4	Rain 5	Rain 6	Rain 7
Na (µmol/l)							
LISA	297	653	538	266	150	158	363
IAAC Q	126	227	189	165	107	64	378
IAAC PE	306	300	440	214	207	194	358
ACD	193	312	155	184	209	181	345
SES	140	267	255	132	152	115	390
Mg (µmol/l)							
LISA	30	70	58	27	15	16	35
IAAC Q	16	26	23	21	12	8	43
IAAC PE	32	33	44	23	23	23	41
ACD							
SES	16	27	27	14	16	12	2
K (µmol/l)							
LISA	6	14	11	5	3	3	8
IAAC Q	3	8	4	4	3		11
IAAC PE	8	6	9	4	5		7
ACD	7	18	10	9	8	8	11
SES	4	7	8	5	5	3	9
Ca (µmol/l)							
LISA	6	14	12	6	3	3	7
IAAC Q	3	5	5	4	2	0	9
IAAC PE	9	7	11	5	5	4	8
ACD							
SES	3	6	6	2	3	2	8
Cl (µmol/l)							
LISA	336	710	602	290	165	170	414
IAAC Q	132	241	206	183	100	72	420
IAAC PE	315	562	439	218	222	211	415
ACD	192	368	294	187	243	190	420
SES	161.5	266.6	284.4	134.4	165.6	117.35	424.5
Sulfate (µmol/l)							
LISA	20	40	33	17	11	11	25
IAAC Q	9	14	12	10	7	5	24
IAAC PE	20	32	24	14	13	12	24
ACD	16	22	19	14	13	14	25
SES	13	21	21	11	12	9	32

Table 4: anions and cations measurements.

Assuming that a "rain event" reflects in fact some showers interrupted with rain periods of lower intensity, this automatic rain sampler will be closed during low intensity rain and then will collect less dry deposition and marine brine. This probably explains the consistently low values of conductance and sea salt component in this sample (Fig. 1). Some funnels were bent into the wind direction (especially LISA in Rain 5); to improve collection efficiencies, this configuration should also increase dry deposition because sea salt aerosol and sea spray may impact much more efficiently to a bent funnel than a horizontally exposed funnel: small sea spray aerosol particles should follow the wind flow curves better than rain drops and then are collected more efficiently by funnels bent to the wind direction than by horizontal funnels. This probably explains the consistently high values in the titled collectors LISA and IAAC-PE in Figure 1.

This intercomparison of different samplers shows that in this coastal area, heavily loaded with sea spray and sea salt particles, dry deposition may be a large part of the major ion concentrations even for collectors manually opened at the start of the rain event and closed at the end of it. Moreover, this part is very dependent on the attitude and the exposure geometry of the collector.

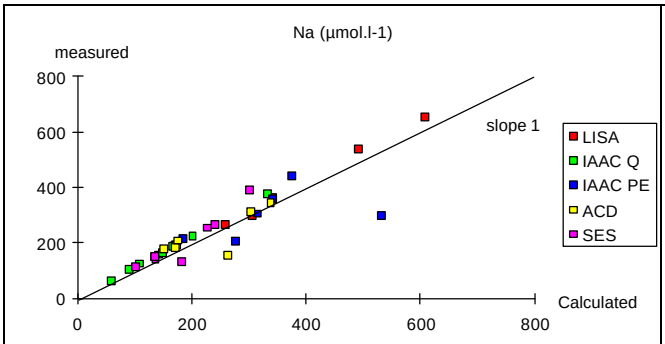

Figure 2: measured concentration of Na^+ versus calculated, assuming sea salt dissolution in water.

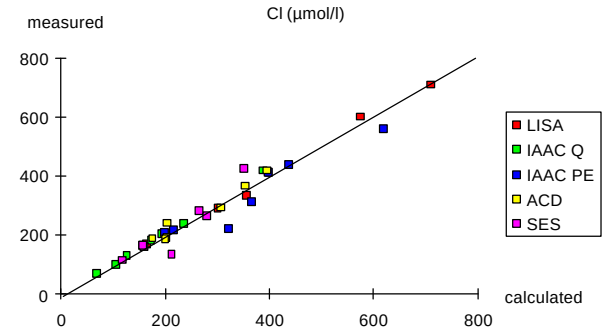

Figure 3: measured concentration of Cl^- versus calculated, assuming sea salt dissolution in water

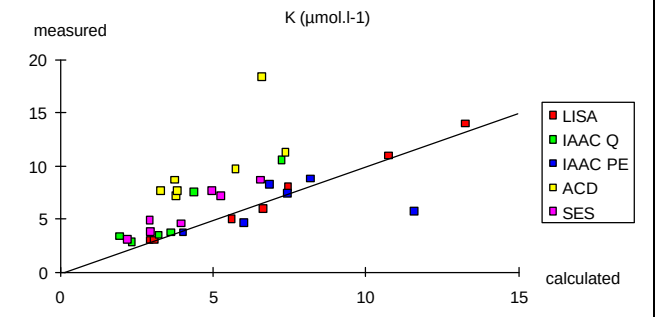

Figure 4: measured concentration of K^+ versus calculated, assuming sea salt dissolution in water

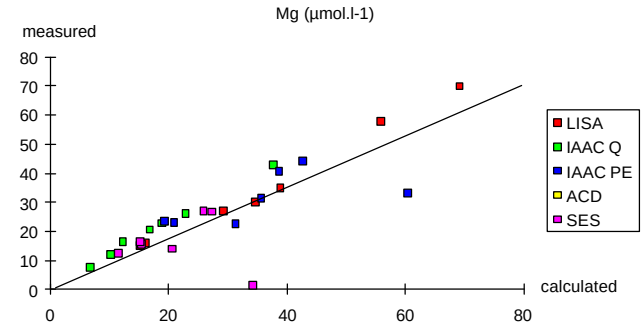

Figure 5: measured concentration of Mg^{2+} versus calculated, assuming sea salt dissolution in water.

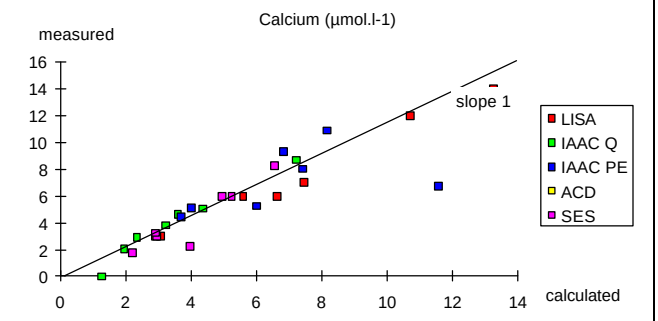

Figure 6: measured concentration of Ca^{2+} versus calculated, assuming sea salt dissolution in water

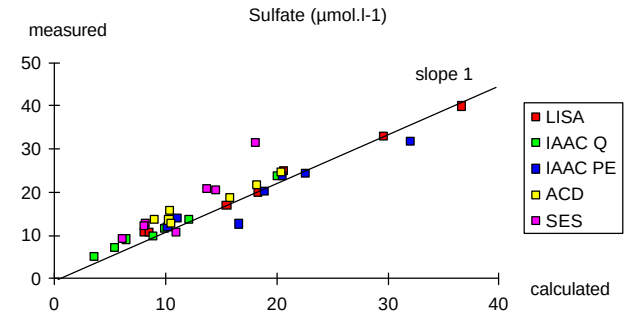

Figure 7: measured concentration of SO_4^{2-} versus calculated, assuming sea salt dissolution in water

8.4.5.3 Sea salt component

Though the non-rain deposition proved to be of major importance for the explanation differences in concentration, the purpose of experiment was to intercompare different sampling protocols. The great importance of the sea salt source for the major ion concentrations at a remote site, allows a check of the analytical performance on the basis of conductivity measurements and ionic balance. If we assume that major ions come from dissolved sea salt and additional acids (mainly HNO_3 and H_2SO_4), we can write:

$$\Lambda = D. \sum c_j.L_j + [H+].(\Lambda_{H+} + \Lambda_{A-})$$

where:

- Λ is the conductivity of the rain water.
- D is the dilution factor of sea salt in rain relative to sea water (D= 1 in sea water).
- j is Na^+, Mg^{2+}, K^+, Ca^{2+}, SO_4^{2-}, Cl^-
- c_j is the concentration of j in sea water (Turner et al., 1981)
- Λ_j is the molar conductivity of j at the measured temperature

- Λ_{A^-} is the molar conductivity of the anion of the acid which has given H^+. It can be taken as Λ_{NO3^-} because of small differences between anions equivalent conductivity (here mainly between nitrate and excess sulfate, see below), or neglected because $\Lambda_{H^+} >> \Lambda_{A^-}$.

As we have a diluted solution, we assume:

$$\Lambda_j=\Lambda°_j \text{ and } [H^+]=10^{-pH}$$

were $\Lambda°_j$ is the conductivity given in tables at infinite dilution. The concentrations of the major ions can now be estimated from measurements of conductivity and pH. Figures 2, 3, 4, 5, 6 and 7 indicate a good agreement between calculated and measured concentrations for all the major ions, except for ACD measurements of K which look systematically overestimated, as we previously remarked in analytical quality control section, and for IAAC PE Rain 2 which shows an underestimation for cations only.

For low concentrations and conductivities (Rain 5 and 6), measured sulfate concentrations are higher than calculated, this shows a non sea salt component which should be attributed to dissociation of sulfuric acid coming from antropogenic or biogenic emissions. This observation on the figure 7 is in good agreement with non sea salt sulfate uncertainties measurements (table 5) which are for these rains less than 100%.

	Rain 1	**Rain 2**	**Rain 3**	**Rain 4**	**Rain 5**	**Rain 6**	**Rain 7**
Ammonium (µmol/l)							
ACD	2.9	2.9	2.4	2.9	1.8	2.9	3.5
SES	3.5	1.8	2.4	1.8	1.8	2.4	6.5
Nitrate (µmol/l)							
LISA	1.2	1.7	2.0	0.9	1.6	1.1	2.2
IAAC Q	2.0	1.8	2.5	1.3	1.9	1.8	2.7
IAAC PE	5.0	2.4	3.1	1.4	2.1	1.9	2.9
IAAC Tef	4.1	3.0	3.5	1.5	2.3	2.2	159.7
ACD	1.1	1.0	0.8	0.8	1.6	0.5	4.4
SES	2.1	1.6	3.2	0.6	1.7	1.3	2.7
Non sea salt sulfate (µmol/l)							
LISA	2	1	1	1	2	1	3
IAAC Q	2	0	0	0	1	1	1
IAAC PE	2	14	-2	1	0	0	2
ACD	4	3	9	3	0	3	4
SES	4	5	6	3	3	2	8
Relative incertitude on non sea salt sulfate contribution							
LISA	90%	>100%	>100%	>100%	53%	85%	77%
IAAC Q	55%	>100%	>100%	100%	84%	33%	>100%
IAAC PE	>100%	18%	100%	>100%	>100%	>100%	>100%
ACD	33%	71%	15%	48%	>100%	42%	56%
SES	25%	40%	32%	34%	35%	34%	34%

Table 5: rain water acidity balance

8.4.5.4 pH, nitrate and ammonium:

Comparison of ammonium (figure 8) and nitrate (figure 9) neither of which have a strong marine component shows much closer results in our measurements. In figure 9, nitrate measurements show a better fit than other species, except some high values which can be attributed to contamination, probably caused by nitric acid wash of the sampling equipment.

The pH of the rain is determined by the balance of alkaline and acidic species. Especially in the case of marine rainwater, acidic species are:

- nitric and sulfuric acids which give nitrate, sulfate and hydronium ions when incorporated in water
- carbon dioxide;

bases are:

- ammonia and carbonates which give quantitatively ammonium ion and bicarbonate if pH is less than 8,

- bicarbonate from the sea (sea spray and sea salt).

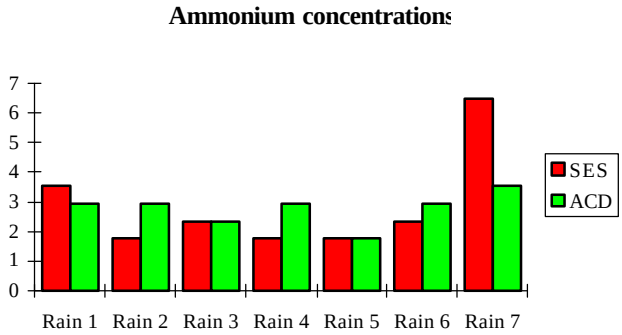

Figure 8: ammonium concentration in rain water comparison SES versus ACD values.

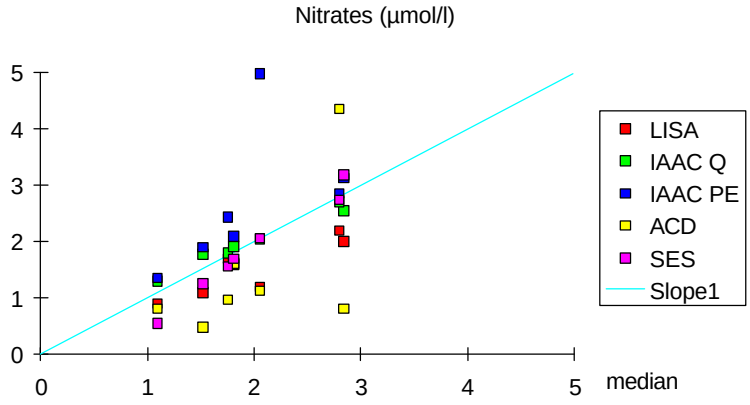

Figure 9: nitrate concentrations versus median concentration.

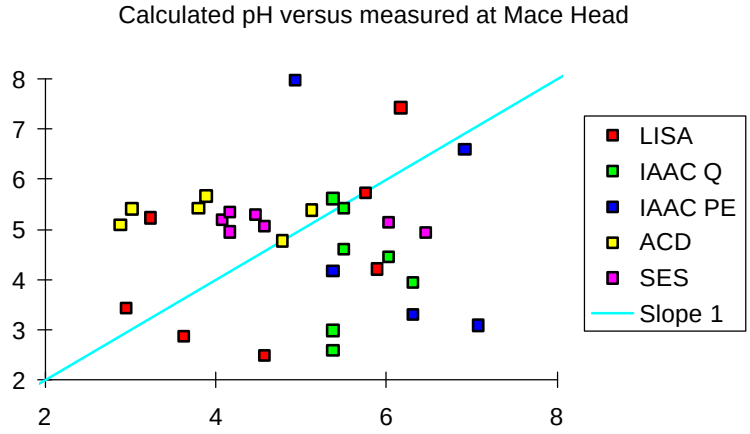

Figure 10: Calculated versus measured pH

The pH balance cannot be written so simply in the general case because of the CO_2/HCO_3^- weak acidity (pK_a= 6.8). So, if pH is low (typically less than 5.8), CO_2 doesn't act as an acid but HCO_3^- reacts quantitatively like a strong base, we can write:

$$[H^+] = [NO_3^-] + 2.[*SO_4^{2-}] - [NH_4^+] - [Alk_{marine}] - [Alk_{crust}]$$

where $[*SO_4^{2-}]$ is the amount of SO_4^{2-} in excess of the sea salt source, $[Alk_{marine}]$ is the amount of neutralized bicarbonate from the sea ($[Alk_{marine}]= D.10^{(-2.89)}$, Turner et al. 1981), $[Alk_{crust}]$ the amount of crustal input of calcite, estimated as $2.[*Ca^{2+}]$ and $[*SO_4^{2-}]$ the amount of incorporated sulfuric acid, that is non sea salt sulfate; but these last measurement have large uncertainties because of the large amount of sea

salt sulfate. Formulas for errors calculation are given in appendix. Under our conditions, it appears that most of the non sea salt values for sulfate are obtained with relative uncertainties greater than 100% (table 5).

Marine alkalinity appears to be negligible compared to other species and ammonium, based on the samples where it was measured (in SES and ACD samples), also appears to be of minor importance. Thus, pH can be calculated with a good accuracy (at ±0.5 unit) from measurement of non sea salt sulfate and nitrates (figure 10). Comparisons, in this case, of non sea salt sulfate and nitrate concentrations show an equivalent contribution of both (table 5) in the acidic budget, in good agreement with previous data collected in some remote marine areas (e.g. Losno et al, 1991).

8.4.6 Conclusion

The different analytical protocols used by the different teams in their laboratories produce similar results if applied on the same sample, as shown by the ACQ results and also the good intercalibration values of nitrate, ammonium, and also non sea salt sulfate if available. At Mace Head, and probably in many remote marine areas, the major ion content of rain water can be explained by sea salt inputs. In local emission conditions (wind speed greater or equal to 10m/s), the rain collection is strongly influenced by dry deposition (up to 100%) and therefore by the rain-sampler geometry, preventing direct intercomparison. However, a simple conductometric model gives accurate values of major ion concentrations.

8.4.7 Acknowledgments

We would like to acknowledge the kind support received from Gerry Jennings and Tom O'Connor, University College of Galway, in providing help and an excellent experimental site.

8.4.8 Funding

Belgian Ministry of Science, French Ministry of Environment and CNRS, UK Department of the Environment, German Ministry of Science and Technology (ENV6 German-Irish Cooperation on Science and Technology).

8.4.9 References

Losno R., Bergametti G. and Buat-Ménard P., (1988), 'Zinc partitioning in Mediterranean Rainwater', *Geophys. Res. L.*, **15**, n°12, 1389-1392.

Losno R. (1989), 'Chimie des éléments-trace dans les précipitations méditerranéennes', *Ph.D. Thesis*, Université Paris 7, 215p.

Losno R., Bergametti G., Carlier P. and Mouvier G., (1991), 'Major ions in marine rainwater with attention to sources of alkaline and acidic species', *Atmos. Environ.*, **25A**, 763-770.

Rendell A.R., Ottley C.J., Jickells T.D. and Harison R.M., (1993), 'The atmospheric input of nitrogen species: the North Sea.', *Tellus*, **45B**, 53-63.

Turner D.R., Whitfield M. and Dickson A.G., (1981), 'The equilibrium speciation of dissolved components in freshwater and seawater at 25°C and 1 atm pressure', *Geochim. Cosmochim. Acta*, **45**, 855-881.

8.4.10 Appendix : uncertainties on non sea salt sulfate concentrations.

If we name $\Delta[X]$ the uncertainty on the concentration of X and R the ratio sulfate/sodium in sea water, we can write:

$$[{}^*SO_4^{2-}] = [SO_4^{2-}] - [Na^+].R$$

$$\Delta[{}^*SO42-] = \left(\frac{D[SO42-]}{[SO42-]}\right)[SO42-] + \left(\frac{D[Na+]}{[Na+]}\right)[Na+].R$$

$$\left(\frac{D[{}^*SO42-]}{[{}^*SO42-]}\right) = \frac{F}{F-1}\left(\frac{D[SO42-]}{[SO42-]}\right) + \frac{1}{F-1}\left(\frac{D[Na+]}{[Na+]}\right)$$

where F is the enrichment factor of sulfate ($F=[SO_4^{2-}{}_{total}]/[SO_4^{2-}{}_{sea\ salt}]$).

8.5 Aluminium Solubility in Rainwater and Molten Snow

R. LOSNO, J.L. COLIN, N. LE BRIS, G. BERGAMETTI, Laboratoire de PhysicoChimie de l'Atmosphère, URA CNRS 1404, Université Paris 7, 2, place Jussieu 75251 Paris CEDEX O5, France.

T. JICKELLS and B. LIM, School of Environmental Sciences, University of East Anglia, Norwich, NR4 7TJ, U.K.

Key words: rainwater chemistry, solubility, aluminium.

ABSTRACT. Large variations of aluminium solubilities are found in marine and rural precipitations. The results of seven field experiments are used to produce a model of the solubilization of aluminium independent of the sampling site. Large variations of solubility appear, and the pH seems to be a major factor explaining this solubility changes. Thermodynamic calculations at T= 278K suggest that, at higher pHs (>5), equilibrium with gibbsite ($\alpha Al(OH)_3$) or a trivalent alkaline insoluble form acts as a limiting of aluminium solubility and at lower pHs (<5), Al could be in equilibrium with a hydroxysulfate salt $Al(OH)_{1.5}(SO_4)_{0.75}$.

1.Introduction.

Numerous studies have underlined the important role of atmospheric inputs to terrestrial and marine ecosystems. Prospero and Nees (1987) have suggested that, on a global basis, the annual atmospheric input of dissolved Al to the oceans is comparable to fluvial inputs. It is now well known that the dominant atmospheric mode of aerosol deposition is by precipitation, especially in the mid-latitude regions (Galloway et al., 1982; Prospero and Nees, 1987). This aqueous medium is favorable for partial or total solubilization of the atmospheric aerosol scavenged by clouds.

The distinction between solid and dissolved fractions is of particular importance as regards the availability of metals to biological food chains. Furthermore the solubility of aerosols appears to be directly involved in the mechanisms of aerosol scavenging by rain droplets as shown by theoretical predictions (Junge and Mac Laren, 1971; Pruppacher and Klett, 1980) as well as by field studies (Martens and Harriss, 1973 ; Jaffrezo and Colin, 1988). Despite its important role in major atmospheric processes the dissolved/particulate distribution of elements in rainwater has rarely been addressed, probably because of sampling difficulties and the complexities of factors which may control it. These controls probably include:

i) Types of aerosol particle; salts from marine or anthropogenic sources which are generally rather soluble while elements from crustal sources (Lim, 1991), included in a mineral lattice, are more insoluble (Colin et al., 1990 ; Jickells et al., 1992).

ii) The complex evolution of aerosols in clouds where they have passed through several cycles of condensation and evaporation (Pruppacher and Klett, 1980). Such processes are able to alter particles due to very strong variations of acidity and ionic strength.

iii) Final conditions of the aqueous medium in raindrops (pH, ligands, ionic strength).

This article focuses on aluminium rain chemistry. In order to attempt to identify the main factors involved in the dissolved/particulate distribution of this metal, we have combined the results of several field experiments from research groups at both the University of East Anglia (England) and the University of Paris 7 (France) (figure 1).

2. Field experiments and analytical methods

2.1. UNIVERSITY OF EAST ANGLIA

2.1.1. *Scotland*. As part of a programme to study the atmospheric transport of contaminants over Europe resulting in "black snow" episodes (Davies et al., 1984), we have collected all snow samples (ScoXX) that fell in 1987 between January 7 and May 1 in the Ciste Mhearad catchment (area 0,4 km^2 located close to the summit of the Cairngorn peak, altitude 1080 m, in Western Scotland). 38 snow samples have been collected and analyzed for a wide range of trace elements. Samples of freshly fallen snow were collected using ultra-clean techniques and stored frozen. On return to the laboratory, samples were thawed and then filtered through 0.4 µm Nuclepore filters within 2 hours and subsequently preserved by acidification to 1% (v/v) with ultra pure nitric acid (Jickells et al., 1992). Insoluble Al was determined by

Instrumental Neutron Activation of the filter (Landsberger et al., 1989; Jickells et al., 1992). Dissolved Al was determined by Inductively Coupled Plasma Mass Spectrometry of the acidified solution (Jickells et al., 1992).

2.1.2. *GCE/CASE/WATOX cruise*. (1988) Shipboard rainwater samples (WatXX) were collected on a wet-only event or sequential sampling basis using ultra clean trace metalstechniques. Rain water was filtered in-situ through (precleaned) 0.2 µm Nuclepore membrane filters. Filtered rainwater samples were immediately retrieved after the rain stopped and stored frozen until analysis in the home laboratory: insoluble Al was determined by Graphite Furnace Atomic Absorption Spectroscopy (GFAAS) after hot HF/HNO_3 digestion of the filter and dissolved Al by GFAAS on the filtered acidified (0.4% nitric acid) thawed samples (Lim and Jickells, 1990).

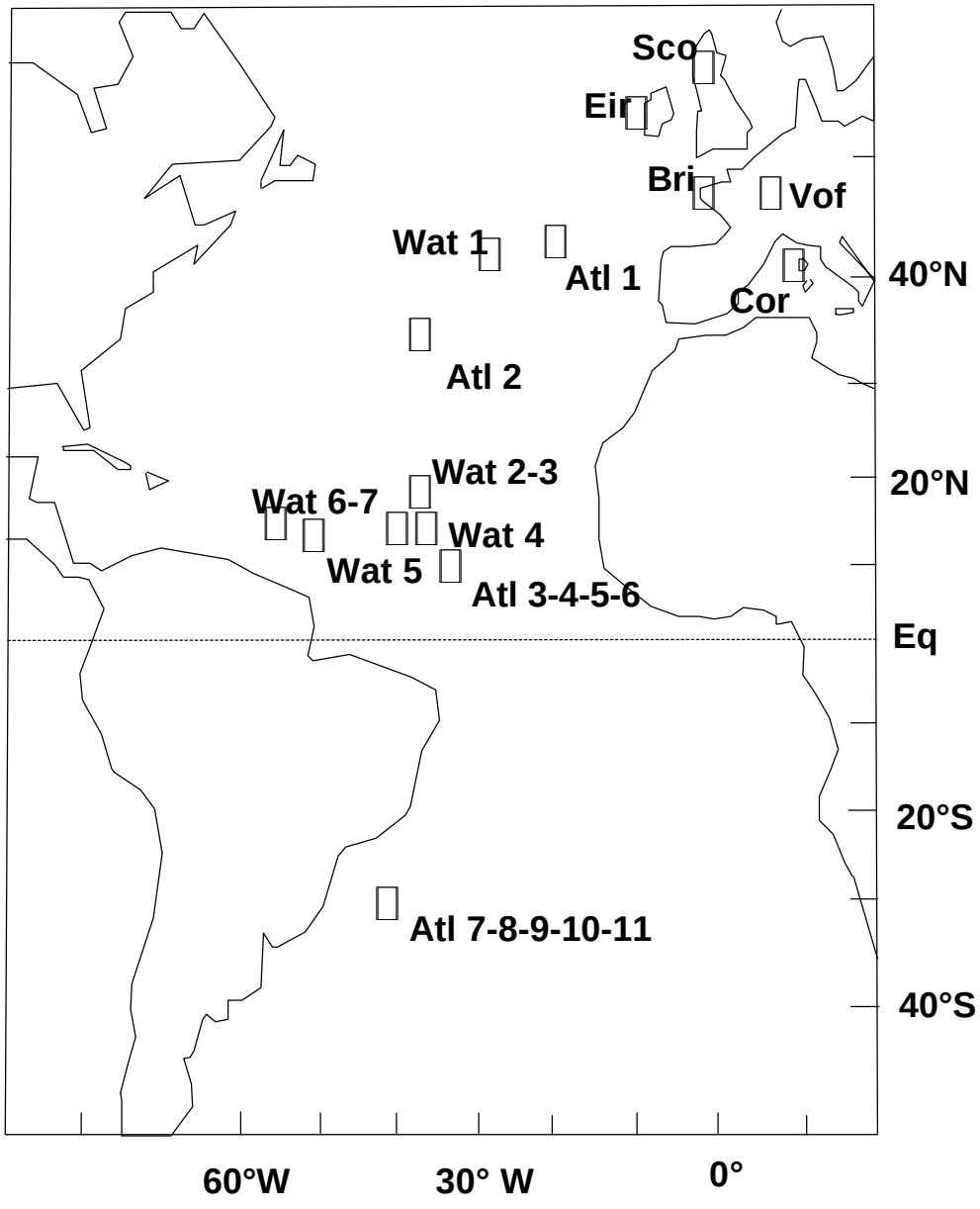

Figure 1: sampling locations.

2.2. UNIVERSITY OF PARIS

Each rain or snow sample was collected separately and filtered immediately after each rain event (in the case of snow, after thawing) under a laminar flow ultra-clean hood through a 0.4 µm porosity Nuclepore filter. When sampling on Corsica, Ireland and on board the Polarstern, single-use pre-washed polyethylene funnels were used and a fraction of the filtered rainwater was stored in a Teflon (FEP) bottle with $0.1 mol.l^{-1}$ ultra pure nitric acid (Losno et al., 1988). For Brittany and the Vosgian forest, a large polyethylene collector

($1m^2$) was used and carefully washed with dilute nitric acid and deionized water before each collection. All the material used for collection and storage of the sample was washed thoroughly and well rinsed with ultra pure reagent (Milli Q water, Prolabo Normatom nitric and hydrochloric acids) to prevent contamination (Ross, 1986; Losno, 1989).

The filters were analyzed for Al by thin layer X-Ray fluorescence by an α10 C.G.R. X-ray wavelength dispersing spectrometer, using a Cr or Sc target and without any sample preparation. For those conditions, the precision of the method was ±7% with a detection limit of 75 ng (2.8 nmol). Soluble Al is analyzed by GFAAS with injections of 20µl or 100µl, depending on the concentration of the analyzed solution, into a tantalum coated pyrolytic tube. The precision is ±20% with a detection limit of 0.04 $\mu mol.l^{-1}$ (20µl) or 0.01 $\mu mol.l^{-1}$ (100µl).

2.2.1. *Corsica.* The samples (CorXX) were taken at Capo Cavallo on the Northwestern coast of Corsica Island. This site (altitude 300 m) is located at about 700 m from the sea. 11 rainwaters have been sampled during two field experiments in March-April 1986 and October-November 1987. All the rains were analyzed for major cations and anions (Losno et al., 1991) and for trace metals including dissolved and particulate Al (Losno, 1989).

2.2.2. *Brittany and Vosgian Forest.* In order to characterize the effect of emission sources, after long and intermediate range transport, on the composition of wet deposition, we have selected two sites in rural areas, remote from local anthropogenic sources.

The first site is located in Brittany (Bri) on the sea coast in the West of France at the "pointe de Penmar'ch". This situation at the extremity of Finistere is very suitable for the observation of the oceanic air masses before they cross France from West to East. 6 rain events have been collected during 2 field campaigns in September and November 1983 and analyzed for Al, among other species. By contrast, the second site is in a continental zone in the East of France. It is located in the west part of the Vosgian forest, at the "Col du Donon" at 700 m altitude. 29 rain and snow events (VofXX) have been collected in March and April 1985 and also analyzed for major species and aluminium. The results are presented in details elsewhere (Colin et al., 1989).

2.2.3. *Polarstern Cruise.* 11 rainwater samples (AtlXX) were collected during the transatlantic cruise of the "Polarstern" ANT VII (Oct-Nov 1988). Rainwater were collected on the ship about 25 m above sea level. Major ions (Losno et al., 1991) and trace metals have been analyzed.

2.2.4. *Ireland.* This campaign (Oct-Nov 1989, EirXX samples) was conducted at "Mace Head" a fairly remote site on the West coast of Ireland. "Mace Head" is in used in the AEROCE programme. 14 rainwaters were collected and analyzed.

2.3. CLASSIFICATION OF SAMPLING SITES

In order to characterize these field sites one can say that, apart from the Vosgian forest in a rural continental area, all the sites are located in marine areas. Nevertheless these latter can be distinguished by their specific environments.

Each site can receive air masses from different origins, Ireland and Brittany are generally exposed to very clean Western air masses. Rains collected at these sites are comparable to those sampled during Polarstern and GCE cruises in the Atlantic Ocean. The Scottish situation on the Cairngorn mountains is more complex. This site can be exposed to very polluted episodes called "black snows" coming from the South which are massively enriched in metals, carbon and acids (Davies et al., 1984) and by contrast air masses from the West with very low concentration levels similar to those observed on Mace Head (Ireland). Corsica is also subject to complex meteorology: generally it is exposed to marine air masses from the Southwest (less polluted) to Northeast (more polluted) but on some occasions, it receives African air from the south with a very high load of crustal material. The associated rains are therefore characterized by a wide range of pH between 4 and 7 (Losno et al. 1988, Losno et al. 1991). In the Vosgian forest, the air masses and their associated precipitation events have three zones of geographical origin, each affected by a main aerosol emission source : north and east by industrial contamination, the west influenced by the Atlantic Ocean and the south dominated by the impact of continental agricultural regions (Colin et al., 1989).

With such a diversity of environments sampled, we will propose conclusions on aluminium dissolution processes that are generally applicable and not site specific.

2.4. FIELD ANALYSES

The pH, temperature and conductivity were usually measured immediately after filtration. Further laboratory pH measurements indicate that these are stable over several weeks.

2.5. MAJOR IONS

Major ions were analyzed by ionic chromatography, flame spectrometry, colorimetry and Gran's titration (bicarbonates) as described in Lim and Jickells (1990), Losno et al. (1991), and Jickells et al. (1992). Fluoride was not detected in the Scottish snow samples, and not measured in the others. Its concentration was calculated (for soluble Al speciation determination), assuming a sea salt origin, from sodium measurements with $\log([Na^+]/[F^-]) = 3.84$ (Turner et al., 1981).

2.6. BLANKS

Blanks were carried out during the field experiments and in our laboratories by pouring ultra pure Milli-Q water through sampling apparatus (bottle + funnel) and analyzing it as a rain sample. No detectable contamination was found.

3. Results and discussion

The dissolved and particulate Al data reported here and the pHs, sulfate and sodium concentrations of the precipitation sample are listed in table 1.

3.1. ALUMINIUM SOLUBILITY

Although Byrne and Kester (1976) indicate that various pore size induce variations in iron solubility measurements, we suggest that aluminium is not strongly influenced by the reduction of pore size from 0.4 to 0.2 µm as shows the similar behaviour to other for GCE samples.

The concentrations of total aluminium in the precipitation considered here varies from 0.2µmol.l^{-1} (Ireland) to 110 µmol.l^{-1} (Corsica) with solubility ranging from 0.2% (Cor3, Sco12, Wat2) up to 91% (Sco9). Beside the very wide range of concentrations, the results from all sites show this wide range of solubilities. Consequently, a mean solubility of Al is not really appropriate. Prospero and Nees (1987), Sequeira (1988) and Losno et al. (1988) have previously underlined the importance of pH variation in the solubility of metal ions in rainwater. It is clear (table 1) that no simple relationship exists between pH and Al solubility, though solubilities tend to be lower at high pHs (Prospero and Nees, 1987). Below we propose an equilibrium model that appears to be able to explain many features of the dissolved/particulate distribution of Al.

3.2 CHEMICAL SPECIATION OF AQUEOUS ALUMINIUM

The first chemical approach involves a thermodynamic description, and needs more information than simply elemental dissolved concentration. However, we can calculate the proportion of each soluble aluminium species from the measured dissolved elemental concentration, assuming an equilibrium between aluminium and some ligands which were also measured (Stumm and Morgan, 1981; Turner et al., 1981). Free aluminium (hydrated Al^{3+} in water) can react with a ligand L by the following reaction:

$$Al^{3+} + nL^{z-} <==> Al(L)_n^{(3-nz)+} \quad (1)$$

with an equilibrium constant β:

$$\beta_n=[Al(L)_n^{(3-nz)+}]/[Al^{3+}][L^{z-}]^n \quad (2)$$

A specific formulation is used for hydroxy complexes:

$$Al^{3+} + nH_2O <==> Al(OH)_n^{(3-n)+} + nH^+ \quad (3)$$

with an equilibrium constant β':

$$\beta'_n=[Al(OH)_n^{(3-n)+}][H^+]^n/[Al^{3+}] \quad (4)$$

In these expressions, we have used the concentrations of species because the low ionic strength of rain water (<10^{-3} mol.l^{-1}, except Eir5, 6, 8, 9, Atl7 and Cor1) makes concentration, expressed in mol.l^{-1}, essentially equal to activity. Published equilibrium data are often given at 298K, which is not within the range of rain temperatures. When it is possible, equilibrium constants are calculated at 278K using the Van't Hoff law:

$$\frac{d(\ln b)}{dT} = \&\frac{\Delta H^\circ}{RT} \quad (5)$$

where T is the absolute temperature [K], R the gas constant and ΔH° the standard enthalpy of the reaction [kJ.mol^{-1}].

sample	pH	[Na^+]	[SO_4^{--}]	sol. Al	in. Al	sample	pH	[Na^+]	[SO_4^{--}]	sol. Al	in. Al
Watox cruise						Sco 17	4.5	92	19	0.11	0.40
Wat 1	4.59	42	25	0.49	2.95	Sco 18	4.6	45	13	0.06	0.24
Wat 2	5.60	160	16	0.07	30.58	Sco 19	5.0	5	7	0.05	1.06
Wat 3	5.60			1.85	17.86	Sco 20	5.4	34	8	0.02	0.23
Wat 4	5.30		5	0.26	0.31	Sco 21	4.8	224	30	0.07	0.76
Wat 5	5.21		2	0.17	2.45	Sco 22	4.3	32	12	0.52	1.40
Wat 6	5.24	36	1	0.07	0.15	Sco 23	4.7	6	8	0.03	0.25
Wat 7	5.24	64	4	0.02	0.42	Sco 24	4.9	9	18	2.26	21.09
Brittany						Sco 25	3.9	174	76	0.74	0.37
Bri 1	5.13	132	19	1.32	2.01	Sco 26	3.7	104	75	1.82	65.82
Bri 2	5.03	206	23	1.10	2.41	Sco 27	4.5	50	10	0.12	0.21
Bri 3	5.24	504	47	1.26	5.13	Sco 28	4.9	111	16	0.20	0.26
Bri 4	4.70	356	50	0.43	3.30	Sco 29	4.6	9	6	0.01	0.47
Vosgian forest						Sco 30	4.4	93	16	0.25	0.32
Vof 1	3.21	16	76	5.40	23.18	Sco 31	4.4	217	8	0.23	0.60
Vof 2	3.05	12	127	3.96	4.71	Sco 32	4.4	183	27	0.09	0.76
Vof 3	3.15	9	107	1.39	2.30	Sco 33	3.9	4	27	1.15	7.23
Vof 4	3.36	8	104	1.56	6.93	Sco 34	4.0	5	13	0.09	0.36
Vof 5	3.54	16	80	1.87	7.23	Sco 35	4.2	4	13	0.02	0.15
Vof 6	3.81	20	60	1.15	4.24	Sco 36	4.1	21	15	0.25	1.39
Vof 7	5.22	16	21	0.16	4.48	Sco 37	4.5	39	9	0.04	0.90
Vof 8	4.98	7	13	0.33	1.40	**Corsica**					
Vof 9	4.55	7	14	0.43	1.37	Cor 1	4.0	1620	155	0.37	3.88
Vof 10	3.74	13	35	0.36	1.90	Cor 2	6.88	154.88	72.67	0.82	63.8
Vof 11	3.60	10	98	1.43	1.49	Cor 3	6.55	17	9	0.07	35.30
Vof 12	3.89	7	42	<0.2	1.25	Cor 4	5.76	45	13	0.07	15.39
Vof 13	3.71	10	69	<0.2	0.40	Cor 5	4.61	93	16	<0.05	1.15
Vof 14	4.52	9	9	0.31	1.98	Cor 6	4.39	302	44	<0.05	0.54
Vof 15	4.53	5	6	0.15	0.58	Cor 7	6.30	112	47	0.15	46.73
Vof 16	3.81	12	27	0.38	0.96	Cor 8	6.08	89	54	0.56	110.18
Vof 17	3.73	24	68	0.63	2.61	Cor 9	5.84	71	20	12.01	29.83
Vof 18	3.52	30	143	0.84	2.54	Cor 10	4.94	107	27	5.93	12.31
Vof 19	4.14	13	46	0.28	1.61	Cor 11	4.63	91	16	0.82	4.90
Vof 20	4.24	17	30	0.36	1.29	**Ireland (Mace Head)**					
Vof 21	4.49	6	14	0.15	0.63	Eir 1	4.55	137		<0.004	0.16
Vof 22	4.22	14	27	0.30	0.42	Eir 2	5.18	425		<0.004	0.25
Vof 23	4.70	12	29	0.23	4.25	Eir 3	5.39	941		0.004	0.22
Vof 24	4.46	8	15	0.20	1.19	Eir 4	5.20	669		<0.004	0.34
Vof 25	4.71	23	18	<0.2	2.96	Eir 5	5.47	2609		0.003	0.23
Vof 26	4.90	2	9	0.31	2.70	Eir 6	5.85	2744		0.004	0.32
Vof 27	4.96	1	8	0.37	0.80	Eir 7	5.24	383		<0.004	0.20
Vof 28	5.26	4	7	<0.2	0.78	Eir 8	5.22	1992		0.004	0.40
Vof 29	5.10	40	10	<0.2	0.74	Eir 9	6.24	3200		0.011	0.43
Scottish snow						Eir 10	4.74	90	9	<0.004	0.21
Sco 1	4.1	603	92	0.48	3.41	Eir 11	5.39	1032		0.003	0.17
Sco 2	4.3	9	15	0.26	1.15	Eir 12	5.23	611		<0.004	0.27
Sco 3	4.2	14	16	0.06	0.37	Eir 13	5.04	929		0.021	0.31
Sco 4	4.1	91	21	0.13	0.78	Eir 14	4.91	241		<0.004	0.33
Sco 5	3.7	95	53	0.11	0.70	**Polarstern cruise**					
Sco 6	3.8	32	45	0.89	9.75	Atl 1	4.68	280	19	0.10	0.75
Sco 7	5.0	25	8	0.03	0.30	Atl 2	4.81	174	22	3.48	4.47
Sco 8	4.9	6	7	0.08	0.56	Atl 3	5.76	18	2	0.23	12.10
Sco 9	4.8	126	19	4.78	0.48	Atl 4	5.73	7	0	<0.04	1.94
Sco 10	4.9	52	11	0.06	0.41	Atl 5	5.43	29	3	1.30	6.15
Sco 11	5.5	35	7	0.46	0.33	Atl 6	4.19	134	21	0.50	4.70
Sco 12	5.2	46	9	0.00	0.48	Atl 7	4.30	5700	341	0.10	2.63
Sco 13	6.4	2	5	0.01	0.08	Atl 8	4.71	37	4	<0.04	0.90
Sco 14	4.3	99	20	0.05	0.07	Atl 9	4.76	18	3	<0.04	0.66
Sco 15	4.4	103	19	0.45	0.15	Atl 10	4.67	21	3	<0.04	0.95
Sco 16	4.2	98	19	0.09	0.17	Atl 11	3.98			0.96	1.82

Table 1: Analytical results. All concentrations are expressed in µmol.l^{-1}.

If T varies from 298K to 278K, we have:

$$\log\beta_{278} = \log\beta_{298} - 0.0126\,\Delta H° \quad (6)$$

L may be sulfate, hydroxide, fluoride or carbonate (table 2).
If we consider all the L_i possible ligands, taking account there excess with regards to [Al], the concentration of free aluminium, $[Al^{3+}]$, can be calculated as (Stumm and Morgan, 1981):

$$[Al^{3+}] = [Al]\,(1 + \Sigma\,\beta_{i,n}\,[L_i]^n + \Sigma\,\beta'_n\,[H^+]^{-n})^{-1} \quad (7)$$

and the concentration of each species $Al(L_i)_n$ is given by

$$[Al(L_i)_n] = [Al^{3+}]\,[L_i]^n\,\beta_{i,n} \text{ or } p[Al(L_i)_n] = p[Al^{3+}] + n\,p[L_i] + p\,\beta_{i,n} \quad (8)$$

where:

$$p[X] = -\log([X]). \quad (9)$$

ligands	$\log\beta_1$	$\log\beta_2$	$\log\beta_3$	$\log\beta_4$
sulfate	2.9	4.8		
hydroxyde	-5.6	-11.2	-15*	-23.23
fluoride	6.9	12.7		
carbonate	8.43*			

Table 2: complexation constants for aluminium dissolved species. These values are calculated at 278K from data (K and ΔH°) given by Schecher and Driscoll (1987), except those marked by * which come from Turner et al. (1981) and are given at 298K.

Calculations performed on the presented data show that Al^{3+} and $Al(OH)_2^+$ are the major dissolved aluminium species in our samples (figure 2), except for Sco1, Atl7 and Cor1 where fluoride complexes appear to be important (>30%). $Al(SO_4)^+$ appears as a minor species, with higher concentrations (5 to 10%) in polluted acidic rains (Vof2, Vof3, Vof4, Vof11, Vof17, Vof18, Sco26). Other species are negligible (except $Al(OH)_4^-$ in Cor2).

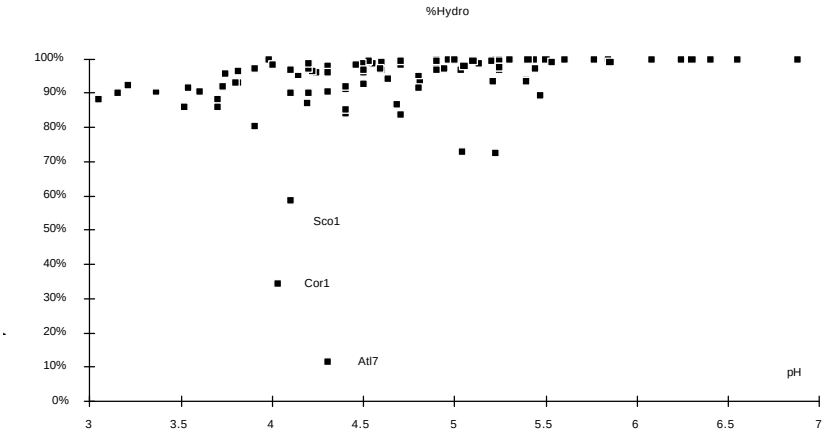

Figure 2: percent of hydroxy and and hydrated aluminium(III) concentration (sum of concentrations of Al^{3+}, $Al(OH)^{2+}$, $Al(OH)_2^+$, $Al(OH)_3°$ and $Al(OH)_4^-$) as function of pH.

Calculations on some polymerized species ($Al_2(OH)_2^{4+}$, $Al_3(OH)_4^{5+}$, $Al_{13}O_4(OH)_{24}^{7+}$) with data found in Stumm and Morgan (1981) (at ionic strength=0 and 298K) show that polyhydroxides $Al_m(OH)_n^{(3m-n)+}$ do not appear in our samples.

3.3 EQUILIBRIUM BETWEEN SOLUBLE AND PARTICULATE ALUMINIUM

Aluminium may form an insoluble salt with:

(i) phosphate (variscite) (Stumm and Morgan, 1981):

$$AlPO_4.2H_2O\downarrow = Al^{3+} + PO_4^{3-} + 2H_2O \qquad pK_{var,298K} = 21 \qquad (10)$$

(ii) hydroxide anions(amorphous or gibbsite)(Stumm and Morgan, 1981, $\Delta H°$ calculated from Bard et al., 1985):

$$amAl(OH)_3\downarrow + 3H^+ = Al^{3+} + 3H_2O \qquad pK_{am,278K} = -12.0 \qquad (11)$$

$$\alpha Al(OH)_3\downarrow + 3H^+ = Al^{3+} + 3H_2O \qquad pK_{\alpha.gib,278K} = -9.7 \qquad (12)$$

May et al. (1979) indicates variations on gibbsite solubility, particularly if "synthetic" gibbsite is used where its pK is 0.5 unit lower, probably caused by an entropic effect.

(iii) basic-sulfates (Johnson et al., 1981), for example among others:

$$Al(OH)SO_4\downarrow + H^+ = Al^{3+} + SO_4^{2-} + H_2O \qquad pK_{sulf,298K} = 3.2 \qquad (13)$$

Calculations on samples for which phosphate concentrations were available show that the solubility product of variscite is never exceeded by several orders of magnitude and we therefore conclude this species is not of importance.

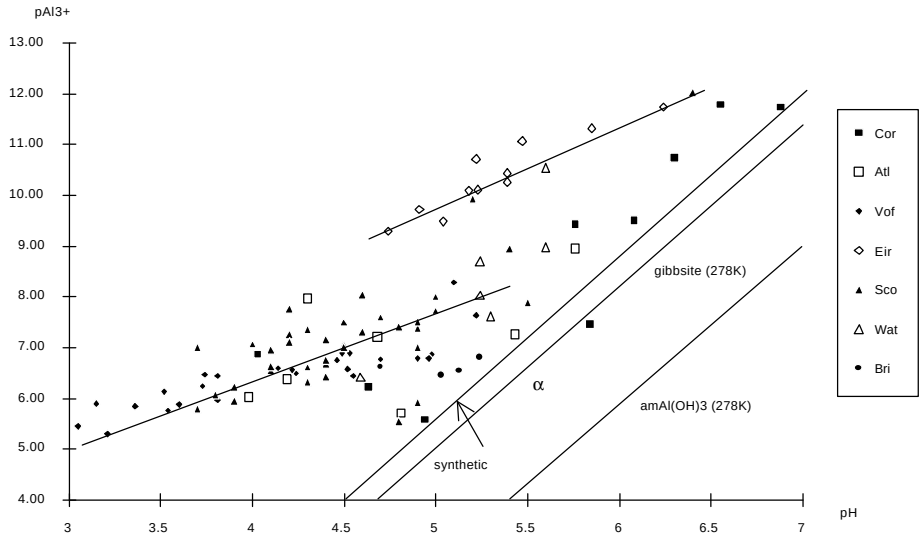

Figure 3: logarithmic concentration of "free" aluminium ($p[Al^{3+}]$) as function of pH

In the case of equilibrium with insoluble salts, equations (11 and 12) indicate a strong dependence of the concentration of Al^{3+} species on pH, where:

$$p[Al^{3+}] = pK_{am} + 3pH \qquad (14a)$$

$$p[Al^{3+}] = pK_{gib} + 3pH \qquad (14b)$$

and for equation (13):

$$p[Al^{3+}] = pK_{sulf} - p[SO_4^{2-}] + pH \qquad (15)$$

We show $p[Al^{3+}]$ as a function of pH in figure 3. Three behaviours appear for the samples: $p[Al^{3+}]$ is dependent on pH with a slope close to 1 between pH 3 and 5, with a slope close to 3 for pH>5 and with a slope close to 2 for very low loaded rains (mainly Eir samples). This indicates that an equilibrium like (13) may be predominant at pHs between 3 and 5 (typically polluted rains or snows) and like 11 or 12 for higher pHs.

3.3.1 *Aluminium Hydroxysulfate Salt*. The equilibrium reported in equation (13) implicates sulfate concentrations at pHs<5. It can be modified by different stoichiometry coefficients:

$$Al(OH)_x(SO_4)_{(3-x)/2}\downarrow + x\ H^+ <==> Al^{3+} + x\ H_2O + (3-x)/2\ SO_4^{2-} \qquad (16)$$

with an equilibrium constant:

$$pK_{x,sulf}=p[Al^{3+}]+(3-x)/2p[SO_4^{2-}]-xpH \quad (17)$$

In figure 4, ($p[Al^{3+}]+3/2p[SO_4^{2-}]$) is plotted as a function of (pH + 1/2 $p[SO_4^{2-}]$). By a classical mean square regression on 61 samples at pH<5 (Atl2, Eir10, Sco9-12-13-24-35-38 are discarded because their deviating position), we obtain a line with a slope of x= 1.54 (±0.01) and an intercept of $pK_{x,sulf=}$ 3.6 (±0.3), which allows us to propose the following equilibrium:

$$Al(OH)_{1.5}(SO_4)_{0.75}\downarrow + 1.5\ H^+ <=> Al^{3+} + 1.5\ H_2O + 0.75\ SO_4^{2-} \qquad pK_{1.5,sulf}= 3.6 \quad (18)$$

or:

$$Al_4(SO_4)_3(OH)_6\downarrow + 6H^+ <=> 4\ Al^{3+} + 6H_2O + 3\ SO_4^{2-} \qquad pK= 14.4 \quad (19)$$

which is close to possible aluminium sulfate minerals presented by Johnson et al. (1981) and Nordstrom (1982) for acidic natural waters.

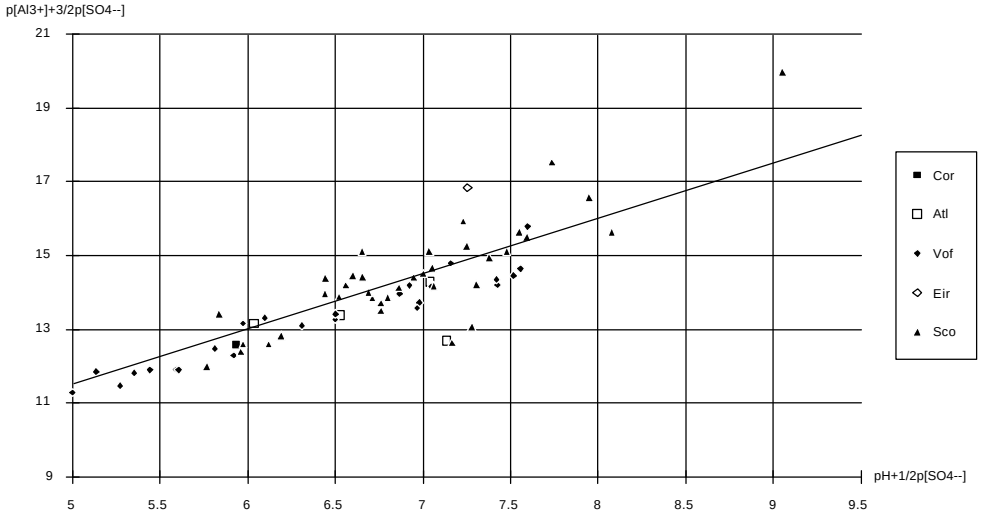

Figure 4: determination of the stoichiometry of hydroxy-sulfate salts for samples at pHs<5, see equation (17).

Then, the solubility of aluminium in such rains or molten snows at pH<5 can be predicted as:

$$p[Al^{3+}] = 3.6 + 1.5\ pH - 0.75\ p[SO_4^{2-}] \quad (20)$$

and more generally taking into account equation (15), pH<5:

$$p[Al_{soluble}] = 3.6 + 1.5\ pH - 0.75\ p[SO_4^{2-}] - \log(1+ \Sigma\ \beta_{i,n}\ [L_i]^n + \Sigma\ \beta'_n\ [H^+]^{-n}) \quad (21)$$

Figure 5 shows the relationship between measured and calculated soluble aluminium in acidic rains. It is clear that equation (21) only approximately fits the logarithmic data.

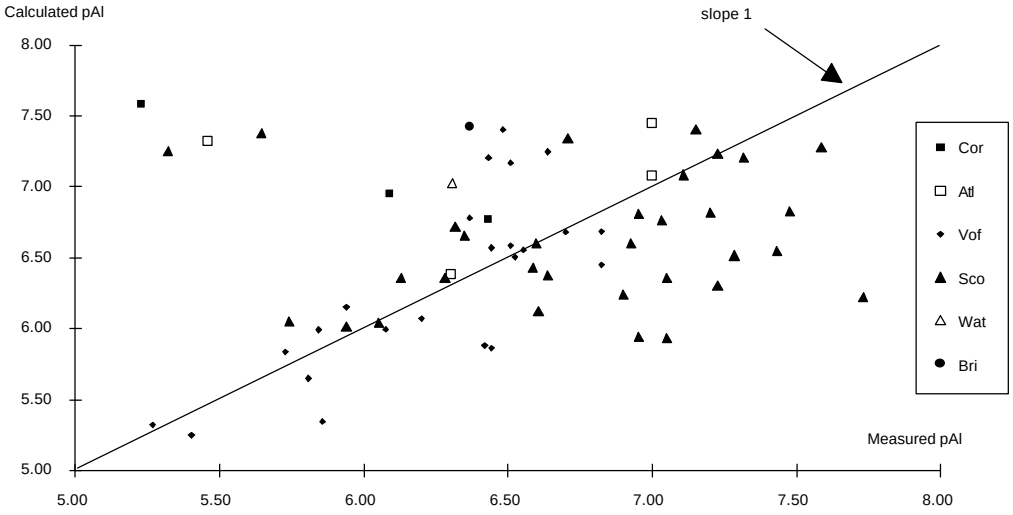

Figure 5: calculated soluble aluminium concentration versus measured in acidic (pH<5) rains and snows.

Consequently, for rain and molten snow with a pH<5, the solubility of aluminium may not depend on the concentration of its particulate fraction and therefore on its origin and history. This behaviour of aluminium in acid rainwater or molten snow, rich in sulfate ions, is thus similar to that in natural surface waters described by Nordstrom and Ball (1986).

3.3.2. *Amorphous aluminium hydroxide and Gibbsite Solubility.* The dispersion of $p[Al^{3+}]$ around the line of slope 3 (figure 3) is greater at pH>5. However, a linear plot of $p[Al^{3+}]$ versus pH with a slope of 3 does approximated fit the data for the most concentrate samples (figure 3). We have drawn on figure 3 the lines which represent equilibrium between Al^{3+} and gibbsite, "synthetic" gibbsite or amorphous hydroxide at 5°C (equation 22). It can be pointed out that the intercept of these line depends on temperature (-0.06 K^{-1}).

$$p[Al^{3+}] = -9.7 + 3\ pH \text{ for } (\alpha) \qquad (22a)$$

$$p[Al^{3+}] = -12.0 + 3\ pH \text{ for (am)} \qquad (22b)$$

The amorphous form is never reached and no sample is over saturated for αgibbsite which may therefore act as a limit in the solubility of aluminium. The line which best fits the data at pH>5 presents an intercept closest of the synthetic (May et al., 1979) than natural gibbsite line; its suggests that a coating is formed and deposited on the solid material enclosed in the rain drops. This coating can be formed by two ways:

(i) "Fast" incongruent dissolution of clays releasing dissolved silica and solid gibbsite (Stumm and Morgan, 1981), as shown by high amounts of dissolved silica (1 to 10 µmol.l^{-1}) observed in Corsican rains (Losno 1989). This may arise because of the high surface/volume ratio for particulate material enclosed in the rain drops, but needs further investigations.

(ii) Neutralization of a previously acidic rain by alkaline material (e.g. carbonates, feldspar) following a mixing of air masses in a frontal event (Losno et al., 1991; Losno et al., 1988): the increase of pH causes the formation of gibbsite from aqueous aluminium and hydroxide ions.

For such rains, the aluminium solubility can be predicted to be less than:

$$p[Al^{3+}] \geq -9.7 + 3\ pH \qquad (23)$$

and considering that only $Al(OH)_2^+$ and $Al(OH)_3°$ are predominant in this pH range:

$$p[Al_{soluble}] \geq -9.7 + 3\ pH - \log(\beta'_2\ [H^+]^{-2} + \beta'_3[H^+]^{-3}) \qquad (24)$$

Irish rains and some Scottish snows are very undersaturated with respect to gibbsite, but still, pAl^{3+} appears to fit a slope of approximately 2 on figure 3. This suggests an equilibrium which involves 2 moles of H^+ ions for one mole of aluminium with another solid phase. This di-alkaline particulate aluminium would then have greater stability (or lower solubility) than gibbsite. This behaviour appears only when total (particulate+soluble) aluminium concentrations are very low ($[Al_{soluble}]$<0.07 µmol.l^{-1}: Sco13, Sco19, Sco20, all Eir samples, Wat6 and Wat7).

4. Conclusions

Many of the features of the dissolved/particulate behaviour of Al can be rationalized by this model. However, this treatment is simplistic and other factors must also be involved. For instance, the major source of Al into the atmosphere is clay minerals in remote areas and the dissolution kinetic processes of Al from there must also be considered. It is possible that at low pH in cloud water and after several wetting and drying cycles during atmospheric transport, sufficient Al is dissolved from clays that as the pH rises during precipitation formation the dissolved/particulate distribution can indeed be poised by equilibrium with $Al(OH)_{1.8}(SO_4)_{0.6}$ and $Al(OH)_3$ though the kinetics of these processes are unknown under cloud water and raindrop conditions. In these conditions, it is not surprising that "synthetic" gibbsite is a better fit than gibbsite for the less acidic samples. However, as previously described for zinc (Losno et al., 1988), the behaviour of aluminium in atmospheric droplets is similar to that described in surface water (Nordstrom and Ball, 1986), especially into the range of pHs 3 to 5, where the grater stability of hydroxysulfate salts is demonstrated by Nordstrom (1982).

Acknowledgments

We thank T.D. Davies, M. Tranter, K. Jarvis and S. Landsberger for permission to use the Scottish data; these analyses were supported by the NERC, ICP-MS unit. We thank all the members of the GCE expedition for help collecting these samples. We thank the French National Navy which allows the sampling program at Capo Cavallo, the German A.W.I., K.F.A. and the crew of the Polarstern vessel, and B.Chatenet, H.Lazar and G.Malingre for help. This work was supported by the NERC in the U.K. and by the CNRS, the French Ministry of the Environment and the EEC (under DEFORPA and EUROTRAC ASE programs). Reviewer's comments are acknowledged for improvements of this paper.

References

Bard, A.J., Parsons, R. and Jordan, J. (1985) 'Standard Potentials in Aqueous Solution', IUPAC, Marcel Dekker Inc., New York and Basel.

Byrne, R.H. and Kester, D.R. (1976) 'Solubility of hydrous ferric oxide and iron speciation in seawater', *Marine Chemistry*, **4**, 255-274.

Colin, J.L., Renard, D., Lescoat, V., Jaffrezo, J.L., Gros, J.M. and Strauss, B. (1989) 'Relationship between rain and snow acidity and air mass trajectory in Eastern France', *Atmos. Environ.*, **23**, 1487-1498.

Colin, J.L., Jaffrezo, J.L. and Gros, J.M. (1990) 'Solubility of major species in precipitations: factors of variation', *Atmos. Environ.*, **24A**, 537-544.

Davies, T., Abrahams, P.W., Tranter, M., Blackwood, I., Brimblecombe, P. and Vincent, C.E. (1984) 'Black acid snow in the remote Scottish Highlands', *Nature*, **312**, 58-61.

Galloway, J.N., Likens, G.E., Keene, W.C. and Miller, J.M. (1982) 'The composition of precipitation in remote areas of the world', *J. Geophys. Res.*, **87**, 8771-8786.

Jaffrezo, J.L. and Colin, J.L. (1988) 'Rain aerosol coupling in urban area: scavenging ratio measurements and identification of some transfer processes', *Atmos. Environ.*, **22**, 929-935.

Jickells, T.D., Davies, T.D., Tranter, M., Landsberger, S., Jarvis, K. and Abrahams, P. (1992) 'Trace elements in snow samples from the Scottish Higlands: sources and dissolved/particulate distributions', *Atmos. Environ.*, **26A**, 393-401.

Johnson, N.J., Driscoll, C.T., Eaton, J.S., Lickens, G.E. and Mc Dowell, W.H. (1981) "Acid rain', dissolved aluminium and chemical weathering at the Hubbard Brook Experimental Forest, New Hampshire.', *Geochim. Cosmochim. Acta*, **45**, 1421-1437.

Junge, C. and Mc Laren, E. (1971) 'Relationship of cloud nuclei spectra to aerosol size distribution and composition', J. *Atmos. Sci.*, **28**, 382-390.

Landsberger, S., Davies, T.D., Tranter, M., Abrahams, P.W. and Drake, J.J. (1989) 'The solute and particulate chemistry of background versus a polluted black snowfall on the Cairngorm mountains, Scotland', *Atmos. Environ.*, **23**, 395-401.

Lim, B. and Jickells, T.D. (1990) 'Dissolved, particulate and total trace metals in North Atlantic precipitation collected on the Global Change Expedition', *Global Biogeochemical Cycles*, **4**,445-458.

Lim B. (1991) 'Trace metals in North Atlantic precipitation', Ph-d Thesis, University of East Anglia, Norwich.

Losno, R., Bergametti, G. and Buat-Ménard P. (1988) 'Zinc partitioning in Mediterranean rainwater', *Geophys. Res. Lett.*, **15**, 1389-1392.

Losno, R. (1989) 'Chimie d'éléments minéraux en trace dans les pluies méditerranéennes', thesis, Paris 7 University, France.

Losno, R, Bergametti, G., Carlier, P. and Mouvier, G. (1991) 'Major ions in marine rainwater with attention to sources of alkaline and acidic species', *Atmos. Environ.*, **25A**, 763-770.

Martens, C.S. and Harriss, R.C. (1973) 'Chemistry of aerosols, cloud droplets and rain in the Puerto Rican marine atmosphere', *J. Geophys. Res.*, **78**, 949-957.

May, H.M., Helmke, P.A. and Jackson, M.L. (1979) 'Gibbsite solubility and thermodynamic properties of hydroxy-aluminium ions in aqueous solution at 25°C', *Geochim. Cosmochim. Acta*, **43**, 861-868.

Nordstrom, D. K. (1982) 'The effect of sulfate on aluminum concentrations in natural waters: some stability relations in the system Al_2O_3-SO_3-H_2O at 298 K', *Geochim. Cosmochim. Acta*, **46**, 681-692.

Nordstrom, D. K. and Ball, J. W. (1986) 'The geochemical behavior of aluminium in acidified surface water', *Science*, **232**, 54-56.

Prospero, M and Nees, R.T. (1987) 'Deposition rate of particulate and dissolved aluminium derived from saharan dust in precipitation at Miami, Florida', *J. Geophys. Res.*, **92**, 14723-14731.

Pruppacher, H.R. and Klett, J.D. (1980) The role of cloudphysics in atmospheric multiphase system: ten basic statements, D. Reidel Publishing Company.

Ross, H. (1986) Trace metals in the atmosphere: the wet deposition of trace metals in Sweden; the selenium cycle, dissertation for Doctor's degree in Chemical Meteorology, University of Stockolm, Sweden.

Schecher, W.D. and Driscoll, C.T. (1987) 'An evaluation of uncertainty associated with aluminium equilibrium calculations', *Water Resources Research*, **23**, 525-534)

Sequeira, R. (1988) 'On the solubility of some natural minerals in atmospheric precipitation', *Atmos. Environ.*, **22**, 369-374.

Stumm, W. and Morgan, J.J. (1981) Aquatic Chemistry: an introduction emphasizing chemical equilibria in natural water. 2nd Ed., John Wiley and Sons, New-York.

Turner, D.R., Whitfield, M. and Dickson A.G. (1981) 'The equilibrium speciation of dissolved components in freshwater and seawater at 25°C and 1 atm pressure', *Geochim. Cosmochim. Acta*, **45**, 855-881.

8.6 Origins of the Atmospheric Particulate Matter over the North-Sea and the Atlantic Ocean

R. LOSNO, G. BERGAMETTI, P. CARLIER
Laboratoire de Physico-Chimie de l'Atmosphère, UA CNRS 1404, Université Paris 7, 2 place Jussieu, 75251 Paris Cedex 05, France.

ABSTRACT

During the ANT VII/1 cruise of the RV Polarstern from Bremerhaven (FGR) to Rio Grande do Sul (Brazil), aerosols were collected with a time step of 36 hours. Elemental analyses have been performed in order to determine atmospheric aerosol concentrations of Al, Si, P, S, K, Ca, Ti, Mn, Fe and Zn over the North-Sea, Channel, North and South Atlantic. The slight and continuous moving in latitude, associated to large variability in concentration levels and chemical composition, allows to point out the relative influence of the major sources of particulate matter: desert soil-dust in the tropical North Atlantic, anthropogenic emissions in the North Sea and Channel and biomass burning and continental biogenic activity in the tropical South Atlantic.

INTRODUCTION:

The atmospheric particulate matter plays a significant role in interactions between continents and oceans, especially by acting on the deep-sea sedimentation (Rea et al., 1985) and on the biogeochemistry of the oceans (Buat-Ménard, 1983). The remote marine areas are primarily interested by such inputs because the atmospheric fallout is one of the major source of matter for these surface oceanic waters.

At this time, a limited number of data concerning the sources and composition of aerosols over the Atlantic ocean has been reported. The most complete studies of aerosol transport over Atlantic Ocean were those dealing with the transport of African dust over the North Tropical Atlantic (Chester et al., 1972; Prospero and Carlson, 1972; Prospero, 1979; Schütz et al., 1981; Coudé-Gaussen et al., 1987; Bergametti et al., 1989). These works shown the hight content of the atmosphere in soil-derived particles over the North Atlantic Ocean, primarily between 30°N and 10°N, and the implications of these dust fallouts on the oceanic water column composition (Buat-Ménard and Chesselet, 1979; Chester et al., 1979) and deep-sea sediment formation (Sarnthein et al., 1982).

The influence of human activities on the atmospheric composition over the Atlantic Ocean has been also pointed out by measuring highly enriched elements as Pb, Zn or Cu (Buat-Ménard and Chesselet, 1979; Völkening et al., 1988), which are well-known pollutants. However, some crucial elements for the biogeochemistry of the oceans as phosphorus or manganese were presently poorly studied. Moreover, data on aerosol composition over the South Atlantic were very scarse.

The cruise track of RV Polarstern in September-October 1988 (ANT VII), allowed us to investigate the elemental composition of the atmospheric aerosol over the North Sea, the Channel, the North and South Atlantic.

SAMPLING AND EXPERIMENT

Aerosol samples were collected from September 14 to October 6 during the expedition ANTVII/1 of the German RV Polarstern. The route of ANTVII/1 started from Bremerhaven (FRG) (54°N, 9°E) to finish in Rio Grande do Sùl (Brazil) (32°S, 52°W). The route of the ship is described in Müller et al., this issue.

Aerosol samples were collected by bulk filtration on 0.4µm pore size Nuclepore filters with a pumping rate of about $1 m^3.h^{-1}$. The sampling duration was generally 36h. The filtration unit was placed at the top of a 3m long pole located in front of the iceberg guard platform which is 25m high above sea level and about 10m high above the highest deck of the ship. Moreover, to prevent possible contaminations by smoke emitted from the chimney of the ship about 40m back, an automatic device stopped the pump when the local wind conditions were not satisfying. We have choosen to sample only when the wind velocity was more than $1.5 m.s^{-1}$ and when the wind direction made an angle less than 80° with the prow. The pumps were stopped immediatly when local wind was not propicious and switched on only 10 to 20 seconds after that better conditions were retrieved.

The sampling locations are listed in table 1 and the local wind conditions were plotted by Müller et al. (this issue).

For all the samples, the concentrations of Al, Si, P, S, K, Ca, Mn, Fe and Zn have been determinated by

wavelength dispersive X-Ray fluorescence spectrometry (CGR Ó10) according to the method described by Losno et al. (1987). Primarily, X-Ray excitation is produced by a chromium target for Al, Si, P, S, K and Ca, a copper target for Mn and Fe and a gold target for Zn. The intensity of fluorescence emission was measured on the K` X-Ray of the element and compared with those given by thin layer standards. The uncertainties of measurements were determinated during calibration and were found to be less than 7%.

Sample	Date begin	Date end	Latitude begin	Latitude end	Longitude begin	Longitude end	Rain
Atlan 1	16/09/88 08:20	17/09/88 10:27	53° 32' N	50° 15' N	04° 57' E	00° 16' E	No
Atlan 2	17/09/88 10:30	18/09/88 09:22	50° 15' N	47° 39' N	00° 16' E	07° 13' W	No
Atlan 3	18/09/88 09:25	19/09/88 13:28	47° 39' N	43° 28' N	07° 13' W	14° 25' W	No
Atlan 4	19/09/88 13:31	20/09/88 13:37	43° 28' N	41° 42' N	14° 25' W	17° 20' W	No
Atlan 5	20/09/88 13:40	21/09/88 10:27	41° 42' N	39° 27' N	17° 20' W	21° 45' W	Yes
Atlan 6	21/09/88 10:30	22/09/88 14:53	39° 27' N	37° 01' N	21° 45' W	26° 04' W	No
Atlan 7	22/09/88 14:56	23/09/88 15:27	37° 01' N	32° 12' N	26° 04' W	28° 47' W	Yes
Atlan 8	23/09/88 15:30	24/09/88 20:22	32° 12' N	26° 14' N	28° 47' W	30° 00' W	No
Atlan 9	24/09/88 20:25	26/09/88 10:22	26° 14' N	17° 35' N	30° 00' W	30° 00' W	No
Atlan 10	26/09/88 10:25	27/09/88 20:19	17° 35' N	10° 00' N	30° 00' W	30° 00' W	No
Atlan 11	27/09/88 20:22	28/09/88 17:13	10° 00' N	05° 06' N	30° 00' W	30° 00' W	Yes
Atlan 12	28/09/88 17:16	29/09/88 19:37	05° 06' N	00° 24' S	30° 00' W	30° 00' W	Yes
Atlan 13	29/09/88 19:40	30/09/88 20:47	00° 24' S	05° 46' S	30° 00' W	30° 00' W	No
Atlan 14	30/09/88 20:50	02/10/88 11:47	05° 46' S	14° 17' S	30° 00' W	30° 00' W	No
Atlan 15	02/10/88 11:50	03/10/88 15:02	14° 17' S	20° 22' S	30° 00' W	30° 00' W	No
Atlan 16	03/10/88 15:05	04/10/88 15:57	20° 22' S	26° 03' S	30° 00' W	30° 00' W	No
Atlan 18	04/10/88 17:15	05/10/88 19:40	26° 20' S	30° 16' S	30° 00' W	32° 54' W	No
Atlan 19	05/10/88 19:43	06/10/88 18:40	30° 16' S	30° 48' S	32° 54' W	37° 56' W	Yes

Table 1: Sampling locations

RESULTS

The elemental concentrations are reported on figure 1 as a function of the sampling latitude. Various behaviours of the elements all along this cruise can be immediatly underlined:

- Over the North Sea and the Channel, S, Zn, K and P as well as Mn exhibit high atmospheric concentrations which decrease continuously between 50°N and 40°N. On the contrary, Al, Si, Ca, Fe show also relatively high atmospheric concentrations but without significant decrease between 50°N and 40°N.
- While between 40°N and equator S and Zn present relatively stable low concentrations, the other elements (Al, Si, P, Mn, Ca, K, Fe) exhibit their higher concentrations between 20°N and 10°N.
- In the south hemisphere, the concentrations of all the elements are the lowest observed during the cruise, excepted for K which shows a second major peak between equator and 20°S.

In view of this brief description of the elemental composition of atmospheric aerosol during this cruise, at least three different periods must be distinguished in order to identify the sources and the source-regions of the collected particles.

DISCUSSION

A/ North Sea and Channel

As indicated above, high concentrations were observed for elements generally associated to anthropogenic emissions (S, Zn, K, P). These concentrations as high as 50ng.m-3 for Zn, 3500ng.m-3 for S, 20ng.m-3 for P and 580ng.m-3 for K, are in good agreement with those obtained in these areas by Deuderwarder et al. (1985) and Cambray et al. (1975). Enrichment factors can also be computed by the well-known formula:

$$E.F. = (X/Si)_{aer} * (Si/X)_{soil\ model}$$

(with silicon as a reference element) in order to point out anormalous highly enriched elements versus an average soil composition (Rahn, 1976). According to wind direction (Müller et al., this issue) and as

indicated by high crustal enrichment factors (table 1), the high concentrations of S, Zn, Pb, Cu primarily result from land based anthropogenic sources in the north European industrial countries.

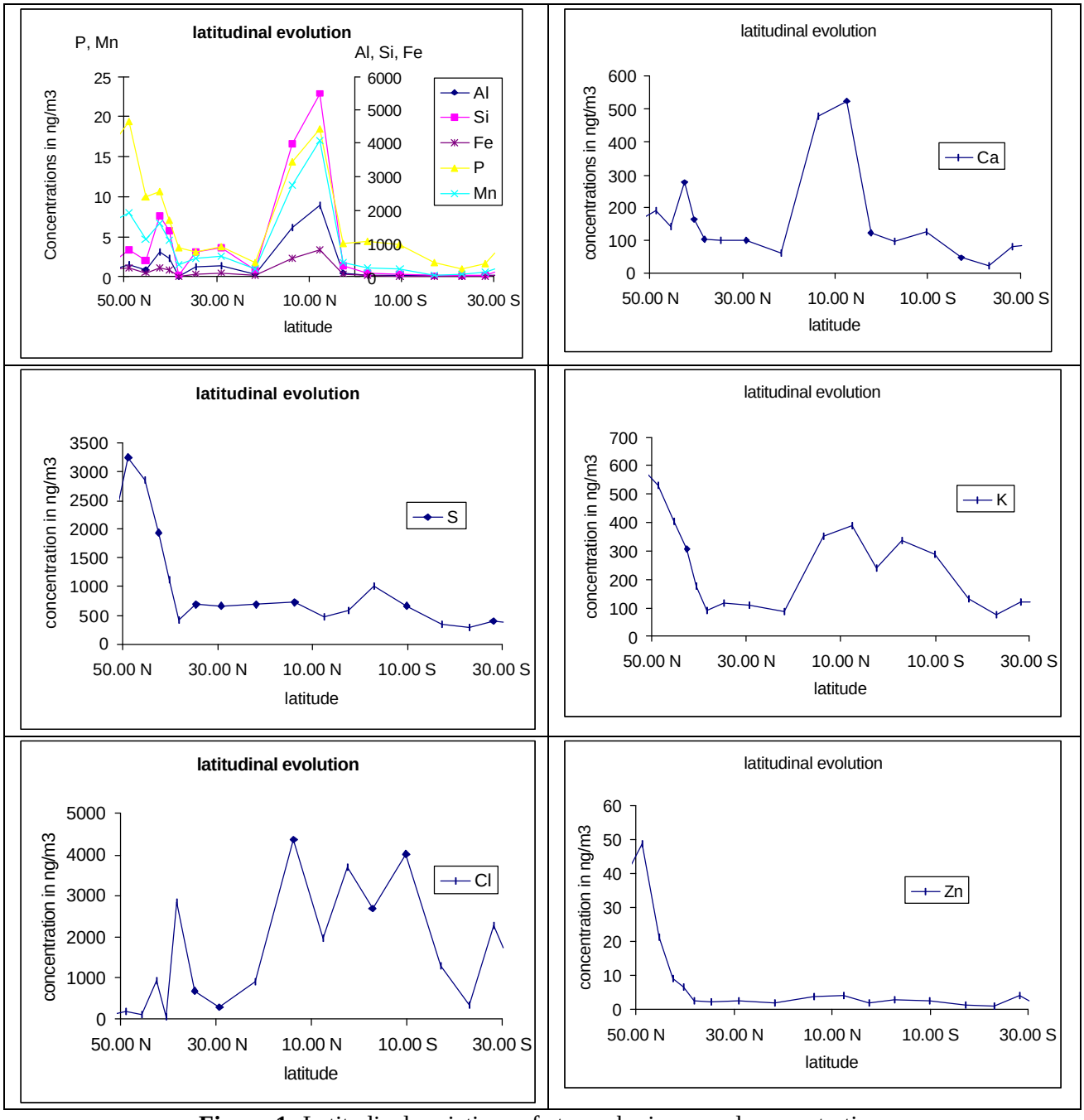

Figure 1: Latitudinal variations of atmospheric aerosol concentrations.

Latitude	Al	Si	P	S	K	Ca	Mn	Fe	Zn
50°15' N	1.7	1	9.7	3140	14	2.5	4.8	3.2	322
47°39' N	1.7	1	7.0	3085	8.1	1.8	3.4	2.2	245

Table 2: Enrichment factors of the analyzed elements over the North Sea and Channel using an earth crust model (Turekian, 1971) with Si as reference.

However, a significant contribution of particulate S could also be produced by sea salt. Measurements of non sea salt SO42- made during this cruise by Bürgermeister et al. (1990) show that more than 3µg.m-3 of S can not be attributed here to the production of sea-salts by bubbling. This indicates that the major part of particulate sulfur concentrations observed over the North sea and the Channel can be probably attributed to anthropogenic activities, even if a small contribution from DMS oxydation can be expected.

Moreover, we can observe on table 2 that some elements as calcium, iron or manganese exhibit lower but significant enrichment factors, indicating also a probable anthropogenic contribution.

A rough estimate of the anthropogenic contribution to the concentrations of these elements in these areas can be obtained by using the classical Chemical Element Balance (CEB) method (Miller et al, 1972). If we assume that Si is only associated to soil-derived particles, and that the ratio of the element X versus silicon is known in the parent-soil, we can write:

$$Xex = Xaer - [(X/Si)_{soil} * Si_{aer}]$$

with: X_{ex}= concentration of X resulting from non-crustal sources
X_{aer} = measured concentration of X in aerosol
Si_{aer}= measured concentration of Si in aerosol
$(X/Si)_{soil}$= ratio of these elements in the parent-soil

If we express this equation as a function of the enrichment factor, we obtain:

$$X_{ex}\ (\%) = [(EF-1)/EF] * 100$$

The precision of such an estimation of the non-crustal contributions (in this case, primarily anthropogenic) is mainly limited by the capability of the soil-model to reflect the relative abundances of the elements in the parent-soil. A comparison of various earth crust and soil models allowed us to estimate this incertainty to be about 25% for the Fe, Ca and Mn elements (Losno, 1989). So, the uncertainty on Xex can be expressed (Losno, 1989):

$$E\%X_{ex} = 1/(EF-1) * (EF * 7\% + [7\% + 25\%])$$

where: EF is the crustal enrichment factor of X.
$E\%X_{ex}$ is the relative uncertainty of non crustal X.

These computations show that values up to 68(+/-17)% for Fe, 60(+/-20)% for Ca and 80(+/-14)% for Mn are obtained for the anthropogenic contributions in these areas. Moreover, these values must be considered as a lower limit according to the hypothesis attributing all the measured Si to the crustal source while it is probable that a part of Si also results from pollution sources. These results of elemental concentrations of trace elements over the North Sea and Channel underline the stress produced by human activities in the atmospheric environment of some regional seas and the role of the atmospheric inputs for these marine environments.

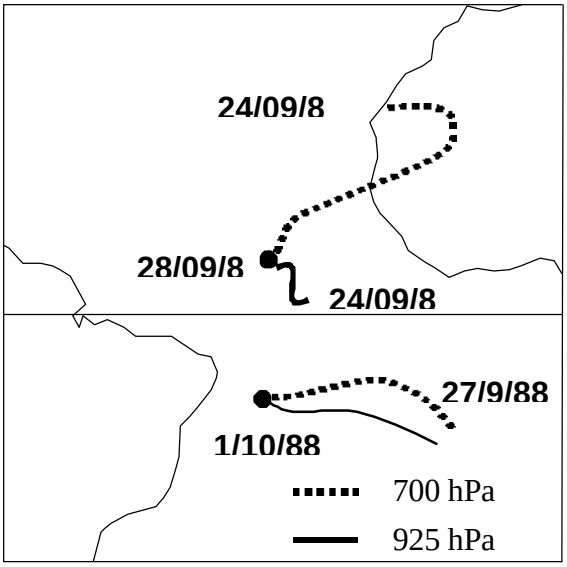

Figure 2: Two barometric levels backward air mass trajectories for the Saharan event observed in the tropical North Atlantic on 28 September and the suspected biomass burning aerosol collected between 30 September and 2 October

B/ The North Tropical Atlantic (TNA)

As previously mentioned, many works were conducted to study Saharan dust transport over this part of the Atlantic Ocean. Our results show a strong increase of soil-derived particles concentrations (as indicated

by the increase in concentrations of all the elements excepted S and at a lesser degree Zn), suggesting a significant contribution of African dust during this period. To point out such an event, four days backward air mass trajectories were computed to finish on the sampling area at two different barometric levels (925 hPa, 700 hPa) (figure 2). If in the lower layers, low wind speeds produced a short trajectory, staying over the TNA, we observe in the upper layers (700 hPa) that the air-mass comes from the arid and semi-arid areas of the African continent.

So, both the strong increase in concentrations of soil-derived particles and air-mass trajectories suggest that, during this time, the atmosphere of the Tropical North Atlantic ocean was affected by African air masses, highly loaded in soil dust. The intensity of this dust event seems to be relatively important since concentrations up to 5.5 µg.m^{-3} for Si and 2.1 µg.m^{-3} for Al were observed. Prospero (1981) reports mineral dust concentrations of about 10 µg/m^3 in this area during GATE experiments. Assuming that Al represents about 8% of the total mass of the mineral dust, we obtain, for this event, a mineral dust concentration in the range of 25 µg/m^3 indicating its strong intensity.

Obviously, during this period, all the elements exhibit their lower crustal enrichment factors (table 3).

Latitude	Al	Si	P	S	K	Ca	Mn	Fe	Zn
10°N	1.3	1	1.1	142	1.2	0.93	1	0.93	4
5°N	1.4	1	0.99	65	0.9	0.74	1.1	0.94	3.1

Table 3: Enrichment factors of the analyzed elements over the Tropical North Atlantic using an earth crust model (Turekian, 1971) with Si as reference.

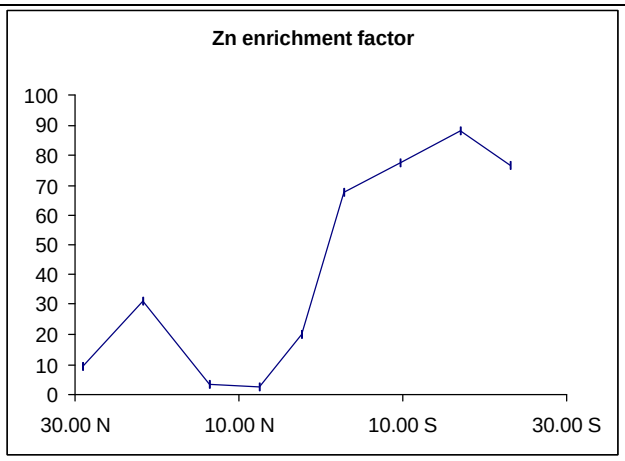

Figure 3: Crustal enrichment factor of Zn in the open Atlantic

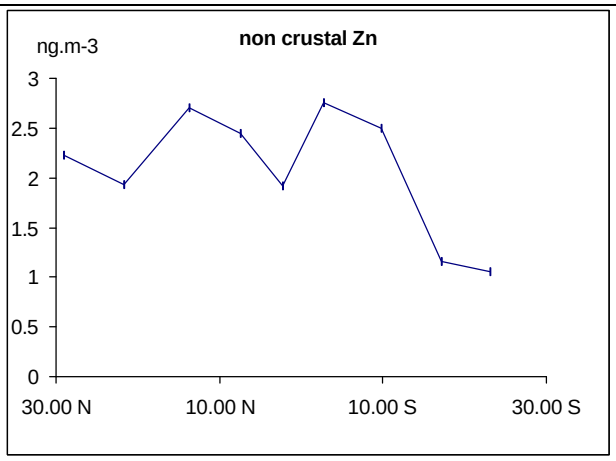

Figure 4: non crustal Zn atmospheric concentrations over the open Atlantic

Most of the concentrations of the elements are mainly controlled by this soil dust input excepted S and Zn. However, for this last element, simultaneously to a slight increase in concentrations, exceptional low values of EF were observed (figure 3). It is obvious that, during this strong dust event, a soil-dust component is superimposed to the oceanic background of Zn. By using the CEB, we can estimate that the crustal contribution represents about 30% of the total zinc measured in this area during such a dust event. By opposite, we can also deduced the oceanic background (without dust event contribution) of Zn which seems to quite stable (about 2 ng.m^{-3}) over the Atlantic Ocean between 30°N and Equator (fig. 4).

C/ the South Tropical Atlantic

Between about 0x and 26°S, the atmospheric elemental concentrations of all the elements decrease to their minimal level which is observed between 20 and 26°S (1 ng.m^{-3} for Zn, 8 ng.m^{-3} for Fe, 13 ng.m^{-3} for Al, 300 ng.m^{-3} for S or 1 ng.m^{-3} for P at 26x S). These values probably correspond to a background level in this part of the southern Atlantic Ocean.

However, between 5°S and 14°S, a significant peak of K is observed, even when its crustal component is eliminated (figure 5). Slight increases were also observed at these latitudes in concentrations of some elements, primarily P, Zn and Ca. Artaxo et al. (1988) have shown, using a factor analysis applied to samples collected in the Amazon Basin, that K, P and Ca are primarily released by the vegetation. Moreover,

K is generally considered as the more efficient tracer of biomass burning and continental biogenic emissions (Crozat, 1978). Hence, these results suggest that the tropical and equatorial forest areas could be responsible of these observed increases in concentrations of K. This hypothesis is reinforced by the work of Bürgermeister et al. (1990) who also observed a peak of non sea-salt potassium around 5 and 10°S during this cruise. Moreover, at the same latitudes, Papenbrock and Stuhl (1990) observed remarkably high concentrations of HNO_3 and Koppman et al. (1990) noted elevated levels of C_2H_2 which could be also relatively well explained by a contribution from biomass burning. Finally, these results confirm the observations made by Andreae (1983) who has pointed out the major role of the biomass burning on the atmospheric particulate matter composition in this area;

At last, from 30°S, the elemental concentrations increase slowly in relation with the arrival near the Brazilian coasts indicating a stronger influence of coastal emissions on the concentrations and composition of aerosols.

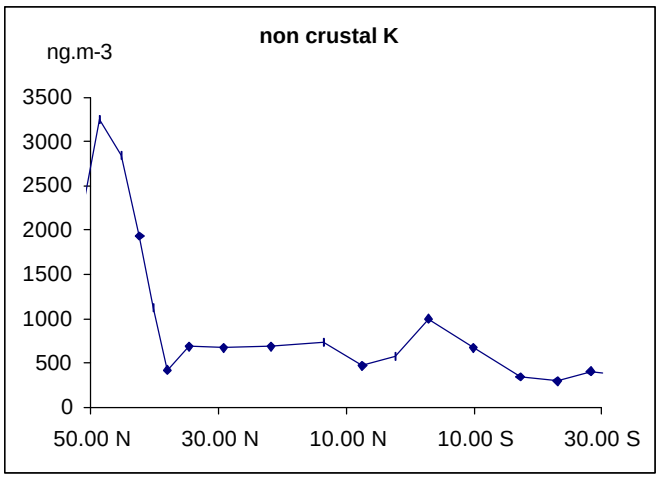

Figure 5: non crustal K concentrations

CONCLUSION

This study of the elemental composition of atmospheric aerosol over the North Sea, Channel, North and South Atlantic ocean allowed us to distinguish three major areas submitted to the major influence of different source-types:

- In the North Sea and Channel, the elemental composition of the atmospheric particulate matter is strongly affected by the anthropogenic emissions. The concentrations of pollutants as Zn and S are obviously particularly influenced by these emissions, but, even elements generally considered as resulting mainly of the crustal source (as Fe or Ca for exemple) have a significant part of their concentration explained by the anthropogenic emissions.
- In the tropical north Atlantic, we have observed a strong dust event coming from arid and semi-arid regions of Africa which controlled significantly the atmospheric concentrations of most of the elements.
- In the south tropical Atlantic, it seems that the major source was the biomass burning and/or vegetation releases which lead to elevated levels for some elements and especially for K.

Finally, only between about 20°S and 26°S, we have observed an atmospheric background level with low concentrations for all the analyzed elements.

ACKNOWLEDGEMENTS

We thank the Alfred Wengener Institute to invit us to participate at the ANT VII/1 cruise of the R.V. POLARSTERN.

REFERENCES

Andreae, M.O., Soot carbon and excess fine potassium: long-range transport of combustion-derived aerosols, *Science*, **220**, 1148-1151, 1983.

Artaxo, P., Storms, H., Bruynseels, F., Van Grieken, R., and Andreae, M.O., Composition and sources of aerosols from the Amazon Basin, *J. Geophys. Res.*, **93**, 1605-1615, 1988.

Bergametti, G., L. Gomes, G. Coudé-Gaussen, P. Rognon and M.N Le Coustumer, African dust observed over Canary Islands: Source-regions identification and transport pattern for some summer situations, *J. Geophys. Res.*, **94**, 14855-14864, 1989.

Buat-Ménard, P., Particle geochemistry in the atmosphere and oceans, in *Air-seaexchange of gases and particles*, NATO ASI Series C, **108**, pp 455-532, P.S. Liss and W.G.N. Slinn ed., D.Reidel Company, Dordrecht, 1983.

Buat-Ménard, P., and R. Chesselet, Variable influence of the atmospheric flux on the trace metal chemistry of oceanic suspended matter , *Earth Planet. Sci. Lett*., **42**, 399- 411, 1979.

Bürgermeister, S., H.W. Georgii, and R. Staubes, Methane sulfonate and non-sea-salt sulfate in the marine aerosol and precipitation, in *Physico-Chemical behaviour of atmospheric pollutants*, G. Restelli and G. Angeletti eds., pp 675-680, Kluwer Academic Publishers, Dordrecht, 1990.

Cambray, R.S., D.F. Jefferies, and G. Topping, An estimate of the input of atmospheric trace elements into the North-Sea and the Clyde Sea (72-73), *U.K. Atom. Energy Pub*. nx AERE-R7733, HMSO London, 30pp, 1975.

Chester, R., Geological, geochemical and environmental implications of the marine dust veil , *The changing chemistry of the ocean*s, Dryssen & Jagner ed., J. Wiley and Sons, , 1972.

Chester, R., A.G. Griffiths, and J.M. Hirst, The influence of soil sized atmospheric particulates on the elemental chemistry of deep-sea sedime nts of the northeastern Atlantic , Mar. Geology , 32, 141- 154, 1979.

Coudé-Gaussen, G., P. Rognon, G. Bergametti, L. Gomes, B. Strauss, J.M. Gros and M.N. Le Coustumer, Saharan dust on Fuerteventura Island (Canaries): chemical and mineralogical characteristics, air-mass trajectories, and probable sources, *J. Geophys. Res.*, **92**, 9753-9771, 1987.

Crozat, G., L'aérosol atmosphérique en milieu naturel: etude des différentes sources de potassium en Afrique de l'Ouest (Côte d'Ivoire), *Ph D Thesis*, Université de Toulouse III, 70pp, 1978.

Dedeurwaerder, H., F. Dehairs, Q. Xian, and B. Nemery, Heavy metals transfered from the atmosphere to the sea in the southern bight of the North Sea, in *Progress in Belgian Oceanographic Research*, 170-177, Bruxelles, 1985.

Koppmann, R., F.J. Johnen, C. Plass, and J. Rudolph, The latitudinal distribution of light non-methane hydrocarbons over the Mid-Atlantic between 40°N and 30x S, in *Physico-Chemical behaviour of atmospheric pollutants*, G. Restelli and G. Angeletti eds., pp 657-662, Kluwer Academic Publishers, Dordrecht, 1990.

Losno, R. Chimie d'éléments minéraux en trace dans les pluies méditerranéennes, *Ph D Thesis*, Universit de Paris VII, 189pp, 1989.

Losno, R., G. Bergametti, and G. Mouvier, Determination of optimal conditions for atmospheric aerosols analyses by X-Ray Fluorescence, *Environ. Technol. Letters*, **8**, 77-87, 1987.

Miller, M.S., S.K. Friendlander, and G.M. Hidy, A chemical element balance for the Pasadena aerosol, *J. of Colloid and Interface Sci.*, **39**, 165-176, 1972.

Papenbrock, T., and F. Sthul, Detection of nitric acid in air by a laser-photolysis fragment-fluorescence (LPFF) method, in *Physico-Chemical behaviour of atmospheric pollutants*, G. Restelli and G. Angeletti eds., pp 651-656, Kluwer Academic Publishers, Dordrecht, 1990.

Prospero, J. M., Mineral and sea-salt aerosol concentrations in various ocean regions , *J. Geophys._Res* , **84**, 725- 731, 1979.

Prospero, J.M., Arid regions as sources of mineral aerosols in the marine atmosphere, Geol. Soc. Amer. Spec. Paper,**186**, 71-86, 1981.

Prospero, J.M., and T.N. Carlson, Vertical and areal distribution of Saharan dust over the western equatorial North Atlantic ocean , *J. Geophys. Res.* , **77**, 5255- 5265, 1972.

Rahn, K.A., The chemical composition of the atmospheric aerosol, *Tech. Report*, University of Rhode Island, 1976.

Rea, D.K., M. Leinen and T.R. Janecek, Geologic approach to the long-term history of atmospheric circulation, *Science*, **227**, 721-725, 1985.

Sarnthein, M., J. Thiede, U. Pflaumann, H. Erlenkeuser, D. Fütterer, B. Koopmann, H. Lange, and E. Seibold, Atmospheric and oceanic patterns off northwest Africa during the past 25 million years, in *Geology of the Northwest African Continental Margin*, edited by U. Von Rad, K. Linz, M. Sarnthein, and E. Seibold, pp 545-604, Springer-Verlag, Berlin, 1982.

Schütz, L., R. Jaenicke, and H. Pietrek, Saharan dust transport over the North Atlantic Ocean , *Geol. Soc. Amer. Spec. Paper* , **186**, 87- 100, 1980.

Turekian, K.K., Geochemical distribution of the elements, in *Mac Graw Hill Encyclopedia of Science and Technology*, **Vol 4**, pp 627-630, 1971.

Völkening, J., H. Baumann, and K.G. Heumann, Atmospheric distribution of particulate lead over the Atlantic Ocean from Europe to Antarctica, *Atmos. Environ*., **22**, 1169-1174, 1988.

9 Programme de recherche proposé au 5ème PCRDT: INCHAAC

9.1 Objectives

This proposal is concerned with the influence of heterogeneous chemistry inside clouds on the atmospheric composition. A cloud is a system, where water condenses on the existing aerosol particles, which partially dissolve themselves. Also gas exchange with air is occuring with the coud drop. Most often, a cloud evaporates giving back to the atmosphere partially changed particles.
The chemistry for gas-water exchange is now well known, however little is known about solid-water interaction. This interaction causes dissolution of transition metals and anions from aerosol particles and also modifies the surface characteristics of the aerosols. Even at nano-molar concentrations, dissolved transition metals are promoting catalytic and photocatalytic cycles in cloud droplets. The importance of these cycles is correlated with the amount of dissolved metals. Metal solubility generally increases with decreasing pH and especially for iron, depends upon the oxidation state. Dissolution of acid gases (e.g., HNO_3), acid precursors (e.g., SO_2) or redox active species (e.g., peroxides, soluble organics, ozone) can increase the amount of chemically reactive transition metals in the aqueous phase. A strongly linked mechanism occurs whereby the redox state of the cloud water influences transition metals dissolution (heterogeneous chemistry), which in turn influences the redox state of the cloud water. This inter-connected mechanism have an effect on the aerosol surface, which must be well characterised. Because the microphysical behaviour of the cloud determines liquid water amount, residence time and overall physico-chemical environment, this parameter is a key to understanding the chemical system.
After drying of a cloud, the surface of the remaining aerosol has changed. This causes an enhancement of their ability to condense water in the next cloud. Therefore, this causes changes in the size distribution of cloud droplets and radiative properties of the cloud. Sometimes, the water content is enough to let droplets grow and fall as rain. Dissolved species and processed aerosols are brought to the ground as wet deposition.
In this work, we propose to improve knowledge on the homogeneous and heterogeneous reactions occurring in a cloud and integrate the heterogeneous ones in a model describing the chemical composition of an air mass. This model will be validated with one joint field experiments where all the critical parameters described above will be measured.
The general goal of the project is to provide an insight into the aspects involved in the chemical activity of clouds. This is of paramount importance because of their possible influence on global atmospheric composition (Walceck et al., 1997; Audiffren et al., 1996; Jacob et al., 1989) and climatic effect. This effect is dependant on the aerosol processes in clouds and cloud condensing capacity changes. This requires a multiphase description of a cloud. We will attempt to:

1.
   1.1. Propose chemical schemes, which describe the aqueous/aerosol interface chemistry and define application domains of these schemes: polluted, rural and marine area.
   1.2. Quantify the concentrations of soluble active transition metals present in the cloud droplets using a dissolution model rather than average trace metal concentration measurements and assessments.
   1.3. Extract the relation between the measured surface structure and the reactivity of aerosols.
   1.4. Quantify the variations of cloud condensation properties of processed aerosols.

2.
   2.1. Because soluble transition metals strongly modify aqueous chemistry and photochemistry, identify the most important aqueous phase oxidation processes and determine the reaction rates necessary to complete the model. Quantify the transition metal catalytic cycles for the radical budget.

2.2. Evaluate the ratio of the in-situ (aqueous) production of radicals and the exchange with the gas phase. Determine if the aqueous phase is a sink or a source of radicals for the gas phase, and if gas phase reactions are important in a cloud, or immediately after cloud evaporation.
2.3. Determine how cloud microphysics influences this chemical balance.

3. Validate proposed schemes by appropriate field and laboratory measurements.

The major innovation of this project will be to join various research teams at a European scale, who will converge their power on cloud research. The different aspects of the cloud chemistry, gaseous chemistry, transition metal chemistry and surface chemistry are strongly linked and concern also heterogeneous chemistry at solid-liquid, liquid-gas and solid-gas interfaces. The proposed objectives cannot be reached at a national scale because of the strong link between all the aspects necessary to solve. It is therefore necessary to undergo a working program, which covers this topical area.
Expected results of this proposal will be to quantify the effect of cloud chemistry on atmospheric chemistry, atmospheric composition and pollution, and to quantify the effect of cloud aerosol process in atmospheric cloud formation. Because most of the trace gases and organic solids are health hazards, an improved forecasting of their behaviour in the atmosphere will be of benefit to populations exposed to air pollution. Because the transition metal chemistry is mainly linked to the cloud chemistry, and because transition metals are potential hazards for biota, the knowledge of their chemical states will enhance the knowledge of their impact on living organisms. Because transition metals are coming from aerosol dissolution, because the aerosol dissolution is the main criterion in defining the cloud condensation nucleus, knowledge of aerosol processing in clouds will improve forecasting of cloud formation and transition metal activity.

9.2 Contribution to programme/key action objectives

This project is build directly in the scope of the paragraph 2.1.1 written in the 2001 work plan document.

- At the European scale this project is related to the atmospheric composition change due to cloud formation. Clouds modify the concentration of oxidising and reducing species present in the dry atmosphere. The "atmospheric composition change" is here understood in gaseous composition change and also in aerosol properties change. The precise knowledge of the chemistry prevailing in clouds improves the knowledge of the fate and behaviour of emitted pollutants. Therefore, this will help the European Community to forecast the range of pollution emission reduction policy.
- At the global scale this project concerns the effect of aerosol cloud processing on cloud formation and then the contribution to the radiative budget of the atmosphere. This is related to the global warming care defined in the Kyoto protocol and cited in paragraph 2.1.1.

This project will examine the effect of transition metal chemistry on the atmospheric composition of tropospheric ozone, nitrogen oxides, sulphur oxides, peroxides, volatile and non volatile organic compounds. The presence and the chemical forms of the transition metals are affected by human activities, by emitting rare elements into the atmosphere (Ni, Cu ...) and by changing the natural emissions conditions of metals. For example, transition metals are emitted in silicated crystals by wind crustal erosion, but rather in an amorphous or organic material by industrial activity.
All these items can have a major influence on the global and local atmospheric composition in trace gases and aerosols. The question asked and answered by INCHAAC can resolve a part of the problem raised by the unknown influence of industrial atmospheric emissions of aerosols and metals on the atmospheric composition.

9.3 Innovation

9.3.1 Transition metals as catalysts in the troposphere

Dissolved transition metals are well known to be highly reactive with many compounds (Graedel et al., 1986; Weschler et al., 1986; Zuo and Hoigné, 1992; Zuo, 1995; Warneck et al., 1996; Losno, 1999). Cloud, fog and rain chemistry has a chemical impact on both a regional and a global scale (Matthijsen et al., 1997; Walceck et al., 1997; Sander & Crutzen 1996; Lelieveld and Crutzen 1991; Jacob et al., 1989). Cloud water droplets condense onto solid aerosol particles, which are present throughout the entire atmosphere, even in remote oceanic area (e.g. Losno et al., 1992; François et al., 1995). Trace metals are introduced into the aqueous phase through the partial dissolution of aerosols into the atmospheric liquid water. If the droplet size increases, it forms rain. Various field experiments report concentrations of dissolved trace metals in rainwater samples (Jickells et al., 1984; Ross, 1987; Lim et al., 1993). Laboratory experiments also demonstrate the transfer of trace metals from the solid to the liquid phase (Spokes et al. 1994, Desboeufs et al., 1999). Because of the known reactivity, abundance in atmospheric liquid water as well as in aerosols and also of analytical possibilities, Fe, Mn and Cu are the most investigated transition metals. The effect of more rare naturally metals also present in polluted plumes is also included. Photochemical reactions occuring either directly or indirectly through organic chromophores, are suggested as important reactions by which the speciation of metals (e.g. iron) in clouds is changed. They influence the solubility of at least iron via the photoreduction of Fe(III) to Fe(II) (Behra and Sigg, 1990; Zhuang et al., 1992; Zhu et al., 1993; Zuo, 1995; Spokes and Jickells, 1996). Organic compounds, most of which are not yet characterized, are ubiquitous in aerosols (Cachier *et al.,* 1986; Havers *et al.,* 1998) and also influence chemical schemes (Grgic et al., 1998, 1999). Other metals that are considered as potential catalysts are manganese, cobalt and copper (Warneck, 1991; Sedlak and Hoigné, 1993).

9.3.2 Cloud as a central point of transition metals and aerosols chemistry

Direct gas-particle reactions involving trace metals may occur in a dry atmosphere (Dentener et al., 1996). However, the major known effects of transition metals occur during homogeneous aqueous phase chemistry, which may also be a water film around aerosol surfaces. Graedel et al. (1985) note the potential of iron(III)-hydroxo complexes in providing a photolytic source of OH radicals in cloud droplets. Reactions occurring at the water-solid interface are currently not well documented. All these chemical reactions are partially driven by local meteorological conditions and hygroscopicity of aerosol, which govern cloud formation and evaporation. The rate of formation of cloud droplets and aerosol size segregation will also determine transition metal fate and behaviour.

When air masses enter clouds, a water layer covers a part of the solid aerosol, aqueous chemical reactions begin and also aerosol surface alteration occurs. The processes involve exchanges between gas, water and solid phases, which change the chemical form and the speciation of metals, and the surface properties of the wet aerosol. Chemical reactions are driven by many acidic species (e.g., nitric, sulphuric, carboxylic acids), reducing or oxidising agents (e.g., sulphur (IV), hydrogen peroxide), radicals and photons. Neutralisation of the acidic species can be accomplished by NH_3 or alkaline soil dust (e.g., silicates, carbonates).

The solubility of metals, and hence the reactivity, is also strongly dependent on the oxidation state of the metal. In-cloud photochemical reactions are directly involved in the determination of the oxidation state of these metals. For example, iron(III) can be extracted from an aluminosilicate or oxo-hydroxide matrix and reduced to the more soluble iron(II) species (Zhuang et al., 1992; Spokes and Jickells, 1996). The oxidised forms Fe(III) and Mn(IV) are not very soluble in rain water, whereas the reduced forms Fe(II) and Mn(II) are soluble (Behra and Sigg, 1990; Spokes and Jickells, 1996). The free dissolved transition metals released by this process can act to convert H_2O_2 into radicals (Losno, 1999) and catalyse SO_2 oxidation to H_2SO_4 (Graedel et al., 1985; Martin et al.,

1991), and thus initiate a direct feedback to the solubilisation of the metals. The redox reactions occur in-situ at the cloud level and are strongly dependent on the presence of light, radical species, oxidising or reducing agents and exposure time, on the microphysics of the cloud (Chaumerliac et al., 1999), and on the availability of transition metals. All these aqueous phase and heterogeneous processes are still poorly understood and not well quantified. The field, laboratory and model studies proposed here are required for their elucidation.

9.3.3 Aerosol weathering in the clouds

pH has been suggested to be a major factor in controlling the solubility of metals in rainwater (Colin et al., 1990). Yet, for many metals this relationship is not simple (Lim et al., 1993; Losno et al., 1993, Desboeufs et al, 1999). Aerosols are exposed to repeated evaporation/condensation cloud cycles before removal by precipitation, which enhances solubility (Desboeufs et al. 2001). As a result of SO_2 oxidation and incorporation of H_2SO_4, HNO_3 or organic acids, the pH value of cloud water can be very low, or alternatively very high if ammonia or carbonate is present. Thus, the final pH of precipitation, which can vary between 4 and 7, does not necessarily reflect the pH conditions to which the aerosol particle is exposed in the atmosphere.

Aerosols are emitted into the atmosphere from both natural and industrial sources: wind erosion, biomass and waste burning, industrial activity and motor emissions. The chemical state and amount of metals emitted depends on the source, with large differences in composition between aerosols produced by combustion processes and those produced by mechanical erosion or sea spray drying. Transport of aerosols allows regional and global dispersion and mixing to occur. Metal elements are processed by atmospheric reactions, mainly within clouds. During atmospheric transport, the chemical reactivity of all the components involved may be increased by the highly energetic chemical and photochemical conditions, which exist in clouds (e.g. Spokes et al., 1994; Spokes and Jickells, 1996). Aerosol removal from clouds occurs in two ways. The first is wet removal with the formation of rain or snow. The second and most frequent (average 90%) is dry removal, where aerosols and gases are ejected back to the dry atmosphere during cloud evaporation, resulting in major changes in the aerosol structure and surface. Once back in the atmosphere, this weathered particulate material can be reincorporated into clouds undergoing continued cycling before removal by wet or dry deposition. Cloud processing is a fundamentally important aspect of atmospheric aerosol cycling (Flossmann, 1998), resulting in large changes in aerosol structure affecting the aerosol size distribution, its chemical reactivity and surface structure. These processes are usually influenced by the presence of other aerosols, meteorological conditions and particularly the liquid phase content of the clouds.

The impact of trace metals on cloud chemistry strongly depends on the chemical form of the metals and on the surface characteristics of aerosol particles. Solubility and subsequent chemical availability vary depending on the chemical weathering and surface modifications of aerosols occurring during atmospheric transport. Three major sources have to be understood when modelling trace metals: wind erosion, industrial production and combustion. Wind erosion produces mineral aerosols in arid and semi-arid regions, where metals are present in a mineral matrix, mainly as silicates, with relative abundance close to natural ground abundance. Industrial production and combustion processes can disperse more rare transition metals like vanadium (in biomass burning), chromium, nickel or mercury, for which atmospheric chemistry is currently not well known. The matrix carrying the metals can be either mineral or organic and the solid particle may be very heterogeneous with a reactive surface. One of the major innovations of this project will be to relate the reactivity of an aerosol particle incorporated into a cloud and its surface chemical property variations.

9.4 Project workplan[1]

9.4.1 Proposed work

This project can be described as three complementary parts: field experiments, laboratory experiments and modelling. Field experiments are necessary: to become time series of measured concentrations of transition metals and to determine the chemical states of transition metals, which will be included in models; to determine the surface properties of the solid particles included in cloud water and to collect raw material (especially aerosols) for laboratory experiments. Results given by the models will also be compared with a specially built field validation. Laboratory experiments will give missing kinetic constants, provide cloud simulation in a cloud chamber or in an aqueous phase reactor and also validate model outputs in term of processes.

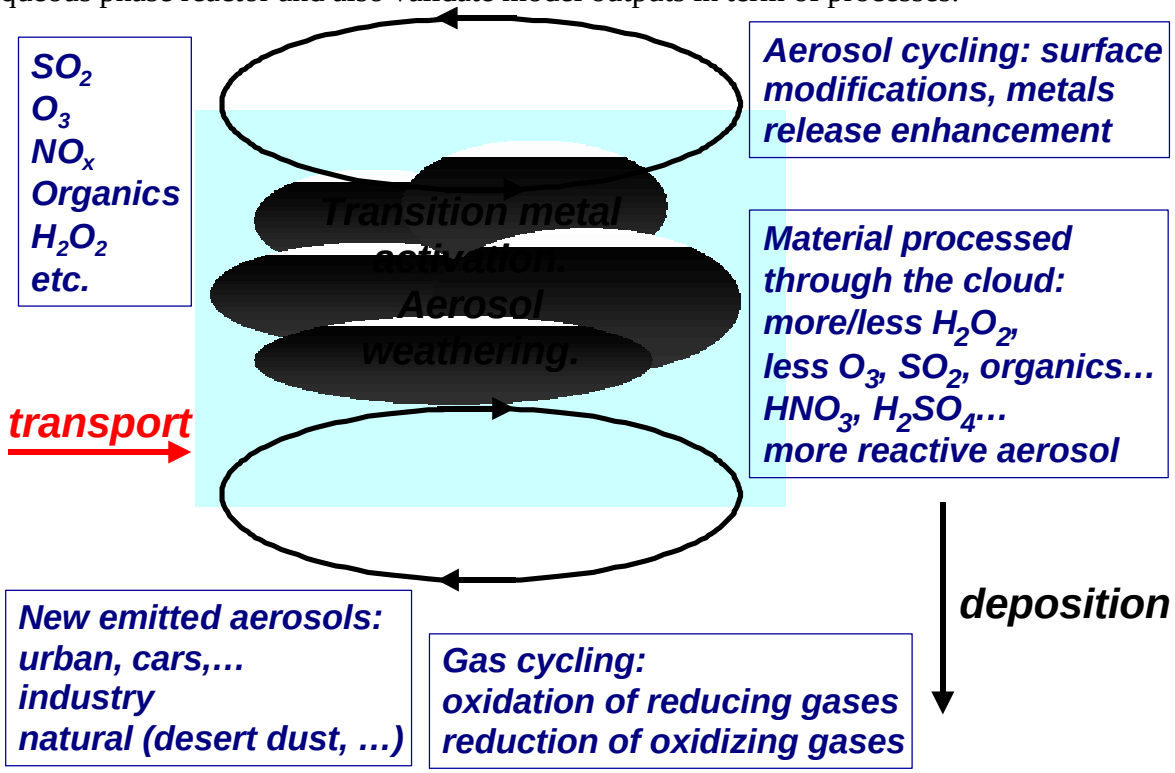

This project cannot be conducted within a single country because of the dispersion of laboratories throughout Europe, which can study processes on the surface of aerosols and the reactivity of metals in clouds. Six laboratories of four countries are therefore implicated.

9.4.1.1 Field experiments

A cloud forms as a consequence of a wet air mass cooling. This occurs during frontal events, convection or orographic conditions. The two first cloud types need an aircraft, and the third type can be accessed with ground based sampling, near the top of cloud-capped mountains. An aircraft may be used to obtain vertical profiles. Cloud condenses on solid aerosol particles and sometimes causes rain (wet output). At various locations under various meteorological situations, we will measure the amount of total and dissolved transition metals and the amount of all known species, which can interact with metals. We will determine the chemical state of dissolved metals in cloud and rainwater, including redox speciation (e.g., Fe^{II}/Fe^{III}) in rain and cloud water after aerosol dissolution. We will collect aerosols in dry conditions to provide raw material for laboratory experiments, and also in wet conditions to separate aerosols without condensed water from aerosols acting as condensation nuclei. We will follow the aerosol behaviour before and after a cloud event to

[1] To maintain the anonymous principle, most of the necessary references have been omitted because only few teams in Europe are working on these subjects.

quantify the cloud processing effect. Such an experiment is possible in the field experiment locations, which are often concerned with orographic clouds. Surface chemical characterisation will be one of the major tools in understanding the aerosol chemistry, including transition metal dissolution and cloud condensation properties evolution.

Aircraft collections will provide a unique tool to sample clouds at different levels and in a wide range of geographical locations covering Europe, but also to better constraint clouds model if coupled with ground based field experiments. One of the partners in this project has developed a cloud collector, which can fly on any research aeroplane, e.g. French research aeroplanes MERLIN or ARAT. Classical physical instrumentation is also available on these aircraft, including particle counters, dynamic of the aeroplane, cloud total water content, temperature, pressure and light irradiation. We will sample the same cloud at different altitudes, which provides various photochemical conditions for the same wet air mass. Aerosols will also be sampled before and after the cloud. Besides this direct sampling and because of the high price of aircraft experiments, we will utilise cloud capped mountains and fog to provide complementary sampling for longer periods and obtaining time series. For this item, we will use an existent field station on the top of a French[2] mountain (altitude 1400 m, **STATION A**) and in Germany (altitude 937 m, **STATION B**). The STATION A will be used for cloud, rain and aerosol sampling during the joint experiment and will be the main station used for model validation.

Several techniques will be employed at various experimental sites. Additionally, cloud water will also be collected by size segregated multiple-stage collectors (Berner type). In-situ measurements in real clouds have been lacking and the set up of a measuring site gathering both microphysical and chemical data in STATION A will go some way to alleviate this. The station has operational devices such as a chalet to host scientific staff, a fully equipped wind tunnel in which microphysical probes can be set up, an instrumented mast for the measurement of ozone, SO_2, CO, NO_2 photolysis rate and meteorological data. The site is also used for hosting the set up of instrumentation in natural clouds or in airborne conditions (nephelometer, instrumentation for detecting riming conditions). Furthermore, routine data are available from a wind profiler.

Rainwater collection will give information on the wet removal from clouds, on the properties of metals in wet deposition and as a picture of cloud processes. It will be collected in France at STATION A, in Germany in a town, at a rural companion site and in STATION B. Rain will be sampled and processed in ultra clean conditions using the unique systems that have been developed within this group of laboratories. Techniques include rapid filtration to determine dissolved particulate distribution and metal speciation using separation of different species on micro-columns. This uses columns with reagents immobilised on them which complex a metal in a particular oxidation state. Aerosol and the insoluble fraction measurements, especially with surface methods, will give required information on the raw solid material captured by the clouds or collected in rain. Aerosol particles will be collected on various filter media, using high and low volume collectors and multi-stage cascade impactors appropriate for the task in hand. In the field campaigns, size segregated aerosols will be routinely collected, while for the laboratory work the larger samples which can be collected by bulk aerosol collector are often more useful. Aerosol will also be collected for laboratory dissolution experiments.

As the trace metal and aerosol chemistry is strongly related to the redox chemistry of a cloud, measurements of oxidising and reducing species within the rain and cloud water will be necessary. H_2O_2 and RO_2H are among the most important compounds to be also measured in both liquid and gaseous phase. Other gases involved in phase exchange with the aqueous phase will also be sampled and analysed by classical methods. These include O_3, NO_x, NO_y, SO_2 and organic gases (such as H_2CO and peroxides).

[2] Geographical precision is omitted to allow this text to be as anonymous as possible

The field work will act to verify whether laboratory simulations and chemical modelling can predict and explain the behaviour of cloud and rain water components. This work will improve our knowledge of metal concentrations in the atmosphere over different areas of global and local significance. This work will also improve our knowledge on the surface chemistry of aerosols and solubility variations.

9.4.1.2 Laboratory experiments

Our aim is to conduct laboratory based investigations to identify more closely the role of the above processes and additional mechanisms which are as yet uncharacterised. These laboratory studies will be paralleled by field campaigns investigating the sensitivity of metal concentrations, the solubility and the aerosol surface modifications to these various parameters. The philosophy underlying this work is that individual processes can only be fully identified in laboratory simulations. Nevertheless, these simulations must be compared to field studies to ensure that the most relevant processes are investigated. In addition to understanding the processes which control the aerosol surface modification and the particulate/dissolved distribution of metals our aim is also to determine the oxidation state of metals in the atmosphere and the role of these metals in SO_2, NO_x, HO_x and RO_x cycling.

Large uncertainties remain in atmospheric heterogeneous chemistry, especially in the exchange reactions occurring between particulate and solution phases. We do not know how these reactions are related to chemical surface speciation. Laboratory experiments are necessary to quantify these reactions to enable better understanding of dissolution processes. The aim of the laboratory experiments is:

- To derive quantitative kinetic and thermodynamic data on the exchange of metals between the particulate and solution phase over time scales of minutes for incorporation into models.
- To improve the database on homogeneous reaction involving trace metals.
- To improve the database on heterogeneous reaction involving aerosol weathering.
- To understand how aerosol are modified during evaporation-condensation cycles.

We will conduct the following laboratory experiments:

1. Particle/water interaction studies using aerosols, time scales and conditions representative of those experienced by wetted aerosols in the atmosphere. A particular focus of these studies will be the role of photochemistry in regulating solubility.
2. Investigation of exchange reaction mechanisms using well characterised particulate material and water solutions to look at the reactions occurring in cloud and rain water in order to improve the chemical description of atmospheric matter which forms aerosol. A particular focus will be applied on surface chemical measurements to understand how the surface chemical structure is related to the aerosol reactivity with water. Extend these mechanisms to natural aerosols considered as internally mixed minerals and organics.
3. Model laboratory experiments (e.g., in a semi-batch continuous stirred tank reactor under controlled conditions) will be carried out in an attempt to understand the role of soluble transition metal ions (single or combination), which are eluted from aerosol particles, in the SO_2, NO_x or RO_2H redox reactions under conditions representative for those of atmospheric liquid water. The effect of organic compounds (e.g., the formation of complexes with transition metal ions) on the reaction rates (i.e., catalytic activity of metal ions) will be studied.

All these techniques are working or are under development in the implicated laboratories. Work will be conducted in clean rooms by people who have extensive experience in trace metal analyses and heterogeneous reactions.

9.4.1.3 Modelling Clouds

The calculations will be conducted using cloud models. This model will incorporate pH and light variation. Outputs will be:

- dissolved metals concentrations in cloud water
- aerosol surface evolution
- gas composition evolution during and after the cloud event
- cloud condensation nuclei capacity of the remaining dry atmosphere after evaporation

Some chemical reactions, especially aqueous homogeneous reactions with transition metals and hydrogen peroxide, are now well known and published, others are not well known or not studied at all. The heterogeneous reactions involving exchange between particulate and dissolved phases and the homogeneous reactions involving direct chemical bonding between transition metals and compounds other than H_2O_2, OH or HO_2, must be incorporated into the model. Also, condensation of soluble compounds from gaseous phase can be important to activate an existing aerosol for its first condensation.

Modelling will run side by side with laboratory and field experiments and thus we will be able to closely identify the processes which should be measured in the laboratory and the parameters which should be measured in the field. Laboratory and field experiments are necessary to validate a model and it is an important feature of this project that the modelling effort will be integrated within the chemical work to maximise the synergy between the two components.

We propose to incorporate the following:

1. Solubilization of aerosol particles upon water attack: A parameterization of this process needs to take into account the pH of the cloud and rainwater, the thermodynamic and kinetic considerations regarding the solubilization of the different minerals and substances to be expected in aerosols. Acidity will be calculated from published large scale simulations and the cloud water content derived from the reanalysis of the meteorological fields. Relevant thermodynamic and kinetic data will be asssembled both by an intense literature survey and through evaluation of the experiments of this project (Keene and Savoie, 1998; Keene et al., 1998).
2. Water attack in combination with photochemically induced redox-reactions: The impact of photochemistry will be assessed for the case of iron, where changes in the oxidation state changes the solubility, bioavailability and catalytic activity. The feedback mechanisms of increased sulphate production and higher solubility will be studied in detail.
3. Aggregation of aerosol particles by cloud processing: The multiple uptake of aerosol particles by cloud droplets produces both a changed cloud droplet environment and a change in the aerosol size distribution during dry output. This involves a change in solubility and size distribution of e.g. mineral particles. Experiments suggest, that a disintegration of the newly formed aggregates is not to be expected. We intend to study this process considering the scavenging efficiency, the aerosol composition and the fractions of aerosol, which have been processed by a cloud in the model work and experimentally in the field.
4. Surface modification of an aerosol particle: the aerosol cycling through a cloud dramatically change the properties of its surface and then further metal dissolution and cloud condensation nuclei (CCN) properties.
5. All of this chemical discussion will be coupled with cloud microphysics.
6. The response of the alteration of particles on cloud system cycle (development and radiative impact) will be modelled. We intend to develop a complete modelling of the processed aerosol cycle in the framework of a mesoscale model: aerosol emission and transport, particle weathering and in-cloud mixing and aggregation as parameterized from the above mentioned studies. The new chemical properties of the cloud droplet will be studied with a dual objective: (1) effects on their optical properties (direct effect), which may modify the column radiative budget and

consequently change to some extent the vertical dynamics, including a possible effect on cloud development; (2) particular attention will be paid brought to the new CCN capabilities of the processed particles, which may result in cloud albedo changes during the further cycles (indirect radiative effect). According to the size and nature of the initial CCN distribution, we expect either a direct Twomey effect (albedo increase by cloud nuclei number increase), or inverse Twomey effect by competitive de-activation of the smaller fraction of the nuclei distribution.

9.4.1.4 Analytical methods

Measurements of pH, and major ions can be measured with high accuracy. Cations will be measured by atomic emission spectrometry (ICP-AES), and ion-exchange chromatography (HPIC). In addition, our sampling and analytical protocols will allow us to determine organic anions (formate, acetate, lactate, glycolate, propionate, MSA, oxalate) by ion-exclusion chromatography. Peroxides will be determined by liquid chromatography and POPHA fluorescence. Elemental trace metals in particulate matter will be measured by X-Ray Fluorescence (XRF), while the concentration of soluble fraction of trace metals will be determined by graphite furnace atomic absorption (GFAAS), ICP-AES or ICP-MS. We have extensive experience of measuring trace metals accurately at low (10^{-9} M) ambient levels.
For redox speciation low pressure chromatographic separation prior to elemental analysis or specific colorimetric techniques (e.g., Ferrozine method for Fe(II)) will be used. Important redox species will be also measured in gaseous and dissolved phase, including H_2O_2 by fluorescence, O_3 by light absorption, NO_x, organics, etc.
The aerosol surface measurement will be conducted by ESCA, TOF-SIMS and near field microscopy (AFM).

9.4.2 Gantt diagram of the project

9.4.2.1 Table

N°	Duration (month)	Begin (month)	End (month)	Work complete
1	0.1	0	0.1	Starting meeting.
2	12	1	12	Aerosol sampling for laboratory experiments at STATION A and B
3	3	0	2	Extensive bibliography survey to prepare new chemical scheme to apply to cloud models.
4	2	1	2	Interlaboratory Analytical protocol validation procedures.
5	6	2	7	First run of laboratory experiments.
6	6	3	8	Sensitivity test of cloud models to prepare the joint campaign.
7	0.25	8	8.25	1st workshop to define activities what to exactly do during the joint experiment; discussion of first results.
8	2	8	9	Interlaboratory analytical protocol validation procedures.
9	3	8	10	Joint field experiment preparation.
10	1	11	11	First joint field experiment in STATION A.
11	3	12	14	Analyses and evaluation of results.
12	0.25	14	14.25	2nd workshop to discuss first experimental results and Individual field experiments (time series).
13	11	14	24	second run of laboratory experiments.
14	17	13	27	Individual field experiment campaigns (time series).
15	12	14	27	Modelling runs and validation of the field experiments.
16	0.25	25	25.5	3rd Workshop, international communications and publications preparation.
17	6	25	30	3rd runs to complete the validation schemes (field, model and lab).

18	.25	32	32.25	Final workshop.
19	6	31	36	Final report redaction including interpretation and publications of results.

9.4.2.2 Diagram

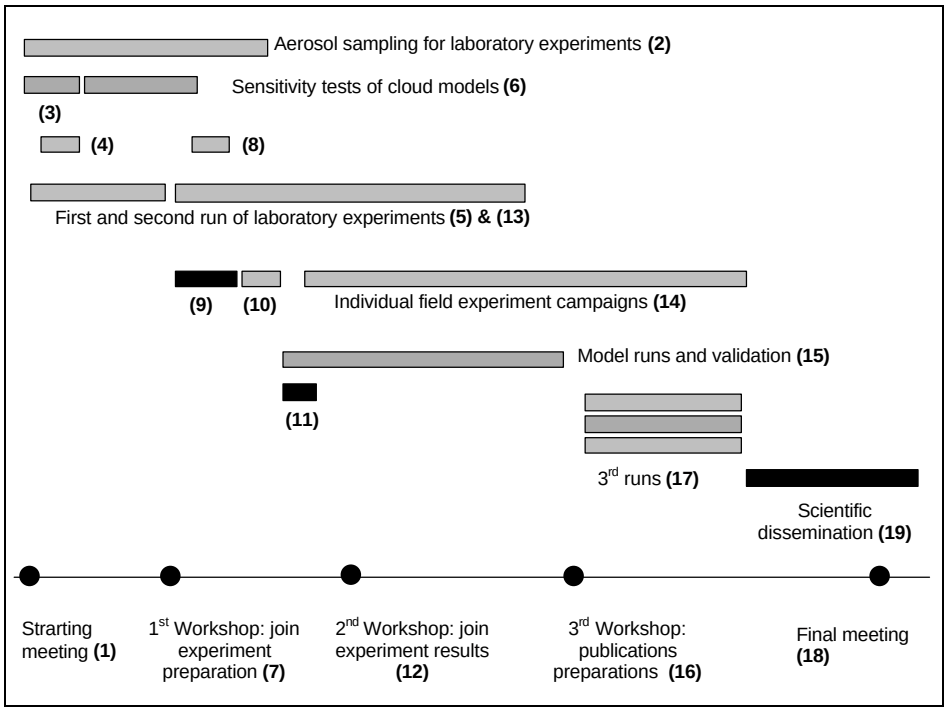

9.4.2.3 Remark on field experiments

For field experiments, and particularly the first (joint experiment), the exact schedule of this event depend on the season. It is without doubt not very efficient to plan a cloud experiment in June or July, or if a high pressure field is firmly installed, but a period in the interval from September to April seems better. The individual experiment campaign will be devoted to explaining particular points not understood in the joint experiment and to obtain time series.

9.4.3 Pert diagram of the project

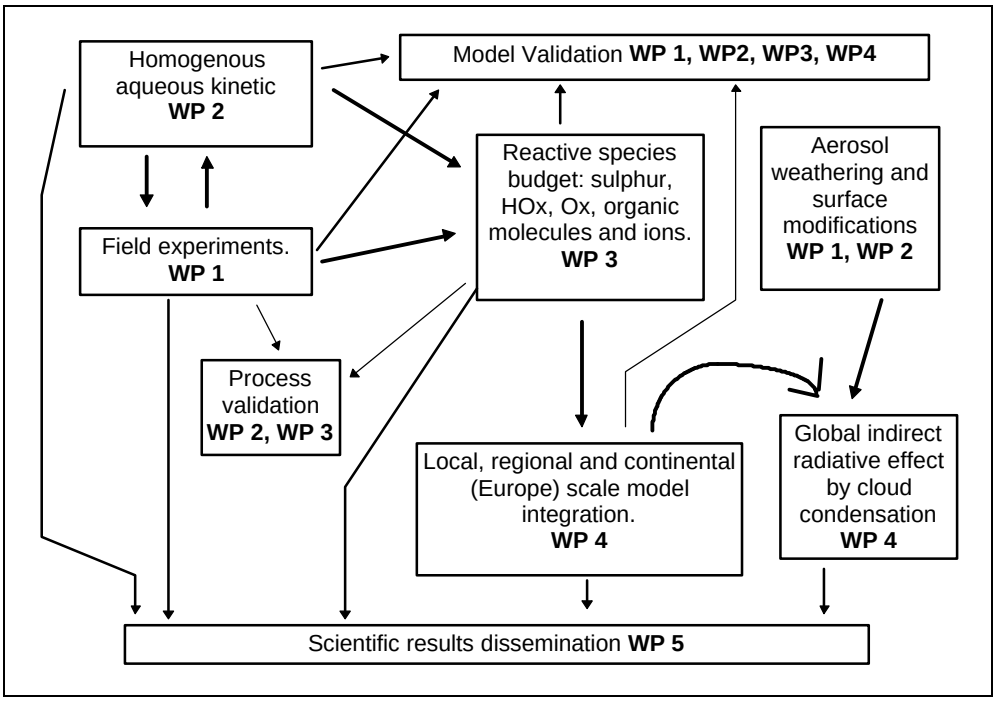

9.4.4 Workpackages

9.4.4.1 Workpackage list

The whole project will be divided in 5 workpackages integrating the 4 self consistent parts of the project which can give scientific deliverable, and a special consideration to the dissemination of the science produced. These workpackages are those written above in the Pert diagram and listed below with more details.

N°	Title	Lead contractor	Person-month	Start month	End month	Deliverable
1	Field measurements	1	60	11	25	3, 5, 6, 9
2	Lab measurements	5	63	2	25	1, 2, 5, 6, 9
3	Results integration	3	65	0	25	4, 7
4	Cloud and Multiphase chemistry	4	65	8	30	8, 9
5	Results dissemination	1	24	31	36	10
	TOTAL		**277**			

9.4.4.2 Workpackage WP1: Field measurements

Start Date: 11 **Lead Contractor N°:** 1 **Person-months:** 60

Objectives

To generate a database for model validation. To measure the amount of chemically reactive species in cloud drops and ambient air: transition metals, sulphur and nitrogen oxides, peroxides, ozone. To follow the aerosol surface evolution during cloud process. To collect raw aerosol for laboratory experiments, to analyse the surface of true aerosol. To evaluate the range of variation of aerosol and cloud water properties.

Methodology / work description

Short intensive experiences

In situ cloud sampling will be made by aircraft with a cloud at different altitudes from bottom to top, by fog collector and wind tunnel on at ground level of cloud capped mountains. Rain will also be sampled because it is a direct product of clouds. We also will made in situ analyses of important physical parameters with microphysic instruments (drop size spectra, temperatures, ...), of variable chemical parameters (pH, reactive gases concentrations and dissolved form). All the samples will be analysed further to the lab to determine its chemical composition of the soluble, the insoluble and the surface. This includes elemental analyse, iron redox speciation and also surface characterisation for the particulate material. A virtual impactor will be used in the wind tunnel sampler to separate dry and wet material in the cloud. Aerosol will be collected by aircraft before and after the cloud, and also continuously on the mountains associated with a precise meteorology survey to become particulate material at various cloud cycles stage.

Time series

Because a close measurement of a cloud system is very expensive, long term experiments will be conducted on selected parameters. This will be aerosol composition and surface chemical properties, quantification of soluble trace metals in fog, clouds and rainwater, gaseous concentration monitoring.

Deliverables

A database for phase transfer reactions, for dissolved and available metals measured concentrations, for associated water content, ice content and chemical composition.

Cost: 32%

Milestone and expected results

The joint experiment will take 4 weeks of field presence, but 6 month for samples analyses. For the time series, one year sampling is necessary to integrate seasonal variability, but analyses can be conducted in the same time.

Cost: 32%

9.4.4.3 Workpackage WP2: Laboratory measurements

Start Date: 2 **Lead Contractor N°:** 5 **Person-months:** 63

Objectives

To define and validate a reaction scheme, which represents what occurs in cloud water, including detection and characterisation of reactive intermediates, monitoring the stoichiometry of the reactions as function of time, determining reactions that are not well known as function of time, investigating the role of transition metals other than Fe, Cu and Mn, investigating the role of organic components. We also need information to heterogeneous mechanisms which transfer trace metals from aerosol to the solution and the evolution of the aerosol's surface.

Methodology / work description

Detection and characterisation of reactive intermediates: to study the kinetic and equilibrium aspects of the reactions of these species and characterise the kinetic features of the studied reactions to establish the rate laws under a variety of experimental conditions. Stopped flow and sequential stopped flow techniques will be used.

Monitoring the stoichiometry of the reactions as a function of time: to determine how the concentration ratios of the products and reactants change over the entire course of the reactions. Procedure will include spectrophotometry, potentiometry and out-of-cell classical analytical methods.

Investigating the role of transition metals in catalytic and photocatalytic cycles: Determination of rate constants that are not well known for redox processes (e.g., SO_2, NO_x or RO_x) in the presence of transition metal ions (single and combination). Studying the influence of organic components present (peroxides, ligands) in atmospheric liquid water on the oxidation rates. Aqueous photochemical and chemical reactors will be used for kinetic experiments; the concentration of reactive and products will be determined by HPICP, ICP-AES and HPLC.
Developing the appropriate mechanisms: The objective is to develop detailed kinetic models which are consistent with the observations and predict the behaviour of the studied systems reasonably well. The mechanisms will be confirmed by simultaneously evaluating all the laboratory experimental data and comparing experimental and calculated kinetic profiles. Box model will be built on existing tools (MODEL A AND B).
Heterogeneous chemistry: Determination of weathering rate of aerosol in a photochemical open-flow reaction cell. The dissolution rate of aerosol will be followed in various conditions: water composition, light flux, different aerosol types including weathered aerosols. Simulation of aerosol cloud processing.
Soluble material will be measured by ICP-AES, insoluble by TOF-SIMS and ESCA.

Deliverables
Validated kinetic constant for the catalytic cycles involving transition metals, quantification of the relative influence of each transition metal in the reaction schemes, quantification of the influence of organic components on redox and photo-redox chemistry, guidelines to make reaction schemes more simple for 1D, 2D and 3D models. Quantification of the aerosol evolution as it is included in a cloud droplet. Structure-reactivity relationship for the aerosol surface.
Cost: 28%

Milestone and expected results
All the work to do in this workpackage can progress simultaneously. Kinetic constant will be delivered at month 18 and reaction scheme at month 24. The results are expected for WP3 and 4.
Cost: 28%

9.4.4.4 Workpackage WP3: Results integration

Start Date: 0 **Lead Contractor N°:** 3 **Person-months:** 65

Objectives
To integrate homogeneous and heterogeneous (including particulate-soluble and gas-soluble transfer) cloud model and determine the chemical budget of a cloud. Inputs are deliverables from WP1 and WP2

Methodology / work description
We will build a cloud model at a cloud scale to determine what is the quantitative impact of aerosol dissolution and transition metals on the chemical budget of a cloud.
Mechanism development: Based on the existing multiphase coupled with MODEL B the reaction scheme will be extended considering additional processes of transition metal ions. Beside of processes of Mn, Fe and Cu already included in the scheme highly dynamical processes and equilibria of additional TMI's as mentioned in WP1 will be implemented directly into the multiphase mechanism.
Model Initialisation: The chemical and microphysical data determined by WP2 will be implemented in the model. The resulting data set for the cloud model will allow to determine the quantitative impact of transition metals on the chemical budget of a cloud in different environments

at a cloud scale.

Model calculations: This work will use the homogeneous and heterogeneous kinetic data delivered by WP1 and WP2 to perform a chemical budget of all the reactive species present in a cloudy environment. This includes the phase transfers between gas and dissolved species and between particulate and dissolved species. This phase transfer will be driven using a cloud microphysical model. The validated data obtained from WP1 and WP2 will enhance the accuracy of the developed model. One aspect in the interpretation of the model results will be the close link between the HO_x-ROx and TMI-chemistry in the particle phase possibly influencing the oxidation effectivity of the tropospheric gas phase.

Deliverables

Microphysic, water and ice content of cloud, 0D model and a detailed chemical reaction scheme for the tropospheric multiphase system (gas phase, aqueous phase, solid phase) with a consistent data set for different scenarios, Cloud chemical budget including inorganic and organic species and also a multiphase balance between particulate, aqueous and gas phase.

Cost 17%

Milestone and expected results

The used model will be prepared and tested for the description of solution processes from solid particles (CCN) into the resulting droplets. The implementation of the results of WP1 and WP2 will begin as soon as the first set of experimental data will be obtained. The sensitivity test of the model will lead to guidelines to define further experimental protocols. The major result will be a better understanding of the in-cloud chemical process at the cloud level exceeding current multiphase models considering in general only selected TMI such as Fe, Mn, Cu. The influence of emissions of TMI's will be quantified.

Cost 17%

9.4.4.5 Workpackage WP4: Cloud and Multiphase chemistry

Start Date: 8 **Lead Contractor N°:** 4 **Person-months:** 65

Objectives

To integrate at a local, regional and continental scale the cloud chemistry described in WP3

Methodology / work description

Rain, cloud, aerosol and associated trace gases sampling and analyses, associated with a large meteorological survey will be used to validate the proposed chemical schemes with a 3D simulation.

Cloud models: they involve modelling of the entire cloud or parts of it, in order to develop detailed reference models for the development of parameterisations. A model such as MODEL C will be useful to estimate local budgets of key species (oxidants, radicals) and partitioning of species among gas phase and condensed phase as a function of cloud formation and evolution stage. They will help to document the dependency of transition metal chemistry on drop size, hydrometeors shape and chemical composition, water content,…They will lead to the development of parameterizations to be included in larger scale models.

Regional and continental models: they consist in transport/chemistry models that couple simplified chemical mechanisms and parameterizations of microphysical processes. A model such as MODEL D coupled with a chemical module including gas and aqueous phase chemistry will be extended to more complex species based upon the first types of models already described. These models will integrate field data (microphysics and chemistry) or wind profiler data to initialise the dynamical and chemical fields and quantify the transport of primary aerosols, the fate of secondary aerosols and

the final deposition rates of the metal species. Another MODEL D version will include: (1) an in-cloud scavenging model (already developed); (2) an aerosol source scheme (already existing); (3) a simplified, parameterized chemical module ascribing (from previous WP's) at each time step and grid point the new aerosols solubility properties in view to continuously update the CCN input in the MODEL D built-in cloud sub-model. The radiative EC3 model (ECMWF modified) is already coupled online with MODEL D and will provide the radiative SW/LW fields, and possible dynamics/radiation retroactions.
The models should describe the microphysics of the cloud, either in a fully spectral way (MODEL C) or in a parameterised way. In both cases, it is important to consider the nucleation process and the evaporation stage of the cloud in order to account for aerosol changes in structure or surface. Then, one can conclude in the possible size segregation of the aerosol particles that can occur during these phase evolution of the cloud.

Deliverables
Atmospheric water chemical compounds and transition metal content. Effect of the transition metals at a continental scale. Mesoscale evaluation of the CCN modification. Quantification of subsequent direct and indirect cloud development and radiative forcing
Cost 18%

Milestone and expected results
This modelling work will start after 5 months of WP3 running and will benefit of the advancements proposed by WP3. The expected results are an overview of the influence of transition metals in atmospheric chemistry, an overview of the solubility of these metals and also the aerosol evolution. We expect a better comprehension of the impact of aerosol weathering on cloud development and radiative budget.
Cost 18%

9.4.4.6 Workpackage WP5: Results dissemination

Start Date: 31 **Lead Contractor N°:** 1 (with 2-5) **Person-months:** 24

Objectives and input to workpackage
To write international top-levels publications on the influence of aerosol dissolution and transition metals for cloud and atmospheric chemistry, with an integration of multiphase chemistry and cloud physics.

Methodology / work description
The large data set obtained along the 30 months of experimental and modelling activity will produce publications around the partial results. We will conduct here a large brain activity, assisted with a close communication with e-mails, and deliver scientific publications which would serve as reference for the next period.

Deliverables
A set of international level publications which report the conclusions of the proposed work
Cost 5%

Milestone and expected results
We expect that the proposed work will enhance the knowledge of multiphase chemistry because of the large part of cloud chemistry covered here. As the working plan is organised to answer to all the remaining obscure points around this subject, the maximum rate of scientifically top levels results production will take place in the last 6 month of the project.

Cost 5%

9.4.4.7 Deliverables list

N°	Title	Date	Nature	Dissemination level
1	Validated kinetic constant	18	Da	Pu
2	Heterogeneous kinetic mechanisms	18	Da, Th	Pu
3	Micro physic, water and ice content of cloud	18	Da, Th	Pu
4	Reduction guidelines for models	24	Me	Pu
5	Measured available dissolved metals concentration	26	Da	Pu
6	Surface structure and reactivity relationship	26	Da, Th	Pu
7	0D model, chemical reaction scheme	26	Th	Pu
8	Cloud chemical budget (sulphur, HO_x, etc...)	30	Th, Re	Pu
9	Role of aerosol weathering at a continental scale	36	Re,Th	Pu
10	International level publications	36 and after (review delays)	Re, Da, Me	Pu

9.5 Appendix: references

Audiffren N., N. Chaumerliac, and Renard, M. (1996), "Effects of a polydisperse cloud on tropospheric chemistry.", *J. Geophys. Res.*, **101,** 25949-25966.

Audiffren N., M. Renard, E. Buisson and N. Chaumerliac (1998) Deviations from the Henry's law equilibrium during cloud events: a numerical approach of the mass transfer between phases and its specific numerical effects, Atmos. Res., **49**, 139-161.

Audiffren N., S. Cautenet, and N. Chaumerliac (1999) A modeling study of the influence of ice scavenging on the chemical composition of liquid-phase precipitations of a cumulonimbus cloud, J. Appl. Meteor., **38** , No. 8 , p. 1148-1160 (AMS).

Behra, P. and Sigg, L. (1990), "Evidence for redox cycling of iron in atmospheric water droplets". *Nature*, **344**, 419-421.

Cachier, H., Buat-Ménard, P., Fontugne, M., Chesselet, R., (1986). Long range transport of continentally-derived carbon in the marine atmosphere: Evidence from stable carbon isotope studies. Tellus 38, 161-177.

Chaumerliac N., N. Audiffren, and M. Leriche (2000) Modelling of scavenging processes in clouds: some remaining questions about the partitioning of species among gas and liquid phases. Atmos. Res., **53**, No. 1-3, p. 29-43.

Colin, J.L., Jaffrezo, J.L. and Gros, J.M. (1990) Solubility of major species in precipitation : factors of variation. *Atmos. Environ*., **24A**, 537-544.

Dentener, F., Carmichael, G., Zhang, Y., Crutsen, P. and Lelifeld, J. (1996) The role of mineral aerosols as a reactive surface in the global troposphere. J. Geophys Res., **101 D17**, 22869-22890.

Desboeufs, K.D., Losno, R., Vimeux, F. and Cholbi, S. (1999) pH Dependant dissolution of Wind transported Saharan Dust, J. Geophys. Res., in press.

Flossmann A.I., (1998), "Clouds and Pollution". *Pure & Appl. Chem.*, **70**, 1345-1352.

Flossmann A.I., (1998), "Interaction of aerosol particles and clouds". *J. Atmos. Sci.*, **55**, 879-887.

Flossmann A.I., (1998), "Richard Goody : Principles of atmospheric physics and chemistry". *J. Atmos. Chem*, **30**, 314-317.

François, F., Maenhaut, W., Losno, R., Colin, J.L., Schulz, M., Haster, T., Spokes, L. and Jickells, T.(1995) Intercomparison of elemental concentrations in total and size-fractionated aerosol samples collected during the Mace Head experiment, April 1991. *Atmos. Environ.*, **27**,837-849.

Graedel T.E., Weschler C.J and Mandich M.L. (1985), "Influence of Transition Metal Complexes on Atmospheric Droplet Acidity." *Nature* **317,** 240-242.

Graedel T.E., Mandich M.L. and Weschler C.J. (1986), "Kinetic Model Studies of Atmospheric Droplet Chemistry: 2. Homogeneous Transition Metal Chemistry in Raindrops", *J. Geophys. Res.*, **91 D4**, 5205-5221.

Grgic, I., Dovzan, A., Bercic, G., and Hudnik, V. (1998), "The Effect of Atmospheric Organic Compounds on the Fe-catalyzed S(IV) Autoxidation in Aqueous Solution." *J. Atmos. Chem.* **29**, 315-337.

Grgic, I., Poznic, M. and Bizjak, M. (1999), " S(IV) Autoxidation in Atmospheric Liquid Water: The Role of Fe(II) and the Effect of Oxalate." *J. Atmos. Chem.* **33**, 89-102.

Havers, N., Burba, P., Lambert, J., Klockow, D., 1998. Spectroscopic characterisation of humic-like substances in airborne particulate matter. J. Atmos. Chem. 29, 45-54.

Jacob D.J., Gottlieb E.W. and Prather M.J. (1989), "Chemistry of a Polluted Cloudy Boundary Layer", *J. Geophys. Res.*, **94 D10**, 12975-13002.

Jickells T.D., Knap A.H. and Church T.M. (1984), "Trace Metals in Bermuda Rainwater", *J. Geophys. Res.*, **89 D1**, 1423-1428.

Keene, W.C., Savoie, D.L. (1998). "The pH of deliquescent sea-salt in polluted marine air", *Geophys. Res. Lett*., **25**, 2181-2184.

Keene, W.C., Sander, R., Pszenny, A.A.P., Vogt, R., Crutzen P.J., Galloway, J.N., (1998) "Aerosol pH in the marine boundary layer: A review and model evaluation", *J. Aerosol Sci.* **29**, 339-356.

Lelieveld J. and Crutzen P.J. (1991), "The role of Clouds in Tropospheric Photochemistry", *J. Atmos. Chem.*, **12**, 229-267.

Leriche, M., Voisin, D. ; Chaumerliac, N., Monod, A., and Aumont, B. (2000) A model for tropospheric multiphase chemistry: application to one cloudy event during the CIME experiment, Atmos. Environ., **34** , No. 29-30 , p. 5015-5036 (Elsevier).

Lim, B., Jickells, T.D., Colin J.L. and Losno, R (1993) Solubilities of Al, Pb, Cu and Zn in rain sampled in the marine environment over the North Atlantic Ocean and Mediterrean Sea. *Global Biogeochemical Cycles*, **8**, 349-362.

Losno, R., Bergametti, G. and Carlier P. (1992) Origin of the atmospheric particulate matter over the North-Sea and the Atlantic Ocean. *J. of Atmos. Chem.*, **15**, 333-352.

Losno, R., Colin, J.L., Le Bris, N., Bergametti, G., Jickells, T. and Lim, B. (1993) Aluminium Solubility in Rainwater and Molten Snow. *J. of Atm. Chem*, **17**, 29-43.

Losno, R. and Martin, D. (1995) NUAC: Une approche de la base de donnée. Première analyse de cohérence et de qualité. Perspectives d'utilisation.. Rapport au Ministère de l'Environnement, 14pp.

Losno, R. (1999) Trace Metals Acting as Catalysts in a Marine Cloud: a Box Model Study, *Phys. Chem. Eart (B)*, **24**, 281-286.

Martin, L.R., Hill, M.W., Tai, A.F. and Good, T.W. (1991) The iron catalysed oxidation of sulfur(IV) in aqueous solution: differing effects of organics at high and low pH. J. Geophys. Res. 96, 3085-3097.

Matthijsen J., Builtjes P.J.H., Meijer E.W. and Boersen G. (1997), "Modelling cloud effects on ozone on a regional scale: a case study", *Atmos. Environ.*, **31**, 3227-3238.

Ross H.B. (1987), "Trace metals in precipitation in Sweden", *Water Air and Soil Pollution*, **36**, 349-363.

Sander R. and Crutzen P.J. (1996), "Model study indicating halogen activation and ozone destruction in polluted air masses transported to the sea", *J. Geophys. Res.*, **101 D4**, 9121-9138.

Sedlak, D.L. and Hoigné, J. (1993), "The role of copper and oxalate in the redox cycling of iron in atmospheric waters". *Atmos. Environ.* **27A** (14), 2173-2185.

Spokes, L. J., Jickells, T.D. and Lim, B. (1994) Solubilisation of aerosol trace metals by cloud processing : a laboratory study. *Geochem. Cosmochim. Acta*, **58**, 3281-3287.

Spokes, L.J. and Jickells, T.D. (1996) Factors controlling the dissolved-particulate distribution of aerosol trace metals in the atmosphere and on mixing to seawater. *Aquatic Geochemistry*, **1**, 355-374.

Voisin D., M. Legrand and N. Chaumerliac (2000) Investigation of the scavenging of acidic gases (HCOOH, CH3COOH, HNO3, HCl, and SO2) and ammonia in mixed liquid-solid water clouds at the Puy de Dome mountain (France), J. Geophys. Res., **105** , No. D5 , p. 6817-6836.

Walcek C. J., Yuan H.H., and Stockwell W.R. (1997) "The influence of aqueous-phase chemical reactions on ozone formation in polluted and nonpolluted clouds", *Atmos. Environ.*, **31**, 1221-1237.

Warneck P. (1991) "Chemical Reactions in Clouds", *Fresenius J. Anal. Chem.* **340**, 585-590.

Warneck P., Mirabel P., Salmon G.A., van Eldik R., Vinckier, C., Wannowius K.J. and Zetzsch C. (1996): Review of the activities and achievements of the EUROTRAC subproject HALIPP, *Transition metal ions and their role in atmospheric waters*, in P. Warneck (ed), Heterogeneous and Liquid Phase Processes, Laboratory studies related to aerosols and clouds, Springer-Verlag, Berlin. pp. 20-26.

Weschler C.J., Mandich M.L. and Graedel T.E. (1986), "Speciation, Photosensitivity, and Reactions of Transition Metal Ions in Atmospheric Droplets", *J. Geophys. Res.*, **91 D4**, 5189-5204.

Zhu, X, Prospero, J.M., Savoie, D.L., Millero, F.J., Zika, R.G. and Saltzman, E.S. (1993) Photoreduction of iron (III) in marine aerosol solutions. *J. Geophys. Res.* **98**, 9039-9046

Zhuang, G., Yi Z., Duce, R.A. and Brown P.R. (1992) Link between iron and sulphur suggested by the detection of Fe(II) in remote marine aerosols. *Nature*, **355**, 537-539.

Zuo, Y. (1995) Kinetics of photochemical cycling of iron coupled with organic substances in cloud and fog droplets. *Geochim. Cosmochim. Acta.* **59**, 3123-3130.

Zuo Y. and Hoigné J. (1992), "Formation of Hydrogen Peroxide and Depletion of Oxalic Acid in Atmospheric Water by Photolysis of Iron(III)-Oxalato Complexes", *Environ. Sci. & Technol.*, **26**, 1014-1022.